TECHNICAL REPORT STANDARD PAGE

1. Report No.	2. Government Accession No.	3. Recipient's Catalog No.
FHWA/LA.13/519		

4. Title and Subtitle	5. Report Date
Evaluation of Dynamic Shear Rheometer Tests for Emulsions	December 2014
	6. Performing Organization Code LTRC Project Number: 11-2B State Project Number: 30000163

7. Author(s)	8. Performing Organization Report No.
Nazimuddin Wasiuddin, Saeid S. Ashani, and M. Readul Islam Louisiana Tech University	

9. Performing Organization Name and Address	10. Work Unit No.
Department of Civil Engineering Louisiana Tech University Ruston, LA 71272	11. Contract or Grant No.

12. Sponsoring Agency Name and Address	13. Type of Report and Period Covered
Louisiana Department of Transportation and Development P.O. Box 94245 Baton Rouge, LA 70804-9245	**Final Report** **09/2010-11/2013**
	14. Sponsoring Agency Code

15. Supplementary Notes
Conducted in Cooperation with the U.S. Department of Transportation, Federal Highway Administration

16. Abstract
DSR-based rheological tests of 20 different asphalt emulsion residues were performed and relationships with elastic recovery (AASHTO T301) and force ductility (AASHTO T300) were investigated. In strain sweep test from 2% to 52%, it was observed that emulsions prepared of hard pen base asphalt have relatively lower strain tolerances. Using frequency sweep data, complex modulus master curves were constructed at 25°C to understand overall rheological behavior. Temperature sweep of phase angle from 52°C to 94°C showed that a maximum phase angle in the range of 75° to 85° may be used as a criterion for polymer identification. MSCR (AASHTO TP70) at 58°C has been recommended to replace the elastic recovery test (AASHTO T301). At 0.1kPa creep stress, a minimum percent recovery of 25 and at 3.2kPa, a minimum percent recovery of 9 are recommended to identify the presence of polymer replacing elastic recovery test (AASHTO T301). Also, percent recovery of MSCR and phase angle can be used to replace force ductility requirements (AASHTO T300). It is recommended that at 58°C, a maximum phase angle of 81° and a minimum MSCR percent recovery (at 0.1kPa creep stress) of 30 can be specified to replace the force ductility test (AASHTO T300). These criteria are applicable for emulsion residues prepared according to the low temperature evaporative method specified in ASTM D7497. However, a comparative study among ASTM D7497 (24 hr at 25°C and 24 hr at 60°C), ASTM D6934 (3 hr at 163°C), AASHTO TP 72 Method B (6 hr at 60°C), vacuum dry method (6 hr at 60°C, a method developed in this study) and field curing have been performed in order to develop a low temperature low duration recovery method. It was observed that the MSCR test on residue prepared with the vacuum dried method can be used for polymer identification replacing elastic recovery and force ductility tests. Finally, the current specification viscosity range for low and high viscous emulsions using the saybolt furol viscometer to ensure quality control and quality assurance can also be replaced by the rotational viscometer. The ranges recommended are 220 - 730 cP and 5 – 90 cP (gives 98% probability) at 50 rpm and 30°C for high and low viscous emulsions, respectively.

17. Key Words	18. Distribution Statement
Dynamic Shear Rheometer, Asphalt Emulsion, Multiple Stress Creep and Recovery, Force Ductility, Elastic Recovery, Viscosity	Unrestricted. This document is available through the National Technical Information Service, Springfield, VA 21161.

19. Security Classif. (of this report)	20. Security Classif. (of this page)	21. No. of Pages	22. Price

Project Review Committee

Each research project will have an advisory committee appointed by the LTRC Director. The Project Review Committee is responsible for assisting the LTRC Administrator or Manager in the development of acceptable research problem statements, requests for proposals, review of research proposals, oversight of approved research projects, and implementation of findings. LTRC appreciates the dedication of the following Project Review Committee Members in guiding this research study to fruition.

LTRC Administrator

William "Bill" King, Jr., P.E.
Materials Research Administrator

Members

Danny Smith, DOTD Construction
Luanna Cambas, DOTD District 02 Lab
Jason Davis, DOTD Materials Lab
Jay Collins. DOTD District 04
John Wells, DOTD Contracts and Specifications
Don Weathers, LAPA
Hector Santiago, FHWA
Gaylon Baumgardner, Paragon Services

Directorate Implementation Sponsor

Richard Savoie, P.E.
DOTD Chief Engineer

Evaluation of Dynamic Shear Rheometer Tests for Emulsions

by

Nazimuddin M. Wasiuddin
Saeid S. Ashani
M. Readul Islam

Department of Civil Engineering
Louisiana Tech University
Ruston, Louisiana, 71272

LTRC Project No. 11-2B
State Project No. 30000163

conducted for

Louisiana Department of Transportation and Development
Louisiana Transportation Research Center

December 2014

ABSTRACT

DSR-based rheological tests of 20 different asphalt emulsion residues were performed and relationships with elastic recovery (AASHTO T301) and force ductility (AASHTO T300) were investigated. In strain sweep test from 2% to 52%, it was observed that emulsions prepared of hard pen base asphalt have relatively lower strain tolerances. Using frequency sweep data, complex modulus master curves were constructed at 25°C to understand overall rheological behavior. Temperature sweep of phase angle from 52°C to 94°C showed that a maximum phase angle in the range of 75° to 85° may be used as a criterion for polymer identification. MSCR (AASHTO TP70) at 58°C has been recommended to replace the elastic recovery test (AASHTO T301). At 0.1kPa creep stress, a minimum percent recovery of 25 and at 3.2kPa, a minimum percent recovery of 9 are recommended to identify the presence of polymer replacing elastic recovery test (AASHTO T301). Also, percent recovery of MSCR and phase angle can be used to replace force ductility requirements (AASHTO T300). It is recommended that at 58°C, a maximum phase angle of 81° and a minimum MSCR percent recovery (at 0.1kPa creep stress) of 30 can be specified to replace the force ductility test (AASHTO T300). These criteria are applicable for emulsion residues prepared according to the low temperature evaporative method specified in ASTM D7497. However, a comparative study among ASTM D7497 (24 hr at 25°C and 24 hr at 60°C), ASTM D6934 (3 hr at 163°C), AASHTO TP 72 Method B (6 hr at 60°C), vacuum dry method (6 hr at 60°C, a method developed in this study) and field curing have been performed in order to develop a low temperature low duration recovery method. It was observed that the MSCR test on residue prepared with the vacuum dried method can be used for polymer identification replacing elastic recovery and force ductility tests. Finally, the current specification viscosity range for low and high viscous emulsions using the saybolt furol viscometer to ensure quality control and quality assurance can also be replaced by the rotational viscometer. The ranges recommended are 220 - 730 cP and 5 – 90 cP (gives 98% probability) at 50 rpm and 30°C for high and low viscous emulsions, respectively.

ACKNOWLEDGMENTS

This project was funded by the Louisiana Transportation Research Center (LTRC). The authors sincerely acknowledge their support and contributions. The authors also want to thank the emulsion producers who provided samples for this project.

IMPLEMENTATION STATEMENT

This report documents several new methods for testing and evaluating asphalt emulsions. As described in the report, implementing the use of these test methods will reduce testing time and will provide a greater reliability.

MSCR (AASHTO TP70) at 58°C has been recommended to replace the elastic recovery test (AASHTO T301). At 0.1kPa creep stress, a minimum percent recovery of 25 and at 3.2kPa, a minimum percent recovery of 9 are recommended to identify the presence of polymer replacing elastic recovery test (AASHTO T301).

Also, it was concluded from this study that percent recovery of MSCR and phase angle can be used to replace force ductility requirements (AASHTO T300). It is recommended that at 58°C, a maximum phase angle of 81° and a minimum MSCR percent recovery (at 0.1kPa creep stress) of 30 can be specified to replace force ductility test (AASHTO T300).

These criteria are applicable for emulsion residues prepared according to the low temperature evaporative method specified in ASTM D7497. However, a comparative study among ASTM D7497 (24 hr at 25°C and 24 hr at 60°C), ASTM D6934 (3 hr at 163°C), AASHTO TP 72 Method B (6 hr at 60°C), vacuum dry method (6 hr at 60°C, a method developed in this study) and field curing have been performed in order to develop a low temperature low duration recovery method. It was observed that the MSCR test on residue prepared with the vacuum dried method can be used for polymer identification replacing elastic recovery and force ductility tests.

The current specification viscosity range for low and high viscous emulsions using saybolt furol viscometer to ensure quality control and quality assurance can also be replaced by the rotational viscometer. The ranges recommended are 220 - 730 cP and 5 - 90 cP (gives 98% probability) at 50 rpm and 30°C for high and low viscous emulsions, respectively.

TABLE OF CONTENTS

LIST OF TABLES

LIST OF FIGURES

INTRODUCTION

The Strategic Highway Research Program (SHRP) research on asphalt was carried out almost exclusively with unmodified asphalt cements, so the applicability of the Superpave performance graded (PG) specifications and test methods to modified binders was not validated. Similarly, polymers are added to all types of paving asphalt emulsions to improve performance of surface treatments, cold mix asphalt, recycling, and other applications. The dosage rates vary, but are generally one to five percent polymer by weight of asphalt; two to three percent is the most common for chip seal and slurry seal/microsurfacing applications [*1*]. Currently, Louisiana DOTD requires a ductility test at 25°C according to AASHTO T51 for emulsions and two other tests, namely force ductility ratio at 4°C and elastic recovery at 10°C according to AASHTO T300 and AASHTO T301 respectively for polymer modified emulsions. These test methods are not directly and fully related to pavement performance and there is an immense need to develop performance graded emulsion specifications.

Background and Literature Review on Elastic Recovery (AASHTO T301)

It was reported by D'Angelo that the PG-Plus tests including the elastic recovery test (AASHTO T301) in most cases do not relate to performance and only indicate the presence of a particular modifier in the binder [*2*]. It was also concluded in that study that AASHTO T301, used by many highway agencies to verify the presence of polymer in the asphalt binder, did not identify the nature of the polymer structure because the test is performed at 25ºC, a temperature where the base binder is significantly stiff enough to provide support for the polymer, thus masking the nature and extent of the polymer network. Besides, current methodology for measuring elastic properties of asphalt binders requires the use of a ductility bath, which has several disadvantages: inconsistency of the testing sample geometry, time consuming sample preparation, and manual data collection. It is also known that manually cutting the asphalt sample and moving it back to estimate recovery is subject to operator's variability [*3*]. AASHTO T301 recommends 20 cm elongation and sample hold time of 5 min while ASTM D6084 specifies 10 cm elongation and immediate cut. The researchers conducted a survey of several state DOTs and observed many different methods in the elastic recovery test method. The survey revealed that for modified PG binders, some states such as Louisiana and Kentucky specify 25°C and 10 cm elongation while some other states such as Tennessee, California and West Virginia specify 25°C and 20 cm elongation and Texas uses 10°C and 20 cm elongation. For modified asphalt emulsion, Louisiana uses 10°C and 20 cm elongation while some other states such as Kentucky specifies 4°C and 10 cm elongation.

Several researchers investigated the use of dynamic shear rheometer (DSR) based tests to replace elastic recovery test using a ductility bath. The ability of the multiple stress creep and recovery test (MSCR according to AASHTO TP70) to identify the extent and strength of the polymer network in a PG binder replacing AASHTO T301 method was demonstrated by D'Angelo through a comparison of different blending techniques in one base binder[*2*]. In another study, based on the data produced at the Mathy Technology and Engineering Services, Inc., it was concluded that the MSCR produces data trends similar to those of the elastic recovery test for PG binders. A correlation between the two tests led the FHWA researchers to select 15 % as the minimum requirement for MSCR percent recovery at a 3.2-kPa stress level [*4*]. Anderson reported better correlation between percent recovery at 100Pa in MSCR and elastic recovery in AASHTO T301 for PG binders [*5*]. Recently, Clopotel and Bahia developed a new procedure for measuring elastic recovery in the DSR (ER-DSR) and correlated it to the standard ductility bath test for elastic recovery (ER-DB) [*6*]. They observed a very good correlation (R^2=0.97) between ER-DSR and ER-DB for PG binders and recommended that the procedure for measuring the elastic recovery in the ductility bath be replaced with the DSR. A good correlation (R^2=0.78) between ER-DSR and % recovery from the MSCR test at 3.2 kPa was also observed. In summary, most of the previous studies observed good correlation between a DSR based test and elastic recovery that will help maximize the use of the DSR for asphalt binder testing. Besides, DSR based tests have the following advantages over elastic recovery: small sample size, reduction in the testing time, easy preparation, good repeatability, and automated measurements.

Updated test methods and specifications using newly available tools for PG asphalt binders could provide more accurate characterization of emulsified asphalt residues. To this end, this study has been performed to evaluate dynamic shear rheometer tests for asphalt emulsion residues.

Background and Literature Review on Force Ductility (AASHTO T300)

The force ductility test is used to estimate the potential for fatigue and thermal cracking, and/or raveling [*7*]. It was first introduced by Anderson and Wiley in 1976 to indicate expected low temperature performance of asphalt binders by comparing their relative strength at low temperatures while being pulled at a fixed deformation rate [*8-9*]. Later on in 1985, Shuler modified the test procedure to improve the precision and practicality, particularly for use with polymer modified asphalt binders [*10-11*]. Currently, AASHTO T300 is used for force ductility by some agencies in characterizing polymer modified asphalt

binders where, an asphalt binder sample is elongated typically at 4°C and 5 cm/min deformation rate until fragile fracture or reaching the elongation of at least 30 cm. AASHTO T300 specifies that the force ratio (ratio of the force at the second peak to the force at the initial peak) be reported. The first peak is related to the base asphalt and the second peak characterizes the polymer [*10-11*].

However, the force ductility test is a time and material consuming process. It is subject to reproducibility difficulties and can exhibit significant variability at low to intermediate temperatures (4º-25ºC.) [*7, 12-13]*. Regarding variability, Neoprene and SBR modifiers generally produce comparatively high ductility, while SB and SBS additives yield much lower ductility [*12*]. King characterizes the low ductility of the latter as a function of "too much" rather than "too little" strength, as SB/SBS modified mixes are comparatively thick when elongated and snap much in the way a thick rubber band does when pulled too far [*12*]. This suggests that with some SB and SBS modified mixes, ductility testing could under-predict performance measures of strength. Besides variability in results, the force ductility test requires the use of a ductility bath, which has several disadvantages including inconsistency of the testing sample geometry. Most importantly, these tests are empirical and often fail to accurately and comprehensively characterize the performance characteristics associated with polymer modified emulsion [*14-16*]. The researchers in this study conducted a survey of several state DOTs that specify force ductility test, such as Louisiana and Illinois, and observed many different specifications in force ductility tests. For example, for PG76-22m, Louisiana requires force ratio to be 0.3 or higher; whereas, for PG70-22m, it specifies force at 30 cm elongation to be higher or equal to 0.5 lb. For CRS-2P and PAC-15, the force ratio needs to be 0.3 or higher, and for SS-1P it is to be 0.15 or higher.

The use of (DSR) tests has become increasingly advocated as one method through which the viscoelastic properties of modified emulsion residue and modified asphalt binders may be assessed [*15-21*]. Glover et al. found an excellent correlation for unmodified asphalts between ductility (at 15°C, 1 cm/min) below 10 cm and the DSR function G'/(η'/G') at 15°C and 0.005 rad/s [*13*]. For modified asphalts, the DSR-ductility results were complex. Generally for a given value of the DSR function, the ductility was better than indicated by the DSR function correlation for unmodified asphalts. Larger amounts of modifier produced increasing values of ductility for a given function value. This result was very asphalt dependent and no general correlation could be found for modified binders. Glover et al. also reported that as modified binders oxidize, the asphalt hardens, and the improvement to ductility imparted by modifiers decreases [*13*]. After enough aging, the improvement is gone, and modified binders perform no better than their aged, unmodified counterpart.

Nevertheless, modifiers appear to provide added life to binders. In this regard, Airey reported that the phase angle (δ) is usually considered to be much more sensitive to the structure of the binder than is G*, and as such, provides a better indication of the type and extent of polymer modification [*15*]. Within this context, smaller δ values are indicative of a greater elastic (less viscous) response, and thus suggest a higher degree of polymer network formation, particularly at higher temperatures. Some of the states that use phase angle in PG plus specifications include Florida, Georgia, and Ohio. For PG76-22m, Georgia and Florida specify a maximum phase angle of 75° while Ohio allows a maximum of 76° at 76°C.

In summary, polymer improves the ductility of asphalt binders and emulsion residues depending on the base asphalt characteristics and some states require force ductility, a primarily empirical test for polymer characterization in their PG Plus specifications without enough validation. To this end, this study has been performed to evaluate dynamic shear rheometer tests to replace the force ductility test for asphalt emulsion residues.

Background and Literature Review for Recovery Methods

Several methods are available to recover asphalt from the asphalt emulsion for further rheological characterization or to determine the asphalt content of the emulsion. If the recovery of the residue is focused only on determining the asphalt content, any method can be used as long as it completely removes the water from the emulsion. On the other hand, processes which recover the binder without changing its characteristics are preferred in case of further rheological characterization.

Many manufacturers of polymer modified emulsions believe that high temperature involved in any recovery process can harm the polymer modifier additives. Recently, many researchers have used ASTM D7497, a low temperature recovery method for latex and polymer modified emulsions and have found consistent rheological data. ASTM D7497 and EN 13074 procedures were developed on the basis of the work of Takamura, in which the procedure involved curing of an emulsion film approximately 1 mm thick in a force draft oven for 5 hours at 22°C [*22*]. Measurement of rheological properties of neat and polymer modified emulsion residues at high temperatures showed an increase in G*/sinδ with increasing polymer concentration, verifying that recovery at lower temperatures maintained polymer network [*22*]. It has been made clear that, based on the evaluation of strain tolerance, elastic recovery, and total accumulated strain, the ASTM D7497 procedure allows for the recovery of modified binders from emulsions without degrading the polymer network [*19*]. The only concern with this method is the length of time (48 hours) required to finish the

recovery process. Many DOTs have their own modified version of recovery method to reduce the time of the experiment. AASHTO specifies a different recovery method which is also a low temperature evaporative method but requires only 6 hours. But lowering the time in a low temperature evaporative method may be insufficient for the complete removal of the water from the emulsion which will eventually affect the stiffness of the binder.

Another issue with emulsion recovery methods is that they do not produce emulsion residue with the same rheological properties of their corresponding unaged base binder. Kadrmas found that the values of $G^*/\sin\delta$ for the emulsion are significantly higher than their corresponding unaged base binder, concluding that the recovery method does not produce materials with properties similar to those of the base binders [*23*]. Hanz et al. suggested that the ASTM D7497 evaporative recovery method produced residues with rheological properties similar to those of oven-cured or RTFO-aged base asphalt. The differences of the emulsion residue and corresponding unaged base binder in rheological response, as observed in evaluations of strain tolerance and percent strain recovery can be attributed to the effects of emulsifier or remaining water in the emulsion [*19*]. Previous research efforts by many authors could not identify if these differences are exactly due to oxidative aging, remaining moisture, chemistry of the emulsifier, or a combination of these factors.

Also, one can argue that a procedure should be chosen to match the properties of the road binder when the traffic is reopened. It is clear from the previous studies that there is no ideal standard to compare emulsion residue rheological properties. But a good recovery method is one which removes the water completely from the emulsion, produces a residue representing on-the-road binder and shows the benefits of the polymer without harming its structure [*24*].

To summarize, ASTM D7497 is currently a well-practiced standard method that can produce emulsion residue that is close to RTFO-aged base binder in properties and does not harm the polymer modifier but there is a clear need to reduce the length of time for this procedure. Further research is needed to understand the level of aging that occurs in the field in between the application of emulsion and time of traffic reopening. Rheological properties of the residue change due to recovery time, remaining moisture, and chemical change, but it needs to be understood which of these effects has a significant role to strain tolerance and stiffness.

To this extent, the theme of this research effort is to verify the possibility of time reduction in the low temperature evaporative recovery method and to answer some fundamental questions associated with the emulsion recovery process. To achieve this goal, a new recovery method is evaluated which requires significantly less time along with other methods. To remove the

moisture completely from the residue and to accelerate the evaporation process in such a less time, a high pressure vacuum (0.072 - 0.725 psi) was applied using a vacuum drying oven. Another method is proposed in the study to grossly estimate the initial field aging of the emulsion at the time of traffic reopening. In this process, the emulsion is cured outside for 48 hours (field curing time) in ambient temperature and humidity (on typical Louisiana summer days that were dry). These two new methods, along with ASTM D7497, AASHTO TP 72 (6 hours at 60°C) and ASTM D6934 (3 hours at 163°C), were conducted on six different emulsions including anionic, cationic, slow setting, rapid setting, polymer modified, latex modified, and neat emulsions with the objective of reducing the time of low temperature recovery. Base asphalts of these emulsions were also tested to compare the rheological properties of the emulsion residue.

OBJECTIVE

One of the objectives of this study was to evaluate the DSR-based test parameters to replace the elastic recovery test (AASHTO T301) and the force ductility test (AASHTO T300) using ductility bath for emulsified asphalt residues. Another important objective was to develop a new residue recovery method that will require a shorter time period and lower temperature. Also, this study will evaluate the use of rotational viscometer replacing the saybolt fural viscometer.

SCOPE

Temperature sweep, strain sweep, frequency sweep, and multiple stress creep and recovery tests of commonly used emulsion residues were performed. The DSR-based test parameters were evaluated to replace the elastic recovery test (AASHTO T301) and the force ductility test (AASHTO T300). Residues were obtained using several different methods to develop a lower duration and lower temperature recovery method. A rotational viscometer was used to develop emulsion state viscosity test specifications.

METHODOLOGY

Materials for Elastic Recovery and Force Ductility Tests

Table 1 shows the 20 asphalt emulsions that were used in this study. The emulsions vary in particle charges (cationic and anionic), modifications (non-modified, polymer and latex modified), sources, application types (chip seal, micro-surfacing, fog seal, tack coat, etc.), curing time (slow, medium, and rapid setting), and in some other properties (high float for gelling, hard binder in fog seal, etc.).

Table 1
Emulsion residue experimental plan

Emulsions[1]	Strain Sweep	Freq. Sweep	Temp. Sweep	MSCR	Elastic Recovery and Force Ductility
SS-1 (E)	Temp.: 52°C and 70°C Strain: 2%, 12%, 22%, 32%, 42% and 52% 3 mat samples[2]	Temp.: 10°C, 25°C, 52°C and 70°C Ang. Freq.: 0.1 rad/s – 100 rad/s and data intervals: 10 points/decade 3 mat samples[2]	Temp.: from 52°C to 94°C at 6°C intervals Strain and Ang. Freq.: 12% and 10 rad/s 3 mat samples[2] and 3 DSR mold samples	Temp.: 10°C, 25°C, 58°C, 70°C and one equal-stiffness temperature (2.2 kPa stiffness) Stress: 0.1kPa, 3.2 kPa (0.1kPa, 0.2 kPa, 0.5 kPa and 3.2 kPa at 2.2 kPa stiffness temp.) 3 mat samples[2] for 0.1 and 3.2 kPa and 3 mat samples[2] for 0.2 and 0.5 kPa	Temp. Elastic Recovery: 10°C and 25°C Temp. Force Ductility: 4°C 2 mat samples[2] for Elastic Recovery and 2 mat samples[2] for Force Ductility
SS-1 (B)					
SS-1 (U)					
SS-1H (B)					
SS-1H (U)					
SS-1HP					
SS-1L					
CRS-2 (E)					
CRS-2 (B)					
CRS-2 (U)					
CRS-2P (E)					
CRS-2P (B)					
CHFRS-2P					
CMS-1P					
CSS-1HP					
PME					
NTSS-1HM (B)					
NTSS-1HM (C)					
NTSS-1HM (U)					
Fog Seal					

[1]Letter inside parenthesis denotes the source of the emulsion
[2]Seperate batch of samples for each type of test

Sample Preparation for Elastic Recovery and Force Ductility Tests

Several researchers conducted rheological comparisons between two low temperature evaporative methods, ASTM D7497 and Texas DOT method for emulsion residue preparations. ASTM D7497 uses two consecutive 24-h curing periods, one at 25°C and the other at 60°C, in a forced draft oven while the Texas DOT method uses 6-h curing at 60°C [*17-18*]. It was concluded from those studies that these two methods are compatible while ASTM D7497 samples produced higher stiffness. Hanz et al. concluded that the effects of the remaining moisture after ASTM D7497 procedure can be considered negligible relative to the effect of oxidation [*19*]. Therefore, ASTM D7497 has been used in this study for emulsion residue preparations.

At first, asphalt emulsion was poured into a tin can and the covered tin can was placed in an oven at 60°C for 30 minutes. To prepare big mat samples for elastic recovery and force ductility, about 120 gm of an asphalt emulsion was poured from the tin can in to a silicon mat, and immediately was spread out on the mat with a spatula (Figure 1 a-d). The mat was placed in a force draft oven at 25°C for one day and then another day at 60°C. After taking the mat out of the oven, residue was removed from the mat gently using spatula and was placed in a tin can to be used for elastic recovery and force ductility (Figure 1 e-l) tests.

To make small mat samples for DSR testing, about 1.5 grams of an asphalt emulsion was poured into the mat, and immediately was spread out on the mat with a spatula (Figure 2 a-e). The mat was placed in a force draft oven at 25°C for one day and then another day at 60°C. After taking the mat out of the oven, the residue was removed from the mat gently, placed on the bottom plate of DSR, and pressed with the thumb (Figure 2 f-l).

Experimental Plan for Elastic Recovery and Force Ductility Tests

In this study, a strain sweep test was performed between 2% and 52% strain at 10% intervals at two temperatures, 52°C and at 70°C. A frequency sweep test was performed between 0.1 rad/s and 100 rad/s angular frequency at four temperatures 10°C, 25°C, 52°C and 70°C to draw rheological master curves at 25°C. A temperature sweep test was performed between 52°C and 94°C at 6°C intervals using an angular frequency of 10 rad/s and 12% strain. Multiple stress creep and recovery testing was performed at 10°C, 25°C, 58°C, 70°C and one equal-stiffness (2.2 kPa) temperature according to AASHTO TP70 method. At the 2.2 kPa stiffness temperature, MSCR was also performed at 0.2 and 0.5 kPa stresses in addition to the standard 0.1 and 3.2 kPa stresses. An elastic recovery test was performed at 10°C and 25°C according to AASHTO T301. A force ductility test was performed at 4°C according to AASHTO T300.

First, the temperature sweep test was performed with 3 mat samples and 3 DSR mold samples. Percent water content and G*/sinδ values indicated that mat samples are better cured. Therefore, all other tests were performed using mat samples. Separate batches of three samples were used for strain sweep, frequency sweep, temperature sweep, and MSCR. In the case of MSCR, three more samples were used for 0.2kPa and 0.5kPa stresses at the 2.2kPa stiffness temperature. For elastic recovery, two mat samples were used for each temperature. Also for force ductility, two mat samples were used.

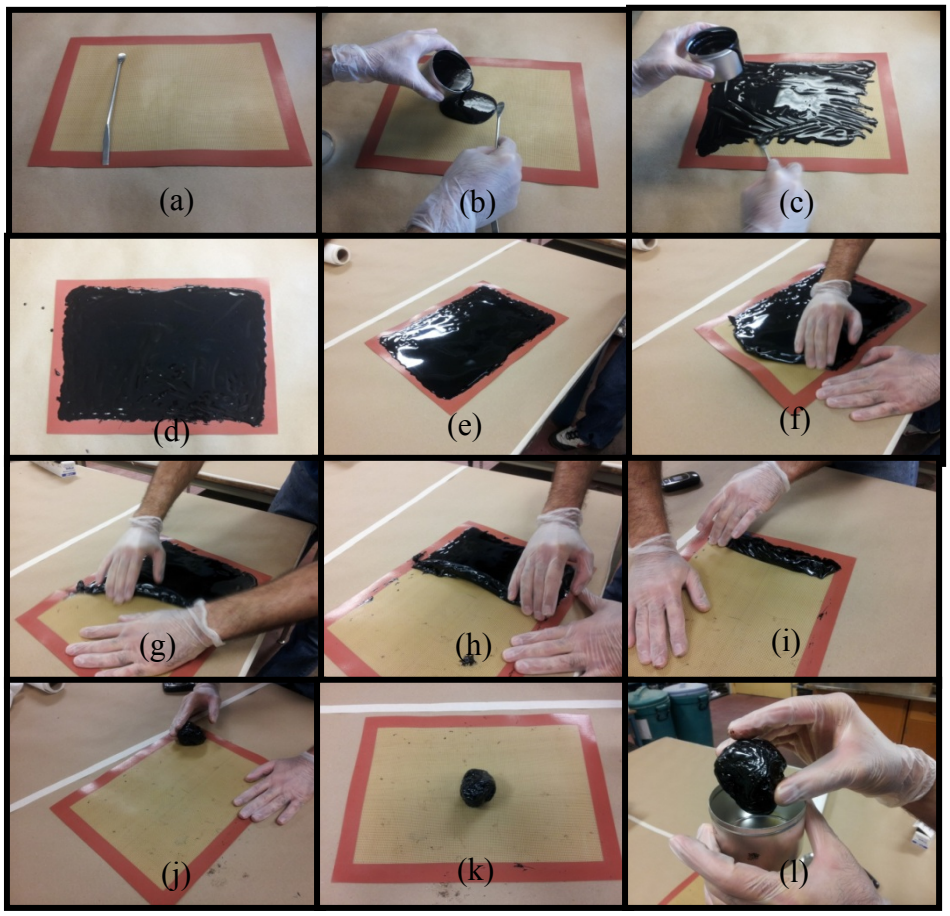

Figure 1
Emulsion residue preparations for elastic recovery and force ductility tests

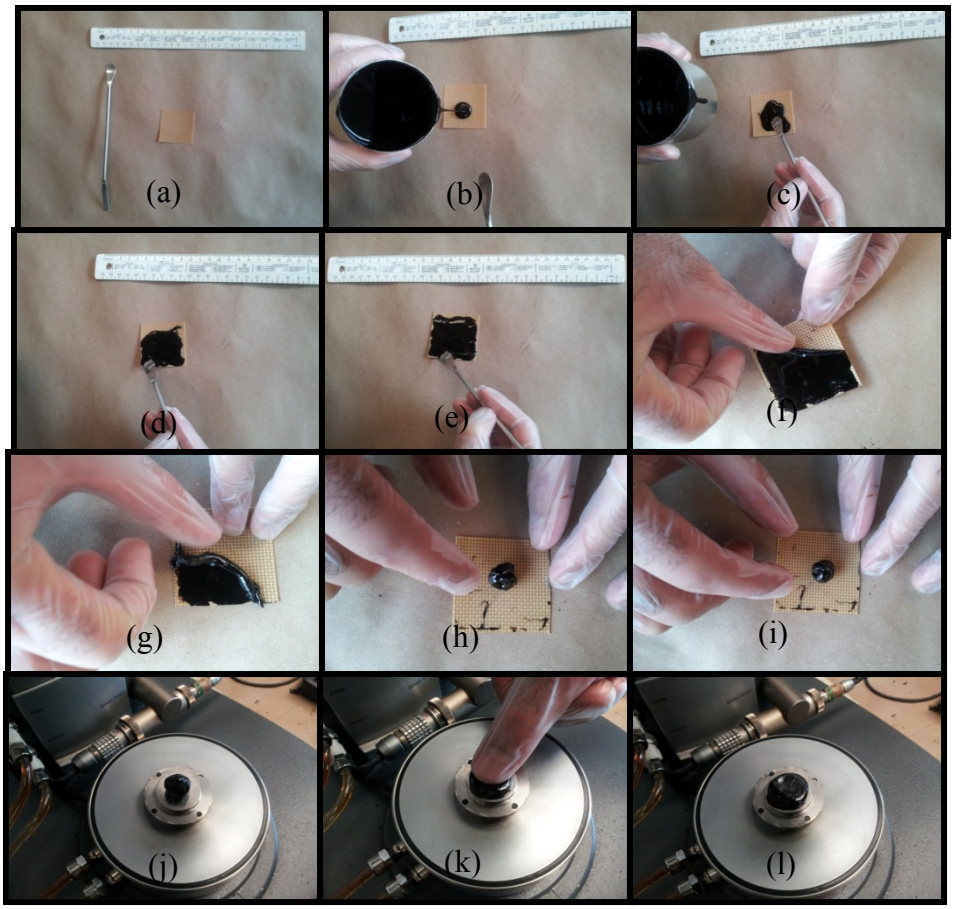

Figure 2
Emulsion residue preparations for DSR tests

Materials and Experimental Plan for Recovery Methods

Recovery Methods

In this study, the ASTM D7497-09 procedure was used to obtain residue from emulsified asphalt. The lower evaporative temperatures of this procedure provided conditions that are very close to that of application techniques for these materials. It specifies curing of an emulsion film of approximately 0.059 in thick on a silicone mat for 24 hrs at 25°C and the subsequent curing of 24 hrs at 60°C. Emulsion was poured on a 2-in. x 2-in. silicone mat and was spread with a spatula. After the curing, residue was peeled off from the mat by hand wearing nitrile gloves. For some of the emulsion samples where peeling off had not been possible, a wooden tongue depressor was used to take out the residue from the mat. This peeled off sample was kneaded into a small ball and placed in the DSR plate without any reheating. It should be noted that heating may affect the polymer structure of the residue.

Another method used in this study was evaporation (ASTM D6934), a standard rapid procedure for determining the asphalt content of asphalt emulsions. In this procedure, a 50 g emulsion sample was pre-weighed in a beaker and was heated in a oven at 163°C (325°F) for 2 hrs, stirred with a glass stick, heated for another hour, and weighed again. The sample was poured on the mat after being removed from the oven. This method is the fastest of all of the methods used for emulsion recovery. It produces a larger amount of sample than the other methods without being affected by external environmental factors such as humidity or lab temperature. One major disadvantage of this test is that it involves high temperatures which adversely affect the polymer modifiers, producing a residue which may not represent the emulsion residue in the field. As this method has the highest temperature of all the methods used in the study, it is expected to remove all the water from the residue and to give the value of maximum moisture content of the emulsion.

Although the ASTM D7497 procedure produces consistent results, one of the major issues with this recovery method is the length of time required (two days). Several DOTs tried their own modified recovery method to reduce the length of time. AASHTO introduced a new recovery method which requires a total of six hours. AASHTO TP 72 Method B is also used in this study. In this procedure, emulsion is poured on a silicone mat of 4 inch X 4 inch and spread with a spatula, creating a thin film with a thickness around 0.015 in. Then the silicone mat is placed inside a forced draft oven for 6 hours at 60°C. Another advantage of this method is that it requires a lower curing temperature which does not affect the polymer structure negatively. On the other hand, due to less time and low temperatures, the results may be prone to retaining moist.

A general understanding of the evaporation process is that water will quickly evaporate from a thin film of emulsion rather than a thick film and also high temperatures remove more water from the emulsion than low temperatures. At ambient pressure (14.69 psi or 101.325 kPa), the water boiling temperature is around 100°C. The boiling point of water decreases at lower pressure; below 1.885 psi (13 kPa), the boiling point of water goes below 60°C. So it is possible to accelerate the evaporation process or even boil out the water from the emulsion without increasing the temperature, but this only applies in a vacuum. A new method is used in this study based on this assumption. In this method, the sample is prepared according to ASTM D7497, placed inside a vacuum drying oven, and the pressure brought down to 0.072 – 0.725 psi (0.5 – 5 kPa). The temperature was kept at 60°C for all the samples and suction was applied for three hours. Figure 3 shows the vacuum drying oven (Yamato Scientific America, Inc., ADP 200C) setup with the pump used in the study. To identify the polymer network development, a few samples were further dried at 60°C temperature with the same vacuum suction. A major advantage of this method over the others is that it allows the sample to be cured at low

temperatures but ensures high water removal from the emulsion in a significantly reduced time. The system goes to extreme low pressure and all the air is sucked out of the chamber, which is another great advantage of the method: theoretically, there is no chance for the residue to experience any oxidative aging inside the chamber without the presence of any air. This method can produce samples that are not unnecessarily aged, which deviates from the rheological property from the base binder. In this paper, this method is referred as “vacuum drying method.”

Another recovery method used in this study involves outside ambient temperature curing for two days. Currently, this method is not a standard procedure. In this procedure, the sample was prepared following ASTM D7497-09 and then cured outside in an open place without any shade. The curing place was selected as such that it represented the exact field curing condition. The test was conducted during the last week of July. The daily average outside mean temperature was 26°C and humidity was 57 - 59%. It must be noted that it did not rain during the curing period of selected samples. This method is highly dependent on weather (outside temperature, humidity, dust, and wind) and all of these add variability to the test results. Still, this method was followed to understand the field condition of the emulsion residue. In this paper, this method is referred as “field curing method.”

The reason for comparing these residue recovery methods is to understand the effect of emulsifier chemicals, aging, and remaining moisture in the recovery process in order to reduce the duration of curing in the low temperature evaporative method.

Figure 3
Setup for vacuum drying method (vacuum drying oven with pump)

Materials and Experimental Plan

Anionic, cationic, slow setting, rapid setting, polymer modified, latex modified, and neat emulsions along with their unaged bases were tested. Residues were produced following five different recovery methods for six emulsions. In all cases except ASTM D6934 (163°C evaporation method), the sample was prepared in the mat; after the recovery process, it was collected from the mat, kneaded into a ball, and placed in the DSR mold. The ball was placed in the DSR plate and final geometry was given without any reheating. The process of sample preparation is illustrated in Figure 2. For ASTM D6934, the sample was poured on the mat after the recovery process and collected from the mat, as explained earlier. For each sample, the total amount of evaporated water was calculated from the initial and final weight. After that, the temperature sweep test at 58°, 64°, and 70°C was performed using an angular frequency of 10 rad/s and 12% strain. This test was performed on 30 different combinations (six emulsions recovered with five recovery methods). Three replicates of this test for each combination were

performed for each type of emulsion. The same test was done on all the base binders of the emulsions used in the study. To identify the polymer network development as a function of time, the MSCR test was conducted on three emulsions namely CRS-2, CRS-2P, and CRS-2L at three different curing times of 3 hours, 6 hours and 8 hours. The test was done at 58°C at stress levels of 100 Pa and 3200 Pa. The MSCR test is specified in ASTM D7405. For both MSCR and the temperature sweep test, 25-mm parallel plate geometry was used. Summaries of the materials used, recovery process used, and tests conducted for the experimental design are provided in Table 2 and Table 3.

Table 2
Summary of material and testing procedure

<table>
<tr><th>Emulsions[1]</th><th>Rate of Setting</th><th>Modifier</th><th>Emulsion Charge</th><th>Typical Field Application</th><th>Recovery Method</th><th>Temperature Sweep</th></tr>
<tr><td>CRS-2P (E)</td><td>Rapid Setting</td><td>Polymer</td><td>Cationic</td><td>Chip Seal</td><td rowspan="7">ASTM D7497

ASTM D6934

AASHTO TP 72 Method B

Vacuum Drying Method

Field Curing Method</td><td rowspan="7">Temp.: 58°C, 64°C and 70°C

12% Strain, 10 rad/s Angular Frequency

25-mm Parallel Plate Geometry

3 Replicates</td></tr>
<tr><td>CRS-2 (E)</td><td>Rapid Setting</td><td>Neat</td><td>Cationic</td><td>Chip Seal</td></tr>
<tr><td>CRS-2L (A)</td><td>Rapid Setting</td><td>Latex</td><td>Cationic</td><td>Chip Seal</td></tr>
<tr><td>SS-1 (E)</td><td>Slow Setting</td><td>Neat</td><td>Anionic</td><td></td></tr>
<tr><td>SS-1H (B)</td><td>Slow Setting</td><td>Neat</td><td>Anionic</td><td>Tack Coat, Fine - graded mixes, Fog Seal</td></tr>
<tr><td>SS-1L (A)</td><td>Slow Setting</td><td>Latex</td><td>Anionic</td><td></td></tr>
<tr><td colspan="6">CRS-2P (E)Base</td></tr>
<tr><td colspan="6">CRS-2 (E) Base</td></tr>
<tr><td colspan="6">CRS-2L (A) and SS-1L (A) Base</td></tr>
<tr><td colspan="6">SS-1 (E) Base</td></tr>
<tr><td colspan="6">SS-1H (B) Base</td></tr>
</table>

[1]Letter inside parenthesis denotes the source of the emulsion.

Table 3
Experimental plan to identify polymer modification as function of time

Emulsions	Recovery Method	Curing time	Temperature Sweep	MSCR
CRS-2 (E)	ASTM D7497 Vacuum Drying Method	3 hrs, 6 hrs, 8hrs (Vacuum Drying Method) 48 hrs (ASTM D7497)	Temp.: 58°C, 64°C, and 70°C 12% Strain, 10 rad/s Angular Frequency 25-mm Parallel Plate Geometry 2 Replicates	Temperature: 58°C Creep Stress: 100 Pa and 3200 Pa 25-mm Parallel Plate Geometry 2 Replicates
CRS-2P (E)				
CRS-2L (A)				
CRS-2 (E) Base				
CRS-2P (E)Base				
CRS-2L (A) Base				

Materials and Experimental Plan for Rotational Viscosity Tests

Anionic, cationic, slow setting, rapid setting, polymer modified, and latex modified emulsions were tested. From there, three low viscosity emulsions, namely SS-1, SS-1H, and SS-1L and two high viscous emulsions, namely CRS-2 and CRS-2P, were selected for the study. Water content of the emulsions was determined following the evaporation method (ASTM D6934). In this procedure, a 50 g emulsion sample was preweighed in a beaker and was heated in a oven at 163°C (325°F) for two hours, stirred with a glass stick, heated for another one hour, and weighed again. From the difference of the initial and final weight, evaporated water or the water content of the emulsion was calculated.

A rotational viscometer was used to determine the viscosity of the emulsion in the emulsion state. AASHTO T 316-10 was followed to determine the viscosity with some minor modifications in the standard as needed to test the emulsions instead of asphalt binders. Emulsion was taken inside the sample holder and placed inside the thermo cell; the spindle (C 21) was placed inside the sample at the same time. Both the spindle and sample holder were pre heated at test temperature. Ten minutes of temperature equilibration time was given, after which the rotation was started at 20 rpm (round per minute) and 15 minutes were allowed to stabilize the flow. The first reading was taken at 25 minutes starting from the beginning of the experiment and at one minute intervals, two more readings were taken. After the completion of three readings at a certain shear rate, the rpm was stepped up from that position without reducing the rotational speed of the spindle. The speed was increased gradually from 20 to 100 rpm and 20, 30, 50, 60 and 100 rpm was selected for the experiment. After stepping up to a certain rpm, an equilibration time of five minutes was given and readings were taken at one minute intervals from the stepping up point. In

this progression, the experiment was finished at 55th minute from the beginning. Fresh emulsion was taken inside the sample holder from the air tight gallon of the emulsion for every sample; the emulsion was stored in a small tin can for the length of time required to complete one batch. Different batches were run on different days.

Six samples of two batches, each batch containing three samples of each emulsion were tested. One data point of a certain sample, at a certain shear rate, and a certain temperature represents the average of readings. Therefore, at a certain shear rate and certain temperature, there are 18 readings (three readings of two samples of two batches). Two test temperatures of 30°C and 60°C were chosen for 5 different shear rates of 20, 30, 50, 60, and 100 rpm. 60°C temperature was chosen based on the consideration of field application temperature. Normally most of the thermo cell equipped rotational viscometers do not come with a cooling system; therefore, testing below 30°C was not conducted in this research. 30°C test temperature ensures better control over the temperature. A total of ten (2 temperatures by 5 rpm) different test conditions were selected for the study. A summary of the experimental plan is provided in Table 4.

Table 4
Details of experimental plan

Emulsion	Viscosity type	Viscosity test temperature	Shear rate (rpm)	Water content	Time of reading Taken (minute)	Replicates
SS-1	Low Viscous	30°C and 60°C	20,30, 50,60 and 100	ASTM D6934	20 rpm: 25th, 26th and 27th 30 rpm: 32th, 33th and 34th 50 rpm: 39th, 40th and 41th 60 rpm: 46th, 47th and 48th 100 rpm: 53th, 54th and 55th	2 batches. 3 samples for each batch. 6 (2 X 3) samples for each emulsion.
SS-1L	Low Viscous					
SS-1H	Low Viscous					
CRS-2	High Viscous					
CRS-2P	High Viscous					

DISCUSSION OF RESULTS

Strain Sweep Test Results

The average complex modulus (G*) of three samples at initial 2% strain and at final 52% strain are shown in Table 5. The coefficient of variation for three samples is shown in the parenthesis. The drop in complex modulus from initial strain to final strain has been expressed in percent of initial modulus.

The results in Table 5 indicate that in the non-polymer modified and non-hard pen base asphalt emulsions categories, the largest and smallest drops from initial G* at 52°C happens for SS-1 (E) and CRS-2 (B), which are 6.7% and 2.7% respectively. The highest coefficients of variation for the samples at initial 2% strain are for SS-1 (B) and CRS-2 (U), which is 7.8. The lowest coefficient of variation is for SS-1 (U), which is 2.7. Also, the largest and smallest coefficients of variation for the samples at final 52% strain are for CRS-2 (U) and SS-1 (U), which are 11.4 and 1.9 respectively. Regarding 70°C, the largest and smallest drops from initial G* happen for SS-1 (E) and SS-1 (B), which are 3.8% and 0.4% respectively. The largest and smallest coefficients of variation for the samples at initial 2% strain are for CRS-2 (U) and CRS-2 (B), which are 7 and 0.3 respectively. Also, the largest and smallest coefficients of variation for three samples at final 52% strain are for CRS-2 (U) and CRS-2 (B), which are 7 and 0.2 respectively.

The results in Table 5 show that in polymer modified asphalt emulsion category, the largest and smallest drops from initial G* at 52°C happen for SS-1L and CMS-1P, which are 12.9% and 3.4% respectively. The largest and smallest coefficients of variation for the samples at initial 2% strain are for PME and CRS-2P (E), which are 7.5 and 2.2 respectively. Also, the largest and smallest coefficients of variation for the samples at final 52% strain are for CMS-1P and SS-1L, which are 5.7 and 1.3 respectively. Regarding 70°C, the largest and smallest drops from initial G* happen for SS-1L and CMS-1P, which are 16.4% and 1.9% respectively. The largest and smallest coefficients of variation for the samples at initial 2% strain are for CMS-1P and CRS-2P (E), which are 5.8 and 0.7 respectively. Also, the largest and smallest coefficient of variation for the samples at final 52% strain are for CMS-1P and SS-1L, which are 5.6 and 0.6 respectively.

The results in Table 5 show that in non- polymer modified and hard pen base asphalt emulsions category, NTSS-1HM (C), NTSS-1HM (B), and Fog Seal could not reach 52% strain at 52°C. The largest and smallest drops from initial G* at 52°C, happen for NTSS-1HM (U), and SS-1H (U), which are 44.2% and 15% respectively. Regarding 70°C, the largest and smallest drops from initial G* happen for NTSS-1HM (B) and SS-1H (U), which are 43.3% and 1.2% respectively.

The largest and smallest coefficients of variation for the samples at initial 2% strain are for Fog Seal and SS-1H (B), which are 10.4 and 5.1 respectively. Also, the largest and smallest coefficients of variation for the samples at final 52% strain are for NTSS-1HM (B) and SS-1H (B), which are 17.8 and 4.5 respectively.

The results in Table 5 indicate that in polymer modified and hard pen base asphalt emulsions category, the drop from initial G* of CSS-1HP is higher than SS-1HP at 52°C and 70°C. Also, the coefficient of variation for 3 samples of CSS-1HP is higher than SS-1HP at initial 2% and final 52% at both mentioned temperatures.

The maximum coefficient of variation obtained at 52°C is 15.0% and at 70°C is 17.8%, respectively for fog seal and NTSS-1HM (B). Both of these emulsions are prepared of hard pen base asphalt (denoted by 'H' in the emulsion name) and in most of the cases all of the emulsions prepared of hard pen base asphalt exhibited relatively higher coefficient of variation. The coefficients of variation of all the emulsions without hard pen base asphalt are relatively much lower.

Previous studies concluded that higher stiffness and strain tolerance relate to lower aggregate loss in chip seal as measured by the ASTM D7000 sweep test in the laboratory. In this study, strain tolerance was evaluated by the drop in complex modulus from initial complex modulus and was expressed in percent of initial modulus. It was observed that emulsions prepared of hard pen base asphalt have relatively lower strain tolerance, i.e. relatively higher drop from initial complex modulus. At 52°C, the complex modulus at 2% strain dropped 44.2% at 52% strain in case of NTSS-1HM (U) and dropped 22.5% in case of CSS-1HP both of which are prepared of hard pen base asphalt. NTSS-1HM (B) and NTSS-1HM (C) could not reach 52% strain at 52°C. At 70°C, the worst two drops were 43.3% and 34.8%, respectively by NTSS-1HM (B) and fog seal which also contains hard asphalt. The strain tolerances of all the emulsions without hard pen base asphalt are relatively much higher, i.e. relatively lower drop from initial complex modulus except SS-1L at 52°C.

Table 5
Strain tolerance of emulsion residues

Emulsion	52°C			70°C		
	G* at 2% Strain, Pa (CoV, %)	G* at 52% Strain, Pa (CoV, %)	Drop from Initial G*, %	G* at 2% Strain, Pa (CoV, %)	G* at 52% Strain, Pa (CoV, %)	Drop from Initial G*, %
SS-1 (E)	4829.0	4507.0	6.7	472.8	455.0	3.8
	(3.2)	(2.3)		(4.4)	(2.8)	
SS-1 (B)	4845.3	4682.7	3.4	461.9	460.2	0.4
	(7.8)	(7.6)		(4.6)	(4.7)	
SS-1 (U)	3504.7	3342.3	4.6	379.6	376.4	0.8
	(2.7)	(1.9)		(2.2)	(1.6)	
SS-1H (B)	20676.7	17503.3	15.3	1877.7	1835.0	2.3
	(7.0)	(4.9)		(5.1)	(4.5)	
SS-1H (U)	21336.7	18133.3	15.0	1800.7	1779.0	1.2
	(5.7)	(4.4)		(6.5)	(6.1)	
SS-1HP	11376.7	10283.0	9.6	1362.3	1311.3	3.7
	(7.3)	(8.1)		(7.0)	(7.5)	
SS-1L	6530.0	5686.7	12.9	1083.0	905.5	16.4
	(3.0)	(1.3)		(0.9)	(0.6)	
CRS-2 (E)	4483.3	4297.7	4.1	408.2	405.6	0.6
	(6.5)	(6.0)		(4.8)	(4.8)	
CRS-2 (B)	4200.3	4088.3	2.7	407.6	404.7	0.7
	(3.5)	(3.2)		(0.3)	(0.2)	
CRS-2 (U)	3326.5	3183.5	4.3	360.9	359.1	0.5
	(7.8)	(11.4)		(7.0)	(7.0)	
CRS-2P (E)	7673.0	7101.3	7.5	926.6	892.5	3.7
	(2.2)	(3.0)		(0.7)	(1.1)	
CRS-2P (B)	6405.0	6183.3	3.5	685.5	669.7	2.3
	(4.8)	(4.5)		(4.0)	(3.3)	
CHFRS-2P	10253.3	9603.7	6.3	1449.0	1403.7	3.1
	(3.4)	(3.2)		(3.6)	(3.4)	
CMS-1P	3386.7	3271.3	3.4	383.8	376.6	1.9
	(6.0)	(5.7)		(5.8)	(5.6)	
CSS-1HP	40173.3	31126.7	22.5	4880.3	4515.3	7.5
	(9.7)	(8.8)		(8.1)	(8.2)	
PME	7536.3	6877.0	8.7	986.9	943.4	4.4
	(7.5)	(3.8)		(3.1)	(3.1)	
NTSS-1HM (B)	789100.0	Could Not Reach 52% Strain		61770.0	35003.3	43.3
	(10.6)			(10.3)	(17.8)	
NTSS-1HM (C)	511300.0	Could Not Reach 52% Strain		31320.0	23953.3	23.5
	(12.6)			(8.4)	(15.6)	
NTSS-1HM (U)	98940.0	55180.0	44.2	6291.5	6062.5	3.6
	(0.1)	(1.6)		(9.1)	(7.7)	
Fog Seal	615550.0	Could Not Reach 52% Strain		44446.7	28990.0	34.8
	(15.0)			(10.4)	(11.5)	

Frequency Sweep Test Results

One advantage of master curve is that it can be used to find the complex modulus in a wide range of frequency values at a constant temperature. Frequency sweep tests were performed to draw different master curves using time-temperature superposition principle for overall understanding of the rheological behavior.

Figures 4 and 5 show the complex modulus master curves constructed at 25°C. Typically, the complex modulus of emulsion residue increases with decreasing temperature and increasing frequency. By shifting the complex modulus-frequency relationship for various temperatures horizontally with respect to a chosen reference temperature, a complete complex modulus-frequency behavior curve was assembled and a polynomial equation was developed. The minimum R^2 obtained in polynomial fitting of the three tack coats (NTSS-1HM) and single fog seal emulsion residues is 0.956 while the minimum R^2 obtained for rest of the 16 emulsion residues is 0.9903.

Figure 4 shows that two tack coats (NTSS-1HM (U) and NTSS-1HM (C)) and the fog seal emulsion residues exhibit a relatively high complex modulus. SS-1H (B) and SS-1H (U) also show a relatively high complex modulus. It is to be noted here that all these are produced by hard pen base asphalt. Similarly in Figure 5, NTSS-1HM (B) and CSS-1HP exhibit a relatively high complex modulus because of the presence of the hard base asphalt. SS-1 (U) in Figure 4 and CRS-2 (U) in Figure 5 exhibit relatively lower stiffness. Overall, the 20 emulsion residues show significant differences in complex modulus at lower frequencies (or higher temperatures) but they all tend to approach towards one glassy modulus as previously obtained for SHRP core asphalt cements.

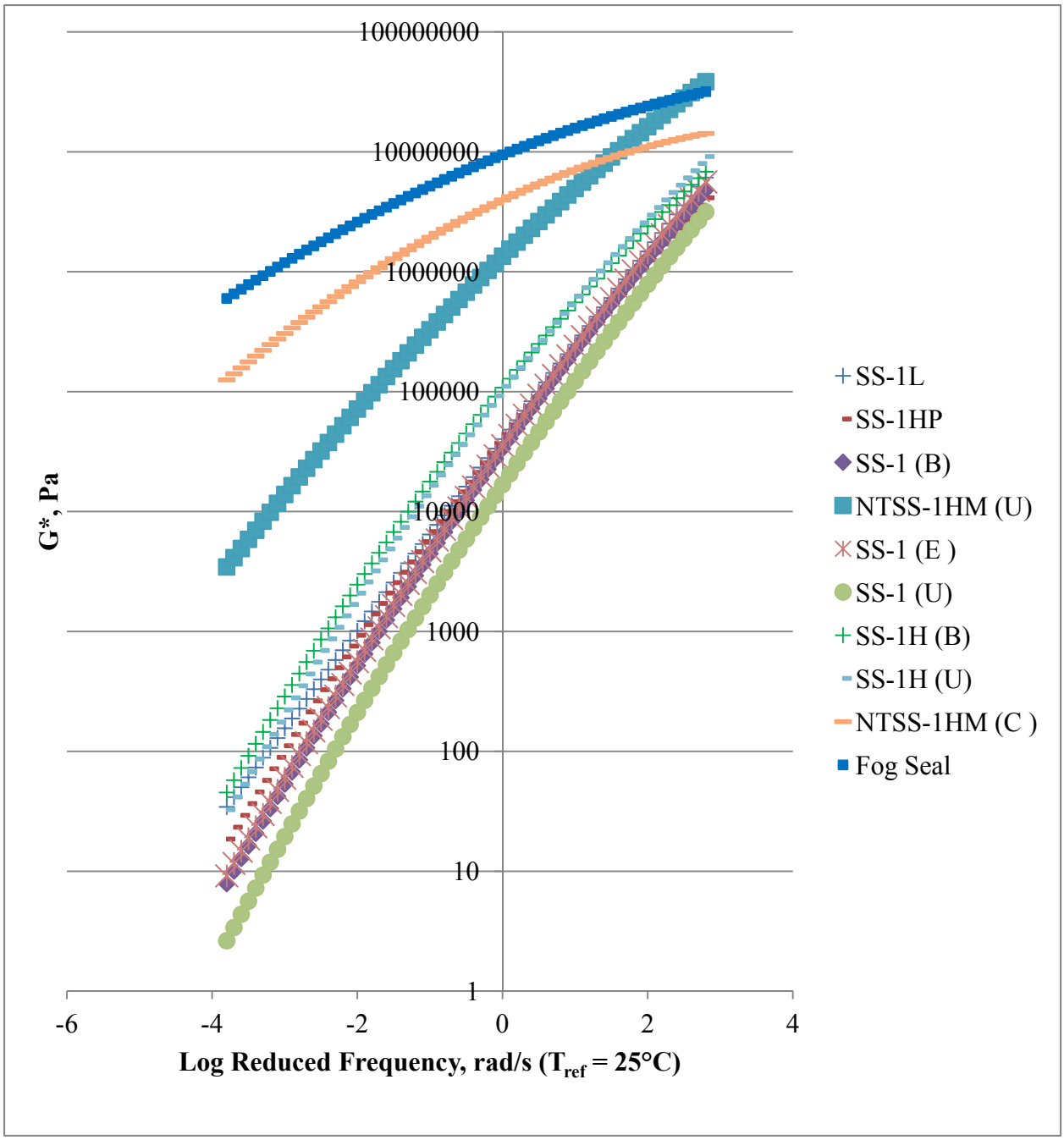

Figure 4
Complex modulus master curves at 25°C (part 1 of 2)

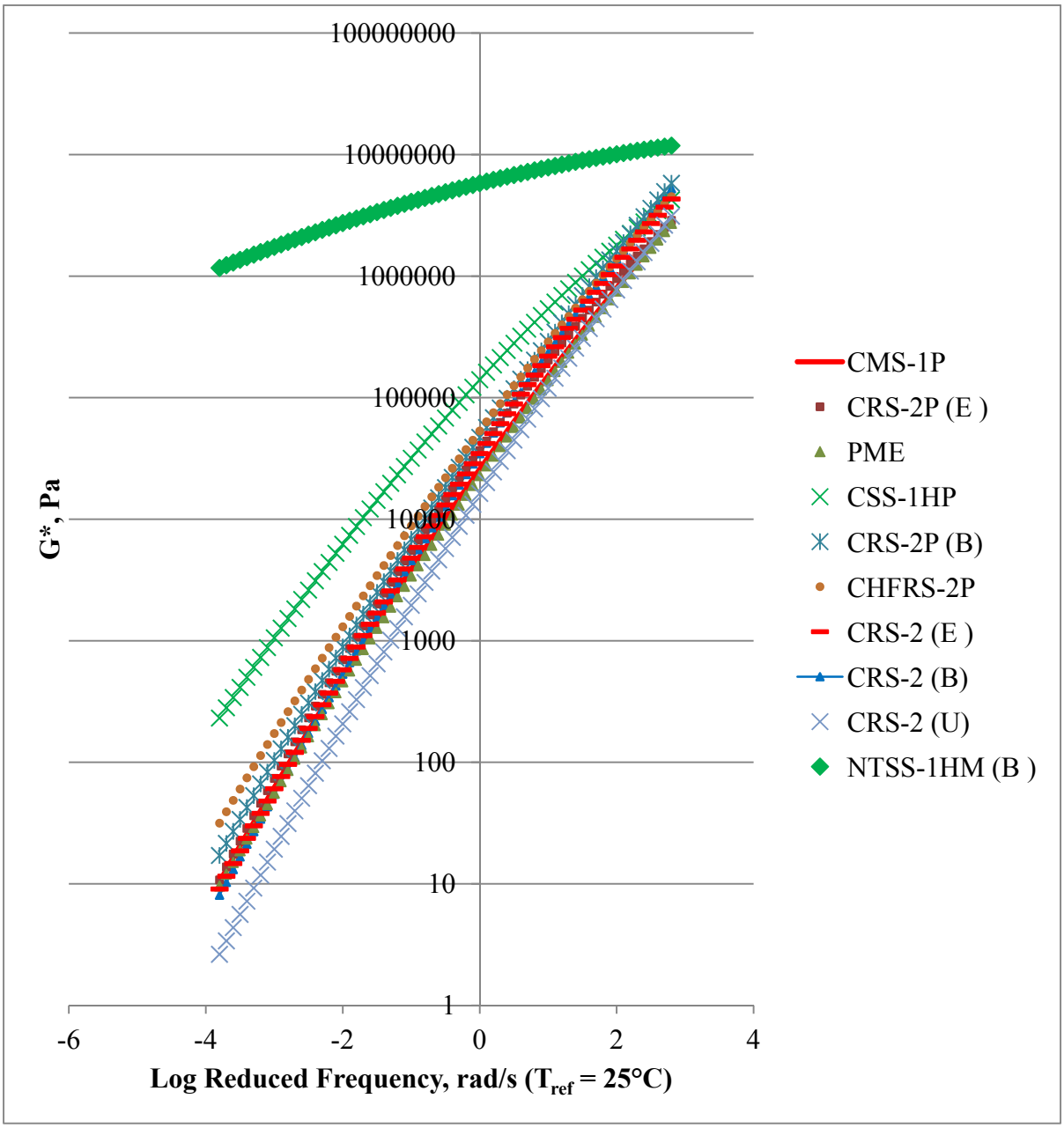

Figure 5
Complex modulus master curves at 25°C (part 2 of 2)

Temperature Sweep Test Results

In conducting temperature sweep tests of the DSR from 52°C to 94°C at 6°C intervals on asphalt emulsion residues, a common trend for phase angle (δ) was obvious, in that there is an increase, and then a decrease in phase angle while temperature increases. This trend happened for all

emulsion residues in three categories, including polymer modified asphalt emulsions, non-polymer modified, and non-hard pen base asphalt emulsions, and polymer modified and hard pen base asphalt emulsions. Also, it should be mentioned that in hard pen base asphalt emulsions, the trend happened only for SS-1H (B), SS-1H (U), NTSS-1HM (B) and NTSS-1HM (C); for NTSS-1HM (U) and Fog Seal, there was just an increase in phase angle while temperature increased. Figure 6 shows G*/sinδ values from 52°C to 94°C at 6°C intervals. It can be observed that the emulsions made of hard pen asphalts namely, CSS-1HP, SS-1H (U), SS-1H (B), SS-1HP, NTSS-1HM (U), NTSS-1HM (C), NTSS-1HM (B), and Fog Seal have higher G*/sinδ values than all other emulsion residues. Stiffness of some hard pen base emulsions could not be measured at lower temperature.

Hanz et al. reported that oxidative aging contributes significantly to the discrepancy between emulsion residue properties and asphalt base materials [*19*]. They found that the ASTM D7497 evaporative recovery method produced residues with rheological properties similar to those of oven-cured or RTFO-aged base materials. Therefore, in this study, temperature at 2.2 kPa stiffness (G*/sinδ) for each emulsion residue was determined and was used as a reference temperature for equal stiffness.

Figure 7 shows that as temperature increases, the phase angle of an emulsion residue increases, reaches a maximum, and then decreases. It was observed that the maximum phase angle of all the non-hard pen polymer modified asphalt emulsion residue falls between 75° to 85°. The maximum phase angles of hard pen polymer modified asphalt emulsions, SS-1HP and CSS-1HP are above 85° and below 75°, respectively. Therefore, a maximum phase angle in the range of 75° to 85° may be used as a criterion for polymer identification as observed from the 20 emulsions tested in this study.

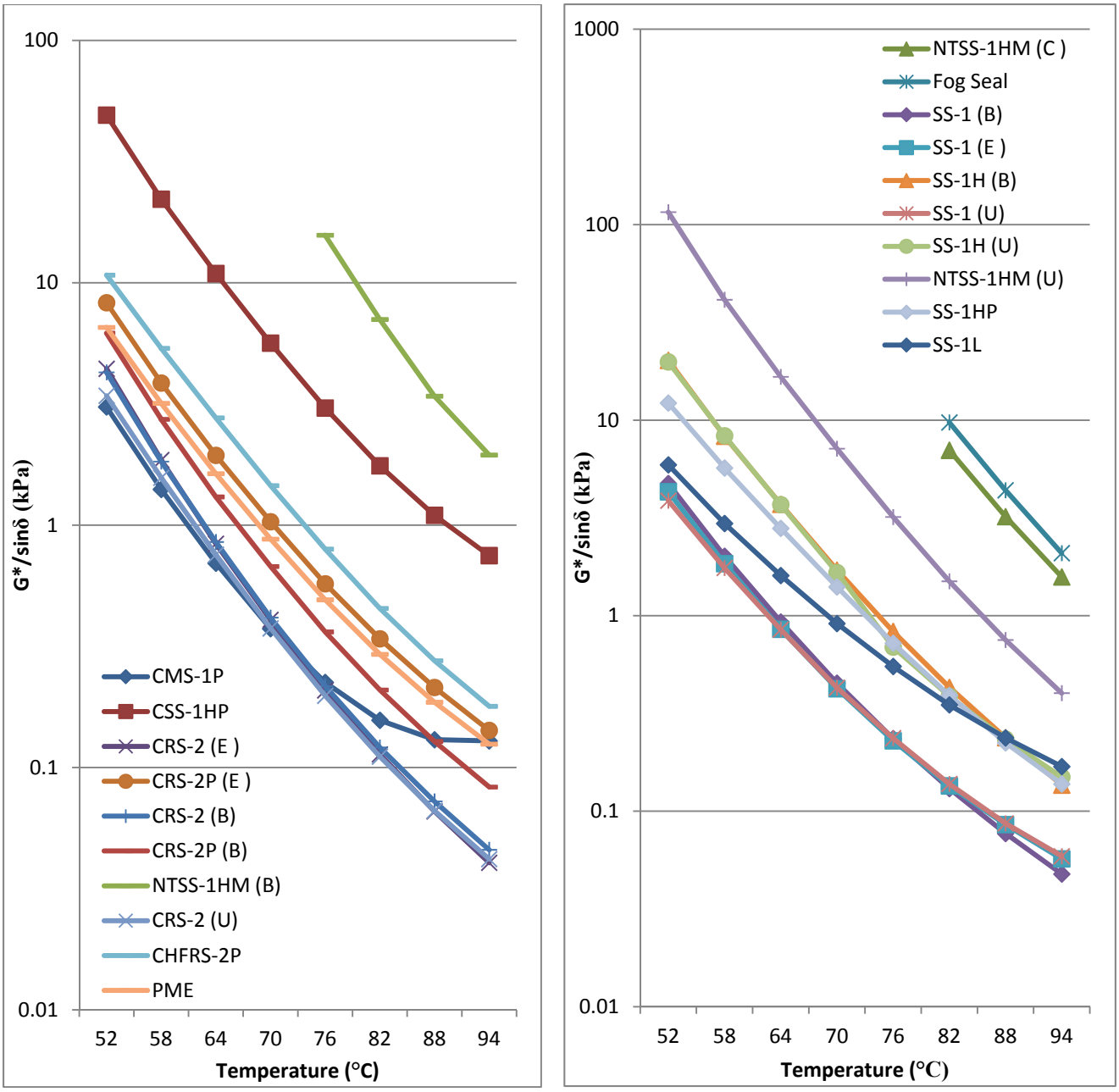

Figure 6
G*/sinδ values at temperature ranges from 52°C to 94°C

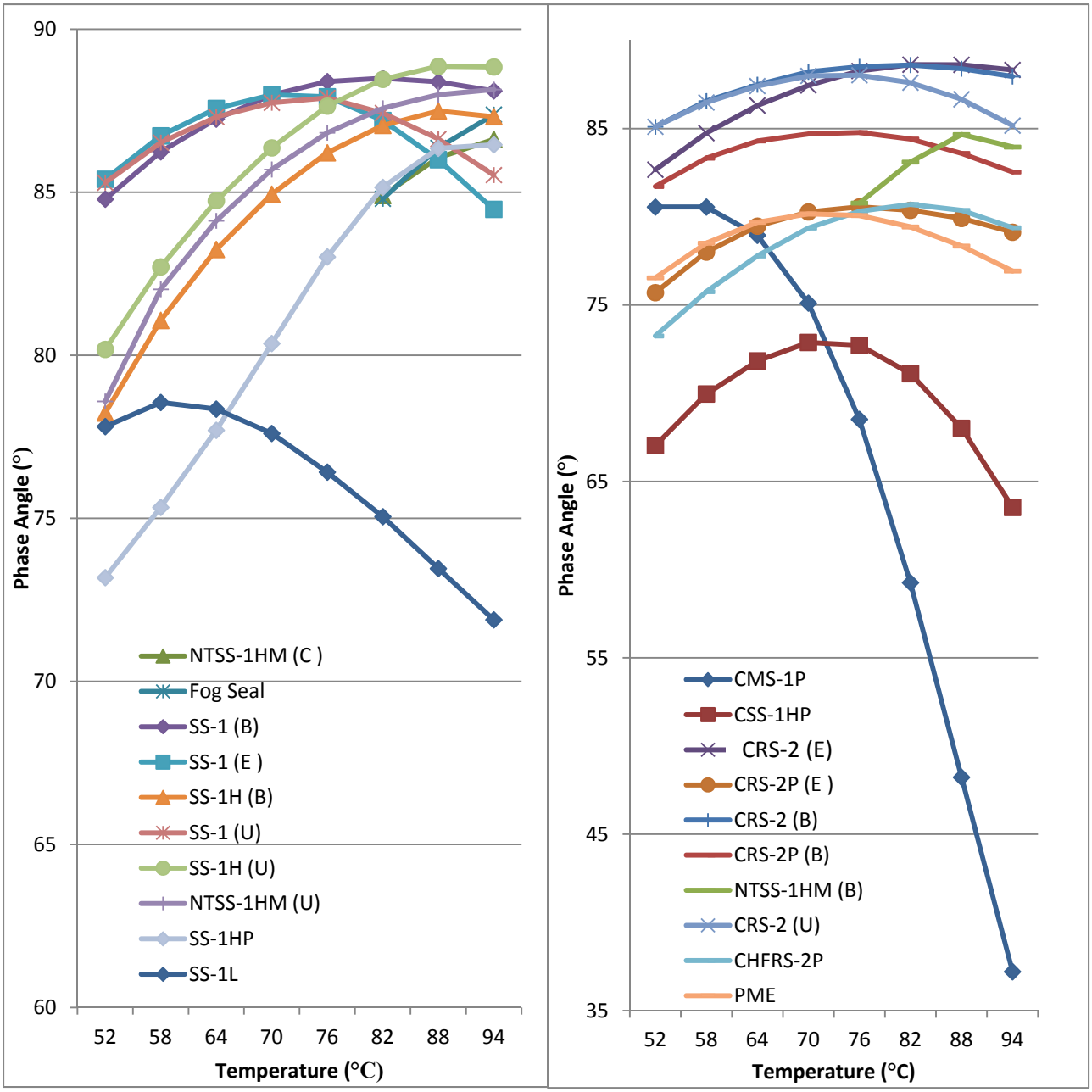

Figure 7
Phase angles at temperatures ranges from 52°C to 94°C

Elastic Recovery Test (AASHTO T301) Results

Emulsion residues were heated at 150°C for 30 min to prepare elastic recovery samples except some hard pen emulsion residues that were heated at 160°C for 30 min. Table 6 shows the elastic recovery (%) of two samples at 10°C and two samples at 25°C. NTSS-1HM (U), NTSS-1HM (C),

NTSS-1HM (B) and fog seal did not produce any results as the samples broke during elongation.

Table 6 presents results in four categories: polymer modified emulsions, polymer modified and hard pen base emulsions, non-polymer modified and non-hard pen base emulsions, hard pen base emulsions.

At 10°C, the maximum elastic recovery is 11.25% for non-polymer modified and non-hard pen base emulsions while the minimum elastic recovery is 36.25% for polymer modified emulsions. Similarly at 25°C, the maximum elastic recovery is 18.5% for non-polymer modified and non-hard pen base emulsions while the minimum elastic recovery is 50% for polymer modified emulsions. This justifies the use of elastic recovery test for polymer identification. It is to be noted here that polymer modified hard pen asphalt emulsions have lower elastic recovery than polymer modified asphalt emulsions at 25°C.

Multiple Stress Creep and Recovery (MSCR) Test Results

Table 7 shows the average percent recovery at 10°C, 25°C, 58°C and 70°C. A general trend is that as temperature increases, percent recovery decreases. All non-polymer modified non-hard pen base emulsions follow the trend. For example, the average percent recoveries of CRS-2 (B) at 0.1 kPa creep stress are 55.5, 37.9, 7.7 and 0.6, respectively at 10°C, 25°C, 58°C, and 70°C. However, very few polymer modified emulsions tend to deviate from this trend. For example, the average percent recoveries of CHFRS-2P at 0.1 kPa creep stress are 72.7, 67.5, 36.8, and 38.1 respectively at 10°C, 25°C, 58°C, 70°C.

It can be observed that at high temperature and/or high creep stress i.e., 3.2 kPa, some asphalt emulsions show negative percent recovery values. Creep and recovery curves for these emulsions indicate that just after the 3.2 kPa creep stress is withdrawn, strain continues to grow for a while before it starts recovering. Therefore, these negative values are actual and not due to error. However, some hard pen asphalt emulsions, namely, NTSS-1HM (U), NTSS-1HM (C), NTSS-1HM (B) and Fog Seal, show erratic behavior at 10°C and 25°C and percent recovery values of 100 or higher were reported.

Table 6
Elastic recovery test (AASHTO T301) results

Emulsions	Elastic Recovery (%)			
	10°C		25°C	
Polymer Modified Emulsions				
PME	52.5	52.75	50	50
CHFRS-2P	51.875	52.5	64.375	65
CRS-2P (E)	36.25	48.75	73.75	75
CMS-1P	58.75	55	87.5	84.5
CRS-2P (B)	36.25	37	53	53.75
SS-1L	61.25	62.5	63.75	66.25
Polymer Modified and Hard Pen Base Asphalt Emulsions				
SS-1HP	53.75	54.375	29.5	32.5
CSS-1HP	23.75	*	38.75	40
Non-Polymer Modified and Non-Hard Pen Base Asphalt Emulsions				
CRS-2 (E)	10	10	7.5	18.5
CRS-2 (B)	9.25	8.75	16	13.75
SS-1 (B)	2.5	1.25	15	13.75
SS-1 (E)	8.75	8.75	6.25	10
CRS-2 (U)	2.5	1.25	6.25	5
SS-1 (U)	10	11.25	5	4.5
Hard Pen Base Asphalt Emulsions				
SS-1H (B)	10	11.25	12.5	11.25
SS-1H (U)	8.75	8.75	5	3.75
NTSS-1HM (U)	Samples Broke During Elongation			
NTSS-1HM (C)				
Fog Seal				
NTSS-1HM (B)				

*One sample got damaged. Therefore, only one sample was tested for CSS-1HP at 10°C.

Table 7 clearly demonstrates that at temperatures 58°C and 70°C and at creep stress of 0.1 kPa, the average percent recovery values of polymer modified asphalt emulsions are significantly higher than those of non-polymer modified and non-hard pen asphalt binders. In the case of 58°C and 0.1 kPa creep stress, the maximum average percent recovery is 7.7 for non-polymer modified and non-hard pen base asphalt emulsions while the minimum average percent recovery is 25.9 for polymer modified emulsions. For 70°C and 0.1 kPa creep stress, the maximum average percent recovery is 0.6 for non-polymer modified and non-hard pen base asphalt emulsions while the minimum average percent recovery is 21.7 for polymer modified emulsions. Similar observations can be made for 3.2 kPa creep stress at 58°C.

Table 7
Average percent recoveries (MSCR) at different temperatures

Emulsions	Percent Recovery (MSCR)							
	Creep Stress 0.1 kPa				Creep Stress 3.2 kPa			
	10°C	25°C	58°C	70°C	10°C	25°C	58°C	70°C
Polymer Modified Emulsions								
CMS-1P	58.8	46.9	35.1	29.0	57.8	45.1	12.6	-1.9
CRS-2P (B)	60.2	48.1	25.9	21.7	58.1	46.2	9.8	0.9
CRS-2P (E)	76.0	63.0	29.7	30.3	65.9	62.7	9.5	2.2
SS-1L	66.7	58.2	53.1	35.6	62.9	56.8	13.9	0.7
PME	79.5	60.0	36.0	32.0	67.4	60.0	12.2	0.4
CHFRS-2P	72.7	67.5	36.8	38.1	72.8	67.4	17.1	5.2
Polymer Modified and Hard Pen Base Asphalt Emulsions								
CSS-1HP	99.9	81.4	56.7	76.3	73.3	76.9	36.2	10.4
SS-1HP	75.9	68.7	24.1	8.7	73.2	68.7	12.9	1.3
Non-Polymer Modified and Non-Hard Pen Base Asphalt Emulsions								
SS-1 (B)	66.1	44.2	3.7	-1.8	66.1	43.4	0.0	-2.7
SS-1 (E)	66.1	39.8	4.9	-1.1	67.4	37.6	-0.1	-2.6
SS-1 (U)	54.4	41.1	5.4	-0.1	52.8	38.5	-0.1	-2.7
CRS-2 (U)	51.1	34.9	2.9	-1.9	51.7	38.5	-0.2	-2.9
CRS-2 (B)	55.5	37.9	7.7	0.6	52.4	37.3	0.2	-2.6
CRS-2 (E)	59.9	49.0	7.1	0.5	63.1	51.0	0.4	-2.6
Hard Pen Base Asphalt Emulsions								
SS-1H (U)	72.1	59.0	6.5	2.4	73.5	58.5	3.4	-0.1
SS-1H (B)	96.6	63.4	11.6	4.0	80.7	63.6	5.3	0.2
NTSS-1HM (U)	≥100	67.5	12.8	8.8	90.0	68.9	9.7	1.6
NTSS-1HM (C)	≥100	≥100	25.8	13.5	≥100	72.1	24.2	10.2
NTSS-1HM (B)	≥100	≥100	39.7	33.0	≥100	≥100	45.1	28.1
FOG SEAL	≥100	≥100	27.0	14.3	96.9	≥100	26.8	12.1

The MSCR test was also performed at 2.2 kPa stiffness (G*/sinδ) temperatures. Table 8 shows the 2.2 kPa stiffness temperatures for 20 emulsions. It also shows average percent recovery values at 2.2 kPa stiffness temperatures for four different creep stresses: 0.1 kPa, 0.2 kPa, 0.5 kPa, and 3.2 kPa.

At 0.1 kPa creep stress, the maximum average percent recovery is 8.7 for non-polymer modified and non-hard pen base emulsions while the minimum average percent recovery is 16.5 for polymer modified emulsions. Similarly, at 0.2 kPa creep stress, the maximum average percent recovery is 6.0 for non-polymer modified and non-hard pen base emulsions while the minimum average percent recovery is 19.0 for polymer modified emulsions. At 0.5 kPa creep stress, the maximum average percent recovery is 3.4 for non-polymer modified and non-hard pen base emulsions while the minimum average percent recovery is 13.1 for polymer modified emulsions.

Therefore, higher percent recovery values of MSCR indicate the presence of polymer and MSCR percent recovery may be correlated with elastic recovery of AASHTO T301.

Table 8
Average percent recovery (MSCR) at various creep stresses and at 2.2 kPa stiffness temperature

Emulsions	2.2 kPa Stiffness (G*/sinδ) Temperatures °C)	Creep Stresses (kPa)				R^2 Value for Log(stress) vs. Percent Recovery
		0.1	0.2	0.5	3.2	
Polymer Modified Emulsions						
CRS-2P (E)	63°C	27.5	24.6	13.9	1.5	0.98
SS-1L	61°C	60.6	55.4	38.8	7.4	0.99
CHFRS-2P	67°C	34.3	29.8	18.6	2.2	0.99
CMS-1P	55°C	43.0	45.6	37.5	23.3	0.91
CRS-2P (B)	59°C	16.5	19.0	13.1	3.7	0.88
PME	62°C	44.2	39.7	26.1	4.1	0.99
Polymer Modified and Hard Pen Base Asphalt Emulsions						
CSS-1HP	80°C	92.2	86.7	47.5	1.1	0.98
SS-1HP	66°C	11.4	8.7	5.5	0.8	0.99
Non-Polymer Modified and Non Hard Pen Base Asphalt Emulsions						
CRS-2 (U)	56°C	6.2	4.1	1.9	-0.3	0.95
CRS-2 (B)	57°C	7.7	6.0	3.4	0.0	0.99
CRS-2 (E)	57°C	5.7	3.9	2.0	-0.2	0.96
SS-1 (U)	57°C	8.4	5.7	2.5	-0.3	0.95
SS-1 (B)	57°C	5.9	5.8	3.2	0.5	0.96
SS-1 (E)	57°C	8.7	6.0	2.6	-0.3	0.94
Hard Pen Base Asphalt Emulsions						
SS-1H (U)	68°C	4.2	2.8	1.2	-0.3	0.95
SS-1H (B)	68°C	10.7	7.6	3.6	0.0	0.95
Fog Seal	94°C	8.6	6.4	3.2	0.2	0.96
NTSS-1HM (U)	79°C	13.3	9.2	3.8	-0.4	0.94
NTSS-1HM (B)	96°C	21.1	15.7	7.5	0.3	0.96
NTSS-1HM (C)	90°C	15.7	12.3	6.8	0.6	0.98

A general trend observed from Table 8 is that as the creep stress increases the percent recovery decreases. In this study, it was observed that the effect of creep stress on percent recovery is logarithmic. Table 8 also shows the coefficient of determination (R^2) values for logarithmic relationships for all the emulsions.

In summary, all the emulsions show R^2 values of higher than 0.9 except for CRS-2P (B) in which case the R^2 value is 0.88. Similar trends were reported by Mathy Technology and Engineering Services, Inc. for PG binders [*20*].

Four-Element Burgers Model

In this study, a four-element Burgers model (i.e., a Kelvin model and a Maxwell model in series) was used to fit the data of the first cycle as previously used by Bahia et al. for polymer modified asphalt binders [*21*]. Table 9 shows the average values of Maxwell elastic modulus (G0), Maxwell viscosity (η_0), relaxation time (T_0), Kelvin elastic modulus (G_1), Kelvin viscosity (η_1) and retardation time (T_1) obtained for 0.1 kPa creep stress and recovery at 2.2 kPa stiffness temperatures of all emulsion residues. These models can be used to predict material behavior in repetitive cycles. The R^2 values obtained between model creep and recovery of first cycle and actual creep and recovery are more than 0.9 for all the emulsions. It can be observed that average η_0 values of polymer modified emulsions are higher than those of non-polymer modified and non-hard pen base asphalt emulsions. In contrast, the average η_1 values of polymer modified emulsions are significantly lower than those of non-polymer modified and non-hard pen base asphalt emulsions.

Correlation between MSCR Parameters and Elastic Recovery (AASHTO T301)

Out of the 20 emulsions tested in this study, eight were hard pen base asphalt emulsions, of which four hard pen base asphalt emulsions did not produce any elastic recovery (the sample failed in AASHTO T301) values to correlate with MSCR parameters. The remaining four hard pen base asphalt emulsions sometimes behaved inconsistently as discussed during their rheological investigation. Therefore, in this study, 12 emulsions (6 polymer modified and 6 non-polymer modified and non-hard pen asphalt emulsions) were considered for correlation with elastic recovery (AASHTO T301).

Table 10 shows coefficient of determination (R^2) values of a linear correlation between non-recoverable creep compliance (J_{nr}) and elastic recovery (AASHTO T301). It can be observed that the best relationship can be obtained between a MSCR temperature of 58°C and an elastic recovery temperature (AASHTO T301) of 10°C. For this best scenario, R^2 values for 0.1 kPa and 3.2 kPa creep stresses are 0.737 and 0.604, respectively.

Table 9
A four-element Burgers model parameters of emulsion residues

Emulsions	Go, GPa	η_o, Pa.s	T_o, s	G_1, Pa	η_1, Pa.s	T_1, s	Correlation between Actual vs. Model Creep and Recovery Data of 1st Cycle
Polymer Modified Emulsions							
CHFRS-2P	1	223	4519400	238	496	2.1	R^2>0.9
CMS-1P	1	537	1862367	514	1016	2.0	
CRS-2P (B)	1	258	3881350	572	1188	2.1	
CRS-2P (E)	1	225	4451700	331	519	1.6	
PME	1	249	4012350	180	387	2.2	
SS-1L	1	595	1684233	282	481	1.7	
Polymer Modified and Hard Pen Base Asphalt Emulsions							
CSS-1HP	1	2243	448255	271	272	1.0	R^2>0.9
SS-1HP	1	146	6826300	707	786	1.1	
Non-Polymer Modified and Non-Hard Pen Base Asphalt Emulsions							
CRS-2 (U)	1	145	6884800	707	2123	3.0	R^2>0.9
CRS-2 (B)	1	218	4578467	1108	2690	2.4	
CRS-2 (E)	1	142	7044267	1141	2052	1.9	
SS-1 (U)	1	172	5839500	696	1837	2.6	
SS-1 (B)	1	197	5078600	975	2223	2.3	
SS-1 (E)	1	176	5722733	788	1840	2.4	
Hard Pen Base Asphalt Emulsions							
SS-1H (U)	1	163	6129050	954	2789	2.9	R^2>0.9
SS-1H (B)	1	172	5826300	692	1521	2.2	
Fog Seal	1	235	4251833	1165	2675	2.3	
NTSS-1HM (U)	1	203	4928200	556	1274	2.3	
NTSS-1HM (B)	1	208	4817150	404	948	2.3	
NTSS-1HM (C)	1	330	3033550	845	1852	2.2	

Table 10
Correlation between MSCR parameters and elastic recovery (AASHTO T301)

Coefficient of Determination (R^2) for Linear Correlation Between **Percent Recovery** (MSCR) and Elastic Recovery (AASHTO T301)			
MSCR Temperature	MSCR Creep Stress	Elastic Recovery Temperature (AASHT T301)	
		10°C	25°C
58°C	0.1 kPa	0.961	0.798
	3.2 kPa	0.938	0.843
70°C	0.1 kPa	0.957	0.872
	3.2 kPa	0.516	0.493
2.2 kPa Stiffness Temperature	0.1 kPa	0.908	0.692
	3.2 kPa	0.409	0.487
Coefficient of Determination (R^2) for Linear Correlation Between **Non-Recoverable Creep Compliance, J_{nr} (**MSCR) and Elastic Recovery (AASHTO T301)			
MSCR Temperature	MSCR Creep Stress	Elastic Recovery Temperature (AASHTO T301)	
		10°C	25°C
58°C	0.1 kPa	0.737	0.623
	3.2 kPa	0.604	0.472
70°C	0.1 kPa	0.169	0.696
	3.2 kPa	0.502	0.391
2.2 kPa Stiffness Temperature	0.1 kPa	0.734	0.682
	3.2 kPa	0.078	0.139

Table 10 also shows coefficient of determination (R^2) values of linear correlation between percent recovery (MSCR) and elastic recovery (AASHTO T301). Overall it can be concluded that the coefficient of determination values of linear correlation between percent recovery (MSCR) and elastic recovery (AASHTO T301) are significantly higher than coefficient of determination values between non-recoverable creep compliance and elastic recovery (AASHTO T301). Also, a 10°C elastic recovery temperature produces better correlation with MSCR parameters than a 25°C elastic recovery temperature.

It can be observed that the highest coefficient of determination of linear correlation was obtained between MSCR percent recovery at a temperature of 58°C and elastic recovery at a temperature (AASHTO T301) of 10°C. For this strongest relationship, R^2 values for 0.1 kPa and 3.2 kPa creep stresses are 0.961 and 0.938, respectively.

Figures 8 and 9 graphically demonstrate that percent recovery (MSCR) can be used to detect polymer modification instead of elastic recovery (AASHTO T301). Figure 8 shows that at 58°C, both 0.1kPa and 3.2kPa creep stresses can distinguish polymer modified emulsions from non-polymer modified and non-hard pen base asphalt emulsions. Figure 9 shows that 0.1kPa creep stress can be used to detect polymer modifications at 70°C and 2.2 kPa stiffness temperature.

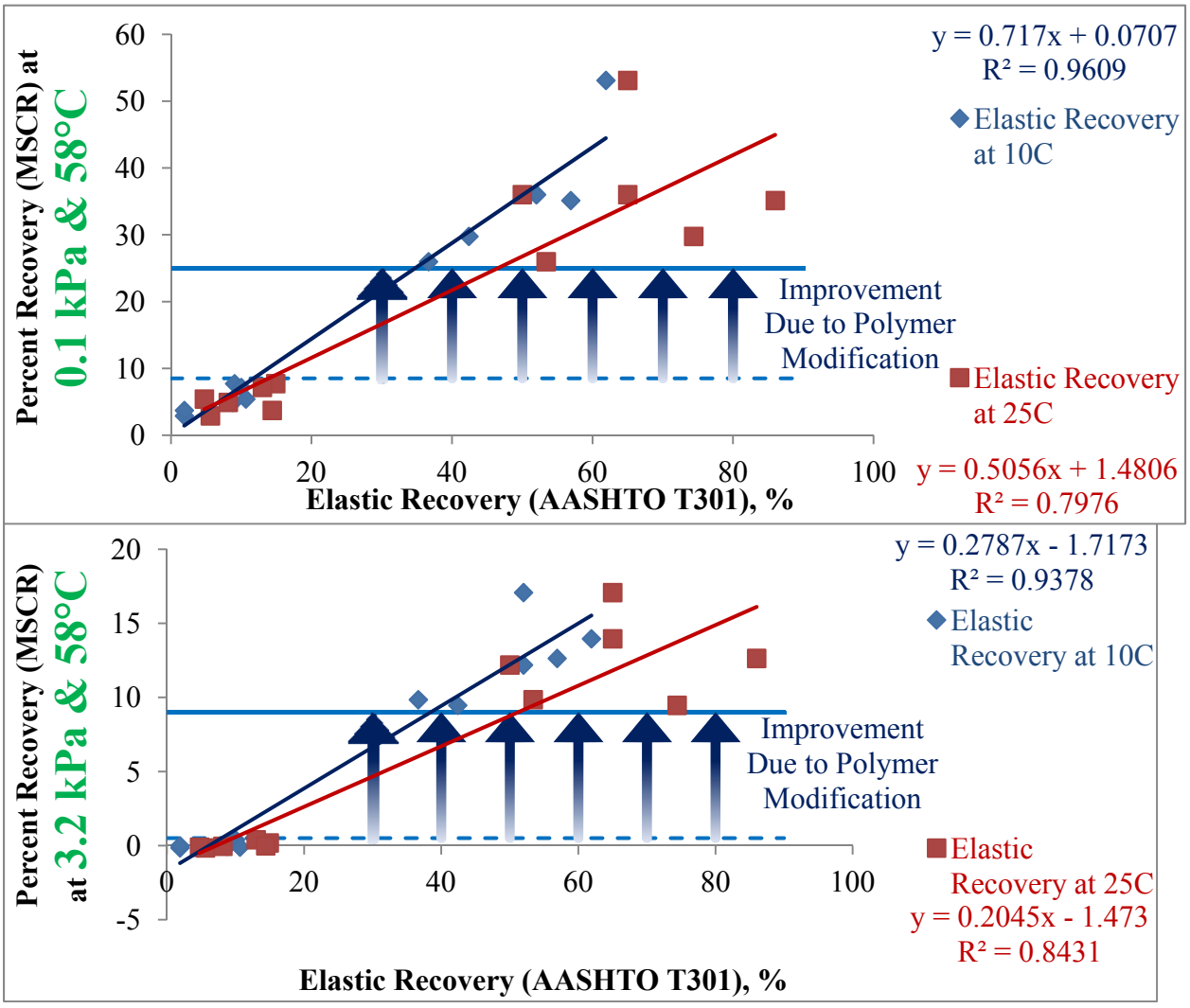

Figure 8
Linear correlation between percent recovery (MSCR at 58°C) and elastic recovery (AASHTO T301)

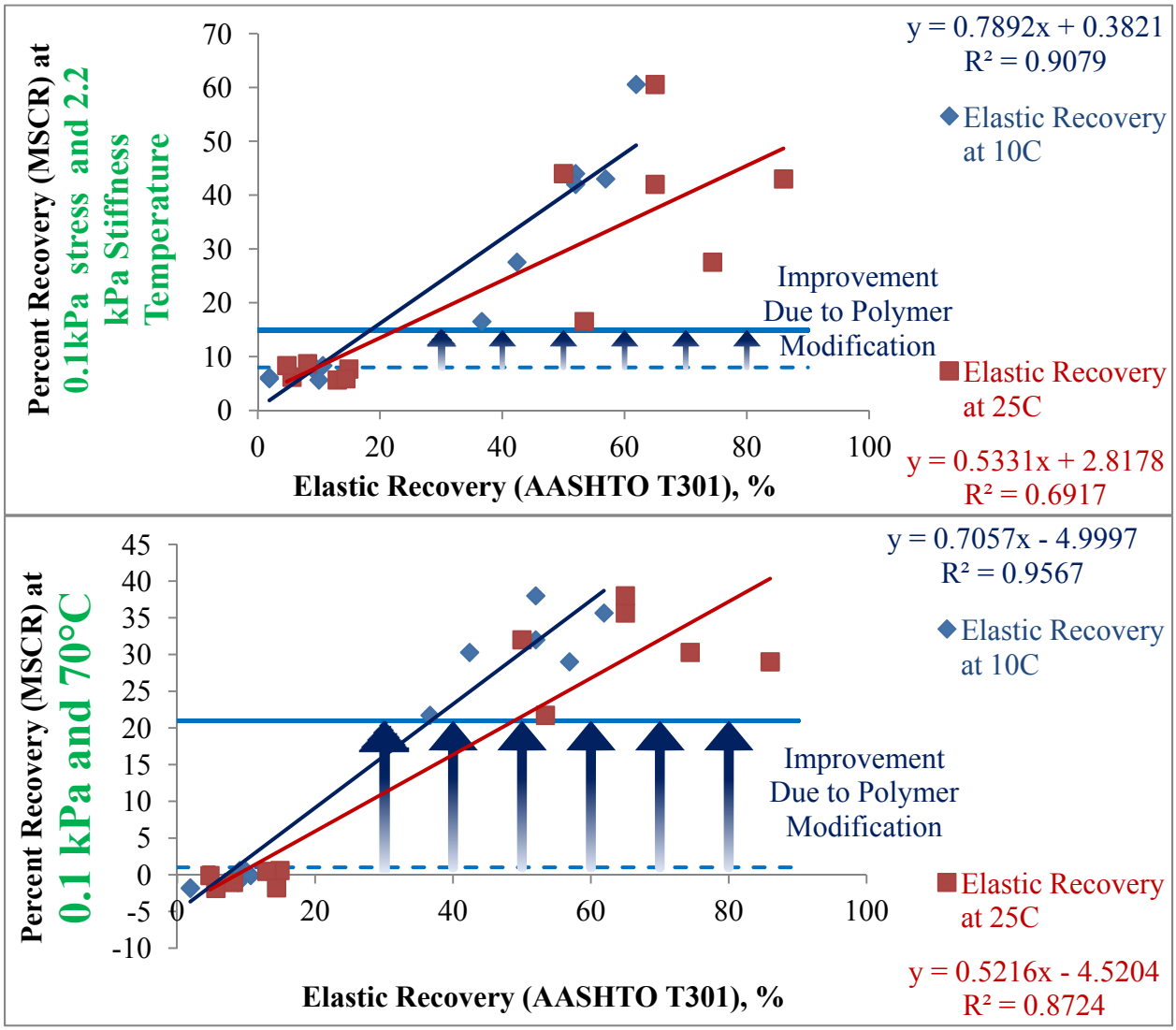

Figure 9
Linear correlation between percent recovery (MSCR at 70°C and at 2.2 kPa stiffness temperatures) and elastic recovery (AASHTO T301)

Therefore, MSCR at 58°C has been recommended as a criterion for polymer identification. At 0.1kPa creep stress, a minimum percent recovery of 25 and at 3.2kPa, a minimum percent recovery of 9 is recommended to identify the presence of polymer.

Force Ductility (AASHTO T300) Test Results

Emulsion residues were heated at 150°C for 30 min to prepare force ductility samples, except some hard pen emulsion residues that were heated at 160°C for 30 min. As mentioned earlier, DOTD requires f_2/f_1 values, and in some cases just f_2 values, in force ductility specifications

where, f_1 is the maximum force in lbs. and f_2 is the force at 30 cm elongation. In this study, the force ductility data acquisition system of LTRC was modified to collect continuous force and elongation data up to about 80 cm elongation. The rate of elongation was 5 cm/min. according to AASHTO T300.

Figure 10 shows force ductility test results for five non-polymer modified and non-hard pen base asphalt emulsion residues. All asphalt emulsion residues in this group, namely, CRS-2 (U), CRS-2 (E), SS-1 (U), SS-1 (B), and SS-1 (E), fail between 30 to 35 cm elongation. It can be concluded here that force ductility values at 30 cm or 35 cm elongation should be used instead of 20 cm elongation as used in elastic recovery (AASHTO T301).

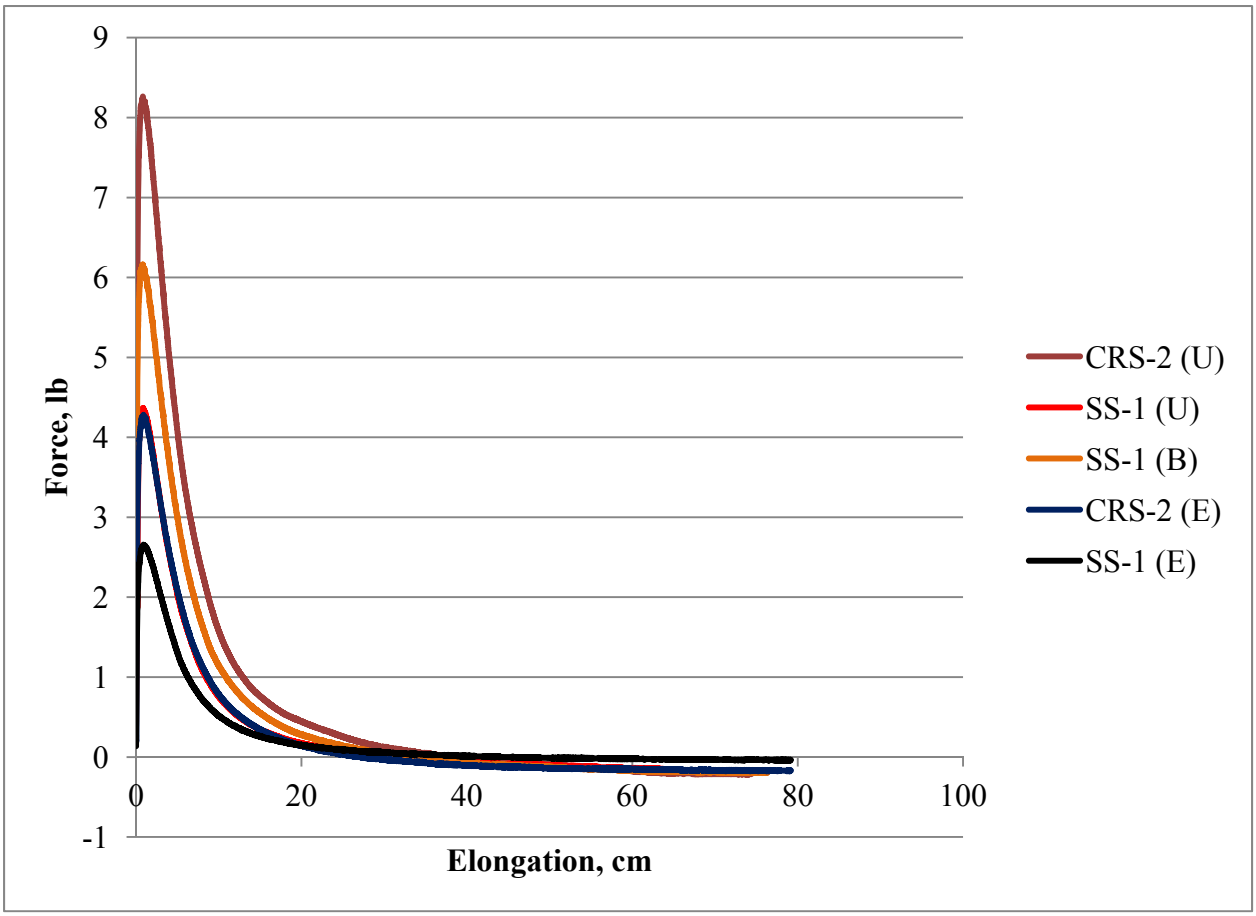

Figure 10
Force ductility test results of non-polymer modified non-hard pen base asphalt emulsions

Figure 11 shows force ductility test results for five polymer modified asphalt emulsions namely, CRS-2P (E), CMS-1P, SS-1L, PME and CHFRS-2P. None of the five polymer modified emulsion residues failed before 45 cm elongation. It can be observed that CMS-1P, CRS-2P (E), and CHFRS-2P never failed.

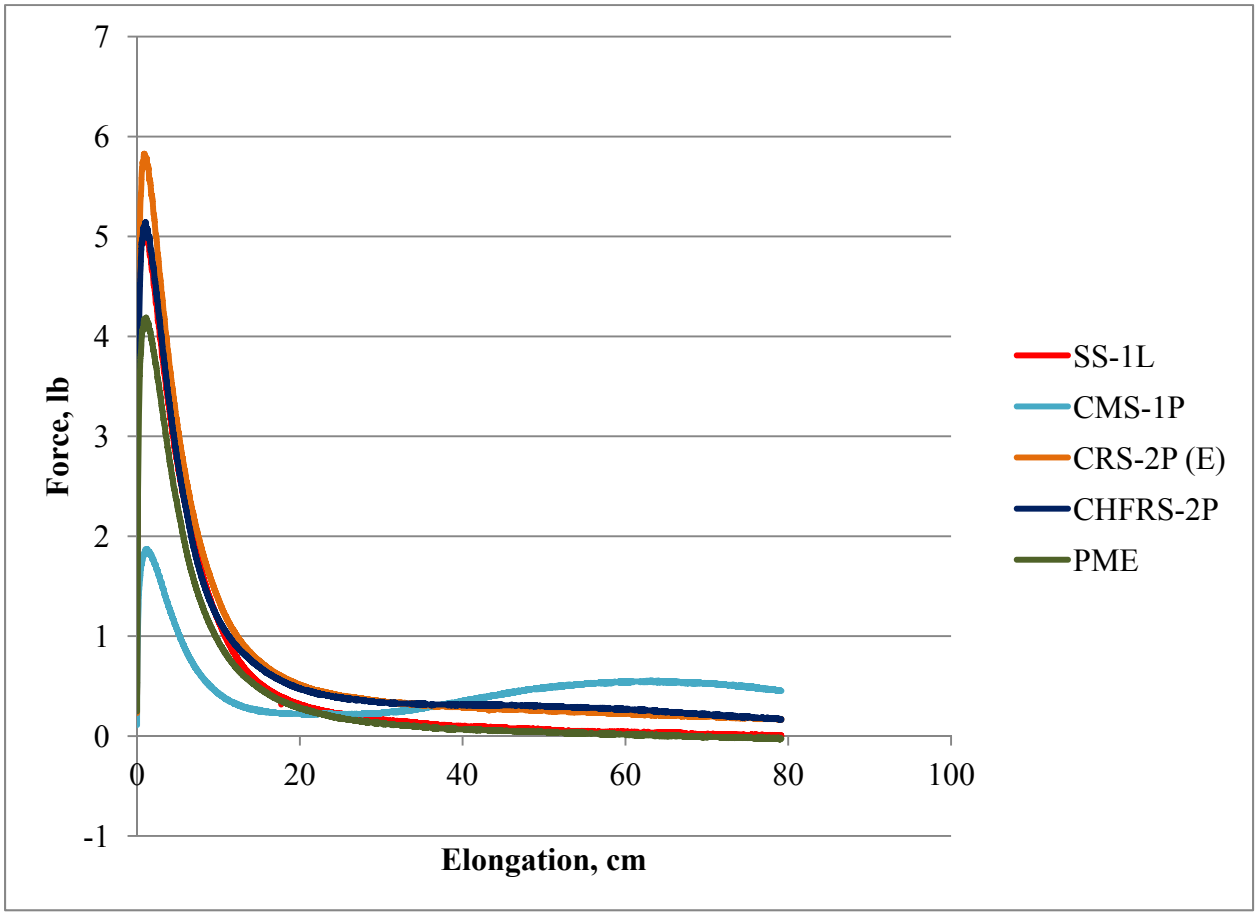

Figure 11
Force ductility test results of polymer modified asphalt emulsions

Figure 12 shows force ductility test results for four hard pen base asphalt emulsion residues namely, SS-1H (U), SS-1H (B), NTSS-1HM (U), and fog seal, and for two polymer modified hard pen base asphalt emulsion residues, namely, CSS-1HP and SS-1HP. It can be observed that all the four hard pen base asphalt emulsion residues have comparatively lower ductility and fail very quickly during elongation. Out of the two polymer modified hard pen base asphalt emulsion residues, SS-1HP exhibits better ductility than CSS-1HP. It can be observed that in general the maximum force is very high for hard pen base asphalt emulsion residues.

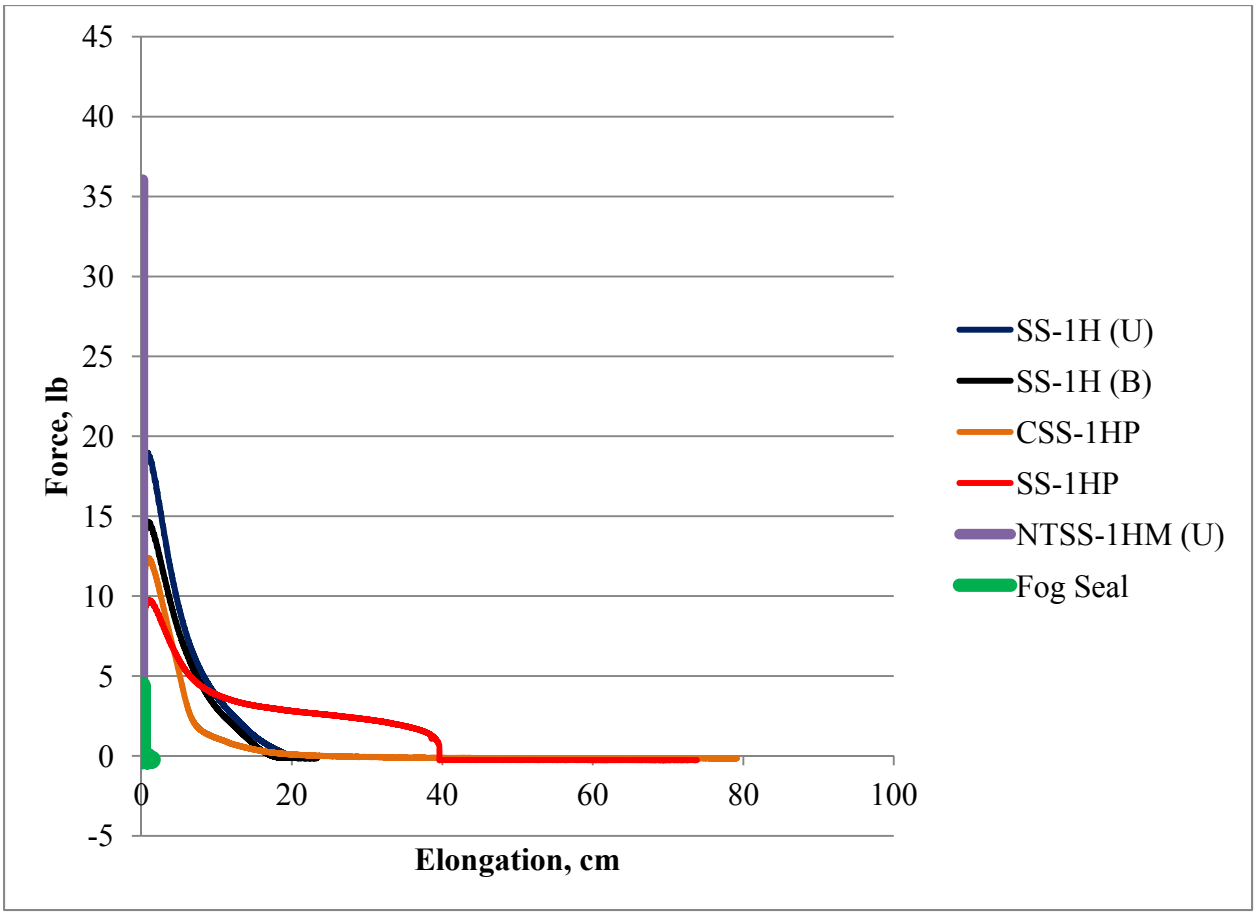

Figure 12
Force ductility test results of hard pen base asphalt emulsions

Table 11 shows maximum force (f_1), force at 30 cm (f_2), f_2/f_1 and force at 35 cm elongation. It can be observed that non-polymer modified and non-hard pen base asphalt emulsions can not be differentiated from polymer modified emulsions based on maximum force (f_1). However, force ductility parameter f_2 (force at 30 cm elongation) can differentiate between these two groups. It can be observed that the lowest value of f_2 for polymer modified emulsion residues is 0.1 lb while the highest value of f_2 for non-polymer modified and non-hard pen asphalt emulsion residue is 0.06 lb. All hard pen base asphalt emulsion residues have an f_2 value of 0 while one polymer modified hard pen base asphalt emulsion residue has an f_2 value of 2.13 lb. Table 11 also shows that the force ductility parameter f_2/f_1 is not as effective as f_2 in differentiating between polymer modified emulsion residue and non-polymer modified non-hard pen base asphalt emulsion residues. The lowest f_2/f_1 value for polymer modified emulsion residues is 0.03 while the highest f_2/f_1 value for non-polymer modified non-hard pen base asphalt emulsion residues is 0.02. The fourth force ductility parameter used in Table 11 is the force at 35 cm elongation. It can be noticed that for polymer modified emulsion residues, the force at 35 cm is much higher than that

of non-polymer modified non-hard pen base asphalt emulsion residues. Overall, force ductility results indicate that polymer modifications significantly increase the ductility of asphalt emulsion residues.

Table 11
Force ductility parameters for emulsion residues

Emulsions	Max. Force, f_1 (lb)		Force at 30 cm, f_2 (lb)		f_2/f_1		Force at 35 cm (lb)	
	Avg.	St. Dev.	Avg.	St. Dev.	Avg.	St. Dev.	Avg.	St. Dev.
Polymer Modified Emulsions								
CHFRS-2p	5.3	0.3	0.38	0.05	0.07	0.01	0.35	0.03
CMS-1p	1.8	0	0.22	0.02	0.12	0.01	0.26	0.01
CRS-2P (E)	5.9	0.1	0.4	0.07	0.07	0.01	0.36	0.06
PME	4.1	0.2	0.1	0.04	0.03	0.01	0.07	0.03
SS-1L	5.3	0.2	0.19	0.04	0.04	0.01	0.15	0.02
Non-Polymer Modified and Non-Hard Pen Base Asphalt Emulsions								
CRS-2 (U)	8.7	0.7	0.06	0.08	0.01	0.01	0.02	0.03
CRS-2 (E)	4.2	0.1	0	0	0	0	0	0
SS-1 (U)	4.3	0.02	0	0	0	0	0	0
SS-1 (B)	6.2	0.02	0.04	0	0.01	0	0	0
SS-1 (E)	2.7	1 sample	0.06	1 sample	0.02	1 sample	0.03	1 sample
Hard Pen Base Asphalt Emulsions								
SS-1H (U)	19.4	0.6	0	0	0	0	0	0
SS-1H (B)	13.8	1.2	0	0	0	0	0	0
Fog Seal	4.3	1 sample	0	0	0	0	0	0
NTSS-1HM (U)	41.2	7.4	0	0	0	0	0	0
NTSS-1HM (B)	18.7	6.2	0	0	0	0	0	0
Polymer Modified and Hard Pen Base Asphalt Emulsions								
CSS-1HP	11.2	1.6	0	0	0	0	0	0
SS-1HP	9.2	0.05	2.13	0.11	0.23	0.01	0.89	1.26

Note: Force ductility could not be performed on CRS-2P (B), CRS-2 (B), and NTSS-1HM (C) because of sample loss during shipping to LTRC.

Correlation between DSR Test Parameters and Force Ductility (AASHTO T300)

Out of the 20 emulsions tested in this study, eight are hard pen base asphalt emulsions of which one hard pen base asphalt emulsions failed before five cm and three failed at around 20 cm, and two hard pen base asphalt emulsions were not tested for force ductility. Out of 12 non hard pen base asphalt emulsions, CRS-2 (B) and CRS-2P (B) could not be tested for force ductility. Therefore, in this study, 10 emulsions (five polymer modified and five non-polymer modified

non-hard pen base asphalt emulsions) were considered for correlation between DSR-based parameters and force ductility test parameters (AASHTO T300).

Based on the force ductility test results as discussed earlier, three force ductility parameters, f_2, f_2/f_1 and force at 35 cm were correlated with two DSR-based parameters, phase angle and percent recovery at 0.1 kPa creep stress. Both the DSR-based parameters were determined at three temperatures, 58°C, 70°C and at equal stiffness (2.2 kPa G*/sinδ) temperatures. Therefore, each temperature produced six coefficient of determination (R^2) values for 6 relationships (3 force ductility parameters X 2 DSR-based parameters = 6). In total, three temperatures produced 18 (3 DSR testing temperatures X 2 DSR-based parameters X 3 force ductility parameters) coefficient of determination (R^2) values. Table 12 shows coefficient of determination (R^2) values of linear correlation of these 18 relationships.

Figure 13 shows how the R^2 values between f_2 and phase angle at 58°C, 70°C and 2.2 kPa temperatures were obtained. Figure 14 show how the R^2 values between f_2 and percent recovery at 58°C, 70°C and 2.2 kPa temperatures were obtained.

It can be observed from Table 12 that both phase angle and percent recovery have linear correlations with force ductility parameters. The highest R^2 value for phase angle is 0.74 and the highest for percent recovery is 0.66. Overall, the phase angle shows a better correlation with force ductility parameters than percent recovery.

For phase angle relationships, the average R^2 values at 58°C, 70°C and 2.2 kPa temperatures are 0.62, 0.62 and 0.57, respectively. For percent recovery relationships, the average R^2 values at 58°C, 70°C and 2.2 kPa temperatures are 0.45, 0.62 and 0.34, respectively. This indicates that the best relationships between force ductility parameters and DSR-based parameters can be obtained at 70°C. The correlations at 58°C are better than those at 2.2 kPa temperature. However, at 70°C, percent recovery of 0.1 kPa stress is sometimes negative. Therefore, the correlation between DSR-based parameters and force ductility parameters should be performed using the 58°C DSR testing temperature.

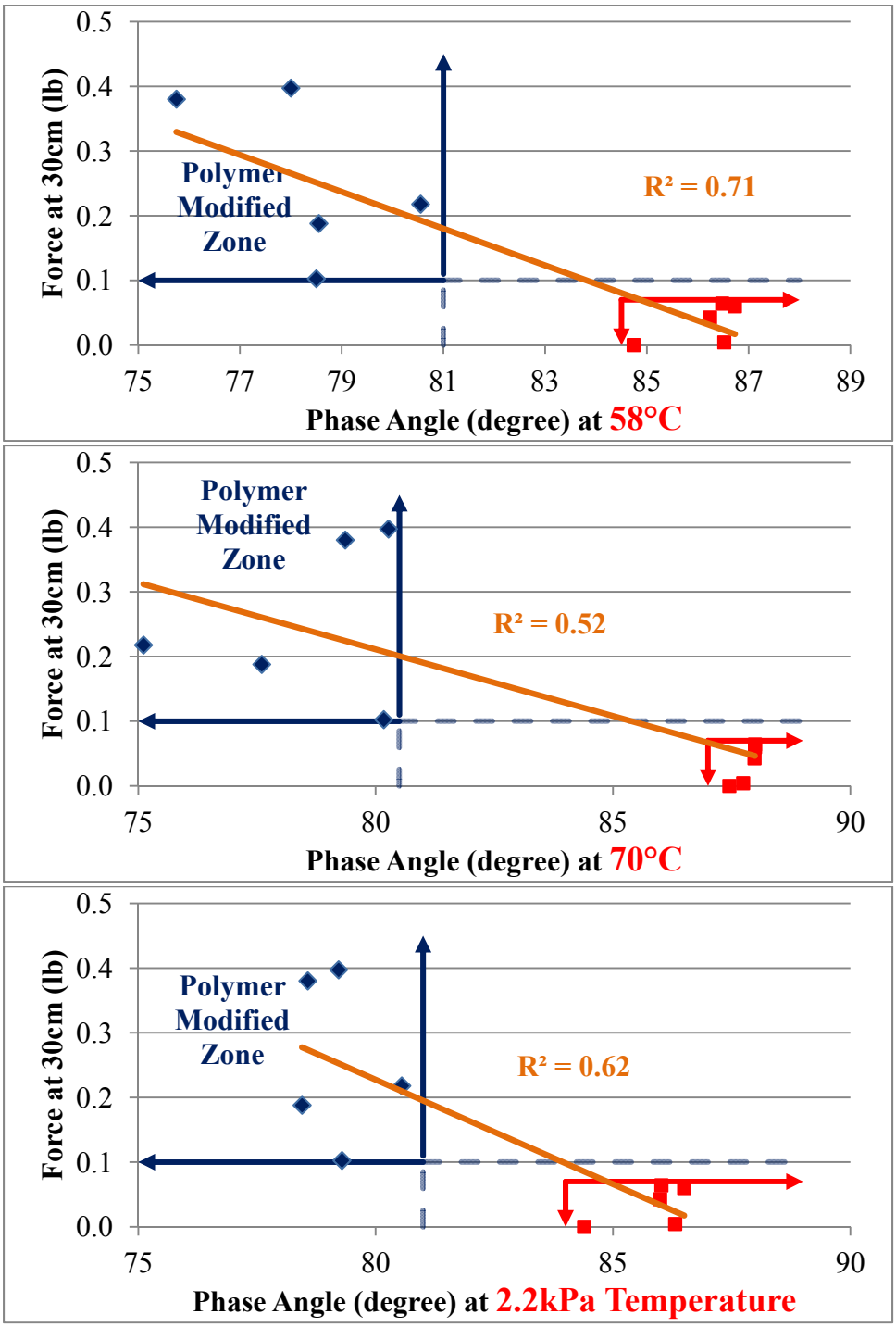

Figure 13
Correlation between phase angle and f_2

Table 12
Coefficient of determination (R^2) between force ductility and DSR-based test results

Linear Correlation with Phase Angle				
Force Ductility Test Parameter	Phase Angle Testing Temperature			
	58°C	70°C	2.2kPa Temp.	Average R^2
Force at 30 cm, f_2 (lb)	***0.71***	***0.52***	***0.62***	0.62
f_2/f_1	0.47	0.74	0.47	0.56
Force at 35 mm (lb)	0.69	0.61	0.62	0.64
Average R^2	0.62	0.62	0.57	0.61
Linear Correlation with Percent Recovery				
Force Ductility Test Parameter	Percent Recovery (at 0.1 kPa Creep Stress) Testing Temperature			
	58°C	70°C	2.2kPa Temp.	Average R^2
Force at 30 cm, f_2 (lb)	***0.46***	***0.65***	***0.31***	0.47
f_2/f_1	0.43	0.54	0.38	0.45
Force at 35 mm (lb)	0.46	0.66	0.33	0.48
Average R^2	0.45	0.62	0.34	0.47

Note: Figures 13-14 show how the bold and italic R^2 values were obtained.

For phase angle relationships, the average R^2 values for force ductility parameters f_2, f_2/f_1 and force at 35 cm are 0.62, 0.56 and 0.64, respectively. For percent recovery relationships, the average R^2 values for force ductility parameters f_2, f_2/f_1, and force at 35 cm are 0.47, 0.45, and 0.48, respectively. This indicates that the best relationships between force ductility parameters and DSR-based parameters can be obtained using the force ductility parameter force at 35 cm. However, the force at 35 cm is sometimes very low. The correlation using f_2 is better than those obtained using force ductility parameter f_2/f_1. Therefore, the correlation between DSR-based parameters and force ductility should be performed using force ductility parameter f_2.

Based on the above analyses, two linear coefficients of determination (R^2) values were selected for further analyses: the R^2 value between phase angle (at 58°C) and f_2 and the R^2 value between percent recovery (at 58°C) and f_2. Figure 13 also shows that the f_2 requirement in the force ductility test can be replaced by a maximum phase angle of 81° at 58°C. Figure 14 shows that the minimum percent recovery (0.1 kPa creep stress) at 58°C can be used to replace the f_2 requirement in the force ductility test.

It was concluded from this study that percent recovery of MSCR and phase angle can be used to replace force ductility requirements (AASHTO T300). It is recommended that at 58°C, a maximum phase angle of 81° and a minimum MSCR percent recovery (at 0.1kPa creep stress) of 30 are specified to replace the force ductility test (AASHTO T300). These criteria are applicable for emulsion residues prepared according to the low temperature evaporative method specified in ASTM D7497.

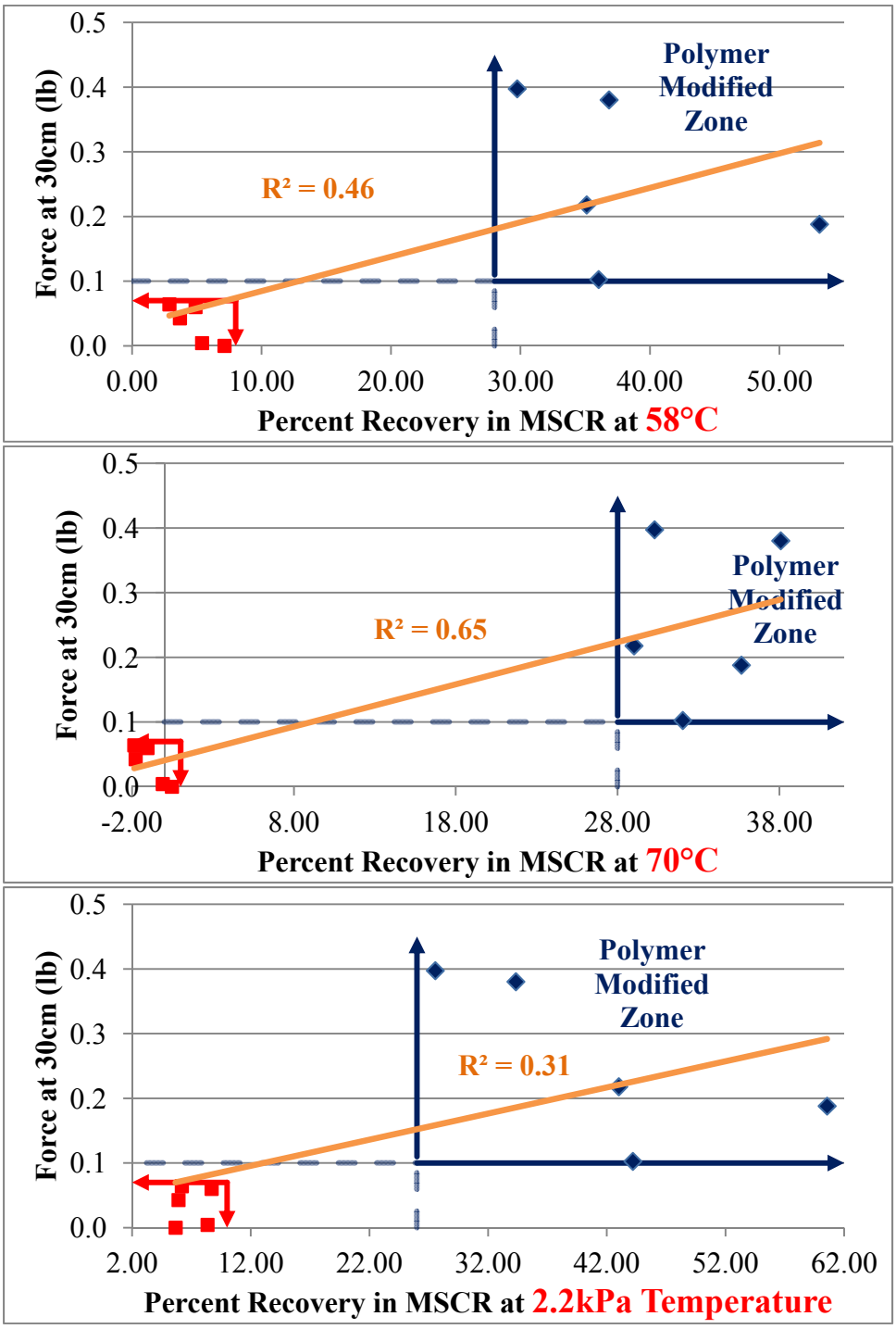

Figure 14
Correlation between percent recovery and f_2

Recovery Methods Test Results

Results of Water Removal

Weight was taken before and after the recovery process for all the samples, and the percentage of water removed was found based on the initial weight. A summary of the water removed by each procedure from all the emulsions is provided in Table 13. ASTM D6934 removed the highest percentage of water from the emulsions which is evident because it uses the highest temperature among all the other methods. Besides, 163°C is well above the boiling point of water which ensures almost complete removal of water from the emulsion.

Table 13
Percent water removal using different recovery methods

Emulsions	ASTM D6934	ASTM D7497	AASHTO TP 72 Method B		Vacuum Drying Method		Field Curing Method	
	Avg % water removal (Std. Dev.)[1]	Avg % water removal (Std. Dev.)	Avg % water removal (Std. Dev.)		Avg % water removal (Std. Dev.)		Avg % water removal (Std. Dev.)	
CRS2P (E)	32.6	32.01 (0.55)	31.14	(0.59)	31.48	(0.23)	29.56	(0.69)
CRS2 (E)	31.2	32.25 (0.53)	30.71	(0.23)	32.38	(0.21)	29.14	(0.85)
CRS2L (A)	31.8	25.68 (0.03)	25.12	(0.51)	28.65	(0.21)	25.97	(1.21)
SS-1 (E)	39.2	37.27 (0.34)	34.75	(0.42)	35.90	(0.51)	34.95	(0.97)
SS-1H (B)	36.2	33.68 (0.54)	32.81	(0.19)	34.94	(0.12)	33.43	(0.92)
SS-1L (A)	37.2	33.27 (1.93)	32.57	(0.34)	34.66	(0.16)	33.02	(0.74)

[1]Three sample was prepared from one recovered residue.

The second most efficient method for water removal is the vacuum drying method which takes approximately three hours to remove the water. The results of ASTM D7497 are very close to the vacuum drying method. If water removal within a short period of time is the only concern, then the vacuum drying method is the most useful among all the low temperature evaporative methods. It removed much more water within 3 hrs than the two days long ASTM D7497 for most of the emulsions. If the percentage of water removed by the ASTM D6934 is considered to be the maximum, then for most of the emulsions ASTM D7497 reached more than 90% of the maximum. It is clear from all of the low temperature evaporative methods data that after the recovery process, a very small amount of water is always left inside. In the field curing method where the field condition is simulated, this phenomenon is even more profound.

Results of Temperature Sweep Test

G*/sinδ is a measure of binder stiffness. Figure 15 summarizes the G*/sinδ values at 64°C for all of the emulsions recovered by five different processes along with their unaged base binder. ASTM D7497 and the field curing method have a curing time of 48 hours. It is clear from Figure 15 that among all the methods, ASTM D7497 and the field curing method showed consistently higher G*/sinδ values than the rest. Other methods using less curing time could not exceed the values of 48 hours curing methods, not even the ASTM D6934 which uses 163°C. This indicates that the increase of stiffness depends much more on curing time than high curing temperature for a short period of time. This statement is also supported by the higher G*/sinδ values obtained from the field curing method where the outside mean temperature was only 26°C but curing time was 48 hours (Figure 15). Both of the latex modified emulsions (CRS-2L and SS-1L) and SS-1H showed higher G*/sinδ values in the field curing method than ASTM D7497 which indicates that these emulsions experience much more oxidative aging in the field condition. In Figure 15, CRS-2L, SS-1L and SS-1H, field curing method showed 22.1%, 37.8% and 23.6% increase in stiffness than ASTM D7497 respectively. A general trend observed in the G*/sinδ values is that latex modified emulsions (SS-1L and CRS-2L) showed higher stiffness than corresponding neat emulsions (SS-1 and CRS-2) in all the other methods. Differences of values due to polymer and latex modification were clearly identifiable in all the methods.

The vacuum drying method (3 hrs) produced well dried sample than the AASHTO TP 62 method even though the curing time is 3h shorter. It was observed that the sample produced by vacuum drying method was easier to peel off from the mat and less sticky than the residue obtained from AASHTO TP 72 method. Except for SS-1H and CRS-2, all the emulsions used in this study showed the lowest G*/sinδ values in the vacuum drying method than the rest, which is good in a sense that this method produces residues that experience less oxidative aging.

Figure 15 shows that G*/sinδ values of polymer and latex emulsions residues almost doubled from their unaged base binder. This was expected for those emulsions because polymer or latex is added to the base binder during emulsification process by the manufacturer. The neat emulsion (SS-1, SS-1H and CRS-2) residues should have a value that is close to the original base binder, as there is no modification present. ASTM D7497 failed to address this issue and higher G*/sinδ values for all emulsions irrespective of modification indicate that the method is prone to oxidative aging (Figure 15). On the other hand, neat emulsion residues recovered by vacuum drying method show almost similar results to their base binder. For CRS-2, SS-1, and SS-1H, the differences in G*/sinδ values to their base binders are 19.9%, 17.2%, and 11%, respectively, which indicates that the vacuum drying method does not produce an unnecessarily aged sample.

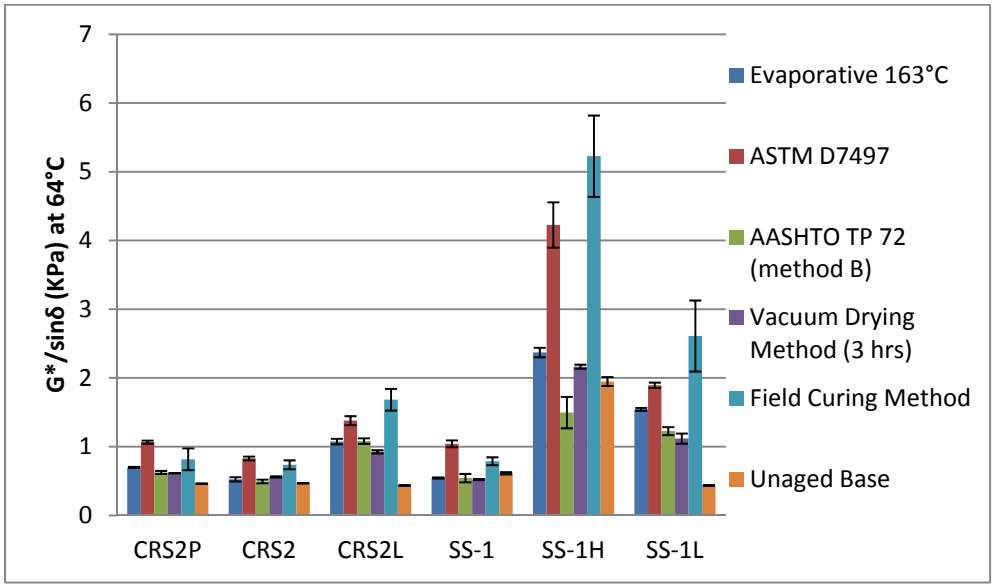

Figure 15
G*/sinδ results at 64°C recovered by different methods

Results of Phase Angle

Airey reports that the phase angle (δ°) is usually considered to be much more sensitive to the structure of the binder than is G*, and as such, provides a better indication of the type and extent of polymer modification [*15*]. Lower phase angle indicates higher elasticity; theoretically, any polymer or latex modification will increase the elasticity of the residue and thus provide a lower phase angle value. Figure 16 presents the phase angle values of all the emulsions recovered by the five different methods along with their unaged bases at 64°C. All the residues recovered in the different methods and their unaged base show very close phase angle values. As the differences of the values are statistically indifferent, polymer identification is not possible, analyzing the values of phase angle. One of the main discrepancies observed in the values of phase angle is that both polymer and latex modified emulsion showed higher values (less elastic) than their corresponding bases which is unexpected; whereas later in this study, it is shown that both these modified emulsions have significantly higher average percent of recovery (more elastic) than their bases. Phase angle changes with temperature and polymer modification could be identifiable at an equiviscous temperature and further research is needed in this direction. Hanz et al. reported that the polymer network development cannot be captured by the G* and δ testing protocols, thus necessitating the use of the multiple stress creep and recovery (MSCR) test for polymer modified binders [*19*].

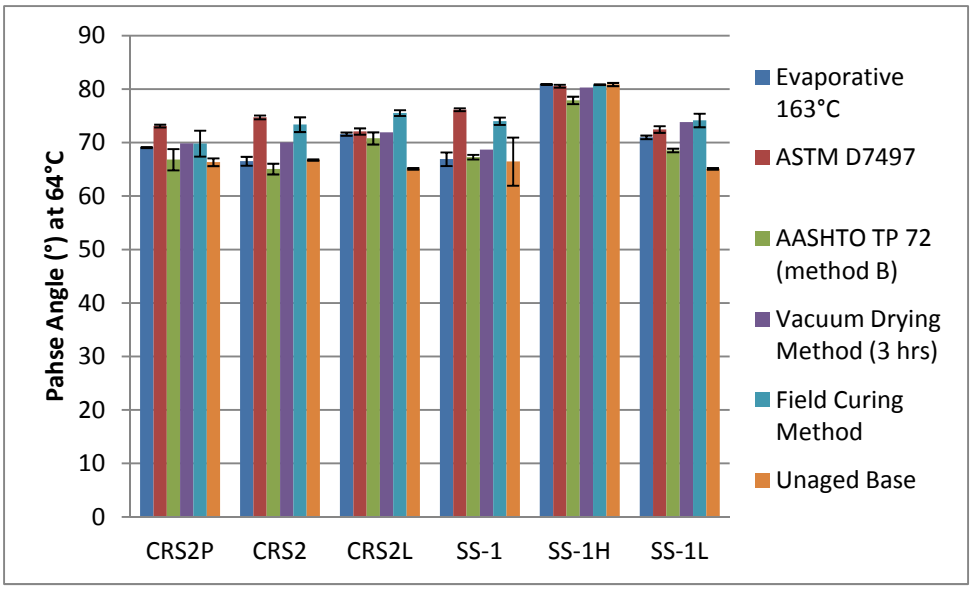

Figure 16
Phase angle (δ°) results at 64°C recovered by different methods

Effect of Remaining Moisture and Curing Time on G*/sinδ

Hanz et al. suggested that a full 48 hours curing period is needed for full development of rheological properties. Within this recovery period, residues are aged similarly to the RTFO aged base asphalt [*19*]. Previous research efforts could not identify the exact reason behind this higher G*/sinδ obtained in ASTM D7497. It is hypothesized that these higher G*/sinδ values may be attributed to oxidative aging, remaining moisture, change in the chemistry of the emulsion or a combination of these factors.

To understand the effect of the remaining moisture and curing time on G*/sinδ, three emulsions namely CRS-2, CRS-2P, and CRS-2L, were selected and recovered using the vacuum drying method. Variable curing times of 3, 6, and 8 hours were used for the recovery process. Figure 17 shows the values of G*/sinδ of the residue recovered by three different curing time. Three emulsions showed gradual increase in the values of G*/sinδ as the time proceeded. The number showed in the graph is the percent water removal of the corresponding point. It is clear that there is no significant water removal from the sample after 3 hours but the gradual increase is still occurring in G*/sinδ values. This phenomenon indicates that after a certain time, water removal remains constant and only curing time affects the residue stiffness. So it is unnecessary for any recovery procedure to be prolonged after a certain time only due to the removal of remaining moisture from the sample. As previously seen in Table 13, the vacuum drying method removes as much or more water within three hours ASTM D7497 does in 48 hours. Even though the sample

recovered by these two methods is dried to the same level, G*/sinδ values demonstrate a great difference. For CRS-2, CRS-2P, and CRS-2L, it is 47.9%, 73.3%, and 48.7% higher for ASTM D7497 respectively than the vacuum drying method. A general misconception of the recovery process is that if any sample has higher remaining moisture, its stiffness should be lower than a completely dried sample. This statement is not completely true if sufficient curing time is given because, in the case of the field curing method, all of the emulsions had higher remaining moisture (see Table 13) but the stiffness of the residue was significantly higher for every sample compared to the vacuum drying method. So it can be concluded that after a certain time, when the sample is almost dried, G*/sinδ is not affected by the remaining moisture.

Another important point to be noted with the vacuum drying method is that while the vacuum is applied, all the air is sucked out of the system and thus, extremely low pressure is achieved. As the system is completely void of air, theoretically there is no chance of oxidative aging of the residue. In Figure 17, the increase in stiffness from 3 to 8 hours is 10.04%, 12.60%, and 21.88% for CRS-2, CRS-2P, and CRS-2L respectively.

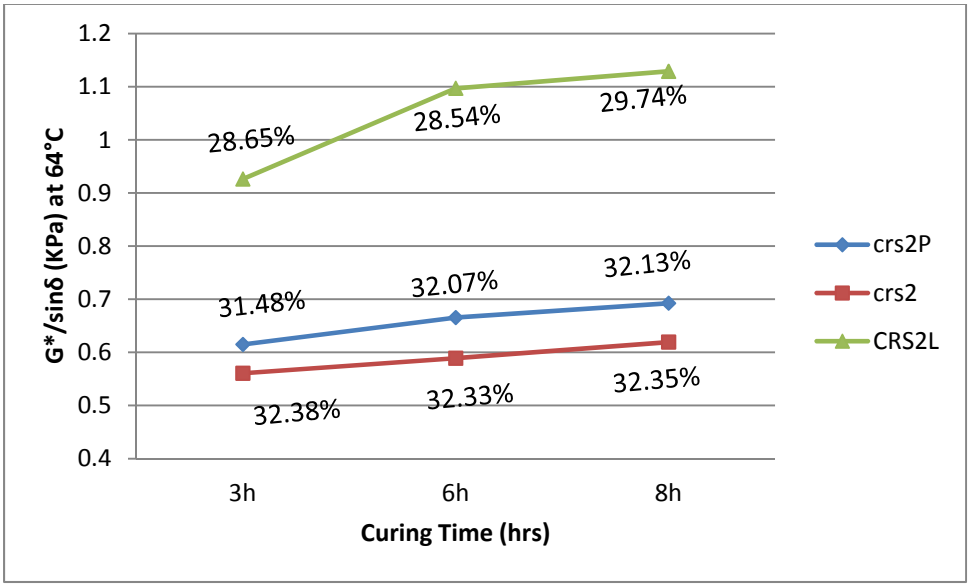

Figure 17
Results of stiffness at 64°C cured by vacuum dry method

This increase in stiffness is not due to water removal because it is constant after three hours, and it is not due to oxidative aging because the chamber is totally void of air. The only conclusion to be drawn, then, is that this change is attributed to chemical changes of the asphalt and emulsifier. This chemical change may correspond to polymer network development or latex structure

formation. So it is anticipated that in three hours of curing time of the vacuum drying method, the polymer network is under-developed and further curing time should be allowed to recognize the full benefits of polymer, latex, or any other chemical change of the emulsifier that plays an important role in emulsion setting and hardening process. But this behavior (polymer network development) cannot be captured by the values of G*/sinδ. So the MSCR test was conducted to evaluate the development of the polymer network as a function of curing time.

Results of Multiple Stress Creep and Recovery

Polymer modification allows the binder to accumulate less permanent deformation due to delayed elasticity; thus a portion of the deformation is recovered after unloading [*25]*. The average percent strain recovery was used to identify the polymer network formation in the residue with respect to time. Figure 18 shows the average percent recovery as a function of curing time at 100 pa stress level and 58°C testing temperature. CRS-2 is a neat emulsion, not modified by any polymer, and showed an insignificant amount of average percent recovery. Both polymer and latex modified emulsion residues showed significantly higher average percent recovery values as the time increased.

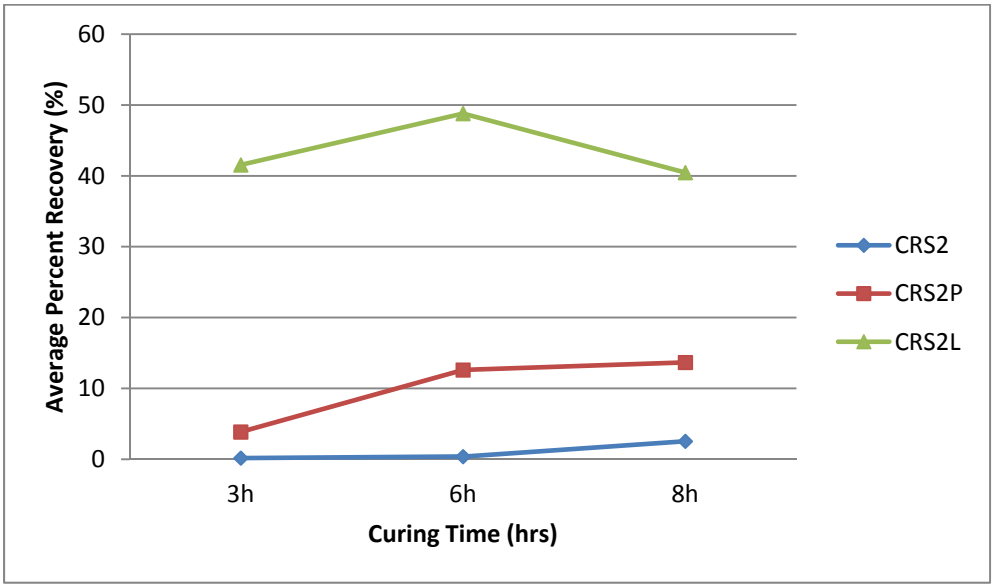

Figure 18
Average percent recovery as function of time at 58°C and 100 Pa

Residues recovered in three hours clearly identified the latex modification from the neat emulsion. It can be said that the rate of reaching a final level of elasticity is slower for the polymer modified emulsion. From three to six hours, the average percent recovery of polymer modified emulsion residue increased 213% whereas for latex modified emulsion residue it is 17%. In the time period of six to eight hours this increase in average percent recovery was

constant for CRS-2P. So it can be said that at three hours curing time the polymer network is still in formation and lowering the curing time to less than 6 hours cannot produce a residue that can show the full benefits of polymer modification.

Table 14 compares the average percent recovery values of each of the emulsions with their unaged base at 58°C and 100 Pa Stress level obtained from the vacuum drying method and ASTM D7497. All the bases show an insignificant amount of percent recovery: less than 0%. Emulsion CRS-2 does not have any polymer modification and it shows no recovery in the vacuum drying method which is expected but shows 5.2% recovery in ASTM D7497. The 6 hours vacuum drying method clearly identified the improvement in elasticity of the modified binders from their corresponding unaged base.

Table 14
Average percent recovery at 58°C and 100 Pa stress level

Emulsion	Vacuum Drying Method			ASTM D7497 Average % recovery (Std. Dev.)	Unaged Base Average % recovery (Std. Dev.)
	3 hrs Average % recovery (Std. Dev.)	6 hrs Average % recovery (Std. Dev.)	8 hrs Average % recovery (Std. Dev.)		
CRS-2	0.15 (0.84)	0.37 (3.73)	2.53 (1.6)	5.20 (2.12)	-3.68 (2.19)
CRS-2P	3.84 (2.35)	12.60 (1.23)	13.66 (3.96)	29.80 (1.41)	-0.49 (0.36)
CRS-2L	41.53 (3.56)	48.795 (3.39)	40.45 (8.75)	43.86 (12.35)	-0.19 (0.31)
		Polymer modification is Identifiable			

Overall Comparison between ASTM D7497 and Vacuum Drying Method

Four major reasons contribute to the higher G*/sinδ value of an emulsion residue than its unaged base binder. Those are polymer or latex modification, emulsifier chemicals, oxidative aging and remaining moisture. It is shown in this study that a slight variation in the remaining moisture after a certain time does not affect the G*/sinδ values of residues. The other three reasons can be separated from one another by comparing the data of the ASTM D7497 and the vacuum drying method together. Figure 19 is a schematic diagram that shows the contribution of different reasons that affect the final stiffness of the residue for a particular binder. To construct this diagram, CRS-2 and CRS-2P were used and recovered with the vacuum drying method but the temperature and time conditions were kept similar to ASTM D7497. Three replicates were tested for each data point of Figure 19. It can be seen in Figure 19 that both base binders have almost the same stiffness value of 0.4623 and 0.4676 for CRS-2P and CRS-2 respectively.

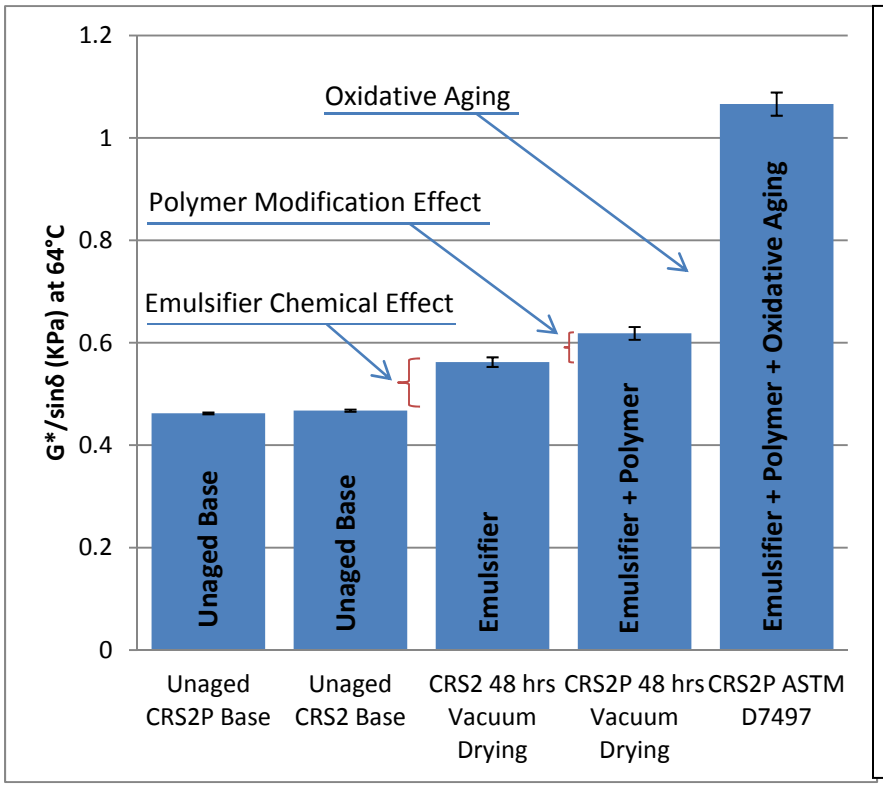

Effect of polymer on elastic recovery is comparatively higher than on stiffness (see Table 14). Therefore, polymer adds a significant value to the performance of emulsions.

Figure 19
Schematic diagram of different reasons affecting final G*/sinδ value of the residue

The difference of the G*/sinδ value between CRS-2 recovered by 48 hours vacuum drying and base binder is 20.2%, this difference is caused by the emulsifier chemicals because there is no presence of polymer in this emulsion and oxidative aging is not possible in the vacuum drying process. The difference between G*/sinδ value of CRS-2 and CRS-2P recovered by 48 hours vacuum drying is 9.9%, this difference is caused by the presence of polymer in CRS-2P as all the other variables were kept same. The jump of G*/sinδ value from CRS-2P recovered by 48 hours vacuum drying and CRS-2P recovered by ASTM D7497 is 72.4%; this significant increase was due to oxidative aging occurring in ASTM D7497 since time and temperature conditions were exactly same in two systems and the only difference was the presence of oxygen in one system. Values of G*/sinδ for CRS-2P and CRS-2 recovered by three hours vacuum drying at 60°C (Figure 15) are 0.615 and 0.5607 whereas these two values for 48 hours that the vacuum drying are 0.6185 and 0.5624. These results are strong evidence indicating vacuum drying system does not experience oxidative aging since even after the time was increased to 45 hours, the stiffness remained almost the same. Table 15 compares the key findings on ASTM D7497 and the vacuum drying methods based on this research.

Table 15
Comparisons of the key findings on vacuum drying method and ASTM D7497

Criteria	Vacuum drying method	ASTM D7497
Water removal	High Water removal.	Relatively less water removal. (Only 2 out of 6 emulsion was higher)
Aging	Theoretically aging is not possible. Less aging observed.	High Aging observed.
Polymer Identification	In 6 hrs polymer modification was clearly identifiable.	Polymer modification was identifiable after 48 hrs.
Temperature	Maximum temperature was 60°C.	Maximum temperature was 60°C.
Time	Less time consuming (6 hrs)	More time consuming (48 hrs)
Residue Stiffness	Stiffness results of Neat emulsion were similar to unaged base binder.	Stiffness results of all the emulsion were almost double of their unaged base binder.
Average percent recovery	Latex modified emulsion showed higher value.	Polymer modified emulsion showed higher value.

Rotational Viscosity Test Results

Repeatability

The viscosity of the emulsions widely varies with different shear rates (rpm) and temperature, as it also does for asphalt binders. It was observed that the variation of the viscosity data at some particular shear rate was higher than others. It is crucial to identify a standard shear rate that produces a minimum amount of variation and high repeatability in the test data. Table 16 shows the coefficient of variation (%) at each shear rate and temperature used in the study. The coefficient of variation shown in the table is calculated for six samples for each two batches. For example, the first coefficient of variation, 7.03% for SS-1 at 20 rpm and 30°C, was calculated from the viscosity result of six samples, which are 39.17 cP (centipoise), 35.83 cP, 35 cP, 34.17 cP, 40.83cP, and 38.33cP; all of these viscosities are the averages of three readings. It is clear from Table 16 that different emulsions showed a minimum coefficient of variation at different test conditions. It is very hard to determine the best test temperature and shear rate that suits all type of emulsions on the basis of data consistency. The last row of Table 16 shows the average coefficient of variation for different test conditions. 50 rpm at 30°C and 30 rpm at 60°C showed a minimum average coefficient of variation. These two test conditions can be selected for a standard test method if data consistency is considered. Table 17 summarizes the average of all the viscosities gathered for the study. The first viscosity value for SS-1 at 20 rpm and 30°C is 37.22 cP, which is the average of the viscosity data of six samples and each of these viscosity data is the average of three readings taken at three different intervals.

Table 16
Coefficient of variation (%) at different shear rate (rpm) and temperature

Temperature	30°C					60°C				
rpm	20	30	50	60	100	20	30	50	60	100
Emulsion	Coefficient of Variation of 6 samples									
SS-1	7.03	3.36	2.25	2.35	1.60	4.84	4.69	6.78	6.06	7.20
SS-1L	4.08	3.33	2.22	2.44	3.16	4.42	4.44	3.98	4.33	4.32
SS-1H	3.93	3.19	2.63	2.80	2.52	3.21	3.03	4.16	4.56	4.51
CRS-2	1.63	2.27	3.69	3.87	4.17	7.46	5.59	4.27	7.73	4.42
CRS-2P	5.31	4.88	2.64	3.65	3.35	4.13	2.25	1.71	2.18	2.73
Average	4.40	3.40	2.68	3.02	2.96	4.81	4.00	4.18	4.97	4.64

Table 17
Average viscosity for different shear rate and temperature

Temperature	30°C					60°C				
Shear rate (rpm)	20	30	50	60	100	20	30	50	60	100
Emulsion	Average Viscosity (cP) of 6 samples									
SS-1	37.22	34.73	34.39	34.10	35.42	62.87	60.00	59.06	59.81	63.81
SS-1L	34.17	31.92	31.17	30.82	31.19	26.67	24.53	22.89	22.60	21.86
SS-1H	92.36	82.49	76.28	73.98	71.11	78.06	75.73	74.22	73.24	72.72
CRS-2	865.28	719.92	596.94	561.18	543.61	436.94	373.56	314.94	282.08	255.81
CRS-2P	432.72	392.11	356.67	340.84	333.94	243.81	216.62	184.22	167.39	141.64

Thixotropic Behavior of Emulsions

All of the emulsions used in the study showed thixotropic behavior. Thixotropy is a shear thinning property of the liquid, where the liquid's viscosity decreases over time and takes a finite amount of time to attain a stabilized viscosity when a particular shear rate is applied. Figure 20 shows multiple runs of CRS-2 and SS-1 at 20 rpm and 60°C. It is obvious from this figure that the viscosity of the emulsion is highly dependent on the time the reading was taken. AASHTO T 316, specified for asphalt binder, allows first reading after 10 minutes for temperature and flow stabilization. But, for emulsions, the first 10 minutes shows the rate of decrease of viscosity as much higher and at this time too much variability in the reading was observed. After around 25 minutes, all of the highly viscous emulsions attained a stabilized viscosity and the rate of decrease of viscosity was lowered; for low viscous emulsions, stabilized viscosity was attained much quicker than high viscous emulsions. To counter the thixotropic effect, the shear rate (rpm) was always applied gradually from low to high and the shear rate was stepped up from low to high without stopping the spindle. It has been observed that once the flow is stabilized at a certain rpm,

it takes a less amount of time to stabilize at the next rpm level if the spindle is not stopped. Previous studies by Salomon at el. also proved that the thixotropic behavior of emulsions follows the first order kinetics. The thixotropic effect on the readings of the viscosity of emulsion using a rotational viscometer cannot be avoided completely, so it is suggested that the time the reading was taken should also be reported with the temperature and shear rate.

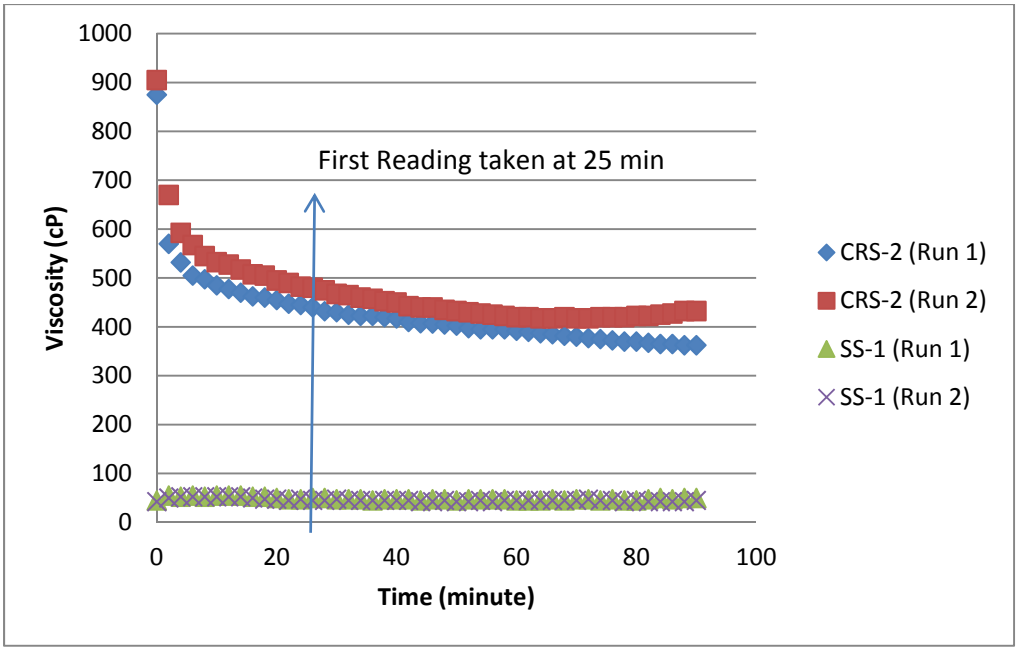

Figure 20
Time dependent change of viscosity for CRS-2 and SS-1

Effect of Shear Rate on Viscosity

Figure 21 shows the effect of different shear rates on emulsion viscosity at 60°C. A general trend observed from this figure is that with the increase of shear rate the emulsion viscosity decreases. This phenomenon is more visible in high viscous emulsions than low viscous emulsions. CRS-2 and CRS-2P decreased 41.4% and 42% respectively whereas SS-1, SS-1L and SS-1H are -1.48% (slightly increased), 18.02% and 6.83% respectively from 20 rpm to 100 rpm. From this figure, it can be said that highly viscous emulsions behave more towards a shear thinning liquid whereas low viscous emulsions behave more towards a Newtonian fluid at 60°C. Similar trend is also observed in Figure 22 which shows the effect of different shear rate on emulsion viscosity at 30°C temperature. CRS-2 and CRS-2P decreased 37.17% and 22.82% respectively whereas SS-1, SS-1L and SS-1H decreased 4.85%, 8.96% and 23% respectively from 20 rpm to 100 rpm.

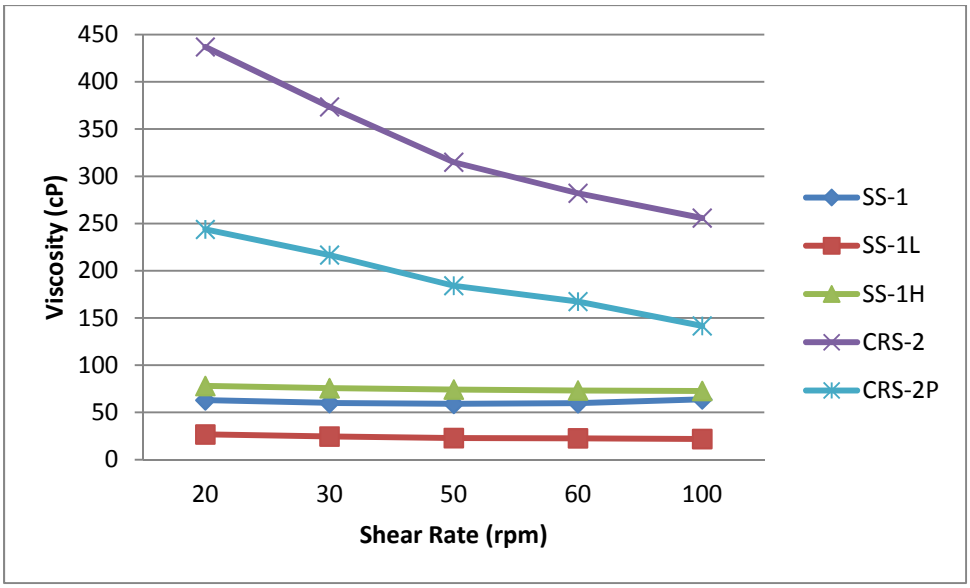

Figure 21
Effect of shear rate on viscosity at 60°C

Effect of Temperature on Viscosity

Table 18 shows the effect of temperature on emulsion viscosity at different shear rates. The values presented in Table 18 are the drop of viscosity from 30°C to 60°C. For all of the emulsions, viscosity decreases with the increase of temperature except SS-1. High viscous emulsions showed a higher drop of viscosity than low viscous emulsions. For CRS-2 and CRS-2P viscosity values dropped 47.2% and 48.3% whereas for SS-1L and SS-1H they are 26.6% and 2.7% at 50 rpm. This trend and a similar amount of drop was also observed for other shear rates.

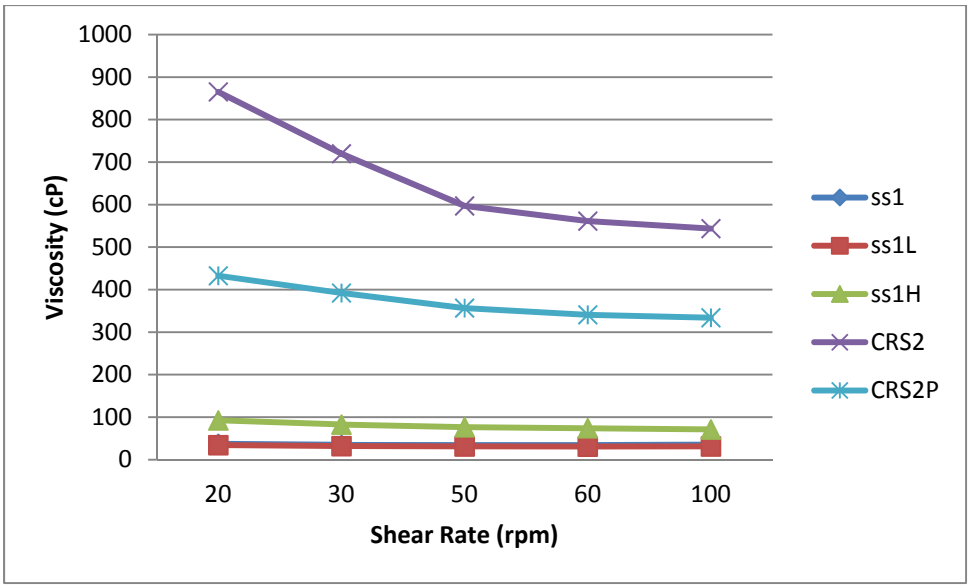

Figure 22
Effect of shear rate on viscosity at 30°C

Table 18
Drop of viscosity from 30°C to 60°C at different temperature

rpm	20	30	50	60	100
Emulsion	(%) Drop of viscosity from 30°C to 60°C				
SS-1	-68.91	-72.77	-71.73	-75.38	-80.16
SS-1L	21.95	23.15	26.56	26.66	29.92
SS-1H	15.49	8.20	2.69	0.99	-2.27
CRS-2	49.50	48.11	47.24	49.73	52.94
CRS-2P	43.66	44.75	48.35	50.89	57.59

Correlation between Water Content of Emulsion and Viscosity

Water content plays the most important role to the viscosity of the emulsion in the emulsion state. Water content is the opposite of the residue content; for example, emulsion with a water content of 32% has a residue content of 68%. In this study, ASTM D6934 was used to determine the water content of the emulsion. Table 19 shows the water content data of the emulsion and viscosity results for a 30 rpm shear rate at 30°C and summarizes the correlation equation at different shear rates. CRS-2 has the lowest water content of 31.2% and SS-1 has the highest value of 39.2%. Lower water content results in higher viscosity and higher water content results to lower viscosity. CRS-2 showed viscosity of 719.92 cP and SS-1 showed a viscosity of 34.73 cP at 30 rpm and 30°C. By carefully observing the data of Table 19, it is clear that a slight change in water content produces a big difference in viscosity of the emulsion, so it is suspected that

relationship of these two variables is either exponential or power. Several curves (linear, logarithmic, exponential, and power) were attempted to find the best correlation, and it was found that at 30°C for all RPMs a power curve fitted the data with the highest R^2 value of any type of curves. Correlation equations for different rpm and different temperatures are shown in Table 19 where x is the water content and y is the viscosity of the emulsion. Figure 23 shows the correlation of these two variables for 30 rpm and 30°C temperature.

Table 19
Correlation of water content and viscosity of the emulsion

Emulsion	Water Content (%)	Viscosity at 30 rpm and 30°C	Correlation equation for water content and viscosity
SS-1	39.2	34.73	At 20 rpm and 30°C: $y = 2E+25x^{-15.03}$ $R^2=0.9524$
SS-1L	37.2	31.92	At 30 rpm and 30°C: $y = 5E+24x^{-14.62}$ $R^2=0.9524$
SS-1H	36.2	82.49	At 50 rpm and 30°C: $y = 4E+23x^{-13.93}$ $R^2=0.9499$
CRS-2	31.2	719.92	At 60 rpm and 30°C: $y = 2E+23x^{-13.69}$ $R^2=0.9493$
CRS-2P	32.6	392.11	At 100 rpm and 30°C: $y = 6E+22x^{-13.44}$ $R^2=0.9463$
			At 20 rpm and 60°C: $y = 2E+18x^{-10.48}$ $R^2=0.7923$
			At 30 rpm and 60°C: $y = 3E+17x^{-10.01}$ $R^2=0.7732$
			At 50 rpm and 60°C: $y = 2E+16x^{-9.274}$ $R^2=0.7392$
			At 60 rpm and 60°C: $y = 2E+15x^{-8.698}$ $R^2=0.7141$
			At 100 rpm and 60°C: $y = 1E+14x^{-7.882}$ $R^2=0.6517$

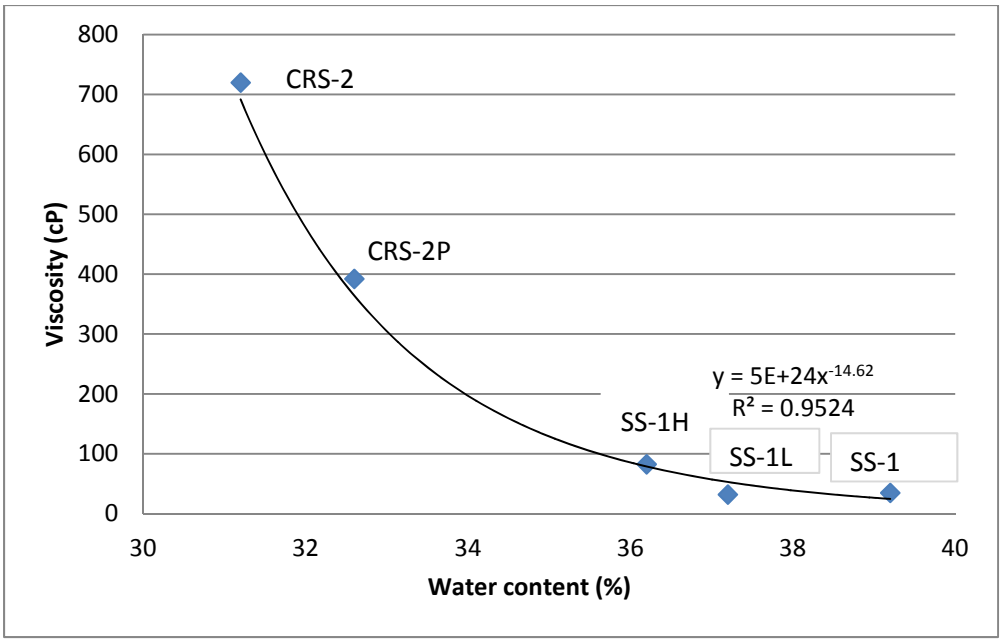

Figure 23
Correlation of water content and viscosity of the emulsion at 30 rpm and 30°C

Identification of Low and High Viscous Emulsions

A saybolt furol viscometer separates low viscosity emulsions from high viscosity emulsion with a range of saybolt furol 50-100 at 25°C and saybolt furol 200-400 at 50°C, respectively, in current Louisiana DOTD specifications. These two ranges to separate two types of emulsions are set at two different temperatures. A rotational viscometer showed a wide range of viscosity at one temperature, and results are far apart for low and high viscous emulsions. It is possible to identify the emulsion type and establish the range for them even at one single temperature using a rotational viscometer. In this study, for each data point at a certain rpm and temperature three readings were taken. Six samples of each emulsion were tested separated by two batches. Figure 24 consists of 90 readings of five emulsions at 50 rpm and 30°C, where each emulsion has 18 readings. The mean viscosity for high viscosity emulsions (CRS-2 and CRS-2P) was found to be 476.8 cP with a standard deviation of 122.96 at 50 rpm and 30°C. The range for high viscosity emulsions lies within 220 - 730 cP with 98% probability, assuming the data is normally distributed. Similarly, a mean viscosity for low viscous emulsions (SS-1, SS-1H and SS-1L) was found to be 47.27cP with a standard deviation of 20.78 cP for 54 readings and the range lies within 5 – 90 cP with 98% probability at 50 rpm and 30°C. The lower limit of high viscosity emulsion and upper limit of low viscosity emulsion showed a gap of 130 cP. These ranges and gaps are calculated for all test conditions in Table 20. At 30 rpm and 60°C where the range were 128-462 cP and 8-99 cP for high and low viscosity emulsions respectively with 98% probability.

It should be noted here that the gap between lower and upper limit of the ranges reduced significantly at 60°C, so the test condition with 50 rpm at 30°C is better for classifying or identifying the type of emulsions based on rotational viscosity data.

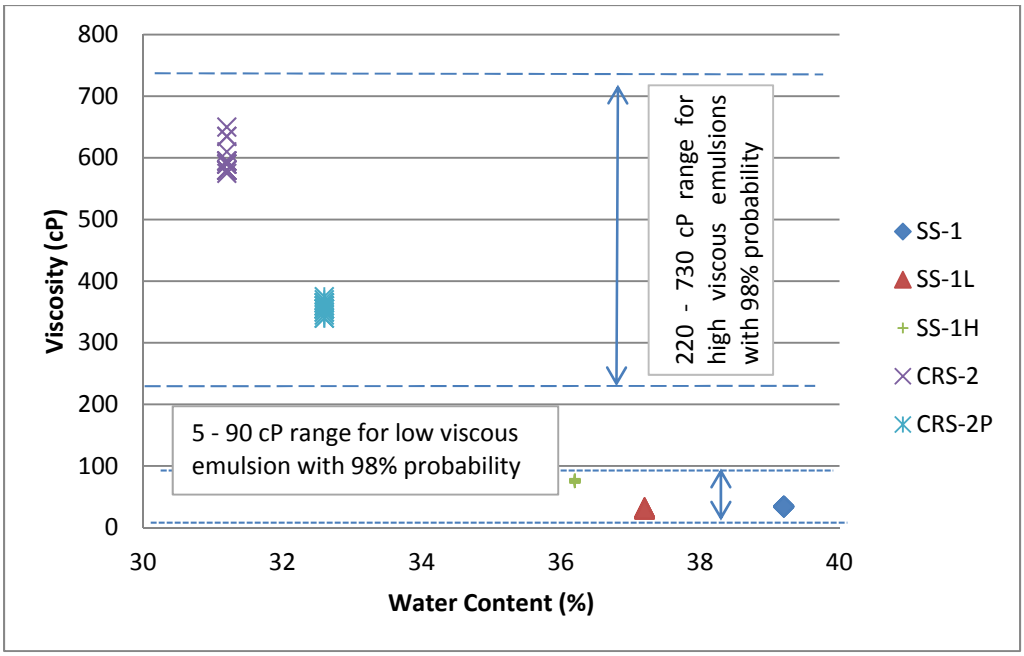

Figure 24
Viscosity limits for high and low viscous emulsions at 50 rpm and 30°C

Table 20
Viscosity range and gap for all test conditions

Test Condition	Range of viscosity (cP)		Gap
	High Viscous	Low Viscous	
30°C and 20 rpm	1102-195	111-0	84
30°C and 30 rpm	901-210	99-1	111
30°C and 50 rpm	730-220	90-5	130
30°C and 60 rpm	684-217	88-5	129
30°C and 100 rpm	661-216	84-8	132
60°C and 20 rpm	548 - 134	101 - 10	33
60°C and 30 rpm	462-128	99-8	29
60°C and 50 rpm	387-111	98-6	13
60°C and 60 rpm	349-101	97-7	4
60°C and 100 rpm	320-78	94-6	Overlap

CONCLUSIONS

Findings on Elastic Recovery and Force Ductility Relationships

Twenty asphalt emulsions were tested in this study. Eight of these are considered hard pen base asphalt emulsions, of which 2 are polymer modified. Out of 12 non-hard pen base asphalt emulsions, 6 are polymer modified. Strain sweep, frequency sweep, temperature sweep, MSCR, elastic recovery (AASHTO T301), and force ductility (AASHTO T300) tests were performed and the following specific conclusions can be drawn from this study.

- It was observed that emulsions prepared of hard pen base asphalt have relatively lower strain tolerance, i.e. relatively higher drop from initial complex modulus. At 52°C, the complex modulus at an initial 2% strain and a final 52% strain dropped 44.2% in the case of NTSS-1HM (U), and dropped 22.5% in case of CSS-1HP, both of which are made with a hard pen base asphalt. Similar observations were made at 70°C. The strain tolerances of all the emulsions without hard pen base asphalt are relatively much higher, i.e. relatively lower drop from initial complex modulus.

- Complex modulus master curves constructed at 25°C demonstrate that all of the 20 emulsion residues possess significant differences in complex modulus at lower frequencies (or higher temperatures) but they all tend to approach one glassy modulus as previously obtained for SHRP core asphalt cements.

- G*/sinδ curves drawn at temperatures from 52°C to 94°C show that hard pen base asphalt emulsions have higher stiffness than all other emulsions. One of the findings of this study is that as temperature increases, phase angle of an emulsion residue increases, reaches a maximum, and then decreases. It was observed that the maximum phase angle of all the non-hard pen polymer modified asphalt emulsion residue falls between 75° to 85°. Therefore, maximum phase angle in the range of 75° to 85° may be used as a criterion for polymer identification as observed from the 20 emulsions tested in this study.

- A general trend in MSCR test results is that as temperature increases, percent recovery decreases. All non-polymer modified emulsions follow the trend. For example, average percent recoveries of CHFRS-2P at 0.1 kPa creep stress are 72.7, 67.5, 36.8, and 38.1 respectively at 10°C, 25°C, 58°C, and 70°C.

- In this study, it was observed that the effect of creep stress on percent recovery (MSCR) is logarithmic. A general trend observed is that as the creep stress increases, the percent recovery decreases.

- A Burgers model prepared for 0.1kPa creep stress and recovery at 2.2 kPa stiffness temperature demonstrates that average Maxwell viscosity, η_0, values of polymer modified emulsions are higher than those of non-polymer modified and non-hard pen base asphalt emulsions. In contrast, the average Kelvin viscosity, η_1, values of polymer modified emulsions are significantly lower than those of non-polymer modified and non-hard pen base asphalt emulsions.

- A significant finding of this study is that higher percent recovery values of MSCR indicate the presence of polymer and MSCR percent recovery is correlated with the elastic recovery of AASHTO T301. It was observed that the highest coefficient of determination of linear correlation was obtained between MSCR percent recovery at 58°C and elastic recovery (AASHTO T301) at 10°C. For this strongest relationship, R^2 values for 0.1 kPa and 3.2 kPa creep stresses are 0.961 and 0.938, respectively. Therefore, MSCR at 58°C has been recommended as a criterion for polymer identification. At 0.1kPa creep stress, a minimum percent recovery of 25 and at 3.2kPa, a minimum percent recovery of 9 is recommended to identify the presence of polymer.

- It was concluded from this study that percent recovery of MSCR and phase angle can be used to replace force ductility requirements (AASHTO T300). It is recommended that at 58°C, a maximum phase angle of 81° and a minimum MSCR percent recovery (at 0.1kPa creep stress) of 30 are specified to replace the force ductility test (AASHTO T300). These criteria are applicable for emulsion residues prepared according to the low temperature evaporative method specified in ASTM D7497.

Findings on Recovery Methods

On the basis of the results on recovery methods, the following conclusions can be drawn:

- The new recovery process proposed in the study using a vacuum drying oven is the most efficient low temperature method to ensure complete drying of the sample within a short period of time. This method ensures two benefits at the same time. One is higher drying of the sample relative to any other methods currently in practice and the other is the system which is totally void of air; theoretically, this method produces a residue that will not

experience any oxidative aging. For neat emulsions, this method produces residue that is not unnecessarily aged and similar to the base binder in stiffness which validates the above statement.

- Curing time can be reduced by up to six hours using this method. Six hours of curing time successfully identified the improvement of polymer and latex modification. It can also differentiate between polymer, latex, and neat emulsion within this period of time. Although in this study only rapid setting emulsion is used for polymer development with respect to time, further research is needed to verify the time reduction possibility and the rate of the polymer network development using slow setting emulsions.

- From the evaluation of the results collected, it can be concluded that the proposed low temperature vacuum drying method allows for the recovery of modified binders from emulsions without degrading the polymer network.

- Some fundamental behavior of the emulsion recovery process is identified by this study. Curing time plays the most important role in stiffness gain; increase of stiffness depends much more on curing time than high curing temperature for a short period of time.

- It is possible that an emulsion can show a higher stiffness value even if it has slightly higher remaining moisture after sufficient curing time is given, which is contrary to the current understanding.

Findings on Rotational Viscosity

On the basis of the viscosity results presented, the following specific conclusions can be drawn:

- This study proposes the use of a rotational viscometer to find the viscosity of the emulsion while in the emulsion state. Results obtained by following the new test procedure proposed in the study were promising and with good repeatability. The new test procedure proposed comprises some slight changes in the current AASHTO T 316 without any equipment modifications thus eliminating the need for buying new equipment; AASHTO T 316 is widely practiced by most of the contractors and state agencies to evaluate the viscosity of asphalt binders.

- Two ideal test conditions have been found to evaluate the viscosity of the emulsion at the emulsion state based on data repeatability, those are 50 rpm at 30°C and 30 rpm at 60°C.

- Emulsions are thixotropic liquids. Thixotropic effects on the viscosity of the emulsion using rotational viscometer is unavoidable, so it is suggested that the time of the reading taken should also be reported with the temperature and shear rate.

- A strong correlation has been found between water content and emulsion viscosity at 30°C temperature with an R^2 value of more than 0.94.

- The current specification of viscosity range for low and high viscous emulsions using saybolt furol viscometer to ensure quality control and quality assurance can be replaced by the rotational viscometer. The recommended range are 220 - 730 cP and 5 - 90 cP with 98% probability at 50 rpm and 30°C for high and low viscous emulsions, respectively.

RECOMMENDATIONS

It is recommended that MSCR (AASHTO TP70) at 58°C be adopted to replace elastic recovery test (AASHTO T301). At 0.1kPa creep stress, a minimum percent recovery of 25, and at 3.2kPa, a minimum percent recovery of 9 are recommended to identify the presence of polymer.

Also, it is also recommended that the percent recovery of MSCR and phase angle be used to replace force ductility requirements (AASHTO T300). Test temperature should be conducted at 58°C, with a maximum phase angle of 81° and a minimum MSCR percent recovery (at 0.1kPa creep stress) of 30 to replace force ductility test (AASHTO T300).

Further research is recommended to determine a better DSR-based parameter to replace force ductility test. A new low temperature low duration residue recovery method called 'vacuum dry method' has been developed and proposed. New specifications for emulsion state viscosity have been proposed using a rotational viscometer.

REFERENCES

1. Field Guide for Polymer Modified Asphalt Emulsions- Composition, Uses and Specifications for Surface Treatments. Federal Highway Administration (FHWA). Washington, D.C., 2009.

2. D'Angelo, J. New High-Temperature Binder Specification Using Multistress Creep and Recovery. In *Development in Asphalt Binder Specifications*. Transportation Research Circular, No. E-C147, 2010.

3. Daranga, C., C. Clopotel, and H. Bahia. Replacing the Elastic Recovery Test of Asphalt Binders with a DSR Test. In *Development of Protocol and Relationship to Binder Fatigue*. Poster presentation at 89th Annual Meeting of the Transportation Research Board, Washington, D.C., 2010.

4. D'Angelo, J. A., Dongre, R., and G. Reinke. *Creep and Recovery. Public Roads*. Vol. 70 (5). Publication FHWA-HRT-07-003. FHWA, U.S. Department of Transportation, 2007.

5. Anderson, M. Evaluation of DSR Creep-Recovery Testing as a Replacement for PG Plus Tests. AMAP Annual Meeting, Boston, MA, 2007.

6. Clopotel, C. S., and H. U. Bahia. Importance of Elastic Recovery in the DSR for Binders and Mastics. *Engineering Journal*. Vol. 16(4), 2012, pp. 99-106.

7. Johnston, J. B., and G. King. Using Polymer Modified Asphalt Emulsions in Surface Treatments, *A Federal Lands Highway Interim Report*, 2008.

8. Anderson, D. I., and M. L. Wiley. Force Ductility – An Asphalt Performance Indicator, *Journal of the Association of Asphalt Paving Technologists*, Vol. 45, 1976, pp. 25-41.

9. Anderson, M. Force Ductility Testing of Asphalt Binders, *Asphalt Magazine of the Asphalt Institute*, Vol. 18(2), 2003.

10. Shuler, T. S., and C. K. Adams, and M. Lamborn. Asphalt-Rubber Binder Laboratory Performance. *Texas State Department of Highways and Public Transportation (SDHPT) Research Report 347-1F*, Texas Transportation Institute, College Station, Texas, 1985.

11. Shuler, T. S., J. H. Collins, and J. P. Kirkpatrick. Polymer-Modified Asphalt Properties Related to Asphalt Concrete Performance. *Asphalt Rheology: Relationship to Mixture ASTM STP 941*, 1987, pp. 179-193.

12. King, G., H. King, R. D. Pavlovich, A. L. Epps, K. Prithvi. Additives in Asphalt. Presented at the 75th Anniversary Historical Review of the Association of Asphalt Paving Technologists, 1998.

13. Glover, C. J., R. R. Davison, C. H. Domke, Y. Ruan, Y., P. Juristyarini, D. B. Knorr, and S. H. Jung. Development of a New Method for Assessing Asphalt Binder Durability with Field Validation, *Texas Transportation Report No. 0-1872-2*, 2005.

14. Angelo, D'. Development of Standard Practice for Superpave Plus Specifications. *Presented at the North East Asphalt User/Producer Group (NEAUPG) Conference*, Burlington, VT, 2005.

15. Airey, G. D. Fundamental Binder and Practical Mixture Evaluation of Polymer Modified Bituminous Materials, *International Journal of Pavement Engineering*, Vol. 5(3), 2004, pp. 137-151.

16. Takamura, K. Pavement Preservation Using the SBR Latex Modified Asphalt Emulsion. *BASF Corporation, Presented at the International Latex Conference*, Charlotte, NC, 2005.

17. Lewandowski, L. Performance Based Emulsion Testing- Residue Testing. AEMA-ARRA-ISSA Annual Meeting. Sunny Isles Beach, Florida, 2010.

18. King, G., King, H., Galehouse, L., Voth, M., Lewandowski, L., Lubbers, C., and P. Morris. Field Validation of Performance-Based Polymer-Modified Emulsion Residue Tests: The FLH Study. Compendium of Papers from the First International Conference on Pavement Preservation. Newport Beach, CA, 2010.

19. Hanz, A. J., Arega, Z. A., and H. U. Bahia. Rheological Behavior of Emulsion Residues Produced by Evaporative Recovery Method. In *Transportation Research Record: Journal of the Transportation Research Board*. No. 2179, Transportation Research Board of the National Academies, Washington, D.C., 2010, pp. 102-108.

20. Reinke, G. MTE Technical Report- Obtaining and Testing Emulsion Residues. Mathy Technology and Technical Services, Inc. Onalaska, WI, 2010.

21. Bahia, H. U., Hanson, D. I., Zeng, M., Zhai, H., Khatri, M. A., and R. M. Anderson. Characterization of Modified Asphalt Binders in Superpave Mix Design. NCHRP Report 459. Transportation Research Board- National Research Council, Washington, D.C., 2001.

22. Takamura, K. Comparison of Emulsion Residues Recovered by Forced Air Flow and RTFO Drying. Presented at AEMA/ISSA joint Annual Meeting. Asphalt Emulsion Manufacturers association, Amelia Island Fla., March 13-16. 2000.

23. Kadrmas, A. Using Dynamic Shear Rheometer and Multiple Stress Creep Recovery to Compare Emulsion Residue Recovery Methods. Presented at 88th Annual Meeting of The Transportation Research Board, Washington D.C., 2009.

24. *Transportation Research Circular E-C122: Asphalt Emulsion Technology Review of Asphalt Emulsion Residue Procedures*. Transportation Research Board of the National Academies, Washington, D.C., 2007.

25. D' Angelo, J. Effect of Polymer- Asphalt Binder Compatibility and Cross-Link Density of Non-Recoverable Compliance in the MSCR Test Method. Presented at Southeast Asphalt User/Producer Group, San Antonio, Tex., 2007.

APPENDIX

Emulsion	G*/sinδ at 58°C	% Recovery (MSCR) at 58°C and 0.1 kpa		Recommendation
CMS-1P	1.403666667	35.1	Non Hard Pen Base Emulsion	Polymer identification by MSCR is recommended for emulsions having G*/sinδ value less than 10 kPa
CRS-2 (U)	1.568666667	2.9		
SS-1 (U)	1.753666667	5.4		
CRS-2 (B)	1.8295	7.7		
SS-1 (E)	1.846	4.9		
CRS-2 (E)	1.856333333	7.1		
SS-1 (B)	2.014666667	3.7		
SS-1L	2.962333333	53.1		
CRS-2P (B)	2.733	25.9		
PME	3.178333333	36		
CRS-2P (E)	3.857666667	29.7		
CHFRS-2P	5.363333333	36.8		
SS-1HP	5.692666667	24.1	Hard Pen Base Emulsion	
SS-1H (U)	8.3245	6.5		
SS-1H (B)	8.2765	11.6		
CSS-1HP	22.12333333	56.7		Polymer identification of very hard pen emulsion by MSCR is not recommended[2]
NTSS-1HM (U)	41.29666667	12.8		
NTSS-1HM (C)[1]	>100	25.8		
Fog Seal[1]	>100	27		
NTSS-1HM (B)[1]	>100	39.7		

[1]Values of G*/sinδ for these binders are extrapolated to 58°C

[2]High stiffness of these binders may contribute more to high percent recovery than polymer modification.

2.2 kPa Temperature MSCR

Temperature @ (G*/sinδ= 2.2kPa) (55°c)									
Shear Stress		0.1 kPa		0.2 kPa		0.5 kPa		3.2 kPa	
Parameter		Re %	J_{nr}	Re %	J_{nr}	Re %	J_{nr}	Re %	J_{nr}
CMS-1P (E)	MT.1	44.32	0.15	46.63	0.14	38.35	0.17	22.52	0.24
	MT.2	44.27	0.14	46.99	0.14	38.35	0.163	24.04	0.23
	MT.3	40.44	0.15	43.32	0.14	35.85	0.162	23.39	0.22
	AVE.	43.01	0.1476	45.65	0.1408	37.52	0.165	23.32	0.231
	St.Dev	2.222	0.0025	2.022	0.003	1.441	0.004	0.761	0.011

Temperature @ (G*/sinδ= 2.2kPa) (56°c)									
Shear Stress		0.1 kPa		0.2 kPa		0.5 kPa		3.2 kPa	
Parameter		Re %	J_{nr}	Re %	J_{nr}	Re %	J_{nr}	Re %	J_{nr}
CRS-2 (U)	MT.1	5.63	0.69	4.00	0.71	1.69	0.74	-0.48	0.85
	MT.2	6.31	0.59	4.25	0.60	2.04	0.62	-0.25	0.71
	MT.3	6.64	0.60	4.10	0.62	2.09	0.64	-0.29	0.73
	AVE.	6.191	0.6229	4.116	0.6422	1.937	0.668	-0.34	0.763
	St.Dev	0.517	0.0568	0.125	0.0562	0.217	0.061	0.124	0.078

Temperature @ (G*/sinδ= 2.2kPa) (57°c)									
Shear Stress		0.1 kPa		0.2 kPa		0.5 kPa		3.2 kPa	
Parameter		Re %	J_{nr}	Re %	J_{nr}	Re %	J_{nr}	Re %	J_{nr}
CRS-2 (B)	MT.1	8.21	0.45	6.20	0.46	3.49	0.49	0.07	0.57
	MT.2	6.94	0.46	5.65	0.47	3.09	0.49	0.01	0.56
	MT.3	8.00	0.45	6.12	0.46	3.69	0.49	0.03	0.57
	AVE.	7.716	0.4521	5.988	0.4655	3.424	0.486	0.034	0.567
	St.Dev	0.683	0.0035	0.294	0.0016	0.307	4E-04	0.029	0.004

Temperature @ (G*/sinδ= 2.2kPa) (57°c)									
Shear Stress		0.1 kPa		0.2 kPa		0.5 kPa		3.2 kPa	
Parameter		Re %	J_{nr}	Re %	J_{nr}	Re %	J_{nr}	Re %	J_{nr}
CRS-2 (E)	MT.1	7.94	0.69	5.51	0.71	2.36	0.75	-0.21	0.87
	MT.2	5.01	0.70	3.47	0.71	1.64	0.74	-0.08	0.83
	MT.3	4.06	0.73	2.79	0.74	1.89	0.76	-0.16	0.85
	AVE.	5.669	0.7029	3.922	0.7235	1.96	0.75	-0.15	0.851
	St.Dev	2.019	0.0199	1.418	0.0153	0.363	0.009	0.063	0.022

Temperature @ (G*/sinδ= 2.2kPa) (59°c)									
Shear Stress		0.1 kPa		0.2 kPa		0.5 kPa		3.2 kPa	
Parameter		Re %	J_{nr}	Re %	J_{nr}	Re %	J_{nr}	Re %	J_{nr}
CRS-2P (B)	MT.1	20.85	0.37	19.76	0.38	14.13	0.41	4.20	0.53
	MT.2	9.18	0.37	20.70	0.35	14.52	0.38	4.42	0.49
	MT.3	19.55	0.35	16.67	0.37	10.53	0.40	2.41	0.51
	AVE.	16.53	0.3623	19.04	0.3628	13.06	0.398	3.678	0.509
	St.Dev	6.396	0.0088	2.109	0.0152	2.201	0.016	1.101	0.021

Temperature @ (G*/sinδ= 2.2kPa) (63°c)									
Shear Stress		0.1 kPa		0.2 kPa		0.5 kPa		3.2 kPa	
Parameter		Re %	J_{nr}	Re %	J_{nr}	Re %	J_{nr}	Re %	J_{nr}
CRS-2P (E)	MT.1	30.44	0.42	22.03	0.48	11.35	0.58	0.80	0.85
	MT.2	30.95	0.41	27.92	0.45	15.81	0.56	1.81	0.85
	MT.3	21.26	0.46	23.70	0.48	14.51	0.57	1.81	0.82
	AVE.	27.55	0.4278	24.55	0.4697	13.89	0.572	1.475	0.84
	St.Dev	5.454	0.0283	3.035	0.0191	2.291	0.01	0.582	0.016

Temperature @ (G*/sinδ= 2.2kPa) (80°c)									
Shear Stress		0.1 kPa		0.2 kPa		0.5 kPa		3.2 kPa	
Parameter		Re %	J_{nr}	Re %	J_{nr}	Re %	J_{nr}	Re %	J_{nr}
CSS-1HP (E)	MT.1	91.58	0.03	86.68	0.04	47.36	0.21	1.54	0.87
	MT.2	92.30	0.02	86.28	0.04	46.05	0.22	1.10	1.00
	MT.3	92.87	0.02	87.16	0.04	49.23	0.20	0.74	1.10
	AVE.	92.25	0.0221	86.71	0.0405	47.55	0.208	1.126	0.99
	St.Dev	0.65	0.0032	0.441	0.0029	1.599	0.011	0.397	0.116

Temperature @ (G*/sinδ= 2.2kPa) (94°c)									
Shear Stress		0.1 kPa		0.2 kPa		0.5 kPa		3.2 kPa	
Parameter		Re %	J_{nr}	Re %	J_{nr}	Re %	J_{nr}	Re %	J_{nr}
FOG SEAL (C)	MT.1	8.49	0.41	6.10	0.42	3.08	0.45	0.12	0.50
	MT.2	9.10	0.42	6.91	0.43	3.36	0.46	0.15	0.52
	MT.3	8.29	0.42	6.21	0.43	3.13	0.46	0.18	0.52
	AVE.	8.629	0.4149	6.404	0.4295	3.192	0.455	0.151	0.515
	St.Dev	0.419	0.0066	0.438	0.0052	0.149	0.007	0.033	0.01

Temperature @ (G*/sinδ= 2.2kPa) (79°c)									
Shear Stress		0.1 kPa		0.2 kPa		0.5 kPa		3.2 kPa	
Parameter		Re %	J_{nr}	Re %	J_{nr}	Re %	J_{nr}	Re %	J_{nr}
NTSS-1HM (U)	MT.1	13.44	0.46	9.52	0.51	4.14	0.59	-0.41	0.77
	MT.2	12.23	0.50	8.29	0.54	3.26	0.61	-0.41	0.76
	MT.3	14.29	0.49	9.86	0.53	4.04	0.61	-0.39	0.77
	AVE.	13.32	0.4846	9.222	0.5246	3.813	0.603	-0.4	0.765
	St.Dev	1.036	0.0216	0.822	0.0174	0.48	0.013	0.014	0.005

Temperature @ (G*/sinδ= 2.2kPa) (96°c)									
Shear Stress		0.1 kPa		0.2 kPa		0.5 kPa		3.2 kPa	
Parameter		Re %	J_{nr}	Re %	J_{nr}	Re %	J_{nr}	Re %	J_{nr}
NTSS-1HM (B)	MT.1	22.29	0.47	16.77	0.50	7.74	0.58	0.15	0.79
	MT.2	19.86	0.42	14.70	0.44	7.21	0.49	0.51	0.62
	MT.3								
	AVE.	21.07	0.441	15.73	0.4739	7.474	0.54	0.331	0.704
	St.Dev	1.72	0.0362	1.461	0.0411	0.373	0.064	0.256	0.116

Temperature @ (G*/sinδ= 2.2kPa) (90°c)									
Shear Stress		0.1 kPa		0.2 kPa		0.5 kPa		3.2 kPa	
Parameter		Re %	J_{nr}	Re %	J_{nr}	Re %	J_{nr}	Re %	J_{nr}
NTSS-1HM (C)	MT.1	14.17	0.29	11.36	0.31	6.20	0.34	0.49	0.42
	MT.2	17.29	0.29	13.24	0.31	7.44	0.35	0.79	0.44
	MT.3								
	AVE.	15.73	0.2916	12.3	0.3095	6.821	0.344	0.641	0.434
	St.Dev	2.21	0.0035	1.331	0.0008	0.877	0.004	0.215	0.014

Temperature @ (G*/sinδ= 2.2kPa) (57°c)									
Shear Stress		0.1 kPa		0.2 kPa		0.5 kPa		3.2 kPa	
Parameter		Re %	J_{nr}	Re %	J_{nr}	Re %	J_{nr}	Re %	J_{nr}
SS-1 (U)	MT.1	7.32	0.64	4.91	0.67	2.02	0.70	-0.46	0.81
	MT.2	6.82	0.58	4.85	0.60	2.37	0.64	-0.23	0.74
	MT.3	10.93	0.52	7.27	0.55	3.07	0.61	-0.28	0.73
	AVE.	8.355	0.579	5.68	0.6071	2.487	0.65	-0.32	0.762
	St.Dev	2.245	0.0595	1.38	0.0562	0.537	0.05	0.125	0.045

Temperature @ (G*/sinδ= 2.2kPa) (57°c)									
Shear Stress		0.1 kPa		0.2 kPa		0.5 kPa		3.2 kPa	
Parameter		Re %	J_{nr}	Re %	J_{nr}	Re %	J_{nr}	Re %	J_{nr}
SS-1 (B)	MT.1	4.04	0.49	4.16	0.49	2.24	0.60	0.44	0.59
	MT.2	8.02	0.50	6.13	0.51	3.33	0.53	0.61	0.60
	MT.3	5.66	0.49	7.11	0.51	4.13	0.53	0.46	0.62
	AVE.	5.907	0.495	5.8	0.504	3.235	0.556	0.502	0.603
	St.Dev	2	0.0017	1.503	0.0088	0.947	0.041	0.093	0.016

Temperature @ (G*/sinδ= 2.2kPa) (57°c)									
Shear Stress		0.1 kPa		0.2 kPa		0.5 kPa		3.2 kPa	
Parameter		Re %	J_{nr}	Re %	J_{nr}	Re %	J_{nr}	Re %	J_{nr}
SS-1 (E)	MT.1	6.10	0.62	4.49	0.64	2.04	0.67	-0.33	0.76
	MT.2	7.08	0.57	4.96	0.59	2.14	0.62	-0.30	0.72
	MT.3	12.90	0.51	8.52	0.55	3.49	0.60	-0.32	0.75
	AVE.	8.692	0.565	5.989	0.5889	2.556	0.633	-0.31	0.743
	St.Dev	3.679	0.0535	2.203	0.0447	0.81	0.034	0.016	0.023

Temperature @ (G*/sinδ= 2.2kPa) (68°c)									
Shear Stress		0.1 kPa		0.2 kPa		0.5 kPa		3.2 kPa	
Parameter		Re %	J_{nr}	Re %	J_{nr}	Re %	J_{nr}	Re %	J_{nr}
SS-1H (U)	MT.1	4.35	0.63	3.02	0.65	1.42	0.67	-0.37	0.76
	MT.2	5.82	0.59	3.68	0.62	1.45	0.65	-0.31	0.74
	MT.3	2.35	0.59	1.67	0.60	0.61	0.61	-0.25	0.67
	AVE.	4.174	0.605	2.791	0.6208	1.16	0.645	-0.31	0.721
	St.Dev	1.741	0.0213	1.021	0.0239	0.473	0.03	0.062	0.049

Temperature @ (G*/sinδ= 2.2kPa) (68°c)									
Shear Stress		0.1 kPa		0.2 kPa		0.5 kPa		3.2 kPa	
Parameter		Re %	J_{nr}	Re %	J_{nr}	Re %	J_{nr}	Re %	J_{nr}
SS-1H (B)	MT.1	8.31	0.60	5.76	0.63	2.88	0.66	-0.09	0.77
	MT.2	10.84	0.55	7.69	0.58	3.66	0.62	0.03	0.74
	MT.3	12.84	0.54	9.41	0.57	4.16	0.62	0.01	0.76
	AVE.	10.66	0.5653	7.621	0.5911	3.567	0.637	-0.02	0.758
	St.Dev	2.267	0.0335	1.824	0.0323	0.643	0.021	0.063	0.013

Temperature @ (G*/sinδ= 2.2kPa) (61°c)									
Shear Stress		0.1 kPa		0.2 kPa		0.5 kPa		3.2 kPa	
Parameter		Re %	J_{nr}	Re %	J_{nr}	Re %	J_{nr}	Re %	J_{nr}
SS-1L (U)	MT.1	63.51	0.11	59.27	0.13	42.76	0.20	9.41	0.47
	MT.2	59.63	0.14	54.20	0.16	36.96	0.24	6.57	0.54
	MT.3	58.54	0.14	52.72	0.16	36.79	0.24	6.35	0.53
	AVE.	60.56	0.1283	55.4	0.1513	38.84	0.23	7.444	0.511
	St.Dev	2.608	0.0124	3.435	0.0164	3.398	0.022	1.709	0.039

Temperature @ (G*/sinδ= 2.2kPa) (67°c)									
Shear Stress		0.1 kPa		0.2 kPa		0.5 kPa		3.2 kPa	
Parameter		Re %	J_{nr}	Re %	J_{nr}	Re %	J_{nr}	Re %	J_{nr}
CHFRS-2P (E)	MT.1	28.89	0.43	23.28	0.47	13.38	0.57	1.21	0.82
	MT.2	31.87	0.45	27.49	0.49	16.14	0.60	1.99	0.87
	MT.3	42.24	0.33	38.53	0.37	26.37	0.47	3.33	0.82
	AVE.	34.34	0.4015	29.77	0.442	18.63	0.546	2.177	0.835
	St.Dev	7.007	0.0598	7.878	0.0666	6.842	0.067	1.069	0.027

Temperature @ (G*/sinδ= 2.2kPa) (62°c)									
Shear Stress		0.1 kPa		0.2 kPa		0.5 kPa		3.2 kPa	
Parameter		Re %	J_{nr}	Re %	J_{nr}	Re %	J_{nr}	Re %	J_{nr}
PME (E)	MT.1	0.93	0.06	28.29	0.43	16.15	0.58	2.32	0.87
	MT.2	46.30	0.33	41.74	0.37	26.83	0.50	3.90	0.86
	MT.3	42.09	0.35	37.64	0.39	25.27	0.52	4.34	0.83
	AVE.	44.2	0.3377	39.69	0.381	26.05	0.507	4.119	0.847
	St.Dev	2.974	0.0173	2.9	0.019	1.1	0.014	0.313	0.017

Temperature @ (G*/sinδ= 2.2kPa) (66°c)									
Shear Stress		0.1 kPa		0.2 kPa		0.5 kPa		3.2 kPa	
Parameter		Re %	J_{nr}	Re %	J_{nr}	Re %	J_{nr}	Re %	J_{nr}
SS-1HP (E)	MT.1	11.24	0.68	9.71	0.70	5.87	0.76	0.85	0.98
	MT.2	11.53	0.68	9.17	0.71	5.55	0.77	0.81	0.97
	MT.3	97.63	0.00	7.16	0.65	4.99	0.72	0.86	0.92
	AVE.	11.39	0.6792	8.68	0.6872	5.472	0.75	0.839	0.954
	St.Dev	0.207	0.0006	1.341	0.029	0.447	0.023	0.022	0.034

MSCR @ 10°C, 25°C, 58°C& 70°C

Asphalt Binder		10° c				25° c				58° c				70° c			
		.1 kPa		3.2 kPa		.1 kPa		3.2 kPa		.1 kPa		3.2 kPa		.1 kPa		3.2 kPa	
		Re %	Jnr	Re %	Jnr	Re %	Jnr	Re %	Jnr	Re %	Jnr	Re %	Jnr	Re %	Jnr	Re %	Jnr
CMS-1P (E)	MT.1	59.9	0.0	60.5	0.0	53.2	0.0	45.3	0.0	33.0	0.4	12.6	0.6	35.5	1.4	-1.5	2.9
	MT.2	58.9	0.0	56.9	0.0	44.7	0.0	45.9	0.0	38.2	0.4	14.7	0.6	27.3	1.7	-1.6	3.0
	MT.3	57.6	0.0	56.0	0.0	42.9	0.0	43.9	0.0	34.1	0.4	10.5	0.7	24.2	2.1	-2.7	3.5
	AVE.	58.8	0.0	57.8	0.0	46.9	0.0	45.1	0.0	35.1	0.4	12.6	0.6	29.0	1.7	-1.9	3.1
	St.Dev	1.2	0.0	2.4	0.0	5.5	0.0	1.1	0.0	2.7	0.0	2.1	0.1	5.8	0.3	0.7	0.4

Asphalt Binder		10° c				25° c				58° c				70° c			
		.1 kPa		3.2 kPa		.1 kPa		3.2 kPa		.1 kPa		3.2 kPa		.1 kPa		3.2 kPa	
		Re %	Jnr	Re %	Jnr	Re %	Jnr	Re %	Jnr	Re %	Jnr	Re %	Jnr	Re %	Jnr	Re %	Jnr
CSS-1HP (E)	MT.1	104.5	0.0	77.1	0.0	83.4	0.0	76.9	0.0	53.7	0.0	35.9	0.0	69.7	0.0	9.1	0.2
	MT.2	95.3	0.0	73.7	0.0	82.6	0.0	76.2	0.0	58.0	0.0	34.0	0.0	78.1	0.0	10.1	0.2
	MT.3	89.1	0.0	69.2	0.0	78.2	0.0	77.7	0.0	58.5	0.0	38.8	0.0	81.1	0.0	12.0	0.2
	AVE.	99.9	0.0	73.3	0.0	81.4	0.0	76.9	0.0	56.7	0.0	36.2	0.0	76.3	0.0	10.4	0.2
	St.Dev	6.6	0.0	4.0	0.0	2.8	0.0	0.7	0.0	2.6	0.0	2.4	0.0	5.9	0.0	1.5	0.0

Asphalt Binder		10° c				25° c				58° c				70° c			
		.1 kPa		3.2 kPa		.1 kPa		3.2 kPa		.1 kPa		3.2 kPa		.1 kPa		3.2 kPa	
		Re %	Jnr	Re %	Jnr	Re %	Jnr	Re %	Jnr	Re %	Jnr	Re %	Jnr	Re %	Jnr	Re %	Jnr
CRS-2 (E)	MT.1	64.1	0.0	63.9	0.0	51.0	0.0	51.2	0.0	6.7	0.4	0.4	0.5	0.9	2.2	-2.5	2.7
	MT.2	58.2	0.0	61.6	0.0	51.6	0.0	50.9	0.0	11.0	0.4	0.3	0.6	0.9	2.4	-2.7	3.0
	MT.3	57.4	0.0	63.6	0.0	44.4	0.0	50.7	0.0	3.7	0.5	0.5	0.6	-0.4	2.3	-2.6	2.7
	AVE.	59.9	0.0	63.1	0.0	49.0	0.0	51.0	0.0	7.1	0.5	0.4	0.6	0.5	2.3	-2.6	2.8
	St.Dev	3.7	0.0	1.2	0.0	4.0	0.0	0.2	0.0	3.6	0.0	0.1	0.0	0.8	0.1	0.1	0.1

Asphalt Binder		10° c				25° c				58° c				70° c			
		.1 kPa		3.2 kPa		.1 kPa		3.2 kPa		.1 kPa		3.2 kPa		.1 kPa		3.2 kPa	
		Re %	Jnr	Re %	Jnr	Re %	Jnr	Re %	Jnr	Re %	Jnr	Re %	Jnr	Re %	Jnr	Re %	Jnr
CRS-2P (E)	MT.1	76.7	0.0	74.8	0.0	63.3	0.0	63.0	0.0	29.7	0.2	7.7	0.2	22.4	0.7	1.0	1.1
	MT.2	71.6	0.0	72.2	0.0	62.8	0.0	62.2	0.0	28.8	0.2	9.2	0.3	28.8	0.6	2.3	1.2
	MT.3	79.9	0.0	50.7	0.0	51.7	0.0	62.9	0.0	30.8	0.2	11.4	0.2	31.8	0.6	3.3	1.2
	AVE.	76.0	0.0	65.9	0.0	63.0	0.0	62.7	0.0	29.7	0.2	9.5	0.2	30.3	0.6	2.2	1.2
	St.Dev	4.2	0.0	13.2	0.0	0.4	0.0	0.4	0.0	1.0	0.0	1.8	0.0	2.2	0.0	1.1	0.0

Asphalt Binder		10° c				25° c				58° c				70° c			
		.1 kPa		3.2 kPa		.1 kPa		3.2 kPa		.1 kPa		3.2 kPa		.1 kPa		3.2 kPa	
		Re %	Jnr	Re %	Jnr	Re %	Jnr	Re %	Jnr	Re %	Jnr	Re %	Jnr	Re %	Jnr	Re %	Jnr
CRS-2 (B)	MT.1	54.4	0.0	53.1	0.0	37.6	0.0	37.1	0.0	5.8	0.5	0.1	0.6	-0.1	2.4	-2.6	2.8
	MT.2	54.7	0.0	54.0	0.0	37.3	0.0	37.0	0.0	5.4	0.5	0.2	0.6	-0.6	2.4	-2.6	2.8
	MT.3	57.4	0.0	50.2	0.0	38.8	0.0	37.7	0.0	11.9	0.5	0.2	0.6	2.4	2.4	-2.7	3.0
	AVE.	55.5	0.0	52.4	0.0	37.9	0.0	37.3	0.0	7.7	0.5	0.2	0.6	0.6	2.4	-2.6	2.8
	St.Dev	1.7	0.0	1.9	0.0	0.8	0.0	0.4	0.0	3.7	0.0	0.0	0.0	1.6	0.0	0.1	0.1

Asphalt Binder		10° c				25° c				58° c				70° c			
		.1 kPa		3.2 kPa		.1 kPa		3.2 kPa		.1 kPa		3.2 kPa		.1 kPa		3.2 kPa	
		Re %	Jnr	Re %	Jnr	Re %	Jnr	Re %	Jnr	Re %	Jnr	Re %	Jnr	Re %	Jnr	Re %	Jnr
CRS-2P (B)	MT.1	60.9	0.0	60.3	0.0	51.6	0.0	47.4	0.0	27.4	0.2	9.6	0.3	18.0	1.1	1.6	1.6
	MT.2	61.9	0.0	59.0	0.0	49.1	0.0	47.4	0.0	30.1	0.2	12.7	0.3	32.8	0.9	1.4	1.6
	MT.3	57.7	0.0	55.0	0.0	43.6	0.0	43.7	0.0	20.3	0.3	7.2	0.5	14.3	1.5	-0.3	2.1
	AVE.	60.2	0.0	58.1	0.0	48.1	0.0	46.2	0.0	25.9	0.3	9.8	0.4	21.7	1.1	0.9	1.8
	St.Dev	2.2	0.0	2.8	0.0	4.1	0.0	2.1	0.0	5.1	0.1	2.7	0.1	9.8	0.3	1.0	0.3

Asphalt Binder		10° c				25° c				58° c				70° c			
		.1 kPa		3.2 kPa		.1 kPa		3.2 kPa		.1 kPa		3.2 kPa		.1 kPa		3.2 kPa	
		Re %	Jnr	Re %	Jnr	Re %	Jnr	Re %	Jnr	Re %	Jnr	Re %	Jnr	Re %	Jnr	Re %	Jnr
FOG SEAL (C)	MT.1									6.3	0.0	25.1	0.0	13.6	0.0	11.3	0.0
	MT.2									29.4	0.0	28.0	0.0	14.4	0.0	12.3	0.0
	MT.3									24.6	-0.2	27.3	0.0	14.9	0.0	12.8	0.0
	AVE.									27.0	-0.1	26.8	0.0	14.3	0.0	12.1	0.0
	St.Dev									3.4	0.1	1.5	0.0	0.7	0.0	0.8	0.0

Asphalt Binder		10° c				25° c				58° c				70° c			
		.1 kPa		3.2 kPa		.1 kPa		3.2 kPa		.1 kPa		3.2 kPa		.1 kPa		3.2 kPa	
		Re %	Jnr	Re %	Jnr	Re %	Jnr	Re %	Jnr	Re %	Jnr	Re %	Jnr	Re %	Jnr	Re %	Jnr
NTSS-1HM (C)	MT.1									25.7	0.0	25.1	0.0	14.2	0.0	10.2	0.0
	MT.2									10.0	0.0	22.0	0.0	12.5	0.0	10.0	0.0
	MT.3									26.0	0.0	25.5	0.0	13.9	0.0	10.3	0.0
	AVE.									25.8	0.0	24.2	0.0	13.5	0.0	10.2	0.0
	St.Dev									0.2	0.0	1.9	0.0	0.9	0.0	0.2	0.0

Asphalt Binder		10° c				25° c				58° c				70° c			
		.1 kPa		3.2 kPa		.1 kPa		3.2 kPa		.1 kPa		3.2 kPa		.1 kPa		3.2 kPa	
		Re %	Jnr	Re %	Jnr	Re %	Jnr	Re %	Jnr	Re %	Jnr	Re %	Jnr	Re %	Jnr	Re %	Jnr
NTSS-1HM (B)	MT.1									36.2	0.0	44.7	0.0	31.7	0.0	27.4	0.0
	MT.2									38.1	0.0	44.2	0.0	32.4	0.0	27.3	0.0
	MT.3									44.8	0.0	46.3	0.0	34.9	0.0	29.7	0.0
	AVE.									39.7	0.0	45.1	0.0	33.0	0.0	28.1	0.0
	St.Dev									4.5	0.0	1.1	0.0	1.7	0.0	1.3	0.0

Asphalt Binder		10° c				25° c				58° c				70° c			
		.1 kPa		3.2 kPa		.1 kPa		3.2 kPa		.1 kPa		3.2 kPa		.1 kPa		3.2 kPa	
		Re %	Jnr	Re %	Jnr	Re %	Jnr	Re %	Jnr	Re %	Jnr	Re %	Jnr	Re %	Jnr	Re %	Jnr
SS-1 (E)	MT.1	67.5	0.0	68.2	0.0	39.2	0.0	37.0	0.0	3.9	0.5	-0.1	0.6	-0.7	2.4	-2.5	2.7
	MT.2	68.0	0.0	67.8	0.0	41.2	0.0	39.5	0.0	6.4	0.4	0.0	0.5	-1.1	2.3	-2.4	2.6
	MT.3	62.7	0.0	66.0	0.0	39.0	0.0	36.5	0.0	4.4	0.5	-0.2	0.6	-1.4	2.6	-2.7	2.8
	AVE.	66.1	0.0	67.4	0.0	39.8	0.0	37.6	0.0	4.9	0.5	-0.1	0.6	-1.1	2.4	-2.6	2.7
	St.Dev	2.9	0.0	1.2	0.0	1.2	0.0	1.6	0.0	1.4	0.0	0.1	0.0	0.4	0.2	0.1	0.1

Asphalt Binder		10° c				25° c				58° c				70° c			
		.1 kPa		3.2 kPa		.1 kPa		3.2 kPa		.1 kPa		3.2 kPa		.1 kPa		3.2 kPa	
		Re %	Jnr	Re %	Jnr	Re %	Jnr	Re %	Jnr	Re %	Jnr	Re %	Jnr	Re %	Jnr	Re %	Jnr
SS-1 (B)	MT.1	67.0	0.0	66.9	0.0	41.1	0.0	40.9	0.0	4.7	0.4	0.6	0.5	-0.4	2.0	-2.0	2.2
	MT.2	67.6	0.0	66.2	0.0	44.7	0.0	45.9	0.0	38.2	0.4	14.7	0.6	27.3	1.7	-1.6	3.0
	MT.3	63.8	0.0	65.3	0.0	46.7	0.0	3.7	0.0	2.7	0.6	-0.7	1.4	-3.2	4.0	-4.6	4.5
	AVE.	66.1	0.0	66.1	0.0	44.2	0.0	43.4	0.0	3.7	0.4	0.0	0.8	-1.8	2.5	-2.7	3.2
	St.Dev	2.1	0.0	0.8	0.0	2.8	0.0	3.6	0.0	1.4	0.1	0.9	0.5	1.0	1.3	1.6	1.2

Asphalt Binder		10° c				25° c				58° c				70° c			
		.1 kPa		3.2 kPa		.1 kPa		3.2 kPa		.1 kPa		3.2 kPa		.1 kPa		3.2 kPa	
		Re %	Jnr	Re %	Jnr	Re %	Jnr	Re %	Jnr	Re %	Jnr	Re %	Jnr	Re %	Jnr	Re %	Jnr
SS-1h (B)	MT.1	96.6	0.0	75.7	0.0	62.1	0.0	62.8	0.0	9.3	0.1	4.4	0.1	2.8	0.5	0.0	0.6
	MT.2	97.4	0.0	83.7	0.0	63.8	0.0	64.0	0.0	12.6	0.1	5.7	0.1	4.6	0.5	0.2	0.5
	MT.3	95.7	0.0	82.8	0.0	64.4	0.0	64.0	0.0	12.8	0.1	5.8	0.1	4.5	0.5	0.3	0.6
	AVE.	96.6	0.0	80.7	0.0	63.4	0.0	63.6	0.0	11.6	0.1	5.3	0.1	4.0	0.5	0.2	0.6
	St.Dev	0.8	0.0	4.4	0.0	1.2	0.0	0.7	0.0	2.0	0.0	0.8	0.0	1.0	0.0	0.1	0.0

Asphalt Binder		10° c				25° c				58° c				70° c			
		.1 kPa		3.2 kPa		.1 kPa		3.2 kPa		.1 kPa		3.2 kPa		.1 kPa		3.2 kPa	
		Re %	Jnr	Re %	Jnr	Re %	Jnr	Re %	Jnr	Re %	Jnr	Re %	Jnr	Re %	Jnr	Re %	Jnr
SS-1 (U)	MT.1	53.4	0.0	54.1	0.0	40.6	0.0	37.5	0.0	4.3	0.5	-0.1	0.6	-0.7	2.5	-2.7	2.9
	MT.2	51.8	0.0	52.6	0.0	42.8	0.0	39.9	0.0	6.9	0.5	-0.1	0.6	-0.9	2.4	-2.6	2.8
	MT.3	57.8	0.0	51.7	0.0	39.8	0.0	38.0	0.0	5.1	0.5	-0.1	0.6	1.2	2.4	-2.6	2.8
	AVE.	54.4	0.0	52.8	0.0	41.1	0.0	38.5	0.0	5.4	0.5	-0.1	0.6	-0.1	2.4	-2.7	2.8
	St.Dev	3.1	0.0	1.2	0.0	1.6	0.0	1.2	0.0	1.3	0.0	0.0	0.0	1.2	0.1	0.0	0.0

Asphalt Binder		10° c				25° c				58° c				70° c			
		.1 kPa		3.2 kPa		.1 kPa		3.2 kPa		.1 kPa		3.2 kPa		.1 kPa		3.2 kPa	
		Re %	Jnr	Re %	Jnr	Re %	Jnr	Re %	Jnr	Re %	Jnr	Re %	Jnr	Re %	Jnr	Re %	Jnr
CRS-2 (U)	MT.1	49.4	0.0	51.0	0.0	39.8	0.0	38.7	0.0	1.5	0.6	-0.1	0.7	-2.4	2.7	-2.8	3.0
	MT.2	52.3	0.0	51.7	0.0	23.7	0.0	38.3	0.0	2.7	0.6	-0.2	0.7	-1.9	2.8	-2.9	3.1
	MT.3	51.7	0.0	52.4	0.0	41.3	0.0	38.4	0.0	4.4	0.6	-0.2	0.7	-1.3	2.7	-2.9	3.0
	AVE.	51.1	0.0	51.7	0.0	34.9	0.0	38.5	0.0	2.9	0.6	-0.2	0.7	-1.9	2.7	-2.9	3.0
	St.Dev	1.5	0.0	0.7	0.0	9.8	0.0	0.2	0.0	1.5	0.0	0.0	0.0	0.6	0.0	0.0	0.1

Asphalt Binder		10° c				25° c				58° c				70° c			
		.1 kPa		3.2 kPa		.1 kPa		3.2 kPa		.1 kPa		3.2 kPa		.1 kPa		3.2 kPa	
		Re %	Jnr	Re %	Jnr	Re %	Jnr	Re %	Jnr	Re %	Jnr	Re %	Jnr	Re %	Jnr	Re %	Jnr
SS-1H (U)	MT.1	63.5	0.0	74.7	0.0	60.7	0.0	58.9	0.0	3.6	0.1	3.5	0.1	2.7	0.5	-0.1	0.6
	MT.2	77.1	0.0	73.6	0.0	58.8	0.0	59.0	0.0	8.4	0.1	3.5	0.1	2.3	0.6	0.0	0.6
	MT.3	75.7	0.0	72.3	0.0	57.4	0.0	57.5	0.0	7.5	0.1	3.2	0.1	2.3	0.6	-0.2	0.7
	AVE.	72.1	0.0	73.5	0.0	59.0	0.0	58.5	0.0	6.5	0.1	3.4	0.1	2.4	0.6	-0.1	0.6
	St.Dev	7.5	0.0	1.2	0.0	1.7	0.0	0.8	0.0	2.6	0.0	0.2	0.0	0.2	0.0	0.1	0.0

Asphalt Binder		10° c				25° c				58° c				70° c			
		.1 kPa		3.2 kPa		.1 kPa		3.2 kPa		.1 kPa		3.2 kPa		.1 kPa		3.2 kPa	
		Re %	Jnr	Re %	Jnr	Re %	Jnr	Re %	Jnr	Re %	Jnr	Re %	Jnr	Re %	Jnr	Re %	Jnr
SS-1L (U)	MT.1	60.9	0.0	63.4	0.0	58.6	0.0	55.5	0.0	51.3	0.1	14.6	0.3	37.0	0.6	1.2	1.4
	MT.2	74.6	0.0	62.8	0.0	58.5	0.0	59.0	0.0	54.6	0.1	13.8	0.3	34.8	0.6	0.5	1.6
	MT.3	64.7	0.0	62.4	0.0	57.5	0.0	55.8	0.0	53.4	0.1	13.4	0.3	35.2	0.6	0.4	1.5
	AVE.	66.7	0.0	62.9	0.0	58.2	0.0	56.8	0.0	53.1	0.1	13.9	0.3	35.6	0.6	0.7	1.5
	St.Dev	7.1	0.0	0.5	0.0	0.6	0.0	2.0	0.0	1.7	0.0	0.6	0.0	1.2	0.0	0.4	0.1

Asphalt Binder		10° c				25° c				58° c				70° c			
		.1 kPa		3.2 kPa		.1 kPa		3.2 kPa		.1 kPa		3.2 kPa		.1 kPa		3.2 kPa	
		Re %	Jnr	Re %	Jnr	Re %	Jnr	Re %	Jnr	Re %	Jnr	Re %	Jnr	Re %	Jnr	Re %	Jnr
NTSS-1HM (U)	MT.1									15.7	0.0	9.4	0.0	11.3	0.1	1.5	0.2
	MT.2									12.1	0.0	9.3	0.0	6.7	0.1	1.4	0.2
	MT.3									10.6	0.0	10.4	0.0	8.3	0.1	2.0	0.2
	AVE.									12.8	0.0	9.7	0.0	8.8	0.1	1.6	0.2
	St.Dev									2.6	0.0	0.6	0.0	2.3	0.0	0.4	0.0

Asphalt Binder		10° c				25° c				58° c				70° c			
		.1 kPa		3.2 kPa		.1 kPa		3.2 kPa		.1 kPa		3.2 kPa		.1 kPa		3.2 kPa	
		Re %	Jnr	Re %	Jnr	Re %	Jnr	Re %	Jnr	Re %	Jnr	Re %	Jnr	Re %	Jnr	Re %	Jnr
PME (E)	MT.1	84.6	0.0	67.4	0.0	59.7	0.0	59.4	0.0	33.9	0.2	7.5	0.3	24.3	0.8	-0.4	1.4
	MT.2	81.0	0.0	63.2	0.0	52.0	0.0	59.9	0.0	29.6	0.2	13.0	0.3	33.6	0.7	0.5	1.5
	MT.3	73.0	0.0	71.5	0.0	60.2	0.0	60.8	0.0	44.6	0.1	16.0	0.3	38.1	0.6	1.0	1.5
	AVE.	79.5	0.0	67.4	0.0	60.0	0.0	60.0	0.0	36.0	0.2	12.2	0.3	32.0	0.7	0.4	1.5
	St.Dev	6.0	0.0	4.2	0.0	0.4	0.0	0.7	0.0	7.7	0.0	4.3	0.0	7.0	0.1	0.7	0.1

Asphalt Binder		10° c				25° c				58° c				70° c			
		.1 kPa		3.2 kPa		.1 kPa		3.2 kPa		.1 kPa		3.2 kPa		.1 kPa		3.2 kPa	
		Re %	Jnr	Re %	Jnr	Re %	Jnr	Re %	Jnr	Re %	Jnr	Re %	Jnr	Re %	Jnr	Re %	Jnr
SS-1HP (E)	MT.1	75.7	0.0	74.2	0.0	69.6	0.0	69.0	0.0	25.2	0.1	13.6	0.1	8.4	0.5	1.5	0.7
	MT.2	74.4	0.0	73.8	0.0	68.3	0.0	68.6	0.0	24.0	0.1	12.5	0.1	8.8	0.6	1.2	0.8
	MT.3	77.7	0.0	71.6	0.0	68.3	0.0	68.6	0.0	23.1	0.1	12.6	0.1	8.9	0.6	1.1	0.8
	AVE.	75.9	0.0	73.2	0.0	68.7	0.0	68.7	0.0	24.1	0.1	12.9	0.1	8.7	0.6	1.3	0.7
	St.Dev	1.7	0.0	1.4	0.0	0.8	0.0	0.2	0.0	1.0	0.0	0.6	0.0	0.3	0.0	0.2	0.1

Asphalt Binder		10° c				25° c				58° c				70° c			
		.1 kPa		3.2 kPa		.1 kPa		3.2 kPa		.1 kPa		3.2 kPa		.1 kPa		3.2 kPa	
		Re %	Jnr	Re %	Jnr	Re %	Jnr	Re %	Jnr	Re %	Jnr	Re %	Jnr	Re %	Jnr	Re %	Jnr
CHFRS-2P (E)	MT.1	70.4	0.0	73.5	0.0	67.8	0.0	67.2	0.0	34.4	0.1	14.6	0.1	34.0	0.4	3.3	0.8
	MT.2	73.2	0.0	73.6	0.0	67.2	0.0	67.4	0.0	36.9	0.1	17.6	0.2	40.8	0.3	5.0	0.8
	MT.3	74.4	0.0	71.3	0.0	67.6	0.0	67.6	0.0	39.2	0.1	19.0	0.1	39.4	0.4	7.5	0.7
	AVE.	72.7	0.0	72.8	0.0	67.5	0.0	67.4	0.0	36.8	0.1	17.1	0.1	38.1	0.4	5.2	0.8
	St.Dev	2.1	0.0	1.3	0.0	0.3	0.0	0.2	0.0	2.4	0.0	2.3	0.0	3.6	0.0	2.1	0.0

STRAIN SWEEP

CMS-1P (E) (52°C)

ang. frequency (rad/s)	temperature (°c)	time (s)	osc. stress (Pa)	strain	Delta (°)	G' (Pa)	G" (Pa)	|G*| (Pa)	|G*|/sin(delta) (kPa)
10	52	25.359	71.52	0.019938	81.49	532.7	3561	3600	3.64
10	52	53.5	429.8	0.1205	81.59	523.7	3541	3579	3.618
10	52	81.609	786.1	0.22112	81.71	514.6	3530	3568	3.605
10	52	109.7	1134	0.32142	81.85	501.8	3505	3541	3.577
10	52	137.67	1474	0.42246	82.02	486.4	3468	3502	3.536
10	52	165.63	1812	0.52474	82.17	472	3432	3465	3.497

ang. frequency (rad/s)	temperature (°c)	time (s)	osc. stress (Pa)	strain	Delta (°)	G' (Pa)	G" (Pa)	|G*| (Pa)	|G*|/sin(delta) (kPa)
10	52	25.422	63.94	0.020093	81.61	466.4	3161	3195	3.229
10	52	53.563	382	0.12011	81.69	461.4	3159	3193	3.227
10	52	81.625	698.5	0.22123	81.82	451.2	3137	3170	3.202
10	52	109.75	1009	0.32142	81.96	440.8	3120	3151	3.182
10	52	137.86	1313	0.42364	82.12	426.7	3083	3112	3.142
10	52	165.89	1610	0.52238	82.27	416.4	3066	3094	3.122

ang. frequency (rad/s)	temperature (°c)	time (s)	osc. stress (Pa)	strain	Delta (º)	G' (Pa)	G" (Pa)	|G*| (Pa)	|G*|/sin(delta) (kPa)
10	52	25.297	66.85	0.019946	81.23	512.8	3326	3365	3.405
10	52	53.328	403.4	0.12063	81.33	506	3319	3358	3.396
10	52	81.391	736.2	0.22078	81.45	497.5	3310	3348	3.385
10	52	109.44	1063	0.3216	81.6	484.6	3282	3318	3.354
10	52	137.58	1385	0.42351	81.76	470.1	3248	3282	3.316
10	52	165.66	1698	0.52356	81.91	457.9	3223	3255	3.288

CMS-1P (E) (70ºC)

ang. frequency (rad/s)	temperature (°c)	time (s)	osc. stress (Pa)	strain	Delta (º)	G' (Pa)	G" (Pa)	|G*| (Pa)	|G*|/sin(delta) (kPa)
10	70	25.422	8.006	0.019993	84.23	40.06	396.6	398.6	0.4006
10	70	53.656	47.98	0.12012	84.36	39.02	395.4	397.4	0.3993
10	70	81.641	87.91	0.22076	84.47	38.18	394.1	395.9	0.3978
10	70	109.86	127.2	0.32029	84.59	37.22	392.7	394.4	0.3962
10	70	137.91	166.7	0.42136	84.71	36.23	391.2	392.8	0.3945
10	70	165.92	205.4	0.52075	84.8	35.48	389.8	391.4	0.393

ang. frequency (rad/s)	temperature (°c)	time (s)	osc. stress (Pa)	strain	Delta (º)	G' (Pa)	G" (Pa)	|G*| (Pa)	|G*|/sin(delta) (kPa)
10	70	25.281	7.214	0.019974	84.01	37.4	356.5	358.4	0.3604
10	70	53.375	43.38	0.12036	84.13	36.56	355.6	357.4	0.3593
10	70	81.531	79.37	0.22086	84.24	35.75	354.3	356.1	0.3579
10	70	109.63	115.1	0.32103	84.35	34.93	353.3	355	0.3567
10	70	137.88	150.4	0.42089	84.47	34.07	352.1	353.8	0.3554
10	70	166.02	185.6	0.52103	84.57	33.31	350.7	352.2	0.3538

ang. frequency (rad/s)	temperature (°c)	time (s)	osc. stress (Pa)	strain	Delta (º)	G' (Pa)	G" (Pa)	|G*| (Pa)	|G*|/sin(delta) (kPa)
10	70	25.359	7.864	0.019904	83.43	45.12	391.9	394.4	0.3971
10	70	53.375	47.56	0.12092	83.9	41.61	389.5	391.8	0.394
10	70	81.5	86.37	0.22059	84	40.78	387.7	389.8	0.392
10	70	109.59	125.3	0.32049	84.11	39.92	387.1	389.1	0.3912
10	70	137.66	163.9	0.42065	84.23	38.95	385.5	387.5	0.3894
10	70	165.76	202.7	0.52171	84.34	38.09	384.2	386.1	0.388

CHFRS-2P (E) (52°C)

ang. frequency (rad/s)	temperature (°c)	time (s)	osc. stress (Pa)	strain	delta (°)	G' (Pa)	G" (Pa)	|G*| (Pa)	|G*|/sin(delta) (kPa)
10	52	25.266	211.7	0.019998	73.24	3062	10170	10620	11.09
10	52	53.36	1268	0.12018	73.38	3025	10140	10580	11.04
10	52	94.203	2293	0.22027	73.68	2933	10020	10440	10.88
10	52	134.92	3289	0.32038	74.04	2831	9898	10290	10.71
10	52	175.74	4251	0.42056	74.39	2728	9762	10140	10.52
10	52	216.66	5172	0.52261	74.73	2613	9573	9924	10.29

ang. frequency (rad/s)	temperature (°c)	time (s)	osc. stress (Pa)	strain	Delta (°)	G' (Pa)	G" (Pa)	|G*| (Pa)	|G*|/sin(delta) (kPa)
10	52	25.329	196.7	0.019889	73.27	2856	9500	9920	10.36
10	52	53.344	1187	0.12049	73.42	2821	9472	9883	10.31
10	52	81.329	2164	0.22175	73.69	2748	9391	9785	10.2
10	52	122.28	3080	0.321	74.07	2642	9253	9623	10.01
10	52	163.27	3988	0.42127	74.42	2550	9144	9493	9.855
10	52	204.13	4850	0.52239	74.75	2448	8983	9311	9.65

ang. frequency (rad/s)	temperature (°c)	time (s)	osc. stress (Pa)	strain	Delta (°)	G' (Pa)	G" (Pa)	|G*| (Pa)	|G*|/sin(delta) (kPa)
10	52	25.312	203.1	0.019928	73.02	2985	9775	10220	10.69
10	52	53.172	1225	0.12031	73.16	2958	9774	10210	10.67
10	52	94.016	2211	0.2204	73.49	2860	9647	10060	10.5
10	52	134.91	3176	0.32136	73.85	2756	9519	9910	10.32
10	52	175.78	4109	0.4216	74.21	2660	9406	9775	10.16
10	52	216.63	4985	0.52206	74.54	2552	9229	9576	9.935

CHFRS-2P (E) (70°C)

ang. frequency (rad/s)	temperature (°c)	time (s)	osc. stress (Pa)	strain	Delta (°)	G' (Pa)	G" (Pa)	|G*| (Pa)	|G*|/sin(delta) (kPa)
10	70	25.25	29.22	0.020002	79.14	278	1449	1476	1.503
10	70	53.281	175.3	0.12007	79.26	275	1449	1475	1.502
10	70	81.406	321.1	0.22125	79.52	266.5	1441	1466	1.491
10	70	109.41	463.5	0.3212	79.88	255.9	1434	1457	1.48
10	70	137.58	603.8	0.42142	80.26	244.7	1425	1446	1.467
10	70	165.58	741.9	0.52209	80.6	234.2	1414	1434	1.453

ang. frequency (rad/s)	temperature (°c)	time (s)	osc. stress (Pa)	strain	Delta (º)	G' (Pa)	G" (Pa)	|G*| (Pa)	|G*|/sin(delta) (kPa)
10	70	25.36	27.45	0.019969	79.14	261.7	1364	1389	1.415
10	70	53.407	164.5	0.12005	79.27	258	1361	1385	1.41
10	70	81.485	301.9	0.22144	79.51	250.7	1354	1377	1.401
10	70	109.53	435.7	0.32134	79.87	241	1348	1370	1.391
10	70	137.56	567.7	0.4227	80.24	229.9	1336	1356	1.376
10	70	165.77	697.4	0.5222	80.56	221	1330	1348	1.366

ang. frequency (rad/s)	temperature (°c)	time (s)	osc. stress (Pa)	strain	Delta (º)	G' (Pa)	G" (Pa)	|G*| (Pa)	|G*|/sin(delta) (kPa)
10	70	25.329	29.29	0.019975	78.82	287.4	1454	1482	1.511
10	70	53.297	175.3	0.12013	78.99	281.4	1447	1474	1.502
10	70	81.375	320.8	0.2215	79.28	272.1	1438	1463	1.489
10	70	109.45	462.1	0.321	79.66	260.9	1430	1454	1.478
10	70	137.47	603.2	0.42288	80.05	248.7	1418	1440	1.462
10	70	165.64	739.5	0.52214	80.39	238.5	1409	1429	1.449

CRS-2 (B) (52°C)

ang. frequency (rad/s)	temperature (°c)	time (s)	osc. stress (Pa)	strain	delta (°)	G' (Pa)	G" (Pa)	|G*| (Pa)	|G*|/sin(delta) (kPa)
10	52	25.266	81.1	0.02012	84.97	353.5	4015	4031	4.046
10	52	53.25	484	0.11986	85.03	350.2	4023	4038	4.054
10	52	81.234	888.7	0.22092	85.09	344.4	4008	4023	4.038
10	52	109.25	1283	0.32067	85.16	337.6	3988	4003	4.017
10	52	137.27	1679	0.42313	85.25	328.8	3954	3967	3.981
10	52	165.31	2056	0.52168	85.33	320.6	3927	3941	3.954

ang. frequency (rad/s)	temperature (°c)	time (s)	osc. stress (Pa)	strain	Delta (°)	G' (Pa)	G" (Pa)	|G*| (Pa)	|G*|/sin(delta) (kPa)
10	52	25.344	85.41	0.02	84.84	383.8	4254	4271	4.288
10	52	53.485	511.7	0.11981	84.91	379.2	4254	4271	4.288
10	52	81.641	939.6	0.22113	84.98	371.9	4233	4249	4.266
10	52	109.7	1355	0.32102	85.06	363.4	4205	4220	4.236
10	52	137.64	1768	0.42353	85.15	353	4161	4175	4.19
10	52	165.8	2160	0.52245	85.24	343.1	4121	4135	4.149

ang. frequency (rad/s)	temperature (°c)	time (s)	osc. stress (Pa)	strain	Delta (°)	G' (Pa)	G" (Pa)	|G*| (Pa)	|G*|/sin(delta) (kPa)
10	52	25.391	86.36	0.02009	84.96	377.7	4282	4299	4.315
10	52	53.5	516.8	0.12003	85.02	374.1	4290	4306	4.322
10	52	81.672	945.3	0.22002	85.08	368.7	4281	4297	4.312
10	52	109.66	1368	0.32125	85.16	359.4	4242	4257	4.273
10	52	137.69	1787	0.42378	85.25	349.3	4202	4217	4.232
10	52	165.69	2193	0.52352	85.33	341.2	4176	4189	4.203

CRS-2 (B) (70°C)

ang. frequency (rad/s)	temperature (°c)	time (s)	osc. stress (Pa)	strain	Delta (°)	G' (Pa)	G" (Pa)	|G*| (Pa)	|G*|/sin(delta) (kPa)
10	70	25.39	8.173	0.020006	87.98	14.39	408.3	408.5	0.4088
10	70	53.328	48.99	0.12006	88.14	13.23	407.8	408	0.4082
10	70	81.422	89.67	0.22069	88.17	12.98	406.1	406.3	0.4065
10	70	109.47	130.2	0.31987	88.2	12.8	406.9	407.1	0.4073
10	70	137.42	170.5	0.41936	88.21	12.7	406.3	406.5	0.4067
10	70	165.42	210.9	0.52066	88.23	12.48	404.9	405.1	0.4053

ang. frequency (rad/s)	temperature (°c)	time (s)	osc. stress (Pa)	strain	Delta (º)	G' (Pa)	G" (Pa)	|G*| (Pa)	|G*|/sin(delta) (kPa)
10	70	25.531	8.12	0.019984	88.08	13.59	406.1	406.4	0.4066
10	70	53.734	48.81	0.12038	88.14	13.13	405.3	405.5	0.4057
10	70	81.922	89.41	0.2206	88.17	12.96	405.1	405.3	0.4055
10	70	109.97	129.7	0.31959	88.19	12.78	405.5	405.7	0.4059
10	70	138.06	169.8	0.41947	88.22	12.6	404.7	404.9	0.4051
10	70	166.17	210.3	0.52117	88.23	12.48	403.4	403.6	0.4038

ang. frequency (rad/s)	temperature (°c)	time (s)	osc. stress (Pa)	strain	Delta (º)	G' (Pa)	G" (Pa)	|G*| (Pa)	|G*|/sin(delta) (kPa)
10	70	25.312	8.16	0.020007	88.28	12.23	407.7	407.8	0.408
10	70	53.422	48.86	0.11976	88.47	10.92	407.8	407.9	0.4081
10	70	81.593	89.5	0.21992	88.47	10.83	406.8	407	0.4071
10	70	109.53	130.2	0.32056	88.5	10.62	406	406.2	0.4063
10	70	137.61	171	0.42039	88.51	10.55	406.6	406.8	0.4069
10	70	165.81	211.1	0.52067	88.52	10.48	405.4	405.5	0.4056

CRS-2 (E) (52°C)

ang. frequency (rad/s)	temperature (°c)	time (s)	osc. stress (Pa)	strain	delta (°)	G' (Pa)	G" (Pa)	|G*| (Pa)	|G*|/sin(delta) (kPa)
10	52	25.344	96.96	0.020173	82.41	636.7	4776	4819	4.861
10	52	66.204	569.9	0.11994	82.42	628.7	4721	4763	4.805
10	52	94.11	1043	0.22112	82.52	615.5	4690	4730	4.771
10	52	122.19	1510	0.32303	82.67	598.1	4646	4685	4.723
10	52	150.2	1961	0.42383	82.82	579.3	4601	4637	4.674
10	52	178.13	2400	0.524	82.98	561	4557	4592	4.626

ang. frequency (rad/s)	temperature (°c)	time (s)	osc. stress (Pa)	strain	Delta (°)	G' (Pa)	G" (Pa)	|G*| (Pa)	|G*|/sin(delta) (kPa)
10	52	25.312	85.69	0.020034	82.38	568.6	4251	4289	4.327
10	52	53.391	513.5	0.12046	82.48	559.6	4238	4274	4.312
10	52	81.391	937.9	0.22087	82.58	549.6	4222	4258	4.294
10	52	109.44	1351	0.32144	82.72	533.9	4182	4215	4.25
10	52	137.45	1758	0.4234	82.88	515.9	4131	4163	4.195
10	52	178.27	2137	0.52117	83.04	498	4080	4111	4.141

ang. frequency (rad/s)	temperature (°c)	time (s)	osc. stress (Pa)	strain	Delta (°)	G' (Pa)	G" (Pa)	|G*| (Pa)	|G*|/sin(delta) (kPa)
10	52	25.312	86.63	0.020004	82.43	572.2	4305	4342	4.381
10	52	53.297	521	0.12035	82.49	567.4	4304	4341	4.378
10	52	81.437	953.7	0.22111	82.59	557.6	4289	4325	4.361
10	52	109.52	1375	0.32264	82.74	540.4	4240	4274	4.309
10	52	137.55	1787	0.42333	82.89	524	4200	4232	4.265
10	52	165.67	2187	0.52329	83.05	507.3	4159	4190	4.221

CRS-2 (E) (70°C)

ang. frequency (rad/s)	temperature (°c)	time (s)	osc. stress (Pa)	strain	Delta (°)	G' (Pa)	G" (Pa)	|G*| (Pa)	|G*|/sin(delta) (kPa)
10	70	25.438	8.764	0.020049	87.4	19.51	430.5	430.9	0.4314
10	70	53.703	52.48	0.11994	87.5	18.83	430.8	431.2	0.4316
10	70	81.828	96.11	0.21986	87.52	18.6	430.3	430.7	0.4311
10	70	109.95	139.6	0.31958	87.56	18.36	429.9	430.3	0.4307
10	70	137.94	183	0.41983	87.56	18.28	429	429.4	0.4298
10	70	166.05	226	0.5199	87.55	18.33	427.7	428.1	0.4285

ang. frequency (rad/s)	temperature (°c)	time (s)	osc. stress (Pa)	strain	Delta (º)	G' (Pa)	G" (Pa)	|G*| (Pa)	|G*|/sin(delta) (kPa)
10	70	25.36	8.107	0.020063	87.1	20.12	397	397.5	0.398
10	70	53.485	48.5	0.11987	87.27	18.97	397.3	397.7	0.3982
10	70	81.516	88.93	0.22059	87.31	18.62	395.7	396.2	0.3966
10	70	109.64	129.1	0.32019	87.36	18.28	395.9	396.3	0.3967
10	70	137.64	169.1	0.41981	87.39	18	395.3	395.8	0.3962
10	70	165.74	209.2	0.52118	87.43	17.67	393.8	394.2	0.3946

ang. frequency (rad/s)	temperature (°c)	time (s)	osc. stress (Pa)	strain	Delta (º)	G' (Pa)	G" (Pa)	|G*| (Pa)	|G*|/sin(delta) (kPa)
10	70	25.407	8.089	0.020062	87.36	18.22	395.7	396.1	0.3965
10	70	53.36	48.37	0.11977	87.38	18.12	396.3	396.8	0.3972
10	70	81.36	88.7	0.22034	87.4	17.91	395	395.4	0.3958
10	70	109.45	128.9	0.32005	87.44	17.69	395.3	395.7	0.3961
10	70	137.41	168.8	0.42014	87.46	17.47	394.1	394.5	0.3949
10	70	165.58	209	0.5201	87.49	17.28	394.2	394.6	0.3949

CRS-2 (U) (52°C)

ang. frequency (rad/s)	temperature (°c)	time (s)	osc. stress (Pa)	strain	delta (°)	G' (Pa)	G" (Pa)	|G*| (Pa)	|G*|/sin(delta) (kPa)
10	52	25.422	69.93	0.019965	85.16	296.4	3497	3510	3.522
10	52	53.657	419.3	0.1197	85.2	293.6	3498	3510	3.522
10	52	81.688	770.2	0.22063	85.26	288.7	3486	3498	3.51
10	52	109.69	1119	0.3219	85.33	283.6	3472	3483	3.495
10	52	137.7	1458	0.42101	85.41	277.5	3457	3469	3.48
10	52	165.7	1791	0.52138	85.51	269.5	3430	3441	3.451

ang. frequency (rad/s)	temperature (°c)	time (s)	osc. stress (Pa)	strain	Delta (°)	G' (Pa)	G" (Pa)	|G*| (Pa)	|G*|/sin(delta) (kPa)
10	52	38.187	85.15	0.019767	86.18	287.3	4304	4313	4.323
10	52	91.953	498.9	0.11048	86.78	254.3	4513	4520	4.527
10	52	132.8	808.4	0.22292	85.63	276.9	3622	3632	3.643
10	52	160.84	1107	0.31798	85.49	274.4	3477	3488	3.499
10	52	188.89	1435	0.4213	85.49	268.4	3402	3412	3.423
10	52	216.94	1763	0.52395	85.51	264.2	3360	3371	3.381

ang. frequency (rad/s)	temperature (°c)	time (s)	osc. stress (Pa)	strain	Delta (°)	G' (Pa)	G" (Pa)	|G*| (Pa)	|G*|/sin(delta) (kPa)
10	52	51.094	886.2	0.28252	85.74	233.2	3134	3143	3.151
10	52	91.844	371.3	0.12115	85.66	232.3	3062	3070	3.079
10	52	119.94	659.2	0.22151	85.49	234.5	2973	2982	2.991
10	52	147.95	946.3	0.3203	85.54	230.3	2951	2960	2.969
10	52	175.97	1241	0.42256	85.62	225	2934	2943	2.951
10	52	204.08	1522	0.52123	85.7	219.6	2917	2926	2.934

CRS-2 (U) (70°C)

ang. frequency (rad/s)	temperature (°c)	time (s)	osc. stress (Pa)	strain	Delta (°)	G' (Pa)	G" (Pa)	|G*| (Pa)	|G*|/sin(delta) (kPa)
10	70	25.453	7.76	0.020034	88.4	10.54	377.9	378	0.3782
10	70	53.453	46.42	0.11972	88.53	9.696	378.1	378.2	0.3783
10	70	81.563	85.08	0.22007	88.56	9.478	376.9	377	0.3771
10	70	109.69	123.8	0.32063	88.6	9.211	376.4	376.5	0.3767
10	70	137.8	162.5	0.42087	88.62	9.067	376.3	376.4	0.3766
10	70	165.8	200.8	0.5203	88.64	8.948	376.1	376.2	0.3763

ang. frequency (rad/s)	temperature (°c)	time (s)	osc. stress (Pa)	strain	Delta (º)	G' (Pa)	G" (Pa)	|G*| (Pa)	|G*|/sin(delta) (kPa)
10	70	25.406	7.643	0.019982	88.54	9.467	372.6	372.8	0.3729
10	70	53.563	45.81	0.12004	88.56	9.347	371.8	371.9	0.372
10	70	81.609	84.1	0.21996	88.57	9.278	372.4	372.5	0.3727
10	70	109.7	122	0.32002	88.61	9.027	371.3	371.4	0.3715
10	70	137.72	160.4	0.41937	88.66	8.736	372.4	372.5	0.3726
10	70	165.83	198.3	0.52086	88.65	8.71	370.6	370.7	0.3708

ang. frequency (rad/s)	temperature (°c)	time (s)	osc. stress (Pa)	strain	Delta (º)	G' (Pa)	G" (Pa)	|G*| (Pa)	|G*|/sin(delta) (kPa)
10	70	25.297	6.855	0.020014	88.25	10.15	331.7	331.8	0.332
10	70	53.438	41.08	0.12	88.36	9.474	331.3	331.4	0.3315
10	70	81.484	75.34	0.21977	88.38	9.36	331.7	331.9	0.332
10	70	109.59	109.6	0.32062	88.42	9.108	330.7	330.9	0.331
10	70	137.59	143.7	0.41937	88.45	8.96	331.4	331.6	0.3317
10	70	165.58	177.6	0.5201	88.48	8.767	330.3	330.4	0.3305

CRS-2P (B) (52°C)

ang. frequency (rad/s)	temperature (°c)	time (s)	osc. stress (Pa)	strain	delta (°)	G' (Pa)	G" (Pa)	|G*| (Pa)	|G*|/sin(delta) (kPa)
10	52	25.36	135.4	0.020082	81.38	1011	6666	6742	6.819
10	52	53.297	805.8	0.11996	81.46	997.1	6644	6718	6.794
10	52	81.235	1474	0.22138	81.6	972.7	6588	6659	6.731
10	52	122.16	2110	0.32019	81.79	941.4	6522	6590	6.658
10	52	150.13	2766	0.4236	81.94	915.4	6467	6531	6.596
10	52	178.16	3403	0.52434	82.09	893.4	6429	6491	6.553

ang. frequency (rad/s)	temperature (°c)	time (s)	osc. stress (Pa)	strain	Delta (°)	G' (Pa)	G" (Pa)	|G*| (Pa)	|G*|/sin(delta) (kPa)
10	52	25.36	126	0.019913	81.57	927.8	6260	6328	6.397
10	52	53.329	759.6	0.12012	81.65	918.3	6257	6324	6.392
10	52	81.329	1385	0.22126	81.8	893.3	6197	6261	6.326
10	52	109.49	2002	0.32169	81.96	870.8	6162	6223	6.285
10	52	137.47	2604	0.42344	82.13	842.4	6093	6151	6.209
10	52	165.5	3197	0.52269	82.27	822.6	6062	6117	6.173

ang. frequency (rad/s)	temperature (°c)	time (s)	osc. stress (Pa)	strain	Delta (°)	G' (Pa)	G" (Pa)	|G*| (Pa)	|G*|/sin(delta) (kPa)
10	52	25.422	122.8	0.019985	81.4	918.8	6076	6145	6.215
10	52	53.422	738.9	0.12023	81.49	909.1	6079	6146	6.215
10	52	81.547	1347	0.22123	81.64	885.9	6026	6091	6.157
10	52	109.67	1949	0.32207	81.8	863	5990	6052	6.114
10	52	137.56	2531	0.42246	81.96	837.4	5932	5991	6.05
10	52	165.59	3114	0.52416	82.12	814.4	5886	5942	5.999

CRS-2P (B) (70°C)

ang. frequency (rad/s)	temperature (°c)	time (s)	osc. stress (Pa)	strain	Delta (°)	G' (Pa)	G" (Pa)	|G*| (Pa)	|G*|/sin(delta) (kPa)
10	70	25.515	14.31	0.019988	84.37	70.26	712.4	715.8	0.7193
10	70	53.671	85.13	0.1199	84.47	68.41	706.7	710	0.7134
10	70	81.765	156.1	0.22114	84.59	66.54	702.7	705.9	0.709
10	70	109.8	225.1	0.32073	84.76	64.16	699	701.9	0.7049
10	70	137.8	294.4	0.42229	84.94	61.46	694.5	697.2	0.6999
10	70	165.88	361.6	0.52091	85.12	59.09	691.6	694.1	0.6966

ang. frequency (rad/s)	temperature (°c)	time (s)	osc. stress (Pa)	strain	Delta (º)	G' (Pa)	G" (Pa)	|G*| (Pa)	|G*|/sin(delta) (kPa)
10	70	25.344	13.56	0.020001	84.68	62.81	675.1	678	0.681
10	70	53.407	81.42	0.12028	84.76	61.82	674.1	676.9	0.6798
10	70	81.61	148.6	0.22002	84.88	60.26	672.8	675.5	0.6782
10	70	109.7	215.9	0.3215	85.05	57.97	668.9	671.4	0.6739
10	70	137.66	281.1	0.42067	85.21	55.79	666	668.3	0.6707
10	70	165.88	347.2	0.52267	85.39	53.44	662.1	664.3	0.6665

ang. frequency (rad/s)	temperature (°c)	time (s)	osc. stress (Pa)	strain	Delta (º)	G' (Pa)	G" (Pa)	|G*| (Pa)	|G*|/sin(delta) (kPa)
10	70	25.391	13.29	0.020055	84.43	64.31	659.7	662.8	0.666
10	70	53.469	79.63	0.12012	84.53	63.16	659.9	662.9	0.666
10	70	81.532	145.7	0.22012	84.65	61.69	658.9	661.8	0.6646
10	70	109.52	211	0.32044	84.8	59.68	655.7	658.5	0.6612
10	70	137.61	275.4	0.42036	84.97	57.41	652.7	655.2	0.6577
10	70	165.72	339.7	0.52202	85.13	55.28	648.3	650.7	0.6531

CRS-2P (E) (52°C)

ang. frequency (rad/s)	temperature (°c)	time (s)	osc. stress (Pa)	strain	delta (°)	G' (Pa)	G" (Pa)	|G*| (Pa)	|G*|/sin(delta) (kPa)
10	52	25.266	156.4	0.019979	76.09	1887	7620	7851	8.088
10	52	53.344	936	0.12042	76.29	1848	7574	7797	8.025
10	52	93.922	1686	0.2212	76.68	1761	7440	7645	7.857
10	52	134.61	2408	0.32172	77.08	1679	7317	7507	7.702
10	52	175.34	3105	0.421	77.42	1611	7218	7396	7.578
10	52	203.03	3837	0.5241	77.7	1564	7173	7341	7.514

ang. frequency (rad/s)	temperature (°c)	time (s)	osc. stress (Pa)	strain	Delta (°)	G' (Pa)	G" (Pa)	|G*| (Pa)	|G*|/sin(delta) (kPa)
10	52	25.265	149.2	0.019918	75.84	1838	7285	7513	7.749
10	52	53.312	896.8	0.12067	76.04	1799	7236	7456	7.683
10	52	93.906	1616	0.22062	76.42	1726	7141	7347	7.558
10	52	134.51	2302	0.32	76.81	1646	7027	7217	7.413
10	52	175.08	2980	0.42026	77.17	1579	6934	7112	7.294
10	52	203	3674	0.52468	77.47	1524	6857	7024	7.195

ang. frequency (rad/s)	temperature (°c)	time (s)	osc. stress (Pa)	strain	Delta (°)	G' (Pa)	G" (Pa)	|G*| (Pa)	|G*|/sin(delta) (kPa)
10	52	38.141	153.4	0.020097	76.07	1843	7429	7655	7.887
10	52	78.797	883.3	0.12037	76.25	1750	7151	7362	7.579
10	52	106.81	1609	0.22211	76.52	1693	7066	7266	7.472
10	52	147.48	2275	0.32027	76.94	1611	6942	7126	7.316
10	52	175.47	2969	0.42374	77.28	1548	6856	7029	7.206
10	52	216.31	3597	0.51994	77.6	1490	6777	6939	7.105

CRS-2P (E) (70°C)

ang. frequency (rad/s)	temperature (°c)	time (s)	osc. stress (Pa)	strain	Delta (°)	G' (Pa)	G" (Pa)	|G*| (Pa)	|G*|/sin(delta) (kPa)
10	70	25.265	18.43	0.019998	80.49	154.1	919.9	932.7	0.9457
10	70	53.109	110.3	0.11993	80.64	151.5	918.4	930.8	0.9434
10	70	80.843	202.3	0.22146	80.95	145.3	911.9	923.4	0.9351
10	70	108.72	291.7	0.32184	81.32	138.2	905.3	915.8	0.9264
10	70	136.5	378.9	0.42165	81.69	131.1	897.9	907.5	0.9171
10	70	164.51	465.7	0.52259	82.02	124.8	890.6	899.3	0.9081

ang. frequency (rad/s)	temperature (°c)	time (s)	osc. stress (Pa)	strain	Delta (º)	G' (Pa)	G" (Pa)	|G*| (Pa)	|G*|/sin(delta) (kPa)
10	70	25.344	18.3	0.019976	80.43	154.2	914.2	927.1	0.9402
10	70	53.204	109.6	0.11988	80.56	151.7	912.5	925.1	0.9378
10	70	81.094	200.9	0.22138	80.85	145.9	906.2	917.9	0.9297
10	70	109.03	290.4	0.32252	81.2	139.2	899.5	910.2	0.921
10	70	136.84	377.2	0.42185	81.55	132.8	893.4	903.2	0.9131
10	70	164.94	462.7	0.52103	81.86	126.9	887.5	896.5	0.9057

ang. frequency (rad/s)	temperature (°c)	time (s)	osc. stress (Pa)	strain	Delta (º)	G' (Pa)	G" (Pa)	|G*| (Pa)	|G*|/sin(delta) (kPa)
10	70	25.359	18.09	0.019907	80.2	156.6	906.6	920	0.9336
10	70	53.015	109.2	0.12114	80.42	151.9	899.9	912.6	0.9255
10	70	80.937	198.1	0.22093	80.72	146.2	895.2	907	0.919
10	70	108.61	286.2	0.32274	81.1	138.7	885.8	896.6	0.9075
10	70	136.64	371.3	0.42196	81.47	131.9	879.3	889.1	0.8991
10	70	164.39	457	0.52342	81.81	125.6	872.6	881.6	0.8907

CSS-1HP (E) (52°C)

ang. frequency (rad/s)	temperature (°c)	time (s)	osc. stress (Pa)	strain	delta (°)	G' (Pa)	G" (Pa)	|G*| (Pa)	|G*|/sin(delta) (kPa)
10	52	38.156	806.9	0.019974	68.22	15020	37590	40470	43.59
10	52	78.828	4727	0.12065	68.73	14240	36570	39250	42.12
10	52	119.72	8323	0.22106	69.42	13260	35310	37720	40.29
10	52	160.61	11620	0.32061	70.08	12370	34140	36310	38.62
10	52	214.39	15640	0.4485	70.76	11510	32970	34920	36.99
10	52	268.11	17020	0.53627	71.27	10210	30110	31790	33.57

ang. frequency (rad/s)	temperature (°c)	time (s)	osc. stress (Pa)	strain	delta (°)	G' (Pa)	G" (Pa)	|G*| (Pa)	|G*|/sin(delta) (kPa)
10	52	37.968	873.8	0.019932	66.62	17440	40320	43930	47.86
10	52	78.843	5096	0.12066	67.25	16370	39030	42320	45.89
10	52	119.78	8916	0.22122	68.07	15080	37460	40380	43.53
10	52	160.66	12390	0.32095	68.81	13980	36060	38670	41.47
10	52	201.5	15610	0.4231	69.47	12970	34620	36960	39.47
10	52	255.26	17880	0.53489	70.07	11410	31470	33480	35.61

ang. frequency (rad/s)	temperature (°c)	time (s)	osc. stress (Pa)	strain	delta (°)	G' (Pa)	G" (Pa)	|G*| (Pa)	|G*|/sin(delta) (kPa)
10	52	37.89	719	0.019948	66.96	14130	33240	36120	39.25
10	52	78.812	4203	0.12021	67.56	13370	32380	35030	37.9
10	52	119.76	7390	0.22043	68.35	12390	31220	33590	36.14
10	52	160.78	10320	0.32107	69.07	11500	30080	32200	34.48
10	52	201.81	13080	0.42383	69.7	10720	28990	30910	32.95
10	52	255.59	15000	0.53449	70.2	9522	26450	28110	29.88

CSS-1HP (E) (70°C)

ang. frequency (rad/s)	temperature (°c)	time (s)	osc. stress (Pa)	strain	Delta (°)	G' (Pa)	G" (Pa)	|G*| (Pa)	|G*|/sin(delta) (kPa)
10	70	25.297	97.35	0.020082	73.26	1404	4668	4875	5.09
10	70	53.328	580.8	0.12068	73.72	1357	4645	4839	5.042
10	70	94.297	1042	0.22069	74.42	1275	4572	4747	4.928
10	70	135.16	1485	0.32031	75.1	1198	4503	4660	4.822
10	70	176.22	1916	0.42039	75.73	1129	4439	4580	4.726
10	70	217.17	2333	0.52048	76.33	1065	4377	4505	4.637

ang. frequency (rad/s)	temperature (°c)	time (s)	osc. stress (Pa)	strain	Delta (º)	G' (Pa)	G" (Pa)	|G*| (Pa)	|G*|/sin(delta) (kPa)
10	70	25.329	105	0.020007	72.28	1606	5028	5278	5.541
10	70	66.125	624.3	0.12005	72.92	1536	4997	5228	5.469
10	70	107.09	1124	0.22002	73.62	1448	4929	5138	5.355
10	70	148	1606	0.32023	74.29	1365	4852	5041	5.236
10	70	188.95	2073	0.41989	74.88	1294	4789	4961	5.139
10	70	229.83	2528	0.51959	75.39	1233	4731	4890	5.053

ang. frequency (rad/s)	temperature (°c)	time (s)	osc. stress (Pa)	strain	Delta (º)	G' (Pa)	G" (Pa)	|G*| (Pa)	|G*|/sin(delta) (kPa)
10	70	25.188	88.93	0.019944	72.15	1376	4272	4488	4.715
10	70	65.953	528.7	0.12018	72.8	1309	4229	4427	4.634
10	70	106.92	954.3	0.2207	73.53	1234	4172	4350	4.537
10	70	147.91	1365	0.321	74.21	1164	4115	4277	4.444
10	70	188.91	1763	0.42137	74.82	1101	4061	4208	4.36
10	70	229.91	2149	0.52073	75.35	1050	4016	4151	4.29

FOGSEAL (C) (52°C)

ang. frequency (rad/s)	temperature (°c)	time (s)	osc. stress (Pa)	strain	delta (°)	G' (Pa)	G" (Pa)	|G*| (Pa)	|G*|/sin(delta) (kPa)
10	52	50.782	13880	1.0242	97.09	-1670	13440	13540	13.65
10	52	79.891	13880	0.020252	69.21	2.48E+05	6.53E+05	6.98E+05	746.5
10	52	82.844	13880	0.020252	69.21	2.48E+05	6.53E+05	6.98E+05	746.5
10	52	85.969	13880	0.020252	69.21	2.48E+05	6.53E+05	6.98E+05	746.5
10	52	88.704	13880	0.020252	69.21	2.48E+05	6.53E+05	6.98E+05	746.5
10	52	103.86	65190	0.10423	70.45	2.13E+05	5.99E+05	6.35E+05	674

ang. frequency (rad/s)	temperature (°c)	time (s)	osc. stress (Pa)	strain	delta (°)	G' (Pa)	G" (Pa)	|G*| (Pa)	|G*|/sin(delta) (kPa)
10	52	50.922	13770	0.020569	69.3	2.41E+05	6.37E+05	6.81E+05	727.9
10	52	78.672	65190	0.10797	70.59	2.04E+05	5.78E+05	6.13E+05	649.7
10	52	93.859	65190	0.10885	70.74	2.00E+05	5.74E+05	6.08E+05	643.6
10	52	109.08	65190	0.1087	70.79	2.00E+05	5.75E+05	6.09E+05	644.3
10	52	124.16	65190	0.10886	70.84	1.99E+05	5.74E+05	6.08E+05	643.1
10	52	139.47	65190	0.10867	70.86	2.00E+05	5.75E+05	6.09E+05	644.2

ang. frequency (rad/s)	temperature (°c)	time (s)	osc. stress (Pa)	Strain	delta (°)	G' (Pa)	G" (Pa)	|G*| (Pa)	|G*|/sin(delta) (kPa)
10	52	50.734	14110	0.025952	72.59	1.65E+05	5.25E+05	5.50E+05	576.5
10	52	104.48	65190	0.1139	72.07	1.79E+05	5.52E+05	5.80E+05	609.4
10	52	119.67	65190	0.11052	71.8	1.87E+05	5.68E+05	5.98E+05	629.4
10	52	134.84	65190	0.10827	71.63	1.92E+05	5.80E+05	6.11E+05	643.3
10	52	149.97	65190	0.10651	71.51	1.97E+05	5.89E+05	6.21E+05	654.7
10	52	165.14	65190	0.10529	71.42	2.00E+05	5.95E+05	6.28E+05	662.7

FOGSEAL (C) (70°C)

ang. frequency (rad/s)	temperature (°c)	time (s)	osc. stress (Pa)	strain	delta (°)	G' (Pa)	G" (Pa)	|G*| (Pa)	|G*|/sin(delta) (kPa)
10	70	38.141	828.9	0.019884	80.58	6831	41160	41720	42.29
10	70	78.797	4947	0.12008	80.72	6649	40690	41230	41.78
10	70	119.72	8935	0.22076	80.93	6386	40000	40500	41.02
10	70	160.59	12770	0.32154	81.14	6121	39270	39750	40.23
10	70	214.33	15950	0.43312	81.39	5518	36450	36860	37.28
10	70	267.92	15210	0.57921	81.65	3816	26010	26290	26.57

ang. frequency (rad/s)	temperature (°c)	time (s)	osc. stress (Pa)	strain	delta (°)	G' (Pa)	G" (Pa)	|G*| (Pa)	|G*|/sin(delta) (kPa)
10	70	38.046	846	0.020226	80.6	6840	41300	41860	42.43
10	70	78.875	4927	0.12052	80.67	6635	40380	40920	41.47
10	70	119.78	8868	0.22041	80.86	6398	39750	40270	40.78
10	70	160.55	12680	0.32257	81.08	6099	38870	39340	39.82
10	70	214.19	15630	0.43205	81.3	5478	35800	36210	36.63
10	70	267.75	15740	0.56323	81.5	4135	27660	27970	28.28

ang. frequency (rad/s)	temperature (°c)	time (s)	osc. stress (Pa)	strain	delta (°)	G' (Pa)	G" (Pa)	|G*| (Pa)	|G*|/sin(delta) (kPa)
10	70	38.015	992.4	0.019965	79.89	8734	48980	49760	50.54
10	70	78.703	5872	0.12007	80.07	8444	48210	48950	49.69
10	70	119.76	10530	0.2211	80.32	8020	47010	47690	48.38
10	70	160.63	14880	0.32246	80.61	7538	45570	46190	46.81
10	70	214.39	18390	0.43057	80.84	6806	42190	42740	43.29
10	70	268.11	18500	0.56615	81.01	5110	32310	32710	33.12

NTSS-1HM (U) (52°C)

ang. frequency (rad/s)	temperature (°c)	time (s)	osc. stress (Pa)	strain	delta (°)	G' (Pa)	G" (Pa)	|G*| (Pa)	|G*|/sin(delta) (kPa)
10	52	38.14	2113	0.020112	79.49	19190	1.04E+05	1.05E+05	107
10	52	78.765	12330	0.12074	79.74	18220	1.01E+05	1.02E+05	104
10	52	119.64	21960	0.22211	80.04	17120	97530	99020	100.5
10	52	173.58	1277	0.60723	117.7	-953	1815	2050	2.315
10	52	227.59	365.9	0.24807	127.1	-849	1122	1407	1.764
10	52	281.42	1016	0.46664	125.2	-1217	1728	2113	2.585

ang. frequency (rad/s)	temperature (°c)	time (s)	osc. stress (Pa)	strain	delta (°)	G' (Pa)	G" (Pa)	|G*| (Pa)	|G*|/sin(delta) (kPa)
10	52	38.046	1974	0.01996	79.47	18090	97360	99030	100.7
10	52	78.859	11630	0.12062	79.77	17140	95040	96580	98.13
10	52	119.55	20660	0.22062	80.11	16110	92370	93760	95.18
10	52	160.51	29080	0.32248	80.43	15010	89020	90280	91.56
10	52	214.2	35120	0.44175	80.71	12850	78550	79590	80.65
10	52	267.91	32010	0.57408	80.91	8813	55110	55810	56.52

ang. frequency (rad/s)	temperature (°c)	time (s)	osc. stress (Pa)	strain	delta (°)	G' (Pa)	G" (Pa)	|G*| (Pa)	|G*|/sin(delta) (kPa)
10	52	37.86	1996	0.020216	79.51	17990	97200	98850	100.5
10	52	78.781	11540	0.12012	79.79	17060	94690	96210	97.76
10	52	119.75	20570	0.22046	80.11	16040	92030	93420	94.83
10	52	160.63	29040	0.32309	80.43	14970	88740	90000	91.27
10	52	214.42	34650	0.44305	80.69	12660	77270	78300	79.34
10	52	268.23	31100	0.57067	80.87	8657	53860	54550	55.25

NTSS-1HM (U) (70°C)

ang. frequency (rad/s)	temperature (°c)	time (s)	osc. stress (Pa)	strain	delta (°)	G' (Pa)	G" (Pa)	|G*| (Pa)	|G*|/sin(delta) (kPa)
10	70	51.125	3.259	3.12E-03	75.38	269.1	1032	1066	1.102
10	70	104.88	16.29	1.36E-03	85	1041	11910	11960	12
10	70	145.88	20.05	0.21781	56.02	22.8	33.82	40.79	0.04919
10	70	199.74	30.67	0.30913	65.28	24.03	52.2	57.47	0.06326
10	70	253.66	41.71	0.40993	65.09	30.24	65.14	71.82	0.07918
10	70	294.75	47.63	0.52665	56.51	31.65	47.83	57.36	0.06878

ang. frequency (rad/s)	temperature (°c)	time (s)	osc. stress (Pa)	strain	Delta (º)	G' (Pa)	G" (Pa)	|G*| (Pa)	|G*|/sin(delta) (kPa)
10	70	25.235	126.7	0.02014	86.03	435.6	6282	6298	6.313
10	70	66	686.7	0.12057	81.69	825	5648	5708	5.769
10	70	119.97	1374	0.22037	86.23	410.4	6228	6242	6.256
10	70	148.13	1991	0.32237	86.32	397.2	6168	6181	6.193
10	70	176.25	2579	0.42194	86.41	383.5	6105	6117	6.129
10	70	204.38	3175	0.52464	86.5	369.8	6046	6057	6.069

ang. frequency (rad/s)	temperature (°c)	time (s)	osc. stress (Pa)	strain	Delta (º)	G' (Pa)	G" (Pa)	|G*| (Pa)	|G*|/sin(delta) (kPa)
10	70	25.344	125.1	0.019917	86.05	433.3	6270	6285	6.3
10	70	53.234	751.2	0.12002	86.13	422.5	6251	6265	6.279
10	70	81.266	1379	0.22175	86.23	409.4	6211	6225	6.238
10	70	109.55	1992	0.32246	86.32	397.4	6172	6185	6.197
10	70	137.55	2590	0.42256	86.4	384.8	6122	6135	6.147
10	70	165.67	3174	0.52357	86.5	370.1	6056	6068	6.079

PME (E) (52°C)

ang. frequency (rad/s)	temperature (°c)	time (s)	osc. stress (Pa)	strain	delta (°)	G' (Pa)	G" (Pa)	|G*| (Pa)	|G*|/sin(delta) (kPa)
10	52	38.047	165.7	0.020291	76.99	1843	7976	8186	2.0291
10	52	79.187	924.2	0.11847	76.78	1789	7616	7824	11.847
10	52	120.08	1669	0.22176	76.88	1713	7352	7549	22.176
10	52	161.06	2362	0.32083	77.22	1634	7202	7385	32.083
10	52	201.88	3044	0.42011	77.59	1562	7098	7268	42.011
10	52	242.77	3713	0.52039	77.95	1494	6997	7155	52.039

ang. frequency (rad/s)	temperature (°c)	time (s)	osc. stress (Pa)	strain	delta (°)	G' (Pa)	G" (Pa)	|G*| (Pa)	|G*|/sin(delta) (kPa)
10	52	38.235	142.9	0.020037	76.21	1705	6948	7155	2.0037
10	52	78.875	840.4	0.12036	76.32	1657	6806	7005	12.036
10	52	106.94	1538	0.22192	76.62	1609	6763	6952	22.192
10	52	147.7	2179	0.32079	77.11	1520	6642	6814	32.079
10	52	188.33	2822	0.42166	77.54	1448	6556	6714	42.166
10	52	216.36	3473	0.52477	77.89	1392	6490	6638	52.477

ang. frequency (rad/s)	temperature (°c)	time (s)	osc. stress (Pa)	strain	delta (°)	G' (Pa)	G" (Pa)	|G*| (Pa)	|G*|/sin(delta) (kPa)
10	52	25.297	144	0.019877	76.03	1754	7053	7268	1.9877
10	52	53.235	869	0.12022	76.22	1727	7043	7251	12.022
10	52	81.297	1584	0.22178	76.56	1665	6970	7166	22.178
10	52	122.14	2246	0.31999	77.06	1577	6862	7041	31.999
10	52	162.97	2904	0.42061	77.49	1501	6761	6926	42.061
10	52	191.08	3577	0.52462	77.83	1441	6684	6838	52.462

PME (E) (70°C)

ang. frequency (rad/s)	temperature (°c)	time (s)	osc. stress (Pa)	strain	delta (°)	G' (Pa)	G" (Pa)	|G*| (Pa)	|G*|/sin(delta) (kPa)
10	70	25.25	20.17	0.019981	79.85	180.1	1006	1022	1.9981
10	70	53.39	121.5	0.12105	80.09	174.7	1000	1015	12.105
10	70	81.406	220.9	0.22205	80.52	165.6	992.5	1006	22.205
10	70	109.39	318	0.32263	81.01	155.7	983.7	996	32.263
10	70	137.45	412.1	0.42222	81.45	146.5	974.7	985.6	42.222
10	70	165.66	506.1	0.5227	81.86	138.4	967.4	977.2	52.27

ang. frequency (rad/s)	temperature (°c)	time (s)	osc. stress (Pa)	strain	Delta (º)	G' (Pa)	G" (Pa)	|G*| (Pa)	|G*|/sin(delta) (kPa)
10	70	25.234	19.22	0.020113	79.53	175.9	952.1	968.2	2.0113
10	70	53.328	114.5	0.12056	79.68	172.4	946.5	962.1	12.056
10	70	81.234	209.1	0.22151	80.09	164.4	941.4	955.6	22.151
10	70	109.2	300.7	0.32264	80.59	154.3	930.3	943	32.264
10	70	137.25	391	0.4235	81.05	145.2	922	933.4	42.35
10	70	165.36	477.8	0.52322	81.45	137.2	912.2	922.5	52.322

ang. frequency (rad/s)	temperature (°c)	time (s)	osc. stress (Pa)	strain	Delta (º)	G' (Pa)	G" (Pa)	|G*| (Pa)	|G*|/sin(delta) (kPa)
10	70	25.329	19.17	0.020028	79.35	179.3	953.7	970.4	2.0028
10	70	53.188	114.9	0.11997	79.55	176	954.8	970.9	11.997
10	70	81.266	210.2	0.22138	79.95	167.9	946.7	961.5	22.138
10	70	109.36	303.6	0.32222	80.44	158.4	940.2	953.4	32.222
10	70	137.45	393.7	0.42263	80.92	148.7	930.2	942	42.263
10	70	165.5	482.9	0.52442	81.32	140.4	919.7	930.4	52.442

SS-1 (B) (52°C)

ang. frequency (rad/s)	temperature (°c)	time (s)	osc. stress (Pa)	strain	delta (°)	G' (Pa)	G" (Pa)	|G*| (Pa)	|G*|/sin(delta) (kPa)
10	52	25.422	105.6	0.020023	84.56	500.4	5258	5282	5.306
10	52	53.625	633.2	0.12086	84.67	487.7	5224	5247	5.27
10	52	81.625	1153	0.22059	84.72	481.6	5215	5237	5.26
10	52	109.34	1664	0.32076	84.81	470.1	5174	5195	5.217
10	52	137.34	2170	0.42329	84.92	454.9	5113	5134	5.154
10	52	165.24	2667	0.52453	85.01	442.6	5072	5092	5.111

ang. frequency (rad/s)	temperature (°c)	time (s)	osc. stress (Pa)	strain	delta (°)	G' (Pa)	G" (Pa)	|G*| (Pa)	|G*|/sin(delta) (kPa)
10	52	25.391	92.62	0.020089	84.44	447.2	4597	4619	4.641
10	52	53.375	553.5	0.12003	84.53	440.5	4599	4620	4.641
10	52	81.016	1014	0.22075	84.6	432.7	4582	4603	4.623
10	52	109.02	1468	0.32165	84.69	422.8	4552	4571	4.591
10	52	136.77	1905	0.42156	84.8	410.4	4509	4528	4.546
10	52	164.78	2348	0.52481	84.9	398.5	4463	4481	4.499

ang. frequency (rad/s)	temperature (°c)	time (s)	osc. stress (Pa)	strain	delta (°)	G' (Pa)	G" (Pa)	|G*| (Pa)	|G*|/sin(delta) (kPa)
10	52	25.312	92.84	0.020068	84.39	453.4	4613	4635	4.657
10	52	53.328	555.8	0.12023	84.46	447.1	4610	4632	4.653
10	52	81.125	1013	0.22032	84.55	437.9	4586	4607	4.628
10	52	109.13	1465	0.32218	84.65	424.8	4535	4555	4.575
10	52	136.92	1909	0.42406	84.75	412.8	4492	4511	4.53
10	52	164.78	2338	0.52333	84.85	401.9	4457	4475	4.494

SS-1 (B) (70°C)

ang. frequency (rad/s)	temperature (°c)	time (s)	osc. stress (Pa)	strain	delta (°)	G' (Pa)	G" (Pa)	|G*| (Pa)	|G*|/sin(delta) (kPa)
10	70	25.343	9.797	0.019963	87.73	19.19	484.8	485.1	0.4855
10	70	53.25	59.06	0.12055	87.88	17.9	483.7	484	0.4844
10	70	81.047	107.6	0.22034	87.92	17.54	482.1	482.4	0.4827
10	70	109.03	156.5	0.3197	87.94	17.36	483.1	483.4	0.4837
10	70	136.72	205.1	0.41986	87.98	17.04	482.2	482.5	0.4828
10	70	164.58	254.4	0.51973	88.01	16.79	483	483.3	0.4836

ang. frequency (rad/s)	temperature (°c)	time (s)	osc. stress (Pa)	strain	Delta (º)	G' (Pa)	G" (Pa)	|G*| (Pa)	|G*|/sin(delta) (kPa)
10	70	25.484	9.298	0.020051	87.53	19.75	457.4	457.9	0.4583
10	70	53.515	55.78	0.12003	87.58	19.38	458.4	458.8	0.4592
10	70	81.359	102.1	0.21958	87.63	19.02	458.7	459.1	0.4595
10	70	109.34	148.4	0.32004	87.67	18.61	457.4	457.7	0.4581
10	70	137.25	195	0.41985	87.69	18.46	457.9	458.3	0.4587
10	70	164.98	241.5	0.52165	87.72	18.18	456.3	456.7	0.4571

ang. frequency (rad/s)	temperature (°c)	time (s)	osc. stress (Pa)	strain	Delta (º)	G' (Pa)	G" (Pa)	|G*| (Pa)	|G*|/sin(delta) (kPa)
10	70	25.437	8.951	0.019954	87.27	21.06	442.3	442.8	0.4433
10	70	53.172	53.73	0.12	87.36	20.32	441.3	441.8	0.4423
10	70	81.031	98.57	0.22058	87.41	19.93	440.4	440.8	0.4413
10	70	108.7	143.3	0.32093	87.44	19.66	440.1	440.5	0.4409
10	70	136.67	187.9	0.42045	87.5	19.22	440.2	440.6	0.441
10	70	164.47	232.1	0.51932	87.54	18.92	440.2	440.6	0.441

SS-1 (E) (52°C)

ang. frequency (rad/s)	temperature (°c)	time (s)	osc. stress (Pa)	strain	delta (°)	G' (Pa)	G" (Pa)	|G*| (Pa)	|G*|/sin(delta) (kPa)
10	52	25.344	93.01	0.020023	85.38	374.6	4637	4652	4.667
10	52	53.453	558.9	0.1205	85.52	362.8	4630	4645	4.659
10	52	81.5	1014	0.22065	85.62	351.9	4591	4604	4.618
10	52	122.36	1451	0.32068	85.72	338.1	4519	4532	4.545
10	52	163.3	1875	0.42124	85.82	324.8	4445	4457	4.468
10	52	191.33	2314	0.5244	85.92	314.7	4407	4418	4.43

ang. frequency (rad/s)	temperature (°c)	time (s)	osc. stress (Pa)	strain	delta (°)	G' (Pa)	G" (Pa)	|G*| (Pa)	|G*|/sin(delta) (kPa)
10	52	25.344	99.72	0.020185	84.37	485.4	4925	4949	4.973
10	52	53.375	592.4	0.1211	84.71	451.9	4879	4900	4.921
10	52	81.422	1075	0.2219	84.88	432.6	4831	4850	4.87
10	52	122.3	1521	0.32072	85.08	407.4	4734	4751	4.769
10	52	150.25	1978	0.42394	85.22	389.4	4656	4673	4.689
10	52	178.23	2419	0.52427	85.36	373.8	4606	4621	4.636

ang. frequency (rad/s)	temperature (°c)	time (s)	osc. stress (Pa)	strain	delta (°)	G' (Pa)	G" (Pa)	|G*| (Pa)	|G*|/sin(delta) (kPa)
10	52	38.218	97.39	0.019968	84.61	459.2	4864	4886	4.908
10	52	79.047	571.5	0.12002	84.88	426	4750	4769	4.788
10	52	107.31	1043	0.22191	85	410	4690	4708	4.726
10	52	148.23	1484	0.32163	85.17	388.9	4603	4620	4.636
10	52	189.22	1913	0.4217	85.31	371.3	4529	4544	4.56
10	52	230.22	2332	0.52114	85.47	354.1	4468	4482	4.496

SS-1 (E) (70°C)

ang. frequency (rad/s)	temperature (°c)	time (s)	osc. stress (Pa)	strain	delta (°)	G' (Pa)	G" (Pa)	|G*| (Pa)	|G*|/sin(delta) (kPa)
10	70	25.421	9.125	0.019946	88.37	12.79	449.9	450.1	0.4503
10	70	53.515	54.88	0.12062	88.54	11.39	447.1	447.2	0.4474
10	70	81.64	100.1	0.22053	88.6	10.92	445.9	446	0.4461
10	70	109.66	144.9	0.32086	88.68	10.19	443.4	443.6	0.4437
10	70	137.64	189.8	0.42016	88.71	9.997	443.4	443.5	0.4436
10	70	165.69	235	0.52279	88.68	10.14	441.2	441.3	0.4415

ang. frequency (rad/s)	temperature (°c)	time (s)	osc. stress (Pa)	strain	Delta (º)	G' (Pa)	G" (Pa)	|G*| (Pa)	|G*|/sin(delta) (kPa)
10	70	25.344	9.804	0.019816	86.79	27.52	490	490.8	0.4916
10	70	66.344	58.68	0.12001	87.16	24.02	483.7	484.3	0.4849
10	70	94.5	107.2	0.22131	87.38	21.95	478.8	479.3	0.4798
10	70	122.55	154.4	0.32173	87.61	19.81	473.9	474.4	0.4748
10	70	150.61	201.2	0.42306	87.73	18.62	469.3	469.7	0.4701
10	70	178.73	247.3	0.52304	87.8	17.94	466.4	466.8	0.4671

ang. frequency (rad/s)	temperature (°c)	time (s)	osc. stress (Pa)	strain	Delta (º)	G' (Pa)	G" (Pa)	|G*| (Pa)	|G*|/sin(delta) (kPa)
10	70	38.297	9.654	0.020033	86.92	25.62	476.8	477.5	0.4781
10	70	79.313	57.12	0.12026	87.3	22.14	469.2	469.7	0.4702
10	70	120.33	103.6	0.22035	87.54	19.92	464.1	464.5	0.4649
10	70	148.44	150.5	0.32181	87.71	18.42	461.3	461.6	0.462
10	70	176.52	196.6	0.42184	87.83	17.41	459.4	459.8	0.4601
10	70	204.77	241.4	0.52073	87.92	16.61	456.7	457	0.4573

SS-1 (U) (52°C)

ang. frequency (rad/s)	temperature (°c)	time (s)	osc. stress (Pa)	strain	delta (°)	G' (Pa)	G" (Pa)	|G*| (Pa)	|G*|/sin(delta) (kPa)
10	52	38.188	68.79	0.01993	86.04	238.5	3.45E+03	3.46E+03	3.465
10	52	65.969	414	0.12102	86.17	228.9	3.42E+03	3.43E+03	3.434
10	52	93.938	751.5	0.22062	86.24	223.5	3404	3411	3.419
10	52	121.89	1085	0.32239	86.33	215.8	3364	3371	3.378
10	52	149.95	1410	0.42241	86.41	209.1	3337	3343	3.35
10	52	178.02	1724	0.52369	86.5	201.2	3291	3297	3.303

ang. frequency (rad/s)	temperature (°c)	time (s)	osc. stress (Pa)	strain	delta (°)	G' (Pa)	G" (Pa)	|G*| (Pa)	|G*|/sin(delta) (kPa)
10	52	25.265	69	0.020072	86.14	231.6	3435	3443	3.451
10	52	53.234	413.6	0.12069	86.25	224.4	3425	3432	3.439
10	52	81.344	751.5	0.22018	86.32	219.1	3411	3418	3.425
10	52	109.26	1086	0.32157	86.41	211.9	3375	3381	3.388
10	52	137.33	1415	0.42392	86.49	204.7	3336	3343	3.349
10	52	165.34	1733	0.52372	86.57	198.4	3308	3313	3.319

ang. frequency (rad/s)	temperature (°c)	time (s)	osc. stress (Pa)	strain	delta (°)	G' (Pa)	G" (Pa)	|G*| (Pa)	|G*|/sin(delta) (kPa)
10	52	25.281	72.29	0.020034	85.87	260.3	3605	3614	3.623
10	52	53.187	433.5	0.12098	86.05	247.5	3581	3589	3.598
10	52	81.172	785.9	0.22059	86.13	241	3560	3568	3.576
10	52	109.25	1133	0.32182	86.22	232.3	3517	3524	3.532
10	52	137.14	1472	0.42409	86.31	223.7	3469	3476	3.483
10	52	178.03	1783	0.52236	86.41	214.2	3411	3417	3.424

SS-1 (U) (70°C)

ang. frequency (rad/s)	temperature (°c)	time (s)	osc. stress (Pa)	strain	delta (°)	G' (Pa)	G" (Pa)	|G*| (Pa)	|G*|/sin(delta) (kPa)
10	70	25.297	7.715	2.00E-02	88.76	8.138	375.5	375.6	0.3757
10	70	53.391	46.42	1.20E-01	88.81	7.79	375.9	375.9	0.376
10	70	81.375	84.75	0.22047	88.84	7.578	374.2	374.3	0.3743
10	70	109.38	123.1	0.31988	88.86	7.432	374.7	374.8	0.3749
10	70	137.41	161.5	0.42053	88.86	7.438	373.7	373.8	0.3738
10	70	165.5	199.6	0.52074	88.87	7.331	373	373	0.3731

ang. frequency (rad/s)	temperature (°c)	time (s)	osc. stress (Pa)	strain	Delta (º)	G' (Pa)	G" (Pa)	|G*| (Pa)	|G*|/sin(delta) (kPa)
10	70	25.265	7.708	0.020073	88.8	7.8	373.8	373.9	0.3739
10	70	53.406	46.25	0.12017	88.91	7.123	374.5	374.6	0.3746
10	70	81.5	84.77	0.2206	88.94	6.898	373.9	374	0.374
10	70	109.5	122.8	0.31969	88.98	6.647	373.7	373.7	0.3738
10	70	137.45	161.5	0.42002	89.01	6.438	374.1	374.1	0.3742
10	70	165.61	199.5	0.52056	88.98	6.645	372.8	372.8	0.3729

ang. frequency (rad/s)	temperature (°c)	time (s)	osc. stress (Pa)	strain	Delta (º)	G' (Pa)	G" (Pa)	|G*| (Pa)	|G*|/sin(delta) (kPa)
10	70	25.375	7.962	0.019983	88.49	10.26	389.2	389.3	0.3895
10	70	53.469	48.01	0.12078	88.63	9.269	388	388.1	0.3882
10	70	81.454	87.59	0.22121	88.69	8.867	386.3	386.4	0.3865
10	70	109.52	126.7	0.32036	88.73	8.519	385.7	385.8	0.3859
10	70	137.49	165.7	0.41988	88.77	8.241	384.8	384.9	0.385
10	70	165.45	204.5	0.52008	88.77	8.228	383.3	383.4	0.3835

SS-1H (B) (52°C)

ang. frequency (rad/s)	temperature (°c)	time (s)	osc. stress (Pa)	strain	delta (°)	G' (Pa)	G" (Pa)	|G*| (Pa)	|G*|/sin(delta) (kPa)
10	52	25.344	443.7	0.019983	77.65	4756	21720	22230	22.76
10	52	53.25	2665	0.121	77.83	4650	21560	22050	22.56
10	52	93.875	4738	0.22095	78.13	4417	21010	21470	21.94
10	52	134.64	6713	0.32145	78.44	4191	20490	20910	21.34
10	52	175.5	8578	0.42298	78.76	3958	19910	20300	20.7
10	52	229.16	9858	0.54513	79.11	3420	17780	18110	18.44

ang. frequency (rad/s)	temperature (°c)	time (s)	osc. stress (Pa)	strain	delta (°)	G' (Pa)	G" (Pa)	|G*| (Pa)	|G*|/sin(delta) (kPa)
10	52	25.219	407.9	0.019975	77.64	4377	19980	20450	20.93
10	52	53.25	2452	0.12054	77.77	4316	19910	20370	20.85
10	52	94.312	4399	0.22122	78.04	4126	19480	19910	20.35
10	52	135.22	6279	0.32192	78.33	3951	19130	19530	19.94
10	52	176.13	8048	0.42152	78.62	3771	18740	19120	19.5
10	52	229.8	9517	0.53306	78.94	3428	17540	17880	18.21

ang. frequency (rad/s)	temperature (°c)	time (s)	osc. stress (Pa)	strain	delta (°)	G' (Pa)	G" (Pa)	|G*| (Pa)	|G*|/sin(delta) (kPa)
10	52	25.266	382.8	0.019814	77.65	4137	18900	19350	19.8
10	52	53.25	2319	0.1209	77.78	4066	18770	19210	19.65
10	52	94.141	4175	0.22155	78.01	3919	18460	18870	19.29
10	52	135	5959	0.32255	78.28	3757	18110	18500	18.89
10	52	175.8	7653	0.4242	78.57	3581	17710	18060	18.43
10	52	229.56	8875	0.53806	78.85	3195	16200	16520	16.83

SS-1H (B) (70°C)

ang. frequency (rad/s)	temperature (°c)	time (s)	osc. stress (Pa)	strain	delta (°)	G' (Pa)	G" (Pa)	|G*| (Pa)	|G*|/sin(delta) (kPa)
10	70	25.36	39.46	0.020036	84.77	180.1	1968	1976	1.984
10	70	53.297	235.9	0.12004	84.85	176.8	1963	1971	1.979
10	70	81.391	431.2	0.22083	84.94	172.8	1951	1959	1.966
10	70	109.36	624.5	0.32173	85.04	168.4	1940	1947	1.954
10	70	137.39	813.6	0.42218	85.14	163.8	1926	1933	1.94
10	70	165.41	998.5	0.52203	85.24	159	1912	1918	1.925

ang. frequency (rad/s)	temperature (°c)	time (s)	osc. stress (Pa)	strain	Delta (º)	G' (Pa)	G" (Pa)	|G*| (Pa)	|G*|/sin(delta) (kPa)
10	70	25.296	37.34	0.020034	84.29	186.2	1861	1871	1.88
10	70	53.421	224	0.12005	84.36	184	1864	1873	1.882
10	70	81.453	409.5	0.22027	84.45	180.5	1857	1866	1.875
10	70	109.41	594.7	0.32135	84.55	176.4	1849	1857	1.866
10	70	137.58	775.8	0.42121	84.65	172.3	1840	1848	1.856
10	70	165.73	955.9	0.52317	84.77	167.2	1826	1833	1.841

ang. frequency (rad/s)	temperature (°c)	time (s)	osc. stress (Pa)	strain	Delta (º)	G' (Pa)	G" (Pa)	|G*| (Pa)	|G*|/sin(delta) (kPa)
10	70	25.281	35.62	0.020022	84.37	175.2	1777	1786	1.795
10	70	53.109	213.6	0.11997	84.43	173.4	1779	1788	1.796
10	70	81.172	390.8	0.22075	84.52	169.6	1769	1777	1.785
10	70	109.2	566.6	0.32021	84.61	166.7	1768	1776	1.784
10	70	137.25	739.6	0.42164	84.72	162	1753	1760	1.768
10	70	165.42	912.7	0.52208	84.82	158.2	1747	1754	1.762

SS-1H (U) (52°C)

ang. frequency (rad/s)	temperature (°c)	time (s)	osc. stress (Pa)	strain	delta (°)	G' (Pa)	G" (Pa)	|G*| (Pa)	|G*|/sin(delta) (kPa)
10	52	25.281	450.9	0.019927	80.02	3926	2.23E+04	2.27E+04	23
10	52	53.375	2710	0.12046	80.13	3862	2.22E+04	2.25E+04	22.86
10	52	94.25	4865	0.22093	80.34	3698	21730	22040	22.36
10	52	135.09	6930	0.32236	80.58	3521	21230	21520	21.81
10	52	175.99	8890	0.42479	80.83	3337	20680	20950	21.22
10	52	229.74	10250	0.53973	81.08	2949	18780	19010	19.25

ang. frequency (rad/s)	temperature (°c)	time (s)	osc. stress (Pa)	strain	delta (°)	G' (Pa)	G" (Pa)	|G*| (Pa)	|G*|/sin(delta) (kPa)
10	52	37.938	406	0.020045	80.42	3375	19990	20280	20.56
10	52	66.157	2432	0.12036	80.51	3334	19950	20230	20.51
10	52	106.88	4372	0.22124	80.73	3185	19520	19780	20.04
10	52	147.8	6246	0.32275	80.96	3044	19130	19370	19.62
10	52	188.67	8006	0.42452	81.2	2887	18650	18880	19.1
10	52	242.39	9338	0.53456	81.45	2600	17290	17480	17.68

ang. frequency (rad/s)	temperature (°c)	time (s)	osc. stress (Pa)	strain	delta (°)	G' (Pa)	G" (Pa)	|G*| (Pa)	|G*|/sin(delta) (kPa)
10	52	25.297	421.7	0.020025	80.09	3629	20770	21080	21.4
10	52	53.391	2530	0.12066	80.19	3578	20690	20990	21.3
10	52	94.312	4532	0.22055	80.41	3427	20280	20570	20.86
10	52	135.13	6465	0.32203	80.65	3264	19830	20100	20.37
10	52	175.88	8313	0.42423	80.9	3103	19370	19620	19.87
10	52	229.52	9661	0.53997	81.16	2751	17700	17910	18.12

SS-1H (U) (70°C)

ang. frequency (rad/s)	temperature (°c)	time (s)	osc. stress (Pa)	strain	delta (°)	G' (Pa)	G" (Pa)	|G*| (Pa)	|G*|/sin(delta) (kPa)
10	70	25.406	38.29	2.00E-02	86.33	123	1915	1919	1.923
10	70	53.468	229.2	1.20E-01	86.36	121.7	1914	1918	1.922
10	70	81.437	419.8	0.21988	86.41	119.7	1909	1913	1.916
10	70	109.56	610.8	0.32099	86.47	117.4	1903	1906	1.91
10	70	137.61	800.1	0.42278	86.53	114.7	1892	1896	1.899
10	70	165.73	983.9	0.52105	86.6	112.3	1888	1892	1.895

ang. frequency (rad/s)	temperature (°c)	time (s)	osc. stress (Pa)	strain	Delta (º)	G' (Pa)	G" (Pa)	|G*| (Pa)	|G*|/sin(delta) (kPa)
10	70	25.25	33.68	0.020024	86.6	99.89	1682	1685	1.688
10	70	53.375	201.2	0.11979	86.63	98.87	1679	1682	1.685
10	70	81.391	370	0.22051	86.67	97.67	1678	1681	1.683
10	70	109.39	535.4	0.31955	86.71	96.18	1676	1678	1.681
10	70	137.5	704.8	0.42138	86.77	94.32	1673	1675	1.678
10	70	165.59	870	0.52014	86.83	92.76	1673	1675	1.678

ang. frequency (rad/s)	temperature (°c)	time (s)	osc. stress (Pa)	strain	Delta (º)	G' (Pa)	G" (Pa)	|G*| (Pa)	|G*|/sin(delta) (kPa)
10	70	25.359	35.95	0.020035	86.33	115.1	1794	1798	1.802
10	70	53.297	214.8	0.11985	86.38	113.5	1792	1796	1.799
10	70	81.312	395	0.22054	86.42	112.1	1791	1794	1.798
10	70	109.42	571.2	0.32022	86.48	109.8	1784	1787	1.79
10	70	137.56	749.4	0.42117	86.54	107.6	1779	1783	1.786
10	70	165.64	920.7	0.52111	86.6	104.8	1767	1770	1.773

SS-1HP (E) (52°C)

ang. frequency (rad/s)	temperature (°c)	time (s)	osc. stress (Pa)	strain	delta (°)	G' (Pa)	G" (Pa)	|G*| (Pa)	|G*|/sin(delta) (kPa)
10	52	25.375	243.1	0.019908	73.01	3577	11710	12240	12.8
10	52	66.235	1449	0.12026	73.26	3479	11570	12080	12.61
10	52	107.16	2610	0.22077	73.5	3366	11360	11850	12.36
10	52	148.09	3714	0.32103	73.77	3241	11130	11600	12.08
10	52	188.99	4767	0.42166	74.06	3112	10900	11330	11.79
10	52	229.84	5770	0.5214	74.33	2997	10680	11090	11.52

ang. frequency (rad/s)	temperature (°c)	time (s)	osc. stress (Pa)	strain	delta (°)	G' (Pa)	G" (Pa)	|G*| (Pa)	|G*|/sin(delta) (kPa)
10	52	38.016	211.3	0.020007	72.8	3133	10120	10590	11.09
10	52	78.891	1221	0.11993	73.57	2888	9794	10210	10.65
10	52	119.94	2196	0.2208	73.79	2784	9575	9972	10.38
10	52	160.8	3127	0.32141	74.06	2680	9383	9758	10.15
10	52	201.55	4021	0.42285	74.34	2574	9183	9536	9.904
10	52	229.52	4924	0.52429	74.63	2496	9082	9419	9.768

ang. frequency (rad/s)	temperature (°c)	time (s)	osc. stress (Pa)	Strain	delta (°)	G' (Pa)	G" (Pa)	|G*| (Pa)	|G*|/sin(delta) (kPa)
10	52	38.11	225.7	0.020035	72.8	3340	10790	11300	11.82
10	52	66.047	1356	0.12087	73	3289	10760	11250	11.77
10	52	107	2425	0.2204	73.27	3176	10560	11030	11.52
10	52	147.84	3471	0.3221	73.56	3059	10360	10810	11.27
10	52	188.75	4465	0.42302	73.84	2946	10170	10580	11.02
10	52	229.75	5403	0.52388	74.11	2831	9947	10340	10.75

SS-1HP (E) (70°C)

ang. frequency (rad/s)	temperature (°c)	time (s)	osc. stress (Pa)	strain	delta (°)	G' (Pa)	G" (Pa)	|G*| (Pa)	|G*|/sin(delta) (kPa)
10	70	25.5	28.71	0.019987	80.15	248.1	1428	1450	1.471
10	70	53.563	172.5	0.12072	80.29	243.3	1421	1442	1.463
10	70	81.532	313.4	0.22081	80.41	238.7	1412	1432	1.452
10	70	109.47	453.8	0.32147	80.53	234.3	1405	1424	1.444
10	70	137.55	590.7	0.42104	80.67	229.4	1397	1415	1.434
10	70	165.64	726.7	0.52243	80.83	223.7	1385	1403	1.421

ang. frequency (rad/s)	temperature (°c)	time (s)	osc. stress (Pa)	strain	Delta (º)	G' (Pa)	G" (Pa)	|G*| (Pa)	|G*|/sin(delta) (kPa)
10	70	25.391	24.88	0.019941	80.47	208.6	1242	1260	1.277
10	70	66.016	147.5	0.11987	80.59	203.1	1226	1242	1.259
10	70	119.81	315.6	0.23751	81.58	196.2	1325	1339	1.354
10	70	160.67	401.9	0.32078	81.18	193.9	1249	1264	1.279
10	70	201.72	513.2	0.42052	81.17	189	1217	1232	1.246
10	70	242.67	625	0.52271	81.28	183	1193	1207	1.221

ang. frequency (rad/s)	temperature (°c)	time (s)	osc. stress (Pa)	strain	Delta (º)	G' (Pa)	G" (Pa)	|G*| (Pa)	|G*|/sin(delta) (kPa)
10	70	25.391	27.21	0.019971	79.62	247.9	1354	1377	1.399
10	70	53.313	163.9	0.12113	79.81	241.8	1345	1367	1.389
10	70	81.36	297	0.22133	80.02	234.8	1335	1355	1.376
10	70	109.44	428.8	0.32212	80.19	229	1325	1344	1.364
10	70	137.53	557	0.42137	80.36	223.5	1316	1335	1.354
10	70	165.63	685.9	0.52303	80.52	218.1	1306	1324	1.342

SS-1L (U) (52°C)

ang. frequency (rad/s)	temperature (°c)	time (s)	osc. stress (Pa)	strain	delta (°)	G' (Pa)	G" (Pa)	|G*| (Pa)	|G*|/sin(delta) (kPa)
10	52	38.172	134.2	0.019971	76.02	1629	6.54E+03	6.74E+03	6.949
10	52	79.047	766.3	0.12023	77.14	1423	6.23E+03	6.39E+03	6.559
10	52	119.7	1360	0.22072	77.82	1304	6044	6183	6.325
10	52	160.53	1923	0.32076	78.41	1209	5893	6016	6.141
10	52	201.42	2469	0.42087	78.88	1135	5773	5884	5.996
10	52	242.34	3000	0.52137	79.26	1076	5670	5771	5.874

ang. frequency (rad/s)	temperature (°c)	time (s)	osc. stress (Pa)	strain	delta (°)	G' (Pa)	G" (Pa)	|G*| (Pa)	|G*|/sin(delta) (kPa)
10	52	25.375	128	0.020194	76.96	1435	6197	6361	6.53
10	52	66.219	733.2	0.12014	77.86	1287	5986	6123	6.263
10	52	107.03	1310	0.22051	78.43	1195	5838	5959	6.082
10	52	147.86	1864	0.32118	78.91	1119	5713	5822	5.933
10	52	175.94	2427	0.42417	79.24	1071	5639	5740	5.843
10	52	216.78	2925	0.52065	79.62	1015	5542	5634	5.728

ang. frequency (rad/s)	temperature (°c)	time (s)	osc. stress (Pa)	Strain	delta (°)	G' (Pa)	G" (Pa)	|G*| (Pa)	|G*|/sin(delta) (kPa)
10	52	38.157	129.8	0.020082	76.22	1545	6300	6486	6.678
10	52	78.829	747.3	0.12077	77.23	1373	6055	6209	6.366
10	52	119.75	1327	0.22099	77.87	1265	5890	6024	6.161
10	52	160.75	1879	0.32075	78.43	1179	5758	5878	6
10	52	201.72	2414	0.42059	78.88	1110	5650	5758	5.868
10	52	242.61	2936	0.52083	79.24	1056	5556	5655	5.756

SS-1L (U) (70°C)

ang. frequency (rad/s)	temperature (°c)	time (s)	osc. stress (Pa)	strain	delta (°)	G' (Pa)	G" (Pa)	|G*| (Pa)	|G*|/sin(delta) (kPa)
10	70	25.375	21.2	1.98E-02	74.18	297.8	1051	1092	1.135
10	70	66.141	122.5	1.21E-01	75.59	257.4	1002	1034	1.068
10	70	107.08	215.8	0.2216	76.67	228.7	964.9	991.6	1.019
10	70	148.06	302.8	0.32232	77.5	206.9	932.9	955.6	0.9788
10	70	188.89	386	0.42362	78.13	190.5	906.2	926	0.9462
10	70	230.06	465.8	0.5234	78.58	179	886	904	0.9222

ang. frequency (rad/s)	temperature (°c)	time (s)	osc. stress (Pa)	strain	Delta (º)	G' (Pa)	G" (Pa)	|G*| (Pa)	|G*|/sin(delta) (kPa)
10	70	25.297	20.87	0.019855	74.23	291.6	1033	1073	1.115
10	70	66.203	121	0.12034	75.6	255	993.3	1025	1.059
10	70	107.03	214.1	0.22158	76.66	227.1	957.4	983.9	1.011
10	70	147.97	301.3	0.32286	77.5	205.5	926.7	949.3	0.9723
10	70	188.78	384.2	0.42352	78.15	189.4	902.3	922	0.9421
10	70	229.67	463.9	0.52288	78.65	177.3	883.4	901.1	0.919

ang. frequency (rad/s)	temperature (°c)	time (s)	osc. stress (Pa)	strain	Delta (º)	G' (Pa)	G" (Pa)	|G*| (Pa)	|G*|/sin(delta) (kPa)
10	70	25.406	21.12	0.019871	74.67	286.6	1046	1084	1.124
10	70	66.313	122.9	0.12042	75.9	253.4	1009	1040	1.072
10	70	107.31	216.9	0.22166	76.95	225	970.2	995.9	1.022
10	70	148.34	305.1	0.323	77.77	203.3	938.5	960.3	0.9825
10	70	189.34	388.7	0.42319	78.39	187.7	913.9	933	0.9525
10	70	230.38	469.5	0.52285	78.87	176	894.3	911.4	0.9289

NTSS-1HM (B) (52°C)

ang. frequency (rad/s)	temperature (°c)	time (s)	osc. stress (Pa)	strain	delta (°)	G' (Pa)	G'' (Pa)	|G*| (Pa)	|G*|/sin(delta) (kPa)
10	52	50.718	18170	0.02215	64.57	3.62E+05	7.60E+05	8.42E+05	932.4
10	52	78.781	65190	0.10041	66.75	2.61E+05	6.08E+05	6.62E+05	720
10	52	93.937	65190	0.10238	67.6	2.47E+05	5.99E+05	6.48E+05	701
10	52	109.14	65190	1.03E-01	67.87	2.43E+05	5.98E+05	6.45E+05	696.7
10	52	124.23	65190	0.10302	67.99	2.41E+05	5.97E+05	6.44E+05	694.4
10	52	139.48	65190	0.10342	68.07	2.40E+05	5.95E+05	6.41E+05	691.3

ang. frequency (rad/s)	temperature (°c)	time (s)	osc. stress (Pa)	strain	delta (°)	G' (Pa)	G'' (Pa)	|G*| (Pa)	|G*|/sin(delta) (kPa)
10	52	50.703	16860	0.02078	64.15	3.63E+05	7.49E+05	8.33E+05	925
10	52	78.859	65190	0.090126	65.23	3.10E+05	6.71E+05	7.40E+05	814.4
10	52	94.094	65190	0.090791	65.7	3.02E+05	6.69E+05	7.34E+05	805
10	52	109.28	65190	0.092722	65.93	2.93E+05	6.56E+05	7.18E+05	786.3
10	52	124.39	65190	0.094802	66.15	2.84E+05	6.42E+05	7.02E+05	767.2
10	52	139.53	65190	0.096459	66.36	2.77E+05	6.31E+05	6.89E+05	752.5

ang. frequency (rad/s)	temperature (°c)	time (s)	osc. stress (Pa)	Strain	delta (°)	G' (Pa)	G" (Pa)	|G*| (Pa)	|G*|/sin(delta) (kPa)
10	52	50.765	13970	0.020592	64.53	2.98E+05	6.26E+05	6.93E+05	767.4
10	52	78.89	65190	0.10753	65.77	2.53E+05	5.63E+05	6.17E+05	676.9
10	52	94.109	65190	0.10807	66.11	2.49E+05	5.61E+05	6.14E+05	671.6
10	52	109.36	65190	0.108	66.29	2.47E+05	5.62E+05	6.14E+05	670.9
10	52	124.47	65190	0.10761	66.41	2.47E+05	5.65E+05	6.17E+05	672.7
10	52	139.69	65190	0.10681	66.49	2.48E+05	5.70E+05	6.21E+05	677.4

NTSS-1HM (B) (70°C)

ang. frequency (rad/s)	temperature (°c)	time (s)	osc. stress (Pa)	strain	delta (°)	G' (Pa)	G" (Pa)	|G*| (Pa)	|G*|/sin(delta) (kPa)
10	70	38.125	1362	0.02007	74.61	18030	65510	67950	70.48
10	70	78.703	7858	0.12064	75.25	16600	63060	65210	67.43
10	70	119.7	13910	0.22149	75.81	15420	60970	62890	64.87
10	70	160.5	19430	0.32467	76.4	14080	58210	59890	61.62
10	70	214.31	22740	0.43799	77.09	11610	50650	51970	53.31
10	70	267.95	22530	0.55476	77.65	8689	39690	40630	41.59

ang. frequency (rad/s)	temperature (°c)	time (s)	osc. stress (Pa)	strain	delta (°)	G' (Pa)	G" (Pa)	|G*| (Pa)	|G*|/sin(delta) (kPa)
10	70	38.125	1260	0.020294	74.82	16280	59990	62160	64.41
10	70	78.922	7190	0.12	75.41	15110	58050	59980	61.98
10	70	119.86	12790	0.22058	75.93	14110	56280	58020	59.82
10	70	160.72	17970	0.32433	76.5	12950	53920	55450	57.03
10	70	214.47	21150	0.44032	77.29	10580	46880	48060	49.27
10	70	267.98	20200	0.56036	77.95	7527	35270	36070	36.88

ang. frequency (rad/s)	temperature (°c)	time (s)	osc. stress (Pa)	strain	delta (°)	G' (Pa)	G" (Pa)	|G*| (Pa)	|G*|/sin(delta) (kPa)
10	70	38.219	1097	0.019903	75.08	14210	53340	55200	57.12
10	70	78.969	6405	0.12069	75.69	13130	51470	53120	54.82
10	70	119.86	11380	0.22134	76.2	12280	49980	51470	53
10	70	173.67	15690	0.32546	76.75	11060	46970	48250	49.57
10	70	227.42	17370	0.44892	77.27	8530	37770	38720	39.7
10	70	280.97	15710	0.5553	78	5886	27690	28310	28.94

NTSS-1HM (C) (52°C)

ang. frequency (rad/s)	temperature (°c)	time (s)	osc. stress (Pa)	strain	delta (°)	G' (Pa)	G'' (Pa)	|G*| (Pa)	|G*|/sin(delta) (kPa)
10	52	51.016	11490	0.02022	70.85	1.89E+05	5.44E+05	5.76E+05	610
10	52	104.81	60800	0.12119	72.29	1.54E+05	4.83E+05	5.07E+05	532.5
10	52	132.7	65190	0.13118	72.47	1.51E+05	4.79E+05	5.02E+05	526.9
10	52	147.89	65190	1.31E-01	72.49	1.51E+05	4.80E+05	5.03E+05	527.6
10	52	163.03	65190	0.13136	72.53	1.51E+05	4.79E+05	5.02E+05	526
10	52	178.3	65190	0.13116	72.54	1.51E+05	4.79E+05	5.03E+05	526.7

ang. frequency (rad/s)	temperature (°c)	time (s)	osc. stress (Pa)	strain	delta (°)	G' (Pa)	G'' (Pa)	|G*| (Pa)	|G*|/sin(delta) (kPa)
10	52	50.594	9020	0.020377	70.82	1.47E+05	4.23E+05	4.47E+05	473.6
10	52	91.594	46530	0.11969	72.21	1.20E+05	3.73E+05	3.92E+05	411.8
10	52	119.63	65190	0.18167	72.8	1.07E+05	3.45E+05	3.62E+05	378.5
10	52	134.86	65190	0.18259	72.91	1.06E+05	3.44E+05	3.60E+05	376.4
10	52	149.89	65190	0.18532	73	1.04E+05	3.39E+05	3.54E+05	370.6
10	52	165.01	65190	0.18828	73.08	1.02E+05	3.34E+05	3.49E+05	364.5

ang. frequency (rad/s)	temperature (°c)	time (s)	osc. stress (Pa)	Strain	delta (°)	G' (Pa)	G" (Pa)	|G*| (Pa)	|G*|/sin(delta) (kPa)
10	52	50.875	10610	0.021043	71.22	1.64E+05	4.83E+05	5.10E+05	539.1
10	52	104.42	51550	0.1216	73.13	1.24E+05	4.09E+05	4.28E+05	447
10	52	132.36	65190	0.15867	73.39	1.18E+05	3.97E+05	4.14E+05	432.4
10	52	147.52	65190	0.15985	73.47	1.17E+05	3.94E+05	4.11E+05	429
10	52	162.63	65190	0.16132	73.55	1.15E+05	3.91E+05	4.08E+05	424.9
10	52	177.77	65190	0.16272	73.62	1.14E+05	3.88E+05	4.04E+05	421

NTSS-1HM (C) (70°C)

ang. frequency (rad/s)	temperature (°c)	time (s)	osc. stress (Pa)	strain	delta (°)	G' (Pa)	G" (Pa)	|G*| (Pa)	|G*|/sin(delta) (kPa)
10	70	38.156	673.4	0.02001	81.61	4912	33320	33680	34.05
10	70	78.922	3988	0.11994	81.77	4760	32930	33270	33.62
10	70	119.56	7213	0.22109	81.97	4559	32330	32650	32.97
10	70	160.3	10290	0.32253	82.19	4340	31640	31930	32.23
10	70	201.05	13180	0.4247	82.39	4114	30790	31060	31.34
10	70	254.77	15020	0.5441	82.58	3567	27400	27630	27.86

ang. frequency (rad/s)	temperature (°c)	time (s)	osc. stress (Pa)	strain	delta (°)	G' (Pa)	G" (Pa)	|G*| (Pa)	|G*|/sin(delta) (kPa)
10	70	38.031	567.6	0.019932	81.26	4332	28170	28500	28.83
10	70	78.594	3353	0.12009	81.54	4112	27640	27950	28.25
10	70	119.52	6017	0.22105	81.8	3887	26960	27240	27.52
10	70	160.36	8487	0.32303	82.03	3647	26040	26290	26.55
10	70	214.14	10370	0.42991	82.26	3250	23910	24130	24.35
10	70	267.86	11040	0.54755	82.5	2636	20010	20180	20.35

ang. frequency (rad/s)	temperature (°c)	time (s)	osc. stress (Pa)	strain	delta (°)	G' (Pa)	G" (Pa)	|G*| (Pa)	|G*|/sin(delta) (kPa)
10	70	38	634	0.019963	81.44	4729	31430	31780	32.14
10	70	78.922	3730	0.12034	81.69	4483	30690	31020	31.35
10	70	119.75	6695	0.22193	81.97	4215	29890	30190	30.49
10	70	160.72	9438	0.32246	82.24	3954	29020	29290	29.56
10	70	201.72	11980	0.42405	82.47	3706	28020	28270	28.51
10	70	255.36	13280	0.55253	82.71	3051	23850	24050	24.24

DSR RESULTS

CMS-1P (E)

ang. frequency (rad/s)	temperature (°c)	time (s)	osc. stress (Pa)	strain	delta (°)	G' (Pa)	G" (Pa)	|G*| (Pa)	|G*|/sin(delta) (kPa)
10	52	671.2	388	0.1121	80.72	561.5	3436	3482	3.528
10	58	1447.8	190.1	0.1203	80.91	252.3	1577	1597	1.617
10	64	2224.5	94.46	0.12044	79.78	141.4	784.3	796.9	0.8098
10	70	3001.2	49.57	0.12041	76.66	96.88	408.4	419.7	0.4314
10	76	3777.8	28.47	0.12042	70.9	78.12	225.6	238.7	0.2526
10	82	4554.7	18.77	0.12037	62.38	70.51	134.8	152.1	0.1717
10	88	5331.3	14.01	0.12041	50.98	66.65	82.25	105.9	0.1363
10	94	6108	11.98	0.12086	38.07	62.93	49.29	79.94	0.1296

ang. frequency (rad/s)	temperature (°c)	time (s)	osc. stress (Pa)	strain	delta (°)	G' (Pa)	G" (Pa)	|G*| (Pa)	|G*|/sin(delta) (kPa)
10	52	671.08	348.6	0.11289	80.37	520.1	3065	3109	3.154
10	58	1447.5	169.6	0.12043	80.51	234.9	1406	1425	1.445
10	64	2224.1	84.03	0.12037	79.11	134.3	697.9	710.7	0.7238
10	70	3000.7	44.42	0.12038	75.62	93.57	364.8	376.6	0.3888
10	76	3777.4	26.16	0.1204	69.66	75.84	204.6	218.2	0.2327
10	82	4554	17.79	0.12036	61.35	67.32	123.2	140.4	0.16
10	88	5330.7	14.09	0.12035	51.6	62.98	79.46	101.4	0.1294
10	94	6107.4	12.54	0.12032	42.2	60.19	54.57	81.25	0.121

ang. frequency (rad/s)	temperature (°c)	time (s)	osc. stress (Pa)	strain	delta (°)	G' (Pa)	G" (Pa)	|G*| (Pa)	|G*|/sin(delta) (kPa)
10	52	671.13	284.6	0.11457	80.57	410.4	2470	2504	2.538
10	58	1447.4	134.5	0.12046	80.24	192	1116	1132	1.149
10	64	2223.8	64.16	0.12044	77.97	113.3	531.5	543.4	0.5556
10	70	3000.2	34.09	0.12038	73.05	84.01	275.7	288.2	0.3013
10	76	3776.3	20.74	0.12035	64.99	71.89	154.1	170	0.1876
10	82	4552.4	14.81	0.12039	54.05	65.64	90.5	111.8	0.1381
10	88	5328.8	12.45	0.12035	42.1	62.1	56.1	83.69	0.1248
10	94	6105	11.56	0.12035	31.35	60.21	36.68	70.5	0.1355

CSS-1HP (E)

ang. frequency (rad/s)	temperature (°c)	time (s)	osc. stress (Pa)	strain	delta (°)	G' (Pa)	G" (Pa)	|G*| (Pa)	|G*|/sin(delta) (kPa)
10	52	671.22	1733	0.033519	66.57	20610	47560	51840	56.49
10	58	1447.5	2825	0.12047	69.43	8264	22020	23520	25.12
10	64	2223.7	1404	0.12031	71.28	3761	11100	11720	12.37
10	70	3000.1	725.4	0.12038	72.49	1826	5789	6070	6.365
10	76	3776.4	387.7	0.12033	72.64	973.7	3115	3264	3.419
10	82	4552.8	219	0.12033	71.44	592.6	1765	1862	1.964
10	88	5329.1	131.1	0.12028	68.88	409	1059	1135	1.217
10	94	6105.5	82.96	0.12029	64.93	313.4	669.8	739.5	0.8165

ang. frequency (rad/s)	temperature (°c)	time (s)	osc. stress (Pa)	strain	delta (º)	G' (Pa)	G" (Pa)	|G*| (Pa)	|G*|/sin(delta) (kPa)
10	52	671.03	1678	0.037982	66.93	17360	40760	44300	48.15
10	58	1447.4	2456	0.12038	69.92	7025	19220	20460	21.79
10	64	2223.5	1226	0.12038	71.89	3182	9726	10230	10.77
10	70	2999.8	633.6	0.12033	73.02	1550	5076	5308	5.55
10	76	3776.1	339.3	0.12032	72.89	841.5	2733	2860	2.992
10	82	4552.5	191.5	0.12028	71.28	524.5	1548	1634	1.725
10	88	5328.8	114.5	0.12035	68.1	371.8	924.8	996.8	1.074
10	94	6105.1	72.64	0.12031	63.55	291.8	586.7	655.3	0.7319

ang. frequency (rad/s)	temperature (°c)	time (s)	osc. stress (Pa)	strain	delta (º)	G' (Pa)	G" (Pa)	|G*| (Pa)	|G*|/sin(delta) (kPa)
10	52	671.02	1639	0.041401	67.6	15120	36690	39680	42.92
10	58	1447.3	2202	0.12037	70.52	6118	17300	18350	19.46
10	64	2223.7	1097	0.12034	72.32	2783	8732	9165	9.619
10	70	3000.1	569.6	0.12036	73.13	1385	4569	4774	4.989
10	76	3776.5	306.9	0.1203	72.63	773.7	2474	2592	2.716
10	82	4552.8	174.4	0.12039	70.62	494.9	1407	1492	1.581
10	88	5329.1	105.3	0.12033	67.06	359.6	849.8	922.7	1.002
10	94	6105.3	67.65	0.12028	62.11	288.4	544.9	616.5	0.6975

NTSS-1HM (C)

ang. frequency (rad/s)	temperature (°c)	time (s)	osc. stress (Pa)	strain	delta (º)	G' (Pa)	G" (Pa)	|G*| (Pa)	|G*|/sin(delta) (kPa)
10	82	671.17	718.2	0.088755	84.84	728.9	8068	8101	8.134
10	88	1447.6	440.6	0.12041	86.12	248.3	3656	3665	3.673
10	94	2224	215.5	0.12046	86.8	99.95	1789	1792	1.795

ang. frequency (rad/s)	temperature (°c)	time (s)	osc. stress (Pa)	strain	delta (º)	G' (Pa)	G" (Pa)	|G*| (Pa)	|G*|/sin(delta) (kPa)
10	82	671.03	618.3	0.095707	85.02	561.2	6443	6468	6.492
10	88	1447.4	360.4	0.12039	86.16	200.8	2991	2998	3.005
10	94	2223.7	178.7	0.12032	86.73	84.78	1485	1487	1.49

ang. frequency (rad/s)	temperature (°c)	time (s)	osc. stress (Pa)	strain	delta (º)	G' (Pa)	G" (Pa)	|G*| (Pa)	|G*|/sin(delta) (kPa)
10	82	671	612.8	0.095888	84.84	575.5	6373	6399	6.425
10	88	1447.4	353.7	0.1204	85.9	210.7	2936	2943	2.951
10	94	2223.9	173.8	0.12041	86.33	92.5	1444	1447	1.45

CRS-2 (E)

ang. frequency (rad/s)	temperature (°c)	time (s)	osc. stress (Pa)	strain	delta (°)	G' (Pa)	G" (Pa)	|G*| (Pa)	|G*|/sin(delta) (kPa)
10	52	671.23	492.3	0.10109	82.31	653	4838	4882	4.926
10	58	1447.6	246.1	0.12045	84.47	197.7	2041	2050	2.06
10	64	2224.1	111.1	0.12034	86.11	62.83	922.9	925	0.9272
10	70	3000.5	54.46	0.12045	87.28	21.2	446	446.5	0.447
10	76	3776.7	29.34	0.12042	88.15	7.338	227.1	227.3	0.2274
10	82	4552.9	18.53	0.12033	88.56	3.083	123.1	123.1	0.1231
10	88	5329.4	14.17	0.12031	88.64	1.683	71.06	71.08	0.0711
10	94	6106.1	12.5	0.12031	88.44	1.175	43.26	43.28	0.0433

ang. frequency (rad/s)	temperature (°c)	time (s)	osc. stress (Pa)	strain	delta (°)	G' (Pa)	G" (Pa)	|G*| (Pa)	|G*|/sin(delta) (kPa)
10	52	670.94	476.8	0.10202	82.43	617.6	4645	4686	4.727
10	58	1447.3	236.3	0.12042	84.55	186.9	1960	1969	1.978
10	64	2223.8	107.2	0.12041	86.16	59.75	889.3	891.3	0.8933
10	70	3000.1	52.64	0.12037	87.34	20.01	430.8	431.2	0.4317
10	76	3776.4	28.5	0.12044	88.21	6.855	219.3	219.4	0.2195
10	82	4552.8	18.15	0.1204	88.62	2.869	118.9	118.9	0.1189
10	88	5329	14.02	0.12036	88.63	1.644	68.88	68.9	0.06892
10	94	6105.6	12.45	0.12033	88.45	1.136	42.13	42.15	0.04216

ang. frequency (rad/s)	temperature (°c)	time (s)	osc. stress (Pa)	strain	delta (°)	G' (Pa)	G" (Pa)	|G*| (Pa)	|G*|/sin(delta) (kPa)
10	52	671.17	382.4	0.10733	83.28	418	3548	3572	3.597
10	58	1447.5	183.2	0.12046	85.22	127.2	1520	1526	1.531
10	64	2223.9	83.5	0.12043	86.66	40.35	691.1	692.3	0.6935
10	70	3000.3	42.25	0.1204	87.73	13.54	341.2	341.4	0.3417
10	76	3776.5	23.94	0.12037	88.45	4.8	177	177	0.1771
10	82	4553.1	16.27	0.12037	88.7	2.209	97.71	97.74	0.09776
10	88	5329.4	13.28	0.12038	88.59	1.419	57.5	57.52	0.05754
10	94	6105.7	12.15	0.12034	88.1	1.19	35.85	35.87	0.03589

FOGSEAL (C)

ang. frequency (rad/s)	temperature (°c)	time (s)	osc. stress (Pa)	strain	delta (°)	G' (Pa)	G" (Pa)	|G*| (Pa)	|G*|/sin(delta) (kPa)
10	82	671.08	799	0.082465	84.8	879.4	9658	9698	9.738
10	88	1447.5	525.8	0.1204	86.36	277.3	4364	4372	4.381
10	94	2223.8	251.1	0.12047	87.38	95.53	2085	2087	2.089

CRS-2P (E)

ang. frequency (rad/s)	temperature (°c)	time (s)	osc. stress (Pa)	strain	delta (º)	G' (Pa)	G" (Pa)	|G*| (Pa)	|G*|/sin(delta) (kPa)
10	52	670.81	692.4	0.082176	75.67	2092	8187	8450	8.722
10	58	1447.5	471.9	0.11985	78.01	822.1	3870	3956	4.045
10	64	2223.9	237.4	0.12003	79.56	361.2	1960	1993	2.026
10	70	3000.4	125.7	0.12008	80.4	176.6	1044	1059	1.074
10	76	3777	69.63	0.12	80.81	93.9	580.2	587.8	0.5954
10	82	4553.5	41.53	0.12002	80.72	56.19	343.7	348.3	0.3529
10	88	5330	26.77	0.11998	80.48	36.05	215	218	0.221
10	94	6106.5	19.04	0.12005	79.92	25.25	142.1	144.3	0.1465

ang. frequency (rad/s)	temperature (°c)	time (s)	osc. stress (Pa)	strain	Delta (º)	G' (Pa)	G" (Pa)	|G*| (Pa)	|G*|/sin(delta) (kPa)
10	52	670.77	669.8	0.084014	75.64	1983	7747	7997	8.255
10	58	1447.1	448.9	0.12004	77.97	783.6	3676	3759	3.843
10	64	2223.4	226.2	0.12003	79.45	347.8	1868	1900	1.932
10	70	2999.8	120.4	0.12001	80.25	171.9	1000	1015	1.03
10	76	3776.1	66.72	0.12001	80.46	93.4	556	563.8	0.5717
10	82	4552.7	39.79	0.1199	80.22	56.81	329.6	334.5	0.3394
10	88	5329.2	25.83	0.12001	79.66	37.81	207.3	210.7	0.2142
10	94	6105.8	18.39	0.12001	78.77	27.2	137	139.7	0.1424

ang. frequency (rad/s)	temperature (°c)	time (s)	osc. stress (Pa)	strain	Delta (°)	G' (Pa)	G" (Pa)	|G*| (Pa)	|G*|/sin(delta) (kPa)
10	52	670.89	649.4	0.085687	75.79	1866	7370	7603	7.843
10	58	1447.2	430.1	0.11993	78.02	748.2	3527	3605	3.685
10	64	2223.5	218	0.11996	79.41	336.9	1801	1833	1.864
10	70	2999.9	116.2	0.12001	80.18	167	965.3	979.7	0.9942
10	76	3776.5	64.28	0.12004	80.42	90.39	535.5	543	0.5507
10	82	4552.9	38.3	0.11992	80.17	54.92	316.8	321.5	0.3263
10	88	5329.2	25	0.12004	79.59	36.68	199.7	203	0.2064
10	94	6105.5	17.94	0.11999	78.69	26.49	132.5	135.1	0.1378

CRS-2 (B)

ang. frequency (rad/s)	temperature (°c)	time (s)	osc. stress (Pa)	strain	delta (°)	G' (Pa)	G" (Pa)	|G*| (Pa)	|G*|/sin(delta) (kPa)
10	58	803.42	252.8	0.11342	85.86	160.8	2223	2229	2.234
10	64	1579.7	123.2	0.12004	86.66	59.81	1025	1026	1.028
10	70	2356.3	59.92	0.12005	86.96	26.5	498.4	499.1	0.4998
10	76	3132.7	30.99	0.12	86.82	14.32	257.9	258.3	0.2586
10	82	3909	17.2	0.12004	86.33	9.185	143	143.3	0.1436
10	88	4685.6	10.33	0.12003	84.19	8.711	85.58	86.02	0.08646
10	94	5462.4	6.677	0.12014	79.65	9.986	54.67	55.57	0.05649

ang. frequency (rad/s)	temperature (°c)	time (s)	osc. stress (Pa)	strain	Delta (º)	G' (Pa)	G" (Pa)	|G*| (Pa)	|G*|/sin(delta) (kPa)
10	52	671.17	446.4	0.10538	85.1	361.8	4221	4236	4.252
10	58	1447.3	219.9	0.12047	86.56	109.5	1822	1826	1.829
10	64	2223.8	102.3	0.12045	87.52	36.7	848.6	849.4	0.8502
10	70	3000.2	49.97	0.12046	88.2	13	414.6	414.8	0.415
10	76	3776.7	26.05	0.12035	88.47	5.784	216.4	216.5	0.2165
10	82	4553.2	14.38	0.12036	88.72	2.666	119.5	119.5	0.1195
10	88	5329.7	8.532	0.12032	88.53	1.813	70.89	70.91	0.07093
10	94	6106.2	5.294	0.12034	88.03	1.51	43.96	43.99	0.04402

ang. frequency (rad/s)	temperature (°c)	time (s)	osc. stress (Pa)	strain	Delta (º)	G' (Pa)	G" (Pa)	|G*| (Pa)	|G*|/sin(delta) (kPa)
10	52	671.11	449.8	0.10528	85.11	363.9	4257	4273	4.288
10	58	1447.5	220.1	0.12046	86.57	109.2	1824	1827	1.83
10	64	2224	102.8	0.1204	87.46	37.88	852.6	853.5	0.8543
10	70	3000.5	49.96	0.12032	88.24	12.73	415	415.2	0.4154
10	76	3777.2	26.1	0.12043	88.55	5.485	216.6	216.7	0.2168
10	82	4553.8	14.72	0.12033	88.49	3.218	122.3	122.4	0.1224
10	88	5330.5	8.904	0.12034	88.26	2.244	73.96	73.99	0.07403
10	94	6107.3	5.697	0.12016	87.88	1.755	47.38	47.41	0.04744

CRS-2P (B)

ang. frequency (rad/s)	temperature (°c)	time (s)	osc. stress (Pa)	strain	delta (°)	G' (Pa)	G" (Pa)	|G*| (Pa)	|G*|/sin(delta) (kPa)
10	52	671.06	597.5	0.09431	81.64	921.6	6269	6336	6.404
10	58	1447.3	334.9	0.12042	83.25	327	2762	2781	2.8
10	64	2223.6	159.3	0.12031	84.21	133.6	1318	1325	1.331
10	70	2999.9	81.57	0.12044	84.59	63.85	674.2	677.2	0.6803
10	76	3776.3	44.16	0.12036	84.61	34.46	365.3	366.9	0.3686
10	82	4552.5	25.52	0.12032	84.15	21.62	211	212.1	0.2132
10	88	5329	15.7	0.12034	83.37	15.05	129.6	130.5	0.1313
10	94	6105.4	10.19	0.12032	82.37	11.24	83.94	84.69	0.08545

ang. frequency (rad/s)	temperature (°c)	time (s)	osc. stress (Pa)	strain	Delta (°)	G' (Pa)	G" (Pa)	|G*| (Pa)	|G*|/sin(delta) (kPa)
10	52	671.08	602.5	0.093907	81.55	943.2	6347	6417	6.487
10	58	1447.4	342.4	0.12036	83.23	335.4	2825	2845	2.865
10	64	2223.6	164.2	0.12039	84.28	135.9	1357	1364	1.371
10	70	3000	85.22	0.12028	84.78	64.49	705.6	708.5	0.7115
10	76	3776.1	44.89	0.12041	85.04	32.22	371.4	372.8	0.3742
10	82	4552.6	25.53	0.12037	84.79	19.28	211.3	212.1	0.213
10	88	5328.8	15.57	0.12028	83.9	13.75	128.7	129.4	0.1302
10	94	6105.2	10.03	0.1203	82.81	10.43	82.74	83.39	0.08405

ang. frequency (rad/s)	temperature (°c)	time (s)	osc. stress (Pa)	strain	Delta (°)	G' (Pa)	G" (Pa)	|G*| (Pa)	|G*|/sin(delta) (kPa)
10	52	670.81	548.3	0.09725	81.98	786.9	5583	5638	5.694
10	58	1447.2	302.1	0.12	83.51	284.5	2502	2518	2.534
10	64	2223.4	145.8	0.11993	84.41	118.4	1210	1215	1.221
10	70	2999.8	75.59	0.11991	84.73	57.85	627.7	630.3	0.633
10	76	3776.2	41.24	0.11995	84.7	31.78	342.3	343.8	0.3453
10	82	4552.5	23.91	0.12003	84.29	19.83	198.2	199.2	0.2002
10	88	5329	14.61	0.12	83.52	13.74	121	121.8	0.1226
10	94	6105.4	9.47	0.12001	82.44	10.38	78.22	78.91	0.0796

NTSS-1HM (B)

ang. frequency (rad/s)	temperature (°c)	time (s)	osc. stress (Pa)	strain	delta (°)	G' (Pa)	G" (Pa)	|G*| (Pa)	|G*|/sin(delta) (kPa)
10	82	671.14	976	0.061548	80.83	2531	15670	15880	16.08
10	88	1447.5	866.3	0.12043	83.18	855.1	7154	7205	7.256
10	94	2223.9	413.3	0.12049	84.79	312.1	3423	3438	3.452
10	96	1447.3	232.2	0.012045	83.96	203.7	1924		1.946

ang. frequency (rad/s)	temperature (°c)	time (s)	osc. stress (Pa)	strain	delta (°)	G' (Pa)	G" (Pa)	|G*| (Pa)	|G*|/sin(delta) (kPa)
10	82	670.98	977.8	0.061139	80.64	2603	15800	16010	16.23
10	88	1447.3	865.7	0.12038	82.98	879.7	7149	7203	7.257
10	94	2223.5	424.5	0.12044	84.53	336.8	3517	3533	3.549
10	96	1447.3	232.2	0.012045	83.96	203.7	1924		1.946

ang. frequency (rad/s)	temperature (°c)	time (s)	osc. stress (Pa)	strain	delta (°)	G' (Pa)	G" (Pa)	|G*| (Pa)	|G*|/sin(delta) (kPa)
10	82	671.16	946.5	0.064747	80.88	2319	14450	14640	14.82
10	88	1447.4	795.2	0.12053	83.15	788.5	6561	6609	6.656
10	94	2223.7	383.7	0.12043	84.68	296.2	3180	3194	3.208
10	96	1447.3	232.2	0.012045	83.96	203.7	1924		1.946

SS-1 (B)

ang. frequency (rad/s)	temperature (°c)	time (s)	osc. stress (Pa)	strain	delta (º)	G' (Pa)	G" (Pa)	|G*| (Pa)	|G*|/sin(delta) (kPa)
10	52	670.86	502.8	0.10197	84.93	436.8	4920	4939	4.958
10	58	1447.3	249.4	0.12013	86.45	128.7	2076	2080	2.084
10	64	2223.5	115.1	0.12005	87.48	42.04	957	957.9	0.9589
10	70	3000	56.56	0.12	88.25	14.21	464.2	464.4	0.4647
10	76	3776.3	30.97	0.12002	88.66	5.669	241.8	241.9	0.2419
10	82	4552.6	19.55	0.11994	88.7	3.049	134.1	134.1	0.1342
10	88	5329.2	14.71	0.11995	88.51	2.058	79.08	79.1	0.07913
10	94	6105.7	12.75	0.11994	88.28	1.469	48.99	49.01	0.04904

ang. frequency (rad/s)	temperature (°c)	time (s)	osc. stress (Pa)	strain	Delta (º)	G' (Pa)	G" (Pa)	|G*| (Pa)	|G*|/sin(delta) (kPa)
10	52	670.8	477.9	0.10315	84.71	427.7	4621	4641	4.661
10	58	1447.3	237.1	0.11998	86.13	133.8	1976	1980	1.985
10	64	2223.7	110	0.12	87.12	46.03	915	916.1	0.9173
10	70	3000	54.29	0.12011	87.85	16.71	445	445.3	0.4457
10	76	3776.2	29.83	0.12004	88.28	6.949	232.1	232.2	0.2323
10	82	4552.3	19.02	0.11994	88.41	3.585	129	129.1	0.1291
10	88	5328.6	14.46	0.11998	88.35	2.182	75.93	75.96	0.07599
10	94	6105	12.64	0.11998	88.07	1.588	47.19	47.21	0.04724

ang. frequency (rad/s)	temperature (°c)	time (s)	osc. stress (Pa)	strain	Delta (°)	G' (Pa)	G" (Pa)	|G*| (Pa)	|G*|/sin(delta) (kPa)
10	52	670.84	474	0.10335	84.72	422.9	4574	4594	4.614
10	58	1447.2	236.1	0.12006	86.14	132.8	1966	1971	1.975
10	64	2223.4	109.3	0.12007	87.13	45.61	909.2	910.4	0.9115
10	70	2999.6	54.15	0.11998	87.84	16.78	444.4	444.7	0.445
10	76	3776.1	29.7	0.11995	88.24	7.113	231.2	231.3	0.2314
10	82	4552.3	18.92	0.11998	88.38	3.629	128	128	0.1281
10	88	5328.5	14.42	0.11997	88.29	2.251	75.54	75.57	0.0756
10	94	6104.8	12.61	0.11997	87.97	1.654	46.76	46.79	0.04682

SS-1 (E)

ang. frequency (rad/s)	temperature (°c)	time (s)	osc. stress (Pa)	strain	delta (°)	G' (Pa)	G" (Pa)	|G*| (Pa)	|G*|/sin(delta) (kPa)
10	52	670.92	447.8	0.10528	85.66	322.4	4247	4260	4.272
10	58	1447.2	217.9	0.12003	87.02	94.49	1815	1817	1.82
10	64	2223.6	100.8	0.1201	87.93	30.23	836.7	837.3	0.8378
10	70	2999.8	50.59	0.12002	88.48	10.94	412.9	413.1	0.4132
10	76	3776.2	28.78	0.11997	88.56	5.569	222.3	222.3	0.2224
10	82	4552.5	19.08	0.11987	87.89	4.815	130.6	130.7	0.1308
10	88	5328.7	14.77	0.11989	86.54	5.034	83.31	83.46	0.08361
10	94	6105.1	12.79	0.1199	84.83	5.072	56.1	56.33	0.05656

ang. frequency (rad/s)	temperature (°c)	time (s)	osc. stress (Pa)	strain	Delta (º)	G' (Pa)	G" (Pa)	|G*| (Pa)	|G*|/sin(delta) (kPa)
10	52	670.97	467	0.10401	85.17	378.4	4482	4498	4.514
10	58	1447.4	230.5	0.12007	86.49	117.7	1920	1923	1.927
10	64	2223.7	107.1	0.12002	87.32	41.77	890.9	891.8	0.8928
10	70	3000	54.06	0.11996	87.68	17.97	443.9	444.2	0.4446
10	76	3776.4	30.66	0.12001	87.6	10.1	240.7	240.9	0.2411
10	82	4552.8	19.94	0.11989	86.91	7.602	141	141.2	0.1414
10	88	5329.2	15.1	0.11992	85.82	6.486	88.79	89.03	0.08927
10	94	6105.6	12.89	0.11994	84.52	5.618	58.52	58.79	0.05906

ang. frequency (rad/s)	temperature (°c)	time (s)	osc. stress (Pa)	strain	Delta (º)	G' (Pa)	G" (Pa)	|G*| (Pa)	|G*|/sin(delta) (kPa)
10	52	670.86	434.2	0.10575	85.37	331.8	4100	4113	4.127
10	58	1447.1	214.3	0.12005	86.68	103.5	1785	1788	1.791
10	64	2223.4	99.32	0.12001	87.46	36.68	825.5	826.3	0.8271
10	70	2999.7	50.23	0.12	87.81	15.75	410.9	411.2	0.4115
10	76	3776.1	28.72	0.11989	87.62	9.268	223.4	223.6	0.2238
10	82	4552.3	19.01	0.1199	86.8	7.352	131.6	131.8	0.132
10	88	5328.6	14.62	0.11991	85.64	6.315	82.85	83.09	0.08333
10	94	6105.1	12.65	0.11992	84.07	5.692	54.84	55.13	0.05543

SS-1H (B)

ang. frequency (rad/s)	temperature (°c)	time (s)	osc. stress (Pa)	strain	delta (°)	G' (Pa)	G" (Pa)	|G*| (Pa)	|G*|/sin(delta) (kPa)
10	52	670.91	1053	0.049354	78.03	4431	20910	21370	21.84
10	58	1447.3	1049	0.11994	80.95	1377	8653	8762	8.872
10	64	2223.4	469.9	0.11994	83.18	466.6	3900	3928	3.956
10	70	2999.9	216.8	0.12008	84.92	160.3	1805	1812	1.819
10	76	3776.3	105.7	0.11999	86.21	58.3	880.3	882.3	0.8842
10	82	4552.5	55.35	0.11998	87.06	23.37	455.6	456.2	0.4568
10	88	5328.9	31.8	0.11994	87.5	10.96	251.2	251.5	0.2517
10	94	6105.1	20	0.11999	87.05	7.29	141.3	141.4	0.1416

ang. frequency (rad/s)	temperature (°c)	time (s)	osc. stress (Pa)	strain	delta (°)	G' (Pa)	G" (Pa)	|G*| (Pa)	|G*|/sin(delta) (kPa)
10	52	670.89	1007	0.055236	78.43	3661	17880	18250	18.63
10	58	1447.2	909.8	0.1201	81.19	1163	7501	7590	7.681
10	64	2223.5	412.8	0.12007	83.31	401.8	3425	3448	3.472
10	70	2999.7	190.7	0.12006	84.96	140	1588	1594	1.6
10	76	3776	93.06	0.12005	86.21	51.21	773.9	775.6	0.7773
10	82	4552.5	49.05	0.12002	87.04	20.75	401.7	402.3	0.4028
10	88	5328.9	28.7	0.12005	87.49	9.79	223	223.2	0.2235
10	94	6105.3	19	0.12003	87.58	5.499	130.1	130.2	0.1303

ang. frequency (rad/s)	temperature (°c)	time (s)	osc. stress (Pa)	strain	Delta (º)	G' (Pa)	G" (Pa)	|G*| (Pa)	|G*|/sin(delta) (kPa)
10	58	670.8	698.8	0.08616	80.88	1288	8023	8126	8.23
10	64	1446.8	435.7	0.12001	83.04	440.9	3614	3641	3.668
10	70	2223.2	204	0.12	84.71	157.4	1699	1707	1.714
10	76	2999.5	100.4	0.12005	85.94	59.22	835.2	837.3	0.8394
10	82	3775.7	52.93	0.11997	86.76	24.65	435.5	436.2	0.4369
10	88	4552.1	30.57	0.11997	87.2	11.78	240.5	240.8	0.2411
10	94	5328.3	19.91	0.11995	87.27	6.673	140.1	140.2	0.1404

CRS-2 (U)

ang. frequency (rad/s)	temperature (°c)	time (s)	osc. stress (Pa)	strain	delta (º)	G' (Pa)	G" (Pa)	|G*| (Pa)	|G*|/sin(delta) (kPa)
10	52	962.53	389	0.10803	85.08	309.7	3595	3608	3.622
10	58	1738.8	197	0.12048	86.48	100.5	1635	1639	1.642
10	64	2515.3	94.6	0.12038	87.46	34.72	783.5	784.3	0.785
10	70	3291.9	47.64	0.12033	88.15	12.52	387	387.2	0.3874
10	76	4068.3	26.68	0.12032	88.26	6.171	202.9	203	0.2031
10	82	4844.7	17.52	0.12033	88.04	3.874	113	113	0.1131
10	88	5621.3	13.75	0.12036	87.4	3.038	66.9	66.97	0.06704
10	94	6397.9	12.25	0.12031	86.14	2.816	41.78	41.87	0.04197

ang. frequency (rad/s)	temperature (°c)	time (s)	osc. stress (Pa)	strain	Delta (º)	G' (Pa)	G" (Pa)	|G*| (Pa)	|G*|/sin(delta) (kPa)
10	52	979.31	360.9	0.10932	85.17	278.4	3296	3308	3.32
10	58	1755.6	183.8	0.12033	86.56	91.93	1527	1530	1.533
10	64	2532	88.99	0.12033	87.52	31.88	736.8	737.5	0.7382
10	70	3308.3	45.15	0.12044	88.14	11.85	365.4	365.6	0.3658
10	76	4084.6	25.64	0.12038	88.32	5.655	193	193.1	0.1932
10	82	4860.9	17.08	0.12036	88.08	3.623	108	108	0.1081
10	88	5637.5	13.57	0.12036	87.32	3.01	64.29	64.36	0.06443
10	94	6413.8	12.18	0.12034	86.09	2.751	40.19	40.29	0.04038

ang. frequency (rad/s)	temperature (°c)	time (s)	osc. stress (Pa)	strain	Delta (º)	G' (Pa)	G" (Pa)	|G*| (Pa)	|G*|/sin(delta) (kPa)
10	52	988.5	359.6	0.10932	85.07	283	3284	3296	3.309
10	58	1764.9	183.5	0.12036	86.41	95.75	1525	1528	1.531
10	64	2541.3	89.48	0.12036	87.26	35.42	741	741.8	0.7427
10	70	3317.6	45.62	0.12037	87.68	14.99	370.3	370.6	0.3709
10	76	4094.1	25.83	0.1203	87.51	8.516	196.2	196.4	0.1966
10	82	4870.5	17.13	0.12027	86.7	6.393	111	111.2	0.1114
10	88	5647	13.5	0.12028	85.28	5.516	66.77	67	0.06723
10	94	6423.6	12.05	0.12026	83.29	5.011	42.61	42.9	0.0432

SS-1 (U)

ang. frequency (rad/s)	temperature (°c)	time (s)	osc. stress (Pa)	strain	delta (º)	G' (Pa)	G" (Pa)	|G*| (Pa)	|G*|/sin(delta) (kPa)
10	52	978.53	420.2	0.10691	85.59	302.8	3924	3936	3.948
10	58	1755.1	213.3	0.1204	86.82	98.47	1771	1774	1.777
10	64	2531.8	103.9	0.12039	87.63	35.68	861.3	862	0.8627
10	70	3308.7	53.53	0.12041	88.13	14.24	437	437.3	0.4375
10	76	4085.5	31.75	0.12112	88.51	6.423	246.5	246.6	0.2467
10	82	4862.2	20.55	0.12054	88.16	4.621	144.1	144.2	0.1443
10	88	5639	15.59	0.12035	87.34	4.266	91.74	91.84	0.09194
10	94	6416	13.45	0.11983	86.32	4.175	64.99	65.13	0.06526

ang. frequency (rad/s)	temperature (°c)	time (s)	osc. stress (Pa)	strain	Delta (º)	G' (Pa)	G" (Pa)	|G*| (Pa)	|G*|/sin(delta) (kPa)
10	52	987.52	408.9	0.10729	85.33	310.7	3806	3818	3.831
10	58	1763.8	208.2	0.12043	86.56	103.8	1729	1732	1.735
10	64	2540.2	100.1	0.12044	87.35	38.33	829.5	830.4	0.8313
10	70	3316.5	50.82	0.12041	87.82	15.75	414.5	414.8	0.4151
10	76	4092.7	29.2	0.1201	87.85	8.506	226.9	227.1	0.2273
10	82	4869	19.15	0.12029	87.35	6.085	131.6	131.7	0.1319
10	88	5645.3	14.63	0.12031	86.56	4.871	80.91	81.06	0.08121
10	94	6421.7	12.69	0.1203	85.35	4.285	52.68	52.86	0.05303

ang. frequency (rad/s)	temperature (°c)	time (s)	osc. stress (Pa)	strain	Delta (°)	G' (Pa)	G" (Pa)	|G*| (Pa)	|G*|/sin(delta) (kPa)
10	52	1023.9	410.1	0.10706	84.96	337.3	3823	3838	3.853
10	58	1800.2	209.7	0.12043	86.19	116	1742	1745	1.749
10	64	2576.7	102.6	0.12029	86.95	45.32	851.9	853.1	0.8543
10	70	3353.2	52.7	0.12042	87.28	20.49	431.1	431.6	0.4321
10	76	4129.8	30.01	0.12033	87.32	10.98	234.5	234.8	0.2351
10	82	4906.4	19.59	0.12032	86.78	7.71	137	137.2	0.1374
10	88	5683	14.97	0.12033	85.99	6.048	86.31	86.52	0.08673
10	94	6460	12.92	0.12034	84.91	5.132	57.65	57.87	0.0581

SS-1L (U)

ang. frequency (rad/s)	temperature (°c)	time (s)	osc. stress (Pa)	strain	delta (°)	G' (Pa)	G" (Pa)	|G*| (Pa)	|G*|/sin(delta) (kPa)
10	52	1011.4	552.1	0.09426	77.67	1255	5742	5878	6.016
10	58	1787.5	352.8	0.12035	78.26	600.3	2888	2950	3.013
10	64	2564	190.4	0.12029	77.92	334.8	1565	1600	1.637
10	70	3340.3	107.4	0.1204	77.1	202.9	885.9	908.8	0.9323
10	76	4116.8	64.16	0.1203	75.91	133.6	532	548.5	0.5655
10	82	4893.2	40.48	0.12036	74.45	93.59	336.3	349.1	0.3623
10	88	5669.6	27.24	0.12034	72.76	69.79	224.8	235.4	0.2465
10	94	6446	19.7	0.12027	71.04	54.47	158.5	167.6	0.1773

ang. frequency (rad/s)	temperature (°c)	time (s)	osc. stress (Pa)	strain	Delta (º)	G' (Pa)	G" (Pa)	|G*| (Pa)	|G*|/sin(delta) (kPa)
10	52	1014.7	546.8	0.094503	77.54	1253	5670	5807	5.947
10	58	1791.1	350.6	0.12028	78.28	595.9	2872	2933	2.995
10	64	2567.5	190.1	0.12027	78.06	330.5	1563	1598	1.633
10	70	3343.7	107.6	0.12037	77.28	200.2	887.4	909.7	0.9326
10	76	4120.2	64.15	0.12037	76	132.5	531.7	547.9	0.5647
10	82	4896.5	39.89	0.12035	74.77	90.24	331.4	343.5	0.356
10	88	5673.1	26.81	0.12038	73.34	66.08	220.8	230.4	0.2405
10	94	6449.4	19.26	0.12044	72.07	49.52	153.1	160.9	0.1691

ang. frequency (rad/s)	temperature (°c)	time (s)	osc. stress (Pa)	strain	Delta (º)	G' (Pa)	G" (Pa)	|G*| (Pa)	|G*|/sin(delta) (kPa)
10	52	1024.8	538.1	0.095553	78.23	1153	5532	5651	5.773
10	58	1801	338	0.12025	79.12	533.9	2776	2827	2.879
10	64	2577.4	180.5	0.12028	79.07	287.5	1488	1516	1.544
10	70	3353.5	100.9	0.12029	78.43	171	835.1	852.4	0.8701
10	76	4129.9	59.55	0.12029	77.34	111.2	494.9	507.2	0.5198
10	82	4906.1	37.46	0.12031	75.93	77.89	310.9	320.5	0.3304
10	88	5682.3	25.41	0.12028	74.28	58.52	207.9	216	0.2244
10	94	6458.5	18.61	0.12027	72.55	46.08	146.6	153.7	0.1611

SS-1H (U)

ang. frequency (rad/s)	temperature (°c)	time (s)	osc. stress (Pa)	strain	delta (°)	G' (Pa)	G" (Pa)	|G*| (Pa)	|G*|/sin(delta) (kPa)
10	52	1018.8	1057	0.05151	80.18	3504	20230	20530	20.84
10	58	1795.1	1034	0.12026	82.71	1092	8537	8607	8.677
10	64	2571.3	458.4	0.12047	84.74	349.8	3797	3813	3.829
10	70	3347.6	207	0.12039	86.36	109.4	1720	1723	1.727
10	76	4124.2	98.56	0.12051	87.64	33.61	815.5	816.1	0.8168
10	82	4900.7	51.28	0.12036	88.46	11.2	417.6	417.7	0.4179
10	88	5677	29.43	0.12037	88.86	4.513	226.9	226.9	0.2269
10	94	6453.3	19.23	0.12038	88.84	2.618	129.8	129.8	0.1298

ang. frequency (rad/s)	temperature (°c)	time (s)	osc. stress (Pa)	strain	delta (°)	G' (Pa)	G" (Pa)	|G*| (Pa)	|G*|/sin(delta) (kPa)
10	52	1079.8	1029	0.05529	80.59	3046	18380	18630	18.88
10	58	1855.8	950.5	0.12029	83.05	957.8	7855	7913	7.972
10	64	2632.2	427.4	0.12041	85	310.2	3543	3557	3.57
10	70	3408.5	191.7	0.12046	86.6	94.65	1592	1595	1.597
10	76	4120.2	64.15	0.12037	76	132.5	531.7	547.9	0.5647
10	82	4896.5	39.89	0.12035	74.77	90.24	331.4	343.5	0.356
10	88	5673.1	26.81	0.12038	73.34	66.08	220.8	230.4	0.2405
10	94	6449.4	19.26	0.12044	72.07	49.52	153.1	160.9	0.1691

NTSS-1HM (U)

ang. frequency (rad/s)	temperature (°c)	time (s)	osc. stress (Pa)	strain	delta (°)	G' (Pa)	G" (Pa)	|G*| (Pa)	|G*|/sin(delta) (kPa)
10	52	1040.7	1300	0.011156	78.59	23090	1.14E+05	1.17E+05	119
10	58	1816.8	5056	0.12031	81.98	5868	41640	42060	42.47
10	64	2593.3	2046	0.1203	84.11	1747	16930	17020	17.11
10	70	3369.7	876.8	0.12035	85.73	543.4	7272	7292	7.313
10	76	4146.3	391.7	0.12035	86.9	176.3	3254	3259	3.263
10	82	4922.9	183.3	0.12058	87.73	60.37	1520	1521	1.522
10	88	5699.5	91.55	0.12038	88.32	22.16	756.9	757.2	0.7575
10	94	6476	49.4	0.12031	88.59	9.877	401.5	401.6	0.4017

ang. frequency (rad/s)	temperature (°c)	time (s)	osc. stress (Pa)	strain	delta (°)	G' (Pa)	G" (Pa)	|G*| (Pa)	|G*|/sin(delta) (kPa)
10	52	1095.2	1298	0.011284	78.25	23470	1.13E+05	1.15E+05	117.7
10	58	1871.6	4974	0.12052	81.86	5851	40890	41300	41.72
10	64	2647.8	2014	0.12049	83.96	1759	16630	16730	16.82
10	70	3424.2	868.3	0.12029	85.52	563.8	7203	7225	7.247
10	76	4200.5	389.3	0.12032	86.61	191.5	3234	3240	3.245
10	82	4976.7	183	0.12029	87.35	70.52	1521	1523	1.525
10	88	5753	92.48	0.12037	87.72	30.47	765.6	766.2	0.7668
10	94	6529.2	50.36	0.12035	87.81	15.72	410.8	411.1	0.4114

ang. frequency (rad/s)	temperature (°c)	time (s)	osc. stress (Pa)	strain	delta (°)	G' (Pa)	G" (Pa)	|G*| (Pa)	|G*|/sin(delta) (kPa)
10	52	1068.4	1296	0.011921	78.92	20930	1.07E+05	1.09E+05	111
10	58	1844.8	4736	0.1205	82.23	5318	38970	39330	39.7
10	64	2621.3	1923	0.12027	84.3	1590	15920	16000	16.08
10	70	3397.6	826.7	0.12041	85.84	498.9	6854	6873	6.891
10	76	4173.9	370.6	0.12045	86.96	163.5	3076	3081	3.085
10	82	4950.4	174.4	0.12036	87.64	59.69	1448	1450	1.451
10	88	5726.8	88.02	0.12033	87.92	26.48	728.2	728.7	0.7292
10	94	6503.2	48.17	0.12035	88.05	13.33	391.7	391.9	0.3922

CHFRS-2P (E)

ang. frequency (rad/s)	temperature (°c)	time (s)	osc. stress (Pa)	strain	delta (°)	G' (Pa)	G" (Pa)	|G*| (Pa)	|G*|/sin(delta) (kPa)
10	52	988.64	785.3	0.072778	72.99	3166	1.04E+04	1.08E+04	11.32
10	58	1764.9	648.2	0.12042	75.59	1345	5236	5406	5.582
10	64	2541.1	335.2	0.12035	77.76	594.6	2740	2804	2.869
10	70	3317.5	178.1	0.12041	79.47	273	1469	1494	1.519
10	76	4093.9	97.37	0.12035	80.58	134	808.2	819.2	0.8304
10	82	4870.3	55.84	0.12034	81	73.4	463.5	469.3	0.4751
10	88	5646.7	34.31	0.1204	80.72	45.84	280.6	284.3	0.2881
10	94	6423.1	22.9	0.12023	79.84	32.17	179.6	182.4	0.1853

ang. frequency (rad/s)	temperature (°c)	time (s)	osc. stress (Pa)	strain	delta (º)	G' (Pa)	G" (Pa)	|G*| (Pa)	|G*|/sin(delta) (kPa)
10	52	1017.7	766	0.074693	73.27	2961	9.85E+03	1.03E+04	10.74
10	58	1794.1	621.2	0.12035	75.78	1274	5026	5185	5.349
10	64	2570.5	322.5	0.12033	77.81	569.7	2638	2698	2.761
10	70	3346.9	169.7	0.12052	79.38	262.1	1398	1423	1.448
10	76	4123.2	92.15	0.12032	80.43	129	765.2	776	0.7869
10	82	4899.6	52.69	0.12034	80.82	70.61	437.1	442.8	0.4485
10	88	5676	32.59	0.12031	80.46	44.71	266.1	269.8	0.2736
10	94	6452.3	21.85	0.12036	79.6	31.14	169.7	172.5	0.1754

ang. frequency (rad/s)	temperature (°c)	time (s)	osc. stress (Pa)	strain	delta (º)	G' (Pa)	G" (Pa)	|G*| (Pa)	|G*|/sin(delta) (kPa)
10	52	1001.5	746.4	0.07652	73.48	2782	9.38E+03	9.78E+03	10.2
10	58	1777.8	599.4	0.12036	75.9	1219	4853	5003	5.159
10	64	2554.2	313.1	0.12041	77.78	554.2	2559	2619	2.679
10	70	3330.5	163.7	0.12049	79.24	256.4	1349	1373	1.398
10	76	4106.9	90.02	0.12036	79.93	132.7	747.1	758.8	0.7706
10	82	4883.4	51.18	0.12052	80.3	72.46	424	430.2	0.4364
10	88	5659.9	31.59	0.12042	79.93	45.72	257.5	261.5	0.2656
10	94	6436.5	21.67	0.12046	78.7	33.73	168.9	172.2	0.1756

PME (E)

ang. frequency (rad/s)	temperature (°c)	time (s)	osc. stress (Pa)	strain	delta (º)	G' (Pa)	G'' (Pa)	|G*| (Pa)	|G*|/sin(delta) (kPa)
10	52	1033.3	597.9	0.090398	76.61	1537	6.46E+03	6.64E+03	6.822
10	58	1809.5	386.7	0.12029	78.66	635.8	3169	3232	3.297
10	64	2585.9	197.7	0.12039	79.96	288.6	1631	1656	1.682
10	70	3362.3	105.4	0.12035	80.65	143.9	874.1	885.9	0.8978
10	76	4138.6	58.64	0.12038	80.76	79.23	486.8	493.2	0.4997
10	82	4915	35.06	0.12036	80.37	48.75	287.5	291.6	0.2957
10	88	5691.4	23.01	0.12038	79.59	33.18	180.6	183.6	0.1867
10	94	6467.8	16.73	0.1203	78.46	24.37	119.4	121.8	0.1243

ang. frequency (rad/s)	temperature (°c)	time (s)	osc. stress (Pa)	strain	delta (º)	G' (Pa)	G'' (Pa)	|G*| (Pa)	|G*|/sin(delta) (kPa)
10	52	1370.1	573.4	0.092	76.49	1461	6.08E+03	6.26E+03	6.433
10	58	2146.5	366.9	0.12034	78.4	616.7	3004	3066	3.13
10	64	2922.9	189	0.12038	79.5	288.8	1559	1585	1.612
10	70	3699.3	102.1	0.12031	79.78	152.7	847	860.6	0.8745
10	76	4476	58.05	0.12034	79.38	90.41	482.4	490.8	0.4993
10	82	5252.7	34.72	0.12042	78.42	58.58	286	291.9	0.298
10	88	6029.1	22.54	0.1205	77.06	41.12	179	183.6	0.1884
10	94	6805.6	16.39	0.12029	75.39	31.29	120.1	124.1	0.1282

ang. frequency (rad/s)	temperature (°c)	time (s)	osc. stress (Pa)	strain	delta (°)	G' (Pa)	G" (Pa)	|G*| (Pa)	|G*|/sin(delta) (kPa)
10	52	1429.1	570.2	0.092266	76.54	1443	6.03E+03	6.20E+03	6.378
10	58	2205.2	364.2	0.12032	78.46	608.9	2983	3045	3.108
10	64	2981.5	187.4	0.12036	79.6	283.6	1545	1571	1.598
10	70	3757.8	99.93	0.12037	80.08	145	828.8	841.4	0.8541
10	76	4534.1	55.75	0.12039	80.09	80.85	462.9	469.9	0.477
10	82	5310.4	33.6	0.12034	79.49	51.14	275.7	280.4	0.2852
10	88	6086.6	22.22	0.12031	78.39	35.92	174.8	178.4	0.1821
10	94	6863	16.2	0.12034	76.93	26.85	115.7	118.8	0.1219

SS-1HP (E)

ang. frequency (rad/s)	temperature (°c)	time (s)	osc. stress (Pa)	strain	delta (°)	G' (Pa)	G" (Pa)	|G*| (Pa)	|G*|/sin(delta) (kPa)
10	52	988.84	815.5	0.070312	73.29	3343	1.11E+04	1.16E+04	12.14
10	58	1765.2	655.5	0.12035	75.45	1375	5295	5470	5.652
10	64	2541.4	323.1	0.12049	77.85	568.1	2639	2700	2.762
10	70	3317.8	161.9	0.12044	80.56	222.5	1339	1357	1.376
10	76	4094.2	83.72	0.12038	83.3	81.65	695.3	700.1	0.7049
10	82	4870.5	46.29	0.12024	85.55	29.51	379.2	380.4	0.3815
10	88	5646.9	27.77	0.1204	87	11.24	214.6	214.9	0.2152
10	94	6423.5	18.9	0.1204	87.57	5.455	128.5	128.6	0.1287

ang. frequency (rad/s)	temperature (°c)	time (s)	osc. stress (Pa)	strain	delta (°)	G' (Pa)	G" (Pa)	|G*| (Pa)	|G*|/sin(delta) (kPa)
10	52	1001.3	815.8	0.070201	73.17	3373	1.12E+04	1.17E+04	12.17
10	58	1777.4	660.7	0.12039	75.32	1397	5332	5512	5.698
10	64	2553.8	329.1	0.12042	77.66	588	2688	2752	2.817
10	70	3330.1	166.4	0.12039	80.3	235.1	1375	1395	1.415
10	76	4106.6	86.53	0.12035	82.92	89.3	718.9	724.4	0.73
10	82	4882.8	47.82	0.12042	85.01	34.28	392.3	393.8	0.3953
10	88	5659.1	28.92	0.12032	86.1	15.46	226.6	227.1	0.2277
10	94	6435.5	19.91	0.12025	86.02	9.844	141.6	142	0.1423

ang. frequency (rad/s)	temperature (°c)	time (s)	osc. stress (Pa)	strain	delta (°)	G' (Pa)	G" (Pa)	|G*| (Pa)	|G*|/sin(delta) (kPa)
10	52	1040.4	822.7	0.069465	73.08	3456	1.14E+04	1.19E+04	12.41
10	58	1816.8	663.8	0.12037	75.24	1411	5356	5539	5.728
10	64	2593.3	328	0.12034	77.59	589.6	2681	2745	2.81
10	70	3369.7	166.8	0.12043	80.22	237.6	1378	1398	1.419
10	76	4146.1	86.97	0.12039	82.83	90.87	722.4	728.1	0.7338
10	82	4922.4	47.88	0.12038	84.89	35.18	393.1	394.7	0.3963
10	88	5698.6	28.96	0.12034	85.94	16.11	227.1	227.7	0.2283
10	94	6475.3	19.84	0.12017	85.78	10.44	141.4	141.8	0.1422

ELASTIC RECOVERY TEST

Asphalt Binder	Elastic Recovery TEST					
	@10°C		Average @10°C	@25°C		Average @25°C
CRS-2P (E)	36.25	48.75	42.5	73.75	75	74.375
CRS-2 (E)	10	10	10	7.5	18.5	13
CSS-1HP (E)	23.75		23.75	38.75	40	39.375
CMS-1P (E)	58.75	55	56.875	87.5	84.5	86
NTSS-1HM (C)						
Fog seal (C)						
CRS-2P (B)	36.25	37	36.625	53	53.75	53.375
CRS-2 (B)	9.25	8.75	9	16	13.75	14.875
NTSS-1HM (B)						
SS-1 (B)	2.5	1.25	1.875	15	13.75	14.375
SS-1H (B)	10	11.25	10.625	12.5	11.25	11.875
SS-1 (E)	8.75	8.75	8.75	6.25	10	8.125
CRS-2 (U)	2.5	1.25	1.875	6.25	5	5.625
SS-1 (U)	10	11.25	10.625	5	4.5	4.75
SS-1H (U)	8.75	8.75	8.75	5	3.75	4.375
SS-1L (U)	61.25	62.5	61.875	63.75	66.25	65
NTSS-1HM (U)						
PME (E)	52.5	52.75	52.625	50	50	50
CHFRS-2P (E)	51.875	52.5	52.1875	64.375	65	64.6875
SS-1HP (E)	53.75	54.375	54.0625	29.5	32.5	31

Rotational Viscometer Data

Viscosity results for SS-1 at 30°C

Sample No.	Temp.	RPM	Viscosity (cP)			Average	Stdev.	Covar.
			1st	2nd	3rd			
1	30	20	35	32.5	35	34.17	1.44	4.22
	30	30	33.3	33.3	35	33.87	0.98	2.90
	30	50	34	33	34	33.67	0.58	1.71
	30	60	33.3	33.3	33.3	33.30	0.00	0.00
	30	100	35	35	35	35.00	0.00	0.00
2	30	20	40	40	42.5	40.83	1.44	3.53
	30	30	36.7	36.7	36.7	36.70	0.00	0.00
	30	50	35	35	35	35.00	0.00	0.00
	30	60	35	35	35	35.00	0.00	0.00
	30	100	35.5	35.5	35.5	35.50	0.00	0.00
3	30	20	37.5	37.5	40	38.33	1.44	3.77
	30	30	33.3	35	35	34.43	0.98	2.85
	30	50	35	34	34	34.33	0.58	1.68
	30	60	33.3	33.3	33.3	33.30	0.00	0.00
	30	100	35.5	35	35.5	35.33	0.29	0.82

Viscosity results for SS-1 at 30°C

Sample No.	Temp.	RPM	Viscosity (cP)			Average	Stdev.	Covar.
			1st	2nd	3rd			
1	30	20	37.5	40	40	39.17	1.44	3.69
	30	30	36.7	35	35	35.57	0.98	2.76
	30	50	35	34	35	34.67	0.58	1.67
	30	60	35	34.2	35	34.73	0.46	1.33
	30	100	35	35.5	35	35.17	0.29	0.82
2	30	20	35	37.5	35	35.83	1.44	4.03
	30	30	33.3	35	33.3	33.87	0.98	2.90
	30	50	33	34	33	33.33	0.58	1.73
	30	60	33.3	34	33.3	33.53	0.40	1.21
	30	100	35	35	35	35.00	0.00	0.00
3	30	20	37.5	35	32.5	35.00	2.50	7.14
	30	30	33.3	35	33.5	33.93	0.93	2.74
	30	50	35	35	36	35.33	0.58	1.63
	30	60	35	34.2	35	34.73	0.46	1.33
	30	100	36.5	36.5	36.5	36.50	0.00	0.00

Viscosity results for SS-1 at 60°C

Sample No.	Temp.	RPM	Viscosity (cP)			Average	Stdev.	Covar.
			1st	2nd	3rd			
1	60	20	65	62.5	62.5	63.33	1.44	2.28
	60	30	60	60	58.3	59.43	0.98	1.65
	60	50	61	61	60	60.67	0.58	0.95
	60	60	60.8	60.8	60.8	60.80	0.00	0.00
	60	100	66.5	66.5	66	66.33	0.29	0.44
2	60	20	65	62.5	65	64.17	1.44	2.25
	60	30	63.3	61.7	61.7	62.23	0.92	1.48
	60	50	62	61	62	61.67	0.58	0.94
	60	60	62.5	61.7	61.7	61.97	0.46	0.75
	60	100	65.5	65	65	65.17	0.29	0.44
3	60	20	65	67.5	66.7	66.40	1.28	1.92
	60	30	63.3	61.7	63.3	62.77	0.92	1.47
	60	50	60	59	60	59.67	0.58	0.97
	60	60	60.8	60.8	60.8	60.80	0.00	0.00
	60	100	65.5	65.5	65	65.33	0.29	0.44

Viscosity results for SS-1 at 60°C

Sample No.	Temp.	RPM	Viscosity (cP)			Average	Stdev.	Covar.
			1st	2nd	3rd			
1	60	20	57.5	60	55	57.5	2.50	4.35
	60	30	55	56.7	53.3	55	1.70	3.09
	60	50	52	51	50	51	1.00	1.96
	60	60	52.5	51.7	53.3	52.5	0.80	1.52
	60	100	54.5	54.5	54.5	54.5	0.00	0.00
2	60	20	62.5	62.5	60	61.66667	1.44	2.34
	60	30	61.7	61.7	60	61.13333	0.98	1.61
	60	50	61	61	61	61	0.00	0.00
	60	60	62.5	61.7	61.7	61.96667	0.46	0.75
	60	100	65.5	65	65	65.16667	0.29	0.44
3	60	20	65	65	62.5	64.16667	1.44	2.25
	60	30	60	60	58.3	59.43333	0.98	1.65
	60	50	61	60	60	60.33333	0.58	0.96
	60	60	60.8	60.8	60.8	60.8	0.00	0.00
	60	100	66.5	66.5	66	66.33333	0.29	0.44

Viscosity results for SS-1L at 30°C

Sample No.	Temp	RPM	Viscosity (cP)			Average	Stdev.	Covar.
			1st	2nd	3rd			
1	30	20	32.5	35	32.5	33.33	1.44	4.33
	30	30	31.7	30	31.7	31.13	0.98	3.15
	30	50	32	31	31	31.33	0.58	1.84
	30	60	30.8	30.8	30.8	30.80	0.00	0.00
	30	100	31	31	31	31.00	0.00	0.00
2	30	20	32.5	32.5	35	33.33	1.44	4.33
	30	30	31.7	31.7	31.7	31.70	0.00	0.00
	30	50	31	30	30	30.33	0.58	1.90
	30	60	30.8	30.8	30	30.53	0.46	1.51
	30	100	31	31	30.5	30.83	0.29	0.94
3	30	30	20	32.5	32.5	35	33.33	1.44
	30	30	30	30	31	31.7	30.90	0.85
	30	30	50	30	31	31	30.67	0.58
	30	30	60	30	30	30	30.00	0.00
	30	30	100	31	31	31	31.00	0.00

Viscosity results for SS-1L at 30°C

Sample No.	Temp.	RPM	Viscosity (cP)			Average	Stdev.	Covar.
			1st	2nd	3rd			
1	30	20	37.5	35	37.5	36.66667	1.44	3.94
	30	30	35	33.3	33.3	33.86667	0.98	2.90
	30	50	32	33	32	32.33333	0.58	1.79
	30	60	32.5	31.7	32.5	32.23333	0.46	1.43
	30	100	37.5	31	31	33.16667	3.75	11.31
2	30	20	35	35	35	35	0.00	0.00
	30	30	31.7	31.7	31.7	31.7	0.00	0.00
	30	50	31	32	31	31.33333	0.58	1.84
	30	60	30.8	30.8	30.8	30.8	0.00	0.00
	30	100	30.5	30.5	30.5	30.5	0.00	0.00
3	30	20	32.5	32.5	35	33.33333	1.44	4.33
	30	30	33.3	31.7	31.7	32.23333	0.92	2.87
	30	50	32	31	30	31	1.00	3.23
	30	60	30.8	30.8	30	30.53333	0.46	1.51
	30	100	31	30.5	30.5	30.66667	0.29	0.94

Viscosity results for SS-1L at 60°C

Sample No.	Temp.	RPM	Viscosity (cP)			Average	Stdev.	Covar.
			1st	2nd	3rd			
1	20	27.5	30	25	27.50	2.50	9.09	20
	30	25	26.7	23.3	25.00	1.70	6.80	30
	50	24	23	24	23.67	0.58	2.44	50
	60	24.2	23.3	24.2	23.90	0.52	2.17	60
	100	23.5	23	23.5	23.33	0.29	1.24	100
2	60	20	27.5	30	27.5	28.33	1.44	5.09
	60	30	26.7	25	25	25.57	0.98	3.84
	60	50	22	22	23	22.33	0.58	2.59
	60	60	21.7	22.5	21.7	21.97	0.46	2.10
	60	100	21	21	20	20.67	0.58	2.79
3	60	20	25	25	25	25.00	0.00	0.00
	60	30	23.3	21.7	23.3	22.77	0.92	4.06
	60	50	21	21	22	21.33	0.58	2.71
	60	60	20.8	21.7	20.8	21.10	0.52	2.46
	60	100	21	21	21	21.00	0.00	0.00

Viscosity results for SS-1L at 60°C

Sample No.	Temp.	RPM	Viscosity (cP)			Average	Stdev.	Covar.
			1st	2nd	3rd			
1	60	20	25	27.5	27.5	26.66667	1.44	5.41
	60	30	23.3	25	23.3	23.86667	0.98	4.11
	60	50	23	23	23	23	0.00	0.00
	60	60	22.5	22.5	22.5	22.5	0.00	0.00
	60	100	22	22	22	22	0.00	0.00
2	60	20	25	27.5	27.5	26.66667	1.44	5.41
	60	30	26.7	25	25	25.56667	0.98	3.84
	60	50	24	23	23	23.33333	0.58	2.47
	60	60	23.3	23.3	22.5	23.03333	0.46	2.01
	60	100	22	22	22.5	22.16667	0.29	1.30
3	60	60	20	25	25	27.5	25.83333	1.44
	60	60	30	25	23.3	25	24.43333	0.98
	60	60	50	24	23	24	23.66667	0.58
	60	60	60	23.3	23.5	22.5	23.1	0.53
	60	60	100	22	22	22	22	0.00

Viscosity results for SS-1H at 30°C

Sample No.	Temp.	RPM	Viscosity (cP)			Average	Stdev.	Covar.
			1st	2nd	3rd			
1	30	20	97.5	95	97.5	96.67	1.44	30
	30	30	86.7	86.7	86.7	86.70	0.00	30
	30	50	78	79	79	78.67	0.58	30
	30	60	75.8	76.7	75.8	76.10	0.52	30
	30	100	72.5	73	73	72.83	0.29	30
2	30	20	95	95	92.5	94.17	1.44	30
	30	30	83.3	83.3	83.3	83.30	0.00	30
	30	50	77	77	78	77.33	0.58	30
	30	60	75	75	75	75.00	0.00	30
	30	100	72	72.5	72	72.17	0.29	30
3	30	20	95	95	97.5	95.83	1.44	30
	30	30	83.3	83.3	83.3	83.30	0.00	30
	30	50	77	78	78	77.67	0.58	30
	30	60	75	75	75.8	75.27	0.46	30
	30	100	72.5	72	72.5	72.33	0.29	30

Viscosity results for SS-1H at 30°C

Sample No.	Temp.	RPM	Viscosity (cP)			Average	Stdev.	Covar.
			1st	2nd	3rd			
1	30	20	90	90	87.5	89.17	1.44	30
	30	30	80	81.7	81.7	81.13	0.98	30
	30	50	74	75	75	74.67	0.58	30
	30	60	72.5	72.5	72.5	72.50	0.00	30
	30	100	69.5	69.5	69.5	69.50	0.00	30
2	30	20	87.5	90	87.5	88.33	1.44	30
	30	30	80	78.3	78.3	78.87	0.98	30
	30	50	74	73	73	73.33	0.58	30
	30	60	70.8	70	70.8	70.53	0.46	30
	30	100	68.5	68	68.5	68.33	0.29	30
3	30	20	92.5	90	87.5	90.00	2.50	30
	30	30	81.7	80	83.3	81.67	1.65	30
	30	50	76	76	76	76.00	0.00	30
	30	60	74.2	75	74.2	74.47	0.46	30
	30	100	71.5	71.5	71.5	71.50	0.00	30

Viscosity results for SS-1H at 60°C

Sample No.	Temp.	RPM	Viscosity (cP)			Average	Stdev.	Covar.
			1st	2nd	3rd			
1	60	20	82.5	80	80	80.83	1.44	60
	60	30	78.3	78.3	76.7	77.77	0.92	60
	60	50	77	77	77	77.00	0.00	60
	60	60	76.7	75.8	75.8	76.10	0.52	60
	60	100	76	75.5	75.5	75.67	0.29	60
2	60	20	80	80	80	80.00	0.00	60
	60	30	78.3	78.3	76.7	77.77	0.92	60
	60	50	77	77	77	77.00	0.00	60
	60	60	76.7	75.8	76.7	76.40	0.52	60
	60	100	75.5	75.5	75.5	75.50	0.00	60
3	20	80	80	80	80.00	0.00	20	80
	30	78.3	78.3	76.7	77.77	0.92	30	78.3
	50	77	77	77	77.00	0.00	50	77
	60	75.8	75.8	76.7	76.10	0.52	60	75.8
	100	76	76	75.5	75.83	0.29	100	76

Viscosity results for SS-1H at 60°C

Sample No.	Temp.	RPM	Viscosity (cP)			Average	Stdev.	Covar.
			1st	2nd	3rd			
1	60	20	77.5	75	75	75.83	1.44	60
	60	30	75	75	73.3	74.43	0.98	60
	60	50	73	72	72	72.33	0.58	60
	60	60	71.7	71.7	70.8	71.40	0.52	60
	60	100	71	71	70.5	70.83	0.29	60
2	60	20	75	75	75	75.00	0.00	60
	60	30	73.3	71.7	73.3	72.77	0.92	60
	60	50	70	71	71	70.67	0.58	60
	60	60	68.3	69.2	69.2	68.90	0.52	60
	60	100	69.5	69	68.5	69.00	0.50	60
3	60	20	77.5	77.5	75	76.67	1.44	60
	60	30	75	73.3	73.3	73.87	0.98	60
	60	50	71	72	71	71.33	0.58	60
	60	60	71.7	70.8	69.2	70.57	1.27	60
	60	100	70.5	69	69	69.50	0.87	60

Viscosity results for CRS-2 at 30°C

Sample No.	Temp.	RPM	Viscosity (cP)			Average	Stdev.	Covar.
			1st	2nd	3rd			
1	30	20	850	850	862.5	854.17	7.22	0.84
	30	30	716.7	716.7	708.3	713.90	4.85	0.68
	30	50	595	590	580	588.33	7.64	1.30
	30	60	554.2	545.2	554.2	551.20	5.20	0.94
	30	100	545	542.5	542.5	543.33	1.44	0.27
2	30	20	862.5	850	837.5	850.00	12.50	1.47
	30	30	725	716	700	713.67	12.66	1.77
	30	50	610	595	590	598.33	10.41	1.74
	30	60	570.8	570.8	570.8	570.80	0.00	0.00
	30	100	555	555	555	555.00	0.00	0.00
3	30	20	900	887.5	875	887.50	12.50	1.41
	30	30	766.7	750	741.7	752.80	12.73	1.69
	30	50	650	635	635	640.00	8.66	1.35
	30	60	604.2	600	600	601.40	2.42	0.40
	30	100	575	572.5	572.5	573.33	1.44	0.25

Viscosity results for CRS-2 at 30°C

Sample No.	Temp.	RPM	Viscosity (cP)			Average	Stdev.	Covar.
			1st	2nd	3rd			
1	30	20	887.5	875	862.5	875.00	12.50	1.43
	30	30	725.7	716.7	700	714.13	13.04	1.83
	30	50	580	580	575	578.33	2.89	0.50
	30	60	545.8	545.8	541.7	544.43	2.37	0.43
	30	100	505	505	502.5	504.17	1.44	0.29
2	30	20	850	862.5	862.5	858.33	7.22	0.84
	30	30	725	716.7	708.3	716.67	8.35	1.17
	30	50	595	590	580	588.33	7.64	1.30
	30	60	554.2	545.2	554.2	551.20	5.20	0.94
	30	100	545	542.5	542.5	543.33	1.44	0.27
3	30	20	875	862.5	862.5	866.67	7.22	0.83
	30	30	725	700	700	708.33	14.43	2.04
	30	50	580	590	595	588.33	7.64	1.30
	30	60	554.2	545	545	548.07	5.31	0.97
	30	100	542.5	542.5	542.5	542.50	0.00	0.00

Viscosity results for CRS-2 at 60°C

Sample No.	Temp.	RPM	Viscosity (cP)			Average	Stdev.	Covar.
			1st	2nd	3rd			
1	60	20	482.5	475	465	474.17	8.78	1.85
	60	30	398.3	395	388.3	393.87	5.10	1.29
	60	50	330	328	324	327.33	3.06	0.93
	60	60	305	303.3	302.5	303.60	1.28	0.42
	60	100	270.5	272	272.5	271.67	1.04	0.38
2	60	20	387.5	385	382.5	385.00	2.50	0.65
	60	30	340	338.3	336.7	338.33	1.65	0.49
	60	50	295	293	291	293.00	2.00	0.68
	60	60	274.2	273.3	270.8	272.77	1.76	0.65
	60	100	242.5	241.5	240.5	241.50	1.00	0.41
3	60	20	462.5	460	457.5	460.00	2.50	0.54
	60	30	391.7	386.7	386.7	388.37	2.89	0.74
	60	50	325	326	322	324.33	2.08	0.64
	60	60	300	299.2	296.7	298.63	1.72	0.58
	60	100	261	260	261	260.67	0.58	0.22

Viscosity results for CRS-2 at 60°C

Sample No.	Temp.	RPM	Viscosity (cP)			Average	Stdev.	Covar.
			1st	2nd	3rd			
1	60	20	482.5	475	465	474.17	8.78	1.85
	60	30	398.3	395	388.3	393.87	5.10	1.29
	60	50	330	328	324	327.33	3.06	0.93
	60	60	305	303.3	302.5	303.60	1.28	0.42
	60	100	270.5	272	272.5	271.67	1.04	0.38
2	60	20	387.5	385	382.5	385.00	2.50	0.65
	60	30	340	338.3	336.7	338.33	1.65	0.49
	60	50	295	293	291	293.00	2.00	0.68
	60	60	274.2	273.3	270.8	272.77	1.76	0.65
	60	100	242.5	241.5	240.5	241.50	1.00	0.41
3	60	20	462.5	460	457.5	460.00	2.50	0.54
	60	30	391.7	386.7	386.7	388.37	2.89	0.74
	60	50	325	326	322	324.33	2.08	0.64
	60	60	300	299.2	296.7	298.63	1.72	0.58
	60	100	261	260	261	260.67	0.58	0.22

Viscosity results for CRS-2P at 30°C

Sample No.	Temp.	RPM	Viscosity (cP)			Average	Stdev.	Covar.
			1st	2nd	3rd			
1	30	20	462.5	475	462.5	466.67	7.22	1.55
	30	30	425	425	408.3	419.43	9.64	2.30
	30	50	375	370	365	370.00	5.00	1.35
	30	60	350	354.2	350	351.40	2.42	0.69
	30	100	345	342.5	340	342.50	2.50	0.73
2	30	20	437.5	425	425	429.17	7.22	1.68
	30	30	383.3	383.3	375	380.53	4.79	1.26
	30	50	355	355	350	353.33	2.89	0.82
	30	60	341.7	341.7	337.5	340.30	2.42	0.71
	30	100	337.5	337.5	337.5	337.50	0.00	0.00
3	30	20	462.5	450.7	450.7	454.63	6.81	1.50
	30	30	408.3	408.3	425	413.87	9.64	2.33
	30	50	365	365	355	361.67	5.77	1.60
	30	60	350	350	341.7	347.23	4.79	1.38
	30	100	342.5	340	337.5	340.00	2.50	0.74

Viscosity results for CRS-2P at 30°C

Sample No.	Temp.	RPM	Viscosity (cP)			Average	Stdev.	Covar.
			1st	2nd	3rd			
1	30	20	425	412.5	412.5	416.67	7.22	1.73
	30	30	383.3	375	375	377.77	4.79	1.27
	30	50	345	340	340	341.67	2.89	0.84
	30	60	320.8	316.7	312.5	316.67	4.15	1.31
	30	100	312.5	312.5	310	311.67	1.44	0.46
2	30	20	412.5	400	412.5	408.33	7.22	1.77
	30	30	383.3	383.3	375	380.53	4.79	1.26
	30	50	360	355	350	355.00	5.00	1.41
	30	60	345	341.7	341.7	342.80	1.91	0.56
	30	100	335	335	337	335.67	1.15	0.34
3	30	20	425	425	412.5	420.83	7.22	1.71
	30	30	383.3	383.3	375	380.53	4.79	1.26
	30	50	360	360	355	358.33	2.89	0.81
	30	60	345	350	345	346.67	2.89	0.83
	30	100	335	337	337	336.33	1.15	0.34

Viscosity results for CRS-2P at 60°C

Sample No.	Temp.	RPM	Viscosity (cP)			Average	Stdev.	Covar.
			1st	2nd	3rd			
1	60	20	230	233.5	232.5	232.00	1.80	0.78
	60	30	213.3	215	215	214.43	0.98	0.46
	60	50	189	188	188	188.33	0.58	0.31
	60	60	172.5	170	168.3	170.27	2.11	1.24
	60	100	142.5	141.5	142.5	142.17	0.58	0.41
2	60	20	240	237.5	235	237.50	2.50	1.05
	60	30	210	211.7	213	211.57	1.50	0.71
	60	50	184	183	182	183.00	1.00	0.55
	60	60	166.7	166.5	166.5	166.57	0.12	0.07
	60	100	139.5	139	138	138.83	0.76	0.55
3	60	20	237.5	235	232.5	235.00	2.50	1.06
	60	30	213	210	210	211.00	1.73	0.82
	60	50	188	183	182	184.33	3.21	1.74
	60	60	168.3	166.5	166.5	167.10	1.04	0.62
	60	100	142.5	139	139.5	140.33	1.89	1.35

Viscosity results for CRS-2P at 60°C

Sample No.	Temp.	RPM	Viscosity (cP)			Average	Stdev.	Covar.
			1st	2nd	3rd			
1	60	20	255	252.5	250	252.50	2.50	0.99
	60	30	223.3	221.7	220	221.67	1.65	0.74
	60	50	186	182	179	182.33	3.51	1.93
	60	60	164.2	161.7	160.8	162.23	1.76	1.09
	60	100	140	137	135.5	137.50	2.29	1.67
2	60	20	257.5	255	252.5	255.00	2.50	0.98
	60	30	223.3	221.7	218.3	221.10	2.55	1.15
	60	50	191	187	184	187.33	3.51	1.87
	60	60	168.3	165.8	162.5	165.53	2.91	1.76
	60	100	145	142	140.5	142.50	2.29	1.61
3	60	20	252.5	250	250	250.83	1.44	0.58
	60	30	218.3	218.3	223.3	219.97	2.89	1.31
	60	50	179	182	179	180.00	1.73	0.96
	60	60	174.2	171.7	172	172.63	1.37	0.79
	60	100	151	148	146.5	148.50	2.29	1.54

Recovery Method comparison data (ASTM D6934)

CRS-2P								
Ang. frequency	Temperature	Time	Osc. Stress	Strain	Delta	G'	G"	|G*|/sin(delta)
rad/s	°C	s	Pa		degrees	Pa	Pa	kPa
10	58	1070.7	136.2	0.11809	74.59	317.7	1152	1.24
10	64	1847.1	73.76	0.11999	69.03	235.5	614.4	0.7046
10	70	2623.4	41.89	0.12006	59.49	203.2	344.8	0.4645
CRS-2P								
Ang. frequency	Temperature	Time	Osc. Stress	Strain	Delta	G'	G"	|G*|/sin(delta)
rad/s	°C	s	Pa		degrees	Pa	Pa	kPa
10	58	828.09	140.8	0.11809	75.41	309.9	1191	1.272
10	64	1604.5	72.87	0.11999	69.16	231	606.8	0.6947
10	70	2381	39.94	0.11999	58.89	197.6	327.5	0.4468
CRS-2P								
Ang. frequency	Temperature	Time	Osc. Stress	Strain	Delta	G'	G"	|G*|/sin(delta)
rad/s	°C	s	Pa		degrees	Pa	Pa	kPa
10	58	606.97	148.5	0.11816	77.31	282.9	1257	1.321
10	64	1371.7	75.3	0.11999	71.26	212.4	626	0.698
10	70	2143.2	40.98	0.11999	60.69	187.8	334.5	0.4399
CRS-2								
Ang. frequency	Temperature	Time	Osc. Stress	Strain	Delta	G'	G"	|G*|/sin(delta)
rad/s	°C	s	Pa		degrees	Pa	Pa	kPa
10	58	958.58	95.8	0.11872	75.38	210.2	805.6	0.8605
10	64	1734.8	49.79	0.11999	65.71	184.4	408.5	0.4917
10	70	2511.2	27.58	0.11996	50.94	173.9	214.4	0.3555

CRS-2								
Ang. frequency	Temperature	Time	Osc. Stress	Strain	Delta	G'	G"	|G*|/sin(delta)
rad/s	°C	s	Pa		degrees	Pa	Pa	kPa
10	58	1120.3	111.1	0.11852	75.84	236.3	936.8	0.9964
10	64	1896.8	56.99	0.11995	67.37	196.4	471.3	0.5531
10	70	2672.9	31.18	0.11999	53.8	182.1	248.8	0.382
CRS-2								
Ang. frequency	Temperature	Time	Osc. Stress	Strain	Delta	G'	G"	|G*|/sin(delta)
rad/s	°C	s	Pa		degrees	Pa	Pa	kPa
10	58	1074.1	104.7	0.11863	75.78	223.6	882.1	0.9387
10	64	1850.3	54.03	0.11995	66.5	194	446	0.5304
10	70	2626.8	29.55	0.12004	52.42	180	233.9	0.3723
CRS-2L								
Ang. frequency	Temperature	Time	Osc. Stress	Strain	Delta	G'	G"	|G*|/sin(delta)
rad/s	°C	s	Pa		degrees	Pa	Pa	kPa
10	58	1129.4	202.4	0.11715	74.69	469.4	1714	1.843
10	64	1905.5	110.9	0.12	71.37	311.1	923	1.028
10	70	2681.8	61.43	0.11999	64.83	240.5	511.7	0.6247
CRS-2L								
Ang. frequency	Temperature	Time	Osc. Stress	Strain	Delta	G'	G"	|G*|/sin(delta)
rad/s	°C	s	Pa		degrees	Pa	Pa	kPa
10	58	670.83	225.8	0.1168	74.78	521.1	1915	2.057
10	64	1447.1	118.8	0.12004	71.46	331.1	987.2	1.098
10	70	2223.6	65.7	0.11993	65.38	251.1	547.8	0.6629

CRS-2L								
Ang. frequency	Temperature	Time	Osc. Stress	Strain	Delta	G'	G"	|G*|/sin(delta)
rad/s	°C	s	Pa		degrees	Pa	Pa	kPa
10	58	670.81	226.9	0.11687	75.32	504.7	1926	2.058
10	64	1447.3	119.3	0.12001	71.95	323.3	992	1.097
10	70	2223.6	66.18	0.12	65.82	247.7	551.5	0.6627
SS-1								
Ang. frequency	Temperature	Time	Osc. Stress	Strain	Delta	G'	G"	|G*|/sin(delta)
rad/s	°C	s	Pa		degrees	Pa	Pa	kPa
10	58	1090.7	106.7	0.1186	75.89	226.2	899.5	0.9564
10	64	1867.1	55.43	0.11998	67.52	189.1	457	0.5352
10	70	2643.5	30.75	0.11996	54	176.9	243.5	0.3721
SS-1								
Ang. frequency	Temperature	Time	Osc. Stress	Strain	Delta	G'	G"	|G*|/sin(delta)
rad/s	°C	s	Pa		degrees	Pa	Pa	kPa
10	58	1090.5	104.1	0.11853	74.28	247.1	877.9	0.9475
10	64	1867.1	54.79	0.11995	65.44	207.5	454.2	0.549
10	70	2643.6	31.95	0.11982	53.1	194.7	259.3	0.4056
SS-1								
Ang. frequency	Temperature	Time	Osc. Stress	Strain	Delta	G'	G"	|G*|/sin(delta)
rad/s	°C	s	Pa		degrees	Pa	Pa	kPa
10	58	1097.5	109.5	0.11857	76.16	227.4	923	0.979
10	64	1873.9	56.99	0.12002	67.76	192.3	470.4	0.549
10	70	2650.5	30.95	0.12003	54.03	178.2	245.6	0.3749

SS-1H								
Ang. frequency	Temperature	Time	Osc. Stress	Strain	Delta	G'	G"	|G*|/sin(delta)
rad/s	°C	s	Pa		degrees	Pa	Pa	kPa
10	58	1078.5	566.2	0.11334	81.29	761.6	4970	5.087
10	64	1854.9	272.5	0.12004	80.79	367.8	2267	2.327
10	70	2631.2	126.8	0.11996	77.48	234.7	1057	1.109
SS-1H								
Ang. frequency	Temperature	Time	Osc. Stress	Strain	Delta	G'	G"	|G*|/sin(delta)
rad/s	°C	s	Pa		degrees	Pa	Pa	kPa
10	58	1085.1	572.2	0.1133	81.39	761.2	5025	5.141
10	64	1861.4	273.3	0.11999	80.95	362.3	2275	2.333
10	70	2637.6	128.5	0.12001	77.8	231.5	1071	1.121
SS-1H								
Ang. frequency	Temperature	Time	Osc. Stress	Strain	Delta	G'	G"	|G*|/sin(delta)
rad/s	°C	s	Pa		degrees	Pa	Pa	kPa
10	58	1077.9	599.2	0.11288	81.28	810.3	5280	5.404
10	64	1854.3	287	0.12	80.92	381.6	2389	2.45
10	70	2630.8	134.8	0.11999	77.85	241.8	1123	1.175
SS-1								
Ang. frequency	Temperature	Time	Osc. Stress	Strain	Delta	G'	G"	|G*|/sin(delta)
rad/s	°C	s	Pa		degrees	Pa	Pa	kPa
10	58	1097.5	109.5	0.11857	76.16	227.4	923	0.979
10	64	1873.9	56.99	0.12002	67.76	192.3	470.4	0.549
10	70	2650.5	30.95	0.12003	54.03	178.2	245.6	0.3749

SS-1L								
Ang. frequency	Temperature	Time	Osc. Stress	Strain	Delta	G'	G"	|G*|/sin(delta)
rad/s	°C	s	Pa		degrees	Pa	Pa	kPa
10	58	1063.7	295.5	0.11546	72.88	772.1	2507	2.745
10	64	1840	170.1	0.11996	70.97	482.7	1400	1.566
10	70	2616.2	97.82	0.12001	66.96	344.7	810.4	0.957
SS-1L								
Ang. frequency	Temperature	Time	Osc. Stress	Strain	Delta	G'	G"	|G*|/sin(delta)
rad/s	°C	s	Pa		degrees	Pa	Pa	kPa
10	58	1076.6	292.6	0.11559	73.38	741.8	2485	2.706
10	64	1853.1	167.9	0.11997	71.34	467.2	1384	1.541
10	70	2629.3	96.47	0.11996	67.29	335	800.4	0.9406
SS-1L								
Ang. frequency	Temperature	Time	Osc. Stress	Strain	Delta	G'	G"	|G*|/sin(delta)
rad/s	°C	s	Pa		degrees	Pa	Pa	kPa
10	58	1078.5	285.9	0.11557	72.67	756.4	2423	2.66
10	64	1854.9	165.1	0.12003	70.68	476.1	1358	1.525
10	70	2631.4	94.85	0.12	66.63	339.7	786.1	0.9329

Recovery Method comparison data (ASTM D7497)

CRS-2P								
Ang. frequency	Temperature	Time	Osc. Stress	Strain	Delta	G'	G"	|G*|/sin(delta)
rad/s	°C	s	Pa		degrees	Pa	Pa	kPa
10	58	1090.1	230.3	0.11699	76.68	463.4	1958	2.067
10	64	1866.6	120.1	0.11998	73.16	302.7	1000	1.092
10	70	2643.2	64.34	0.11997	65.95	239.2	536	0.6428
CRS-2P								
Ang. frequency	Temperature	Time	Osc. Stress	Strain	Delta	G'	G"	|G*|/sin(delta)
rad/s	°C	s	Pa		degrees	Pa	Pa	kPa
10	58	1089.4	225.5	0.11711	77.02	442	1917	2.019
10	64	1865.7	116.6	0.12002	73.34	290.4	970.8	1.058
10	70	2642.1	62.12	0.11997	66.04	229.8	517.1	0.6192
CRS-2P								
Ang. frequency	Temperature	Time	Osc. Stress	Strain	Delta	G'	G"	|G*|/sin(delta)
rad/s	°C	s	Pa		degrees	Pa	Pa	kPa
10	58	1091.4	221.5	0.11711	76.61	447.9	1881	1.988
10	64	1867.7	114.9	0.11999	72.82	296	957.1	1.049
10	70	2644	61.12	0.11999	65.27	234.4	509	0.6169
CRS-2								
Ang. frequency	Temperature	Time	Osc. Stress	Strain	Delta	G'	G"	|G*|/sin(delta)
rad/s	°C	s	Pa		degrees	Pa	Pa	kPa
10	58	1056.7	183.9	0.11797	79.84	279.4	1559	1.609
10	64	1833.1	89.12	0.11997	74.54	205	741.1	0.7978
10	70	2609.3	44.98	0.12001	63.96	179.1	366.7	0.4542

CRS-2								
Ang. frequency	Temperature	Time	Osc. Stress	Strain	Delta	G'	G"	|G*|/sin(delta)
rad/s	°C	s	Pa		degrees	Pa	Pa	kPa
10	58	1128	197.5	0.11783	80.01	295.3	1676	1.728
10	64	1904	95.15	0.11999	75.15	209.9	791.6	0.8473
10	70	2680.3	47.63	0.12	65.05	181.3	389.6	0.474
CRS-2								
Ang. frequency	Temperature	Time	Osc. Stress	Strain	Delta	G'	G"	|G*|/sin(delta)
rad/s	°C	s	Pa		degrees	Pa	Pa	kPa
10	58	1141.7	193.1	0.11784	79.65	299.1	1638	1.693
10	64	1917.9	94.04	0.11996	74.51	217	782.9	0.8431
10	70	2694.1	47.69	0.11994	64.46	187.1	391.4	0.4808
CRS-2L								
Ang. frequency	Temperature	Time	Osc. Stress	Strain	Delta	G'	G"	|G*|/sin(delta)
rad/s	°C	s	Pa		degrees	Pa	Pa	kPa
10	58	1022.5	289.3	0.11603	75.79	624.7	2466	2.624
10	64	1798.7	158.6	0.11997	72.77	407.2	1313	1.439
10	70	2575	86.95	0.11997	67	307	723.1	0.8534
CRS-2L								
Ang. frequency	Temperature	Time	Osc. Stress	Strain	Delta	G'	G"	|G*|/sin(delta)
rad/s	°C	s	Pa		degrees	Pa	Pa	kPa
10	58	1071.3	263.5	0.1163	75.07	597.3	2241	2.4
10	64	1847.5	142.4	0.11997	71.76	388.8	1180	1.308
10	70	2623.8	78.45	0.11999	65.56	296.5	652.6	0.7873

CRS-2L								
Ang. frequency	Temperature	Time	Osc. Stress	Strain	Delta	G'	G"	|G*|/sin(delta)
rad/s	°C	s	Pa		degrees	Pa	Pa	kPa
10	58	1074	277.4	0.11608	74.99	632.7	2360	2.529
10	64	1850.5	151.3	0.11997	71.74	413	1252	1.388
10	70	2626.8	83.13	0.11998	65.64	312.8	690.7	0.8323
SS-1								
Ang. frequency	Temperature	Time	Osc. Stress	Strain	Delta	G'	G"	|G*|/sin(delta)
rad/s	°C	s	Pa		degrees	Pa	Pa	kPa
10	58	1091.8	239.8	0.11726	79.57	375.8	2042	2.111
10	64	1868	114.7	0.12	75.9	240.1	955.9	1.016
10	70	2644.3	58.18	0.11996	67.91	195.2	481	0.5602
SS-1								
Ang. frequency	Temperature	Time	Osc. Stress	Strain	Delta	G'	G"	|G*|/sin(delta)
rad/s	°C	s	Pa		degrees	Pa	Pa	kPa
10	58	1094.2	235.3	0.11747	80.07	350.2	2001	2.062
10	64	1870.8	114.7	0.12003	76.43	230.4	954.9	1.011
10	70	2647.6	59.5	0.12009	68.7	191.4	491.1	0.5657
SS-1								
Ang. frequency	Temperature	Time	Osc. Stress	Strain	Delta	G'	G"	|G*|/sin(delta)
rad/s	°C	s	Pa		degrees	Pa	Pa	kPa
10	58	1132.7	257	0.11702	79.34	412.2	2191	2.268
10	64	1909.1	124.3	0.11997	76.16	255.3	1036	1.099
10	70	2685.3	63.77	0.11998	68.9	204.1	528.9	0.6076

SS-1H								
Ang. frequency	Temperature	Time	Osc. Stress	Strain	Delta	G'	G"	|G*|/sin(delta)
rad/s	°C	s	Pa		degrees	Pa	Pa	kPa
10	58	1013.9	1022	0.10499	79.47	1788	9614	9.946
10	64	1790.3	513.4	0.11998	80.39	720.1	4255	4.376
10	70	2566.5	235.1	0.12001	79.43	364.9	1956	2.024
SS-1H								
Ang. frequency	Temperature	Time	Osc. Stress	Strain	Delta	G'	G"	|G*|/sin(delta)
rad/s	°C	s	Pa		degrees	Pa	Pa	kPa
10	58	1071.1	1034	0.10476	79.45	1814	9743	10.08
10	64	1847.2	522.7	0.12	80.44	729.7	4331	4.454
10	70	2623.6	240.2	0.12	79.6	367	1999	2.066
SS-1H								
Ang. frequency	Temperature	Time	Osc. Stress	Strain	Delta	G'	G"	|G*|/sin(delta)
rad/s	°C	s	Pa		degrees	Pa	Pa	kPa
10	58	1079.6	909.9	0.10737	80.08	1467	8388	8.645
10	64	1855.8	452	0.11997	80.88	602.3	3752	3.849
10	70	2631.9	208.6	0.12002	79.79	312.9	1737	1.793
SS-1L								
Ang. frequency	Temperature	Time	Osc. Stress	Strain	Delta	G'	G"	|G*|/sin(delta)
rad/s	°C	s	Pa		degrees	Pa	Pa	kPa
10	58	1083.2	376.6	0.11433	73.9	931.1	3225	3.494
10	64	1859.5	214.1	0.11998	72.21	564.2	1758	1.939
10	70	2635.8	121.8	0.11996	68.46	397	1006	1.163

SS-1L								
Ang. frequency	Temperature	Time	Osc. Stress	Strain	Delta	G'	G"	|G*|/sin(delta)
rad/s	°C	s	Pa		degrees	Pa	Pa	kPa
10	58	1082.4	360.4	0.11456	73.69	900.9	3079	3.343
10	64	1858.5	205.7	0.11999	72.01	548.7	1690	1.868
10	70	2634.8	117.9	0.11997	68.29	387.9	974.2	1.129
SS-1L								
Ang. frequency	Temperature	Time	Osc. Stress	Strain	Delta	G'	G"	|G*|/sin(delta)
rad/s	°C	s	Pa		degrees	Pa	Pa	kPa
10	58	1084.4	368.1	0.11445	74.85	855.8	3160	3.392
10	64	1861.1	208.6	0.11997	73.17	520	1719	1.876
10	70	2637.8	120	0.11998	69.65	368.7	993.8	1.131

Recovery Method comparison data (AASHTO TP72, METHOD B)

CRS-2P								
Ang. frequency	Temperature	Time	Osc. Stress	Strain	Delta	G'	G"	|G*|/sin(delta)
rad/s	°C	s	Pa		degrees	Pa	Pa	kPa
10	58	822.83	107.3	0.11831	72	294.4	905.8	1.001
10	64	1599.3	58.85	0.12002	64.53	233.3	489.7	0.6009
10	70	2375.9	34.9	0.11998	53.88	209.4	286.9	0.4398
CRS-2P								
Ang. frequency	Temperature	Time	Osc. Stress	Strain	Delta	G'	G"	|G*|/sin(delta)
rad/s	°C	s	Pa		degrees	Pa	Pa	kPa
10	58	670.95	125.6	0.11829	75.26	279.4	1062	1.135
10	64	1447.1	65.26	0.12	68.14	217.7	542.4	0.6298
10	70	2223.6	36.44	0.11998	56.81	194.4	297.2	0.4244
CRS-2P								
Ang. frequency	Temperature	Time	Osc. Stress	Strain	Delta	G'	G"	|G*|/sin(delta)
rad/s	°C	s	Pa		degrees	Pa	Pa	kPa
10	58	1078.9	128.7	0.11825	75.17	288	1088	1.164
10	64	1855	66.44	0.11997	67.79	225.8	552.9	0.6451
10	70	2631.5	36.73	0.11998	56.16	202	301.2	0.4366
CRS-2								
Ang. frequency	Temperature	Time	Osc. Stress	Strain	Delta	G'	G"	|G*|/sin(delta)
rad/s	°C	s	Pa		degrees	Pa	Pa	kPa
10	58	670.91	104.8	0.11859	75.25	232.7	883.8	0.9451
10	64	1447.2	52.74	0.12	66.12	192.5	434.8	0.52
10	70	2223.7	28.84	0.11996	51.9	178.1	227.1	0.3667

CRS-2								
Ang. frequency	Temperature	Time	Osc. Stress	Strain	Delta	G'	G"	|G*|/sin(delta)
rad/s	°C	s	Pa		degrees	Pa	Pa	kPa
10	58	791.91	98.52	0.11863	74.59	228.7	830	0.893
10	64	1568.4	49.62	0.11993	64.95	190.9	408.5	0.4977
10	70	2344.8	28.44	0.11989	51.36	179.2	224.2	0.3675
CRS-2								
Ang. frequency	Temperature	Time	Osc. Stress	Strain	Delta	G'	G"	|G*|/sin(delta)
rad/s	°C	s	Pa		degrees	Pa	Pa	kPa
10	58	1073.7	89.02	0.11874	74.07	213.6	748.4	0.8094
10	64	1850	46.2	0.11999	64.12	183.4	378	0.467
10	70	2626.4	26.36	0.11995	49.58	172.9	203	0.3502
CRS-2L								
Ang. frequency	Temperature	Time	Osc. Stress	Strain	Delta	G'	G"	|G*|/sin(delta)
rad/s	°C	s	Pa		degrees	Pa	Pa	kPa
10	58	1139.3	208.3	0.11717	75.62	453	1767	1.883
10	64	1915.6	112.1	0.11998	71.39	314.1	932.9	1.039
10	70	2692	62.52	0.11995	63.97	254.6	521.3	0.6456
CRS-2L								
Ang. frequency	Temperature	Time	Osc. Stress	Strain	Delta	G'	G"	|G*|/sin(delta)
rad/s	°C	s	Pa		degrees	Pa	Pa	kPa
10	58	1146.3	208.7	0.11694	73.71	516	1766	1.917
10	64	1922.6	115.3	0.12	69.49	357.5	955.4	1.089
10	70	2699	65.6	0.11996	62.63	282.8	546.3	0.6926

CRS-2L								
Ang. frequency	Temperature	Time	Osc. Stress	Strain	Delta	G'	G"	|G*|/sin(delta)
rad/s	°C	s	Pa		degrees	Pa	Pa	kPa
10	58	1100.3	223.1	0.11693	75.39	493.4	1893	2.022
10	64	1876.4	121	0.11994	71.51	336.2	1005	1.118
10	70	2652.7	67.13	0.11997	64.65	265.1	559.5	0.6852
SS-1								
Ang. frequency	Temperature	Time	Osc. Stress	Strain	Delta	G'	G"	|G*|/sin(delta)
rad/s	°C	s	Pa		degrees	Pa	Pa	kPa
10	58	1093.7	107.4	0.11862	76.37	219.2	904.4	0.9575
10	64	1870.1	53.4	0.11998	67.43	182.4	438.8	0.5146
10	70	2646.4	28.81	0.11994	52.76	170.3	224	0.3534
SS-1								
Ang. frequency	Temperature	Time	Osc. Stress	Strain	Delta	G'	G"	|G*|/sin(delta)
rad/s	°C	s	Pa		degrees	Pa	Pa	kPa
10	58	1096.8	103.1	0.11866	76.16	213.7	867.5	0.9201
10	64	1873.2	51.52	0.12	66.8	181.1	422.6	0.5002
10	70	2649.7	28.03	0.11998	51.77	171.2	217.3	0.3521
SS-1								
Ang. frequency	Temperature	Time	Osc. Stress	Strain	Delta	G'	G"	|G*|/sin(delta)
rad/s	°C	s	Pa		degrees	Pa	Pa	kPa
10	58	1101.5	121.4	0.1184	75.82	259.3	1026	1.091
10	64	1878	63.13	0.12003	67.65	215.6	524.3	0.613
10	70	2654.5	35.39	0.11989	56.22	192.7	288.1	0.417

SS-1H								
Ang. frequency	Temperature	Time	Osc. Stress	Strain	Delta	G'	G"	|G*|/sin(delta)
rad/s	°C	s	Pa		degrees	Pa	Pa	kPa
10	58	1071.8	337.8	0.1161	80.01	510.4	2899	2.989
10	64	1848.1	166.8	0.12	77.92	297.5	1390	1.454
10	70	2624.5	82.29	0.12	72.21	219.8	684.7	0.7553
SS-1H								
Ang. frequency	Temperature	Time	Osc. Stress	Strain	Delta	G'	G"	|G*|/sin(delta)
rad/s	°C	s	Pa		degrees	Pa	Pa	kPa
10	58	1083.7	294.4	0.1166	79.71	457	2517	2.6
10	64	1860.1	147.4	0.11994	77.21	279.1	1229	1.292
10	70	2636.3	74.55	0.11995	70.99	213.6	620	0.6936
SS-1H								
Ang. frequency	Temperature	Time	Osc. Stress	Strain	Delta	G'	G"	|G*|/sin(delta)
rad/s	°C	s	Pa		degrees	Pa	Pa	kPa
10	58	1091.3	408.1	0.11518	80.02	620	3525	3.634
10	64	1867.7	201.2	0.12001	78.59	338.1	1675	1.743
10	70	2644	98.02	0.12002	73.74	238.2	816.5	0.886
SS-1L								
Ang. frequency	Temperature	Time	Osc. Stress	Strain	Delta	G'	G"	|G*|/sin(delta)
rad/s	°C	s	Pa		degrees	Pa	Pa	kPa
10	58	1156.5	231.4	0.11632	71.69	645.8	1951	2.165
10	64	1932.8	132.7	0.11997	68.28	434.9	1092	1.265
10	70	2709	77.51	0.11996	62.45	334.7	641.5	0.8162

SS-1L								
Ang. frequency	Temperature	Time	Osc. Stress	Strain	Delta	G'	G"	|G*|/sin(delta)
rad/s	°C	s	Pa		degrees	Pa	Pa	kPa
10	58	1159.4	230.3	0.11635	71.76	640.1	1942	2.153
10	64	1935.5	131.9	0.11997	68.42	429.6	1086	1.256
10	70	2711.9	76.94	0.12	62.6	330.2	637	0.8081
SS-1L								
Ang. frequency	Temperature	Time	Osc. Stress	Strain	Delta	G'	G"	|G*|/sin(delta)
rad/s	°C	s	Pa		degrees	Pa	Pa	kPa
10	58	1033.4	210.6	0.11671	72.13	572.5	1776	1.961
10	64	1809.7	122.2	0.12	68.93	389.1	1010	1.16
10	70	2585.8	71.91	0.11998	63.43	299	597.9	0.7475

Recovery Method comparison data (FIELD CURING METHOD)

CRS-2P								
Ang. frequency	Temperature	Time	Osc. Stress	Strain	Delta	G'	G"	|G*|/sin(delta)
rad/s	°C	s	Pa		degrees	Pa	Pa	kPa
10	58	1080.1	149.3	0.1179	74.43	351.8	1263	1.361
10	64	1856.7	79.48	0.12005	69.24	251	662	0.7572
10	70	2633	45.13	0.11997	60.35	212.6	373.6	0.4946
CRS-2P								
Ang. frequency	Temperature	Time	Osc. Stress	Strain	Delta	G'	G"	|G*|/sin(delta)
rad/s	°C	s	Pa		degrees	Pa	Pa	kPa
10	58	1076.2	214.6	0.11713	76.01	453.8	1822	1.935
10	64	1852.4	108.8	0.11999	72.48	286.2	906.4	0.9967
10	70	2628.7	59.16	0.11997	65.34	225.9	492.2	0.5959
CRS-2P								
Ang. frequency	Temperature	Time	Osc. Stress	Strain	Delta	G'	G"	|G*|/sin(delta)
rad/s	°C	s	Pa		degrees	Pa	Pa	kPa
10	58	1078.3	135.6	0.11802	73.58	337.8	1146	1.246
10	64	1854.6	71.7	0.11998	67.74	244.6	597.5	0.6976
10	70	2631	41.12	0.11997	58.26	210	339.6	0.4695
CRS-2								
Ang. frequency	Temperature	Time	Osc. Stress	Strain	Delta	G'	G"	|G*|/sin(delta)
rad/s	°C	s	Pa		degrees	Pa	Pa	kPa
10	58	670.91	194.6	0.11784	79.81	296.8	1651	1.705
10	64	1447.3	89.12	0.12002	74.63	203.6	740.7	0.7967
10	70	2223.5	46.29	0.12	64.83	177.3	377.4	0.4607

CRS-2								
Ang. frequency	Temperature	Time	Osc. Stress	Strain	Delta	G'	G"	|G*|/sin(delta)
rad/s	°C	s	Pa		degrees	Pa	Pa	kPa
10	58	670.89	177.4	0.11797	79.18	287.4	1504	1.559
10	64	1447.3	82.72	0.12001	73.59	202.4	687.1	0.7467
10	70	2223.6	43.74	0.11998	63.58	176.7	355.7	0.4435
CRS-2								
Ang. frequency	Temperature	Time	Osc. Stress	Strain	Delta	G'	G"	|G*|/sin(delta)
rad/s	°C	s	Pa		degrees	Pa	Pa	kPa
10	58	1080.1	145.3	0.11826	78.01	260.9	1229	1.284
10	64	1856.4	72.8	0.11996	71.9	197.4	604	0.6685
10	70	2633	39.32	0.11993	61	176.2	317.7	0.4154
CRS-2L								
Ang. frequency	Temperature	Time	Osc. Stress	Strain	Delta	G'	G"	|G*|/sin(delta)
rad/s	°C	s	Pa		degrees	Pa	Pa	kPa
10	58	670.92	399.2	0.11474	77.51	762.5	3442	3.611
10	64	1447.2	209.7	0.11998	76.1	430.6	1739	1.846
10	70	2223.8	112.5	0.11998	72.27	299.4	936.5	1.032
CRS-2L								
Ang. frequency	Temperature	Time	Osc. Stress	Strain	Delta	G'	G"	|G*|/sin(delta)
rad/s	°C	s	Pa		degrees	Pa	Pa	kPa
10	58	670.84	354.5	0.11536	77.36	682.7	3044	3.197
10	64	1446.8	189.2	0.11997	75.5	406.1	1570	1.675
10	70	2222.9	101.1	0.12001	71.05	289.2	842.2	0.9415

CRS-2L								
Ang. frequency	Temperature	Time	Osc. Stress	Strain	Delta	G'	G"	|G*|/sin(delta)
rad/s	°C	s	Pa		degrees	Pa	Pa	kPa
10	58	670.91	326.8	0.11573	77.23	634.3	2799	2.943
10	64	1447.3	172	0.11996	75.01	382.3	1428	1.531
10	70	2223.5	93.4	0.11999	70.27	279.1	778.2	0.8783
SS-1								
Ang. frequency	Temperature	Time	Osc. Stress	Strain	Delta	G'	G"	|G*|/sin(delta)
rad/s	°C	s	Pa		degrees	Pa	Pa	kPa
10	58	670.92	201.2	0.11776	79.8	307.4	1708	1.763
10	64	1447.3	92.71	0.12005	74.79	209.6	770.9	0.8278
10	70	2223.7	47.05	0.11998	64.95	179.7	384.5	0.4685
SS-1								
Ang. frequency	Temperature	Time	Osc. Stress	Strain	Delta	G'	G"	|G*|/sin(delta)
rad/s	°C	s	Pa		degrees	Pa	Pa	kPa
10	58	670.92	399.2	0.11474	77.51	762.5	3442	3.611
10	64	1447.2	209.7	0.11998	76.1	430.6	1739	1.846
10	70	2223.8	112.5	0.11998	72.27	299.4	936.5	1.032
SS-1								
Ang. frequency	Temperature	Time	Osc. Stress	Strain	Delta	G'	G"	|G*|/sin(delta)
rad/s	°C	s	Pa		degrees	Pa	Pa	kPa
10	58	670.92	170.2	0.11809	79.43	269	1441	1.492
10	64	1447.1	80.04	0.11999	73.47	197.2	664.4	0.7229
10	70	2223.8	42.59	0.11995	63.11	175.2	345.6	0.4344

SS-1H								
Ang. frequency	Temperature	Time	Osc. Stress	Strain	Delta	G'	G"	|G*|/sin(delta)
rad/s	°C	s	Pa		degrees	Pa	Pa	kPa
10	58	1086	1085	0.10392	79.74	1867	10310	10.65
10	64	1862.5	540	0.11999	80.89	718.1	4477	4.592
10	70	2638.6	250.4	0.11999	80.25	358.1	2084	2.146
SS-1H								
Ang. frequency	Temperature	Time	Osc. Stress	Strain	Delta	G'	G"	|G*|/sin(delta)
rad/s	°C	s	Pa		degrees	Pa	Pa	kPa
10	58	1074.4	1321	0.098648	79.15	2529	13190	13.68
10	64	1850.7	678.4	0.12002	80.76	913.3	5615	5.763
10	70	2627	312.1	0.12	80.72	424.2	2595	2.665
SS-1H								
Ang. frequency	Temperature	Time	Osc. Stress	Strain	Delta	G'	G"	|G*|/sin(delta)
rad/s	°C	s	Pa		degrees	Pa	Pa	kPa
10	58	1076.9	1234	0.10063	79.38	2269	12100	12.53
10	64	1853.2	627	0.12004	80.86	835	5191	5.326
10	70	2629.4	288.4	0.11999	80.64	395.4	2399	2.464
SS-1L								
Ang. frequency	Temperature	Time	Osc. Stress	Strain	Delta	G'	G"	|G*|/sin(delta)
rad/s	°C	s	Pa		degrees	Pa	Pa	kPa
10	58	1056.4	597.9	0.11092	75.17	1395	5269	5.639
10	64	1832.6	334.1	0.12002	75.07	731.3	2743	2.938
10	70	2608.9	183.3	0.12	72.93	464.7	1514	1.656

SS-1L								
Ang. frequency	Temperature	Time	Osc. Stress	Strain	Delta	G'	G"	|G*|/sin(delta)
rad/s	°C	s	Pa		degrees	Pa	Pa	kPa
10	58	1069.5	577.8	0.11121	74.94	1366	5076	5.443
10	64	1845.8	326.3	0.11996	74.69	733.1	2678	2.879
10	70	2621.9	179.5	0.11996	72.44	469	1482	1.63
SS-1L								
Ang. frequency	Temperature	Time	Osc. Stress	Strain	Delta	G'	G"	|G*|/sin(delta)
rad/s	°C	s	Pa		degrees	Pa	Pa	kPa
10	58	1068.7	395.8	0.11404	74.03	972.2	3396	3.675
10	64	1845	223.7	0.12001	72.71	571.8	1837	2.015
10	70	2621.4	125.6	0.11997	69.27	392.8	1038	1.187

Recovery Method comparison data (3 Hours Vacuum Drying)

CRS-2P								
Ang. frequency	Temperature	Time	Osc. Stress	Strain	Delta	G'	G"	|G*|/sin(delta)
rad/s	°C	s	Pa		degrees	Pa	Pa	kPa
10	58	606.98	127.6	0.11842	77.32	242.5	1078	1.132
10	64	1372.4	65.28	0.11998	69.83	198.7	541	0.614
10	70	2137.6	35.86	0.11991	57.92	181.3	289.3	0.4029
CRS-2P								
Ang. frequency	Temperature	Time	Osc. Stress	Strain	Delta	G'	G"	|G*|/sin(delta)
rad/s	°C	s	Pa		degrees	Pa	Pa	kPa
10	58	607.09	125.7	0.11844	77.18	241.4	1061	1.116
10	64	1372.3	65.5	0.11996	69.86	199.1	543	0.616
10	70	2143.1	36.25	0.11996	58.18	181.5	292.6	0.4052
CRS-2								
Ang. frequency	Temperature	Time	Osc. Stress	Strain	Delta	G'	G"	|G*|/sin(delta)
rad/s	°C	s	Pa		degrees	Pa	Pa	kPa
10	58	607.06	118.7	0.1186	78.13	210.2	999.7	1.044
10	64	1371	58.93	0.11998	69.75	178.9	484.9	0.5509
10	70	2141.4	31.46	0.11998	55.67	168.6	246.9	0.362
CRS-2								
Ang. frequency	Temperature	Time	Osc. Stress	Strain	Delta	G'	G"	|G*|/sin(delta)
rad/s	°C	s	Pa		degrees	Pa	Pa	kPa
10	58	606.86	124.7	0.11855	78.51	213.7	1051	1.094
10	64	1371	60.92	0.11998	70.33	179.3	501.8	0.5659
10	70	2142.3	32.25	0.11996	56.45	168.3	253.8	0.3654

CRS-2								
Ang. frequency	Temperature	Time	Osc. Stress	Strain	Delta	G'	G"	|G*|/sin(delta)
rad/s	°C	s	Pa		degrees	Pa	Pa	kPa
10	58	606.91	123.1	0.11856	78.26	215.7	1038	1.082
10	64	1371.3	60.56	0.11997	70	181.7	499.2	0.5653
10	70	2135.8	31.91	0.11997	55.9	170.3	251.5	0.3667
CRS-2L								
Ang. frequency	Temperature	Time	Osc. Stress	Strain	Delta	G'	G"	|G*|/sin(delta)
rad/s	°C	s	Pa		degrees	Pa	Pa	kPa
10	58	606.88	187.3	0.11754	76.33	386.2	1588	1.682
10	64	1371.6	97.76	0.11997	71.98	265	814.9	0.9011
10	70	2143.6	54.71	0.12	64.33	218.4	454.3	0.5593
CRS-2L								
Ang. frequency	Temperature	Time	Osc. Stress	Strain	Delta	G'	G"	|G*|/sin(delta)
rad/s	°C	s	Pa		degrees	Pa	Pa	kPa
10	58	607.02	198.4	0.11737	76.1	416.4	1683	1.786
10	64	1371.4	102.9	0.11997	72.07	277.3	857.2	0.9469
10	70	2136.5	56.88	0.11997	64.55	225.1	473.1	0.5802
CRS-2L								
Ang. frequency	Temperature	Time	Osc. Stress	Strain	Delta	G'	G"	|G*|/sin(delta)
rad/s	°C	s	Pa		degrees	Pa	Pa	kPa
10	58	606.95	192.3	0.11741	75.81	412.4	1631	1.735
10	64	1377.4	100.4	0.11997	71.66	277.2	836.5	0.9284
10	70	2142.7	55.48	0.11997	63.91	225.9	461.4	0.572

SS-1								
Ang. frequency	Temperature	Time	Osc. Stress	Strain	Delta	G'	G"	|G*|/sin(delta)
rad/s	°C	s	Pa		degrees	Pa	Pa	kPa
10	58	606.97	116.6	0.11861	78	208.8	982.2	1.027
10	64	1380.3	56.22	0.11998	69.16	175.7	461.5	0.5284
10	70	2147.2	29.93	0.1199	54.4	166.7	232.8	0.3521
SS-1								
Ang. frequency	Temperature	Time	Osc. Stress	Strain	Delta	G'	G"	|G*|/sin(delta)
rad/s	°C	s	Pa		degrees	Pa	Pa	kPa
10	58	606.97	112.4	0.11864	77.64	207.4	946.1	0.9916
10	64	1371	54.22	0.11999	68.35	176.5	444.7	0.5148
10	70	2135	28.73	0.11998	52.98	167.6	222.2	0.3486
SS-1								
Ang. frequency	Temperature	Time	Osc. Stress	Strain	Delta	G'	G"	|G*|/sin(delta)
rad/s	°C	s	Pa		degrees	Pa	Pa	kPa
10	58	606.88	116.1	0.11859	77.6	215.2	978.2	1.026
10	64	1371.2	55.47	0.11997	68.51	179.5	455.9	0.5265
10	70	2135.8	29.27	0.11997	53.29	170	228	0.3548
SS-1H								
Ang. frequency	Temperature	Time	Osc. Stress	Strain	Delta	G'	G"	|G*|/sin(delta)
rad/s	°C	s	Pa		degrees	Pa	Pa	kPa
10	58	607.14	536.2	0.11378	81.32	715.9	4691	4.8
10	64	1371.2	256.8	0.11997	80.45	359.7	2138	2.198
10	70	2141.9	121.2	0.11998	76.92	234.6	1010	1.064

SS-1H								
Ang. frequency	Temperature	Time	Osc. Stress	Strain	Delta	G'	G"	|G*|/sin(delta)
rad/s	°C	s	Pa		degrees	Pa	Pa	kPa
10	58	606.95	533	0.11378	81.18	723.5	4661	4.773
10	64	1377.6	250.4	0.12	80.2	360	2084	2.147
10	70	2141.6	118.9	0.11999	76.49	238.2	991.2	1.048
SS-1H								
Ang. frequency	Temperature	Time	Osc. Stress	Strain	Delta	G'	G"	|G*|/sin(delta)
rad/s	°C	s	Pa		degrees	Pa	Pa	kPa
10	58	606.97	112.4	0.11864	77.64	207.4	946.1	0.9916
10	64	1371	54.22	0.11999	68.35	176.5	444.7	0.5148
10	70	2135	28.73	0.11998	52.98	167.6	222.2	0.3486
SS-1H								
Ang. frequency	Temperature	Time	Osc. Stress	Strain	Delta	G'	G"	|G*|/sin(delta)
rad/s	°C	s	Pa		degrees	Pa	Pa	kPa
10	58	607.06	523.5	0.11391	81.18	709.4	4574	4.684
10	64	1370.5	250.6	0.11998	80.26	358.2	2086	2.148
10	70	2141.3	118.6	0.11995	76.53	236.7	988.2	1.045
SS-1L								
Ang. frequency	Temperature	Time	Osc. Stress	Strain	Delta	G'	G"	|G*|/sin(delta)
rad/s	°C	s	Pa		degrees	Pa	Pa	kPa
10	58	607.08	239	0.11679	76.02	505.6	2031	2.157
10	64	1378.2	125.7	0.11999	73.52	309.6	1047	1.138
10	70	2143.3	69.96	0.11995	67.43	242.3	583.1	0.6837

SS-1L								
Ang. frequency	Temperature	Time	Osc. Stress	Strain	Delta	G'	G"	|G*|/sin(delta)
rad/s	°C	s	Pa		degrees	Pa	Pa	kPa
10	58	606.88	247.6	0.11673	76.52	505	2106	2.227
10	64	1377.1	131	0.11997	73.98	313.1	1091	1.18
10	70	2147.4	73.79	0.11998	68.21	245.9	615	0.7133
SS-1L								
Ang. frequency	Temperature	Time	Osc. Stress	Strain	Delta	G'	G"	|G*|/sin(delta)
rad/s	°C	s	Pa		degrees	Pa	Pa	kPa
10	58	606.92	220.5	0.11719	77.13	428	1874	1.972
10	64	1377.8	114.9	0.11997	73.99	274.7	957.2	1.036
10	70	2148.6	63.87	0.11996	67.36	221.6	531.2	0.6237

Recovery Method comparison data (6 Hours Vacuum Drying)

CRS-2P								
Ang. frequency	Temperature	Time	Osc. Stress	Strain	Delta	G'	G"	|G*|/sin(delta)
rad/s	°C	s	Pa		degrees	Pa	Pa	kPa
10	58	606.95	141.7	0.11829	77.79	259.3	1198	1.254
10	64	1376.6	71.11	0.11998	71.19	200.9	590.1	0.6585
10	70	2140.7	38.71	0.11997	59.95	181.5	313.7	0.4186
CRS-2P								
Ang. frequency	Temperature	Time	Osc. Stress	Strain	Delta	G'	G"	|G*|/sin(delta)
rad/s	°C	s	Pa		degrees	Pa	Pa	kPa
10	58	606.92	141.3	0.11825	77.06	274.6	1195	1.258
10	64	1372.2	72.15	0.11994	70.76	209.3	599.6	0.6727
10	70	2137.5	39.43	0.12002	59.73	187.4	321.1	0.4304
CRS-2								
Ang. frequency	Temperature	Time	Osc. Stress	Strain	Delta	G'	G"	|G*|/sin(delta)
rad/s	°C	s	Pa		degrees	Pa	Pa	kPa
10	58	607.05	126.4	0.11853	78.44	218.1	1066	1.111
10	64	1376.8	62.71	0.11997	70.7	181.1	517.2	0.5806
10	70	2147.5	33.06	0.11997	57.15	168.5	261	0.3697
CRS-2								
Ang. frequency	Temperature	Time	Osc. Stress	Strain	Delta	G'	G"	|G*|/sin(delta)
rad/s	°C	s	Pa		degrees	Pa	Pa	kPa
10	58	606.94	132.2	0.11847	78.45	228.1	1116	1.162
10	64	1372.2	64.36	0.11997	70.64	186.9	531.8	0.5975
10	70	2143.1	33.8	0.11992	57.19	173.6	269.2	0.3811

CRS-2L								
Ang. frequency	Temperature	Time	Osc. Stress	Strain	Delta	G'	G"	|G*|/sin(delta)
rad/s	°C	s	Pa		degrees	Pa	Pa	kPa
10	58	606.97	220.5	0.11699	75.57	481.7	1872	1.996
10	64	1377.8	118.4	0.11999	72.26	315.1	985.3	1.086
10	70	2141.4	66.43	0.11997	65.87	248	553.6	0.6647
CRS-2L								
Ang. frequency	Temperature	Time	Osc. Stress	Strain	Delta	G'	G"	|G*|/sin(delta)
rad/s	°C	s	Pa		degrees	Pa	Pa	kPa
10	58	661.78	220	0.11687	74.59	514	1865	2.006
10	64	1432.4	118.6	0.11997	70.53	348.2	984.7	1.108
10	70	2203.1	66.51	0.11997	63.74	273.4	554.1	0.6891

Recovery Method comparison data (8 Hours Vacuum Drying)

CRS-2P								
Ang. frequency	Temperature	Time	Osc. Stress	Strain	Delta	G'	G"	|G*|/sin(delta)
rad/s	°C	s	Pa		degrees	Pa	Pa	kPa
10	58	606.97	148.5	0.11816	77.31	282.9	1257	1.321
10	64	1371.7	75.3	0.11999	71.26	212.4	626	0.698
10	70	2143.2	40.98	0.11996	60.69	187.8	334.5	0.4399
CRS-2P								
Ang. frequency	Temperature	Time	Osc. Stress	Strain	Delta	G'	G"	|G*|/sin(delta)
rad/s	°C	s	Pa		degrees	Pa	Pa	kPa
10	58	606.92	147.1	0.11821	77.74	270.4	1244	1.303
10	64	1371.9	74.38	0.11998	71.5	206.7	618	0.6871
10	70	2136.4	40.25	0.11998	60.66	184.1	327.5	0.431
CRS-2								
Ang. frequency	Temperature	Time	Osc. Stress	Strain	Delta	G'	G"	|G*|/sin(delta)
rad/s	°C	s	Pa		degrees	Pa	Pa	kPa
10	58	606.86	137.6	0.11841	78.71	231.9	1162	1.208
10	64	1369.7	67.28	0.11997	71.35	187.8	556.6	0.62
10	70	2134.5	35.17	0.12	58.42	172.6	280.7	0.3868
CRS-2								
Ang. frequency	Temperature	Time	Osc. Stress	Strain	Delta	G'	G"	|G*|/sin(delta)
rad/s	°C	s	Pa		degrees	Pa	Pa	kPa
10	58	606.91	137.7	0.11842	78.85	229.3	1163	1.208
10	64	1371	67.44	0.11999	71.64	185	557.5	0.6188
10	70	2135.5	35.29	0.11994	58.73	170.8	281.3	0.385

CRS-2L								
Ang. frequency	Temperature	Time	Osc. Stress	Strain	Delta	G'	G"	|G*|/sin(delta)
rad/s	°C	s	Pa		degrees	Pa	Pa	kPa
10	58	606.89	235.8	0.11682	75.96	501	2004	2.129
10	64	1377.6	124.7	0.11995	72.63	324.5	1037	1.139
10	70	2142.4	69.24	0.11999	66.44	251.7	577.1	0.6868
CRS-2L								
Ang. frequency	Temperature	Time	Osc. Stress	Strain	Delta	G'	G"	|G*|/sin(delta)
rad/s	°C	s	Pa		degrees	Pa	Pa	kPa
10	58	607.08	233.9	0.11681	75.73	505.2	1987	2.115
10	64	1370.4	122	0.11999	72.2	325.9	1015	1.119
10	70	2140.3	66.87	0.11997	65.66	252.2	557.4	0.6715

Unaged Base Binder

CRS-2 Base								
Ang. frequency	Temperature	Time	Osc. Stress	Strain	Delta	G'	G"	|G*|/sin(delta)
rad/s	°C	s	Pa		degrees	Pa	Pa	kPa
10	52	937.63	196.1	0.11805	81.79	239.7	1661	1.696
10	64	1784.6	48.87	0.11997	66.92	169.6	397.9	0.4701
10	76	2631.5	17.98	0.11998	35.6	162.9	116.6	0.3441
CRS-2 Base								
Ang. frequency	Temperature	Time	Osc. Stress	Strain	Delta	G'	G"	|G*|/sin(delta)
rad/s	°C	s	Pa		degrees	Pa	Pa	kPa
10	52	934.72	192.7	0.11808	81.71	237.7	1632	1.667
10	64	1781.6	48.34	0.11999	66.69	169.4	393.2	0.4662
10	76	2628.6	17.86	0.11996	35.32	162.8	115.4	0.3451
CRS-2 Base								
Ang. frequency	Temperature	Time	Osc. Stress	Strain	Delta	G'	G"	|G*|/sin(delta)
rad/s	°C	s	Pa		degrees	Pa	Pa	kPa
10	52	1347.9	193.6	0.11807	81.73	238.2	1640	1.674
10	64	2194.8	48.36	0.12	66.68	169.6	393.5	0.4666
10	76	3041.9	17.8	0.11996	35.16	163.2	115	0.3466
CRS-2P Base								
Ang. frequency	Temperature	Time	Osc. Stress	Strain	Delta	G'	G"	|G*|/sin(delta)
rad/s	°C	s	Pa		degrees	Pa	Pa	kPa
10	52	983.41	190.2	0.11809	81.61	237.7	1611	1.646
10	64	1830.2	47.53	0.11997	66.31	169.6	386.4	0.4608
10	76	2677	17.78	0.11997	35.11	162.6	114.3	0.3457

CRS-2P Base								
Ang. frequency	Temperature	Time	Osc. Stress	Strain	Delta	G'	G"	|G*|/sin(delta)
rad/s	°C	s	Pa		degrees	Pa	Pa	kPa
10	52	938.69	190.1	0.11809	81.54	239.5	1610	1.645
10	64	1785.5	47.6	0.11997	66.3	169.9	387.1	0.4617
10	76	2632.3	17.63	0.11997	34.72	162.8	112.8	0.3477
CRS-2P Base								
Ang. frequency	Temperature	Time	Osc. Stress	Strain	Delta	G'	G"	|G*|/sin(delta)
rad/s	°C	s	Pa		degrees	Pa	Pa	kPa
10	52	934.72	192.7	0.11808	81.71	237.7	1632	1.667
10	64	1781.6	48.34	0.11999	66.69	169.4	393.2	0.4662
10	76	2628.6	17.86	0.11996	35.32	162.8	115.4	0.3451
SS-1 Base								
Ang. frequency	Temperature	Time	Osc. Stress	Strain	Delta	G'	G"	|G*|/sin(delta)
rad/s	°C	s	Pa		degrees	Pa	Pa	kPa
10	52	670.95	422.2	0.1135	73.52	1074	3630	3.947
10	64	1518	159.9	0.12019	66.74	557.3	1296	1.536
10	76	2364.9	74.06	0.12	58.65	369.6	606.9	0.832
SS-1 Base								
Ang. frequency	Temperature	Time	Osc. Stress	Strain	Delta	G'	G"	|G*|/sin(delta)
rad/s	°C	s	Pa		degrees	Pa	Pa	kPa
10	52	670.91	248.5	0.11722	79.59	388.6	2116	2.187
10	64	1518.1	87.2	0.1202	70.83	252.2	725.5	0.8132
10	76	2365.4	43.24	0.12007	58.86	216.2	357.8	0.4884

SS-1 Base								
Ang. frequency	Temperature	Time	Osc. Stress	Strain	Delta	G'	G"	|G*|/sin(delta)
rad/s	°C	s	Pa		degrees	Pa	Pa	kPa
10	52	670.88	149.5	0.11826	78.81	250	1264	1.313
10	64	1518.1	41.23	0.12003	61.83	179.2	334.6	0.4306
10	76	2365.3	17.29	0.11994	34.06	169.4	114.5	0.3652
SS-1L and CRS-2L Base								
Ang. frequency	Temperature	Time	Osc. Stress	Strain	Delta	G'	G"	|G*|/sin(delta)
rad/s	°C	s	Pa		degrees	Pa	Pa	kPa
10	52	936.19	167.3	0.11833	81.54	210.2	1413	1.445
10	64	1783	44.09	0.11998	64.95	166.4	356.1	0.4339
10	76	2629.9	17.45	0.11993	34.27	162.8	110.9	0.35
SS-1L and CRS-2L Base								
Ang. frequency	Temperature	Time	Osc. Stress	Strain	Delta	G'	G"	|G*|/sin(delta)
rad/s	°C	s	Pa		degrees	Pa	Pa	kPa
10	52	1151.7	169.2	0.11832	81.67	209.4	1430	1.46
10	64	1998.6	44.41	0.11997	65.15	166.2	358.9	0.4359
10	76	2845.4	17.35	0.11996	33.97	162.5	109.5	0.3506
SS-1L and CRS-2L Base								
Ang. frequency	Temperature	Time	Osc. Stress	Strain	Delta	G'	G"	|G*|/sin(delta)
rad/s	°C	s	Pa		degrees	Pa	Pa	kPa
10	52	1510.4	169.4	0.11832	81.67	209.5	1431	1.462
10	64	2357.1	44.59	0.11997	65.26	166.1	360.4	0.4369
10	76	3204	17.34	0.11996	33.96	162.5	109.5	0.3508

SS-1H Base								
Ang. frequency	Temperature	Time	Osc. Stress	Strain	Delta	G'	G"	|G*|/sin(delta)
rad/s	°C	s	Pa		degrees	Pa	Pa	kPa
10	52	670.95	970.2	0.10697	81.48	1350	9004	9.207
10	64	1517.6	223.2	0.11995	81.01	294.2	1861	1.907
10	76	2364.4	56.87	0.11999	69	179.5	467.6	0.5365
SS-1H Base								
Ang. frequency	Temperature	Time	Osc. Stress	Strain	Delta	G'	G"	|G*|/sin(delta)
rad/s	°C	s	Pa		degrees	Pa	Pa	kPa
10	52	670.77	974.6	0.10692	81.52	1350	9051	9.252
10	64	1517.4	224.2	0.11998	81.09	293.1	1869	1.914
10	76	2364.2	57.83	0.11997	69.43	178.4	475.6	0.5425
SS-1H Base								
Ang. frequency	Temperature	Time	Osc. Stress	Strain	Delta	G'	G"	|G*|/sin(delta)
rad/s	°C	s	Pa		degrees	Pa	Pa	kPa
10	52	670.75	999.7	0.10627	81.16	1452	9332	9.558
10	64	1517.7	236.5	0.11997	80.54	328.1	1970	2.024
10	76	2364.9	61.83	0.11993	69.12	195.3	511.9	0.5864

SS-1 Base (repeat)								
Ang. frequency	Temperature	Time	Osc. Stress	Strain	Delta	G'	G"	|G*|/sin(delta)
rad/s	°C	s	Pa		degrees	Pa	Pa	kPa
10	58	606.98	127.6	0.11842	77.32	242.5	1078	1.132
10	64	1372.4	65.28	0.11998	69.83	198.7	541	0.614
10	70	2137.6	35.86	0.11991	57.92	181.3	289.3	0.4029
SS-1 Base (repeat)								
Ang. frequency	Temperature	Time	Osc. Stress	Strain	Delta	G'	G"	|G*|/sin(delta)
rad/s	°C	s	Pa		degrees	Pa	Pa	kPa
10	52	606.94	132.2	0.11847	78.45	228.1	1116	1.162
10	64	1372.2	64.36	0.11997	70.64	186.9	531.8	0.5975
10	76	2143.1	33.8	0.11992	57.19	173.6	269.2	0.3811
SS-1 Base (repeat)								
Ang. frequency	Temperature	Time	Osc. Stress	Strain	Delta	G'	G"	|G*|/sin(delta)
rad/s	°C	s	Pa		degrees	Pa	Pa	kPa
10	52	670.95	125.6	0.11829	75.26	279.4	1062	1.135
10	64	1447.1	65.26	0.12	68.14	217.7	542.4	0.6298
10	76	2223.6	36.44	0.11998	56.81	194.4	297.2	0.4244

MSCR Test results for different curing time (CRS-2P)

Time (hours)	Emulsion	Stress level (Pa)	Recovery(%)	J_{nr}
3	CRS2P	100	2.179429	0.019738
3	CRS2P	3200	-0.11634	0.833252
3	CRS2P	100	5.506782	0.019738
3	CRS2P	3200	0.041003	0.833252
6	CRS2P	100	13.47058	0.0208
6	CRS2P	3200	-0.38898	1.003074
6	CRS2P	100	11.7305	0.021519
6	CRS2P	3200	-0.34693	1.013371
8	CRS2P	100	16.46657	-0.0176
8	CRS2P	3200	-0.02801	0.845339
8	CRS2P	100	10.85476	0.019854
8	CRS2P	3200	-0.20565	0.902177

MSCR Test results for different curing time (CRS-2)

Time (hours)	Emulsion	Stress level (Pa)	Recovery(%)	J_{nr}
3	CRS2	100	-0.4386	0.029408
3	CRS2	3200	-0.79118	1.070384
3	CRS2	100	0.751759	0.027846
3	CRS2	3200	-0.76905	1.056422
6	CRS2	100	3.016155	0.02671
6	CRS2	3200	-0.75358	1.00456
6	CRS2	100	-2.27138	0.027342
6	CRS2	3200	-0.72711	0.958049
8	CRS2	100	3.6651	0.024227
8	CRS2	3200	-0.57176	0.935678
8	CRS2	100	1.398862	0.024862
8	CRS2	3200	-0.59356	0.899438